Razvoj i optimiranje nazalne depozicije inovativnih farmaceutskih oblika kortikosteroida

Nižić Nodilo, Laura

Sveučilište u Zagrebu

Farmaceutsko-biokemijski fakultet

Laura Nižić Nodilo

RAZVOJ I OPTIMIRANJE NAZALNE DEPOZICIJE INOVATIVNIH FARMACEUTSKIH OBLIKA KORTIKOSTEROIDA

DOKTORSKI RAD

Zagreb, 2022.

Sveučilište u Zagrebu

Farmaceutsko-biokemijski fakultet

Laura Nižić Nodilo

RAZVOJ I OPTIMIRANJE NAZALNE DEPOZICIJE INOVATIVNIH FARMACEUTSKIH OBLIKA KORTIKOSTEROIDA

DOKTORSKI RAD

Mentorica: prof. dr. sc. Anita Hafner

Zagreb, 2022.

Faculty of Pharmacy and Biochemistry

Laura Nižić Nodilo

DEVELOPMENT AND NASAL DEPOSITION OPTIMISATION OF INNOVATIVE PHARMACEUTICAL FORMS OF CORTICOSTEROIDS

DOCTORAL DISSERTATION

Supervisor: Professor Anita Hafner, PhD

Zagreb, 2022

Doktorski rad je predan na ocjenu Fakultetskom vijeću Farmaceutsko-biokemijskog fakulteta Sveučilišta u Zagrebu radi stjecanja akademskog stupnja doktora znanosti iz područja biomedicine i zdravstva, polje farmacija, grana farmacija.

Rad je izrađen u Zavodu za farmaceutsku tehnologiju Farmaceutsko-biokemijskog fakulteta Sveučilišta u Zagrebu pod mentorstvom prof. dr. sc. Anite Hafner. Dio eksperimenata proveden je tvrtki JGL d. d. Doktorsko istraživanje provedeno je u sklopu uspostavnog istraživačkog projekta Hrvatske zaklade za znanost pod naslovom „Optimiranje depozicije raspršenih *in situ* gelirajućih i praškastih terapijskih sustava u nosnoj šupljini“, voditeljice prof. dr. sc. Anite Hafner (UIP-2017-05-4592).

ZAHVALE/ACKNOWLEDGEMENTS

Prvu od brojnih zahvala koje „dugujem“ upućujem mentorici, prof. dr. sc. Aniti Hafner. Draga mentorice, hvala Vam na pruženoj prilici još u studentskim danima, na stručnom vodstvu, iznimnoj pristupačnosti i vrhunskim savjetima, kako vezano uz doktorski rad, tako i uz životne situacije. Hvala i na iznimnoj brizi oko svega te na inovativnim gastronomskim iskustvima pristiglima od doline Neretve, preko sjevernijih krajeva pa sve do komercijalno dostupnih bombona.

Zahvaljujem prof. dr. sc. Jeleni Filipović-Grčić na podršci i pomoći te svim kolegicama i kolegama sa Zavoda za farmaceutsku tehnologiju. Posebno hvala susjedama i susjedima iz ureda koji su i najcrnje dane znali razvedriti i olakšati.

Zahvaljujem doc. dr. sc. Ivi Ugrini i dr. sc. Dragi Špoljariću na velikoj pomoći oko statističke analize rezultata te dr. sc. Matiji Gretiću na provedbi pretražne elektronske mikroskopije.

Veliko hvala Vesni Saršon i Maši Safundžić Kučuk na pomoći s analizom veličine raspršenih kapljica.

Zahvaljujem doc. dr. sc. Danieli Amidžić Klarić na iznimnoj pomoći oko HPLC analiza.

Hvala ekipi asistenata (sadašnjih i bivših, pravih i HRZZ) na nezaboravnim druženjima na top zagrebačkim lokacijama.

Posebnu zahvalu upućujem Mirni s kojom sam zadnje dvije godine doktorata provela vjerojatno više vremena nego bilo s kojom drugom osobom, što u labosu, a što na pelinu, bez kojega ovog doktorata ne bi ni bilo.

Riječi ne mogu izreći moju zahvalnost mami i tati na ljubavi, podršci i potpori koju mi pružaju oduvijek. Per concludere, kad ni riječi nešto ne mogu reći, najbolje je preko Zvonca prijeći i komunicirati bliže teći.

Nedovoljno je dokumenata na svijetu da napišem zahvale Josipu za sve što bi trebalo, ali nadam se da će mu za početak dovoljna zahvala biti prestanak slušanja o mojem doktoratu.

Zahvaljujem cijeloj obitelji na podršci i veselim trenutcima u životu.

Hvala mojim dragim prijateljicama i prijateljima, Zadranima, trenutnim i bivšim farmaceutima, i svima ostalima koji su sa mnom proživljavali ovaj period. Ne bih uspjela bez svih vas, od žaljenja kad je loše do uvijek spremnog slavlja kad krene na dobro.

SAŽETAK

Nazalna primjena lijeka uobičajena je u liječenju lokalnih oboljenja nosne sluznice. Istražuje se i kao alternativni put sistemske primjene lijekova, a pruža mogućnost i izravne dostave lijeka u središnji živčani sustav. Ograničenja nazalne primjene lijeka uključuju otežanu dostavu lijeka u ciljno područje te mukocilijarni klirens koji skraćuje vrijeme kontakta lijeka i nosne sluznice. Nazalna primjena kortikosteroida česta je u liječenju bolesti nosne sluznice i paranazalnih sinusa, a u novije vrijeme predlaže se i u liječenju neuroupalnih procesa. U okviru ovog doktorskog rada, primjenjujući načela kakvoće utemeljene kroz dizajn, razvijena su tri inovativna *in situ* gelirajuća sustava s uklopljenim kortikosteroidom za nazalnu primjenu u obliku spreja: (i) *in situ* gelirajuća mikrosuspenzija flutikazonpropionata (FP-a), (ii) *in situ* gelirajuća nanosuspenzija FP-a pripravljena uz vlažno mljevenje te (iii) praškasti sustav mikrosfera s natrijevim deksametazonfosfatom (NDF-om) i inertnog nosača. Provedena je njihova temeljita fizičko-kemijska i biofarmaceutska karakterizacija. Polimerni sastav *in situ* gelirajućih mikro- i nanosuspenzija FP-a osigurao je pseudoplastično ponašanje, prikladnost za primjenu raspršivanjem (tj. prikladnu veličinu raspršenih kapljica i kut raspršenja) te svojstvo geliranja u kontaktu sa simuliranim nosnim fluidom (SNF). Mikrosfere s NDF-om, pripravljene sušenjem raspršivanjem, karakterizirane su velikom uspješnošću uklapanja lijeka, odgovarajućim sadržajem ostatne vlage te sposobnošću bubrenja u SNF-u pri čemu nastaje gel. Smjese mikrosfera s NDF-om i inertnog nosača bile su homogene te boljih svojstava tečenja i užeg kuta raspršenja od samih mikrosfera. Postignuta je uspješna depozicija sva tri farmaceutska oblika u ciljnoj regiji nosne šupljine, ovisno o željenom učinku. Razvijeni farmaceutski oblici karakterizirani su boljom mukoadhezivnošću u usporedbi s konvencionalnim oblicima. Oslobađanje lijeka iz svih razvijenih oblika bilo je prikladno za nazalnu primjenu. Nanonizacija FP-a rezultirala je većom mukoadhezivnošću formulacije te većom topljivošću i brzinom oslobađanja FP-a iz *in situ* gela, pružajući mogućnost smanjenja primijenjene doze. Svim sustavima potvrđena je biokompatibilnost *in vitro* na modelu Calu-3 stanica te fizičko-kemijska stabilnost. Praškasti sustav s NDF-om pokazao je potencijal poboljšanja permeacije lijeka kroz nazalni epitel. Prilagođavanjem procesnih, formulacijskih i/ili parametara primjene korištenjem dizajna eksperimenta razvijeni su inovativni farmaceutski oblici kortikosteroida s potencijalom produljenog zadržavanja na mjestu primjene, povoljnih biofarmaceutskih svojstava i optimirane depozicije u nosnoj šupljini.

Ključne riječi: *in situ* gelirajući sustav, nanosuspenzija, mikrosfere, sušenje raspršivanjem, flutikazonpropionat, natrijev deksametazonfosfat, nazalna depozicija

SUMMARY

Introduction: Nasal drug delivery is a well-established administration route for drugs in the treatment of local nasal mucosa and paranasal sinuses diseases. Due to the large absorption area of the nasal mucosa, high vascularisation and low enzyme activity, it is currently being investigated as an alternative route for systemic delivery of drugs with low oral bioavailability and drugs that require fast onset. Furthermore, it provides the possibility of direct drug delivery to the central nervous system via the olfactory and trigeminal nerves. Despite the aforementioned advantages, the potential of nasal drug delivery has not been fully accomplished. The main limiting factors are related to anatomical and physiological properties of the nasal cavity. Complex geometry of nasal cavity hinders drug delivery to the targeted area behind the nasal valve. For local effect and systemic availability, the drug should be delivered to the respiratory area, and for direct nose to brain delivery, it is necessary to ensure the deposition of the drug in the olfactory area. Another impeding factor is the mucociliary clearance which limits contact time of pharmaceutical form with nasal mucosa, and thus the availability of drug at the site of action.

Nasal corticosteroids are widely used in the treatment of nasal mucosa diseases. Recently, nasal administration of corticosteroids has been proposed as an effective strategy to control neuroinflammatory processes in patients with severe Covid-19 disease.

Innovative *in situ* gelling systems are being developed with the aim to prolong drug retention time at the nasal mucosa and ensure a suitable drug release profile. The gelled system slows down mucociliary clearance and ensures longer contact with the nasal mucosa. Liquid pharmaceutical forms are easily prepared and they ensure uniformity of drug dosage. Powdered systems are more stable than liquid forms, allow for a higher drug content, and provide a higher drug concentration at the nasal mucosa. One of the most commonly used methods for the preparation of powder systems is spray drying. By varying formulation and process parameters, it is possible to prepare particles of precisely defined properties. In this work, liquid and powder *in situ* gelling pharmaceutical forms of corticosteroids were prepared and optimised in terms of drug content, rheological properties, drug release profile, spray properties, mucoadhesiveness, biocompatibility, permeability and nasal deposition profile.

Methods: Statistical design of experiment was used to optimize the process, formulation and/or administration parameters of corticosteroid pharmaceutical forms. *In situ* gelling microsuspension was prepared by mixing fluticasone propionate (FP) and polysorbate 80,

followed by the addition of polymer solutions. *In situ* gelling FP nanosuspension was prepared employing wet media milling method to produce FP nanocrystals. Dexamethasone sodium phosphate (DSP)-loaded microspheres were prepared by spray drying. *In situ* gelling FP micro- and nanosuspension were characterised in terms of suspended (nano)particle size, rheological properties including flow curve, zero shear viscosity, gelation time and frequency sweep, droplet size distribution, spray cone angle, and deposition in 3D printed nasal cavity model. Furthermore, for *in situ* gelling FP nanosuspension, zeta potential, surface tension and particle shape were also investigated. For DSP-loaded microspheres, entrapment efficiency and drug loading, surface properties and morphology, moisture content, particle size and swelling properties were determined. Microspheres/inert carrier (lactose or mannitol) powder blends were prepared and characterised in terms of homogeneity, flow properties, spray cone angle and deposition in 3D printed nasal cavity model. For selected *in situ* gelling liquid and powder formulations, biopharmaceutical properties were determined, including *in vitro* drug release profile, *ex vivo* mucoadhesiveness and *in vitro* biocompatibility and permeability using Calu-3 cell line as a model of respiratory epithelium. Optimal process, formulation and/or administration parameters were revealed by statistical analysis performed on characterization results of corticosteroid pharmaceutical forms.

Results: *In situ* gelling FP microsuspension, *in situ* gelling FP nanosuspension and powder form of DSP-loaded microspheres and inert carrier were successfully prepared employing quality by design (QbD) principles. *In situ* gelling FP microsuspensions were prepared using commercially available micronized FP with particle sizes ranging from 0.097 to 10 μm. *In situ* gelling FP nanosuspensions were characterised by mean diameter of FP nanocrystals ranging from 133.0 ± 0.8 nm to 160.7 ± 3.6 nm and the polydispersity index between 0.227 ± 0.027 and 0.273 ± 0.011, proving the suitability of wet media milling for the FP nanonisation. Zeta potential of *in situ* gelling FP nanosuspensions ranged from -93.1 ± 0.6 mV to -77.2 ± 3.7 mV, ensuring sufficient physical stability of the prepared systems. Surface tension of the *in situ* gelling nanosuspensions was within the range of preferred surface tension values for nasal spray. The polymer composition of *in situ* gelling FP micro- and nanosuspensions ensured appropriate viscosity, beneficial effect on suspension stability, pseudoplastic behaviour, suitability for spray application and gelling properties in contact with simulated nasal fluid (SNF).

Optimisation of the spray drying process for the production of DSP-loaded microspheres resulted in high process yield. Obtained DSP-loaded microspheres were characterised by high entrapment efficiency, relatively low residual moisture content, small particle size and suitable swelling (gelling) properties in SNF. *In situ* gelling FP micro- and nanosuspensions as well as DSP-loaded microspheres formed gel instantly after contact with SNF. Droplet size distribution of liquid *in situ* gelling systems met the requirements for nasal drug administration, with > 90% of the droplets larger than 10 μm. Obtained microspheres were characterised by smaller particle size, making them suitable for mixing with an inert carrier of appropriate particle size. Homogeneous blends of DSP-loaded microspheres with lactose or mannitol (particle size 45 - 63 μm) in weight ratios 1:9 and 1:19 were prepared using powder shaker/mixer. Powder blends showed better flow properties compared to the microspheres alone, as seen from the Hausner ratio. Viscosity of *in situ* gelling FP micro- and nanosuspensions increased with the increase of polymer concentration, especially gellan gum. Spray cone angle of liquid *in situ* gelling systems also depended on the polymer composition; it was most influenced by the concentration of sodium hyaluronate, the increase of which resulted in decrease of the spray cone angle. In addition to the polymer concentration, it was demonstrated that polymer(s) type and behaviour at high shear rates obtained by spraying from the spray pump were also crucial for spray properties. Spray cone angle of powder systems depended on the presence of a carrier in the mixture. A positive correlation between the Hausner ratio and the spray cone was shown. Overall approach to nasal deposition studies coupling formulation, process and administration parameters, resulted in successful delivery of *in situ* gelling FP microsuspension, *in situ* gelling FP nanosuspension and DSP-loaded microspheres/mannitol (1:9, *w*/*w*) powder blend to the total turbinate region (>90% of the applied dose), middle turbinate region (51.8% of the applied dose) and olfactory region (17.0% of the applied dose) of the nasal cavity models, respectively. The administration of DSP-loaded microspheres/mannitol powder blend in two halves of nasal cavity (i.e. left and right nostril) resulted in different deposition profiles due to different nasal valve surface areas, emphasizing the need for individualized approach to nasal treatment.

The *in vitro* FP and DSP release from developed *in situ* gelling systems was suitable for nasal delivery. *In situ* gelling FP micro- and nanosuspensions provided slower release in relation to corresponding conventional suspensions. Similarly, DSP-loaded microspheres/mannitol blend decreased the DSP release rate compared to the physical mixture of mannitol and DSP. Nanonisation of water-insoluble FP resulted in increased FP solubility and faster drug release from the *in situ* gelling nanosuspension compared to *in situ* gelling FP

microsuspension. *In situ* gels were stable over a wide range of angular frequencies and showed very little volume expansion, regardless of FP particle size. All developed formulations showed mucoadhesive properties, increasing in the following order: *in situ* gelling FP microsuspension < *in situ* gelling FP nanosuspension < DSP-loaded microspheres/mannitol blend. Namely, *in situ* gelling FP nanosuspension and its *in situ* gelling microsuspension control exhibited lower adhesion work and detachment force compared to the powder system but were still characterised by higher mucoadhesiveness than conventional aqueous FP micro- and nanosuspensions. *In situ* gelling FP nanosuspension showed improved mucoadhesive properties compared to its non-milled control, demonstrating the benefits of particle size reduction to nanoscale. Biocompatibility of developed *in situ* gelling FP and DSP formulations was confirmed by *in vitro* studies on Calu-3 cells. DSP permeability was influenced by osmotic conditions: apparent permeability coefficients of DSP across Calu-3 cell monolayer under isoosmotic and mildly hyperosmotic conditions were similar, while hypoosmotic conditions caused an increase in DSP permeation through the epithelial barrier model, enhancing the potential of direct drug delivery to the central nervous system. Developed *in situ* gelling FP and DSP formulations were characterised by appropriate stability profiles, confirming their potential in nasal corticosteroids delivery.

Conclusion: Statistical design of experiment revealed and elucidated the influence of process and/or formulation parameters on the key FP and DSP nasal formulation properties, enabling optimisation of their production. *In situ* gelling liquid and powder corticosteroid delivery systems were characterised by fair rheological properties, adequate droplet/particle size, appropriate spray cone angle and good stability. Optimal conditions for achieving drug deposition in targeted region of the nasal cavity were uncovered, showing the importance of process, formulation and administration parameter's interplay on targeted drug delivery.

Conclusively, a comprehensive, QbD-based approach employed in this work resulted in the development of functional *in situ* gelling pharmaceutical forms of corticosteroids for nasal administration with the potential of prolonged retention at the site of administration, optimized nasal deposition and favourable biopharmaceutical properties, suting the needs for efficient and safe localised FP delivery and DSP nose to brain targeting. The obtained results represent a solid foundation for further formulations assessment *in vivo*.

SADRŽAJ

1. UVOD

Nazalna primjena lijekova uvriježen je put primjene za liječenje lokalnih oboljenja nosne sluznice, kao što su kongestija, respiratorna infekcija, alergijski rinitis, kronični rinosinuitis te upala nosne sluznice ostalih etiologija (1). Zbog velike apsorpcijske površine nosne sluznice, dobre prokrvljenosti i relativno niske enzimske aktivnosti, nazalni put primjene intenzivno se istražuje kao vrijedna alternativa sistemskoj primjeni lijekova, posebice onih koji podliježu razgradnji u probavnom sustavu ili ekstenzivnom metabolizmu prvim prolaskom kroz jetru (1). Nadalje, nazalni put primjene pruža i mogućnost izravne dostave lijeka u središnji živčani sustav (2).

1.1. Anatomija i fiziologija nosa i nosne šupljine

1.1.1. Anatomija nosne šupljine

Za provođenje brojnih funkcija nosa zaslužna je njegova složena struktura i aerodinamika. Pojam „nos“ kao funkcionalna jedinica obuhvaća vanjski nos, nosnu šupljinu te paranazalne sinuse (3). Nos se sastoji od lijeve i desne polovice koje su odijeljene nosnom pregradom ili septumom. Vanjski nos smješten je u sredini lica, a građen je od hrskavice te nosne kosti. Korijen nosa predstavlja spoj nosa s čelom, dok se ispupčeni dio naziva vrhom nosa. Nosna hrskavica omeđuje dvije nosnice, lijevu i desnu, između kojih se nalazi prednji dio septuma, odnosno kolumel. Pri udisanju, zrak ulazi kroz nosnice koje se otvaraju prema nosnom vestibulu prekrivenom keratiniziranim višeslojnim pločastim epitelom (3). Na kraju nosnog vestibula nalazi se *limen nasi*. On predstavlja granicu između nosne šupljine i vestibula, a prekriven je nekeratiniziranim višeslojnim pločastim epitelom koji prelazi u pseudovišeslojni cilijarni (trepetljikavi) cilindrični epitel, odnosno respiratorni epitel koji prekriva površinu nosne šupljine (3). Dno nosne šupljine proteže se od nosne valvule, suženja na ulazu u nosnu šupljinu (4), do otvora Eustahijeve cijevi, odnosno do ždrijela (5). S gornje strane nosne šupljine nalazi se krov nosne šupljine, dok bočne stijenke čine nosni septum s medijalne te respiratorna regija s lateralne strane. Septum odjeljuje lijevu i desnu polovicu nosa, a sastoji se od hrskavice te koštanog tkiva kojeg čine okomita ploča rešetnice (lat. *lamina perpendicularis ossis ethmoidales*) i raonik (lat. *vomer*). Lateralna strana nosne šupljine sastoji se od tri ispupčenja koja se nazivaju nosnim školjkama ili turbinama, jer su odgovorne za turbulentno strujanje zraka (6). Sukladno tome, respiratorna regija nosne šupljine često se naziva i turbinatnom regijom (7). Prolazi između nosnih školjki i lateralne stijenke nosne šupljine nazivaju se nosnim hodnicima (5). Većinu prostora nosne šupljine zauzimaju donja i srednja nosna školjka, dok je gornja znatno manja, a smještena je u blizini olfaktorne (njušne) regije kod krova nosne šupljine

(3). Donji nosni hodnik povezan je sa suznim kanalom iz kojeg se slijeva suzna tekućina (3,8). Uz nosnu šupljinu nalaze se i četiri para paranazalnih sinusa, šupljih prostora ispunjenih zrakom koji su omeđeni pripadajućim kostima lubanje (3). U srednjem nosnom hodniku nalaze se otvori čeonog sinusa (lat. *sinus frontales*), sinusa gornje čeljusti (lat. *sinus maxillaris*) te prednji otvor sinusa rešetnice (lat. *cellulae ethmoidales anteriores*), dok se stražnji otvor sinusa rešetnice (lat. *cellulae ethmoidales posteriores*) i otvor sinusa klinaste kosti (lat. *sinus sphenoidalis*) nalaze ispod i iza gornje nosne školjke (3). Unutarnja površina sinusa prekrivena je respiratornim epitelom. Sinusi smanjuju relativnu težinu lubanje, služe kao rezonatori za glas te kao izolatori od brzih promjena temperature u nosnoj šupljini, a imaju ulogu i u imunosnom odgovoru organizma (6,9).

Unutrašnjost nosne šupljine prekriva nosna sluznica koja zauzima površinu od 140 – 172 cm^2, od čega površinu od 2,0 – 2,5 cm^2 zauzima olfaktorna sluznica koja se proteže preko gornje nosne školjke i gornjeg dijela septuma (10). Ostatak površine je respiratorna sluznica koja je građena od cilijarnog epitela. Sluznica nosa vrlo je dobro prokrvljena zahvaljujući prednjoj i stražnjoj etmoidnoj arteriji, ograncima očne arterije te sfenopalatinoj arteriji, ogranku arterije gornje čeljusti koja opskrbljuje krvlju oko 90 % nosne šupljine (11). Ogranci arterija tvore anastomoze s arterijama gornje usne te se tako povezuju s arterijom lica. U području nosnog septuma, sfenopalatina arterija postaje nazopalatina arterija koja se proteže prema usnoj šupljini i stvara splet s velikom arterijom nepca (lat. *arteria palatina major*). U prednjem dijelu septuma, prema vanjskom nosu, nalazi se anastomozni splet prednje i stražnje etmoidne arterije, sfenopalatine arterije, velike arterije nepca i arterije gornje usne nazvan Kiesselbachovim područjem (3,11). Vene koje odvode krv iz nosne šupljine vode prema očnoj veni te veni lica (8).

Nosna šupljina je inervirana trigeminalnim i oftalmičkim živcem te živcem gornje čeljusti koji se grana na prednji etmoidni, infraorbitalni živac i veliki živac nepca. Olfaktorni živac inervira olfaktorno područje te je njime posredovan osjet njuha (3).

1.1.2. Fiziologija nosne šupljine

Nos je početni dio respiratornog trakta. Spada u gornji dio dišnog sustava. Glavne fiziološke funkcije nosa su osjet njuha i kondicioniranje udahnutog zraka, što obuhvaća zagrijavanje udahnutog zraka, zatim njegovo ovlaživanje te djelomično filtriranje većih udahnutih čestica (6).

Fiziološki nazalni ciklus obuhvaća spontano bubrenje (oticanje) nosne sluznice koje se izmjenjuje u dvjema polovicama nosne šupljine u trajanju od 2 do 7 sati, što rezultira trostrukim povećanjem otpora protoku zraka u jednoj od nosnih polovica prilikom disanja kroz nos dok ukupni nazalni otpor protoku zraka ostaje nepromijenjen (3).

Pri protoku zraka pri umjerenom disanju, od oko 30 l min^{-1}, strujanje zraka pri ulasku u nosnice je laminarno, zatim ubrzava u nosnom vestibulu te se zbog suženja poprečnog presjeka koje predstavlja nosna valvula razvija u turbulentno strujanje zraka (12). Na epitelu vanjskog nosa nalaze se dlačice koje zaustavljaju najveće čestice iz udahnutog zraka. Manje čestice zaostaju u nosnoj šupljini zahvaljujući turbulentnom strujanju udahnutog zraka koji udara u brojne prepreke, uključujući nosne školjke, septum te stražnju stijenku ždrijela. Čestice imaju puno veću masu i tromost nego zrak pa ne uspijevaju zaobići navedene prepreke, već ostaju zarobljene u mukoznom sloju na površini sluznice.

Građa sluznice nosa prikazana je na Slici 1. Respiratorna sluznica sastoji se od četiri vrste stanica: cilindričnih stanica s trepetljikama (kinocilijama), cilindričnih stanica s citoplazmatskim izdancima (mikrovilima), vrčastih stanica te bazalnih stanica. Na površini respiratorne sluznice nalazi se sloj sluzi koji može biti debljine od 5 do 15 μm (Slika 1) (13,14). Stanice sluznice koje sadržavaju kinocilije odgovorne su za mukocilijarni mehanizam čišćenja. Cilije se koordinirano kreću i prenose sluz prema ždrijelu, odnoseći tako i eventualne čestice u probavni sustav (6,10). Pokretanje cilija pomiče sluz brzinom od 5 do 6 mm min^{-1} te rezultira uklanjanjem sadržaja s nazalne sluznice i izmjenom sluzi već za 15 do 20 minuta (13,15). Takav mehanizam filtracije je vrlo učinkovit te uklanja gotovo sve čestice promjera većeg od 6 μm (6). Sluz sadrži pretežito vodu (oko 95 %, *m*/*m*), zatim mucine, globularne proteine, soli, lipide, DNA i ostatke stanica te čini gusti, viskoelastični sloj na epitelnim stanicama koji služi kao selektivna barijera za razne molekule, uključujući i molekule nazalno primijenjenog lijeka (14). Jedna od najvažnijih sastavnica sluzi su mucini, polimerni glikoproteini visoke molekulske mase (10 – 40 MDa) koje izlučuju vrčaste stanice i submukozne žlijezde (14). Mucini imaju vlaknastu, četkastu strukturu zbog visokog stupnja glikozilacije te su ključni u obrani dišnog sustava od stranih čestica i patogena. Pri blago kiselom pH nazalne sluznice (5,5 – 6,5), visoki sadržaj sijalinske kiseline i sulfata na mucinima rezultira negativnim površinskim nabojem koji učvršćuje strukturu sluzi zbog odbojnih ionskih sila (14).

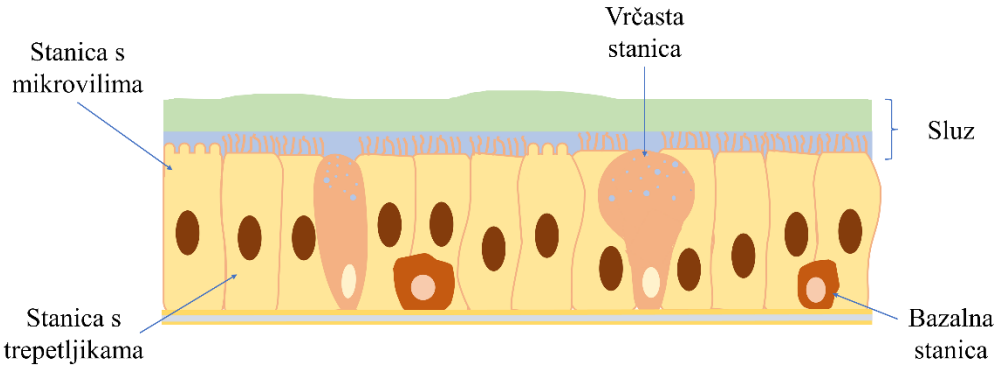

Slika 1. Građa nosne sluznice

Iako je enzimska aktivnost nosne sluznice značajno niža u usporedbi s probavnim sustavom, što je čini pogodnom za primjenu osjetljivih lijekova (15), u nazalnom epitelu ipak su prisutni razgradni enzimi i efluksni prijenosnici (13).

Nazalna sluznica ima važnu ulogu u urođenom i stečenom imunosnom odgovoru organizma (10). U submukozi posteriornog dijela nosne šupljine nalazi se s nazofaringealnom mukozom povezano limfoidno tkivo (engl. *nasopharyngeal mucosa-associated lymphoid tissue*, NALT), nakupina limfoidnog tkiva koja sadrži veliku količinu plazma stanica i limfocita. Na površinu nosne sluznice luče se zaštitna protutijela IgA koja proizvode plazma stanice (16).

Kao što je ranije navedeno, olfaktorni epitel nalazi se u gornjem dijelu nosne šupljine i zaslužan je za osjet njuha, a sastoji se od cilindričnih epitelnih stanica, olfaktornih živčanih stanica (neurona), potpornih stanica, bazalnih stanica i Bowmanovih žlijezda koje proizvode i izlučuju sluz (17). Olfaktorne stanice su nemijelinizirani bipolarni neuroni omeđeni posebnim zaštitnim stanicama (engl. *olfactory ensheating cells*), a proizlaze izravno iz središnjeg živčanog sustava (6,17). Oko sto milijuna olfaktornih stanica raspoređeno je među sustentakularnim stanicama, potpornim stanicama koje iskazuju svojstva epitelnih i neuronskih stanica (18). S mukozne strane olfaktorne stanice imaju olfaktorne cilije (njušne dlačice) koje formiraju gusti pokrov u sluzi te reagiraju na vanjske njušne podražaje, odnosno mirise i stimuliraju olfaktorne neurone, pružajući izravnu vezu središnjeg živčanog sustava s okolinom (6,17). Osim pri vrhu nosne šupljine, otočići njušnog epitela razasuti su i u turbinatnoj regiji (19).

1.2. Patofiziološki poremećaji nosne sluznice

Osim ranije navedenih zaštitnih uloga, stanice nazalnog epitela uključene su i u patogenezu raznih upalnih bolesti dišnog sustava, koje su djelomično posljedica povećane permeabilnosti nosne sluznice. Smanjen integritet čvrstih spojeva, narušen mukocilijarni transport i smanjena proizvodnja antimikrobnih peptida važni su mehanizmi u patofiziologiji nazalnih oboljenja (10).

1.2.1. Epistaksa

Epistaksa je pojam koji označava krvarenje iz nosa i jedan je od najčešćih razloga hitnog prijema u području otorinolaringologije (11). Točna incidencija u populaciji je nepoznata s obzirom da u većini slučajeva krvarenje stane bez potrebe za liječničkom intervencijom. Najčešći izvor epistakse (oko 90 %) je ranije spomenuti Kiesselbachov pleksus (3). Taj splet velike količine krvnih žila nalazi se u području gdje je nazalna sluznica posebno tanka, a zbog blizine nosnici i vanjskom okolišu podložna je oštećenjima uslijed traume, temperaturnih ekstrema i suhoće ili pretjerane vlažnosti (11). Uzroci epistakse mogu se podijeliti na lokalne i sistemske. Lokalni uzroci uključuju traumu lica, umetanje stranog tijela (najčešće kod djece), infekcije, rinosinuitis, nazalnu primjenu lijekova, unošenje zabranjenih tvari kao što je kokain nazalnim putom, zatim strukturne abnormalnosti poput devijacije septuma koja može utjecati na protok zraka, a posljedično i na suhoću nazalne sluznice. Uzroci epistakse mogu biti i jatrogeni, primjerice dijagnostički i operativni otorinolaringološki, maksilofacijalni i oftalmološki zahvati (11). Sistemski uzroci epistakse mogu biti povezani s hematološkim poremećajima, zatajenjem organa, nuspojavama sistemsko primijenjenih lijekova (najčeće antitrombotika), autoimunim bolestima i drugim krvožilnim bolestima (11). Epistaksa je jedna od najčešćih nuspojava korištenja nazalnih kortikosteroida u liječenju alergijskog rinitisa i kroničnog rinosinuitisa (20). Nedavna istraživanja povezuju veću pojavnost epistakse s ipsilateralnom primjenom nazalnog spreja s kortikosteroidom zbog usmjeravanja mlaza prema septumu, odnosno Kiesselbachovom području, što ukazuje na važnost pravilne primjene spreja za nos (21).

Liječenje epistakse najčešće uključuje pritisak na nosnicu, lokalnu primjenu vazokonstriktora i tamponadu nosnice. U primjeni su i kemijska ili elektrokoagulacija, zatim tamponada pomoću komercijalnih nosnih balona te Foley kateter (22,23).

1.2.2. Rinitis

Rinitis je upala nosne sluznice karakterizirana začepljenim nosom (kongestijom) i curenjem nosa. Mogu biti prisutni i simptomi kao što su svrbež nosa, kihanje, anosmija i drugi (24). Podjela rinitisa temeljena je na njegovoj etiologiji, a obuhvaća infekcijski, nealergijski i alergijski rinitis (25). Infekcijski rinitis najčešće je akutna bolest uzrokovana virusom obične prehlade koja prođe bez liječenja, no može se zakomplicirati uslijed sekundarne bakterijske infekcije. Nealergijski rinitis pojam je koji se odnosi na upalu nosne sluznice bez znakova infekcije ili alergijske reakcije. U tu skupinu spadaju rinitis uzrokovan lijekovima, rinitis kod starije populacije, hormonski rinitis uključujući trudnički rinitis, nealergijski profesionalni, okusni te idiopatski rinitis (25,26).

Alergijski rinitis zahvaća 10 – 20 % populacije te je jedna od najčešćih nezaraznih bolesti (25). U podlozi alergijskog rinitisa složena je poveznica između genskih i okolišnih čimbenika (24). Izloženost nazalne sluznice alergenima kao što su pelud, grinje, čestice prašine i drugi iritansi rezultira aktivacijom urođenog i stečenog imunosnog odgovora. Pokreće se stvaranje specifičnih protutijela IgE, aktivacija eozinofila i degranulacija mastocita i bazofila te se posljedično razvijaju klinički simptomi alergijskog rinitisa (24).

Liječenje alergijskog rinitisa temelji se na edukaciji pacijenta o izbjegavanju alergena i iritansa, ispiranju nosne sluznice te lokalnoj i sistemskoj farmakoterapiji i imunoterapiji. U rijetkim slučajevima pribjegava se operativnom zahvatu ili alternativnoj opciji poput akupunkture (24). Farmakoterapija alergijskog rinitisa obuhvaća kratkotrajnu nazalnu primjenu dekongestiva, nazalnu primjenu kortikosteroida te lokalnu i/ili sistemsku primjenu antihistaminika (24,27).

1.2.3. Kronični rinosinuitis i nosna polipoza

Rinosinuitis, odnosno upala sinusa i nosne sluznice, česta je bolest koja u djece najčešće zahvaća etmoidne sinuse, dok je u odraslih zastupljenija upala sinusa gornje čeljusti koja često potječe od upale kutnjaka ili pretkutnjaka (3,28). Akutni rinosinuitis najčešće je posljedica virusne prehlade te prestanak simptoma većinom nastupi i bez farmakoterapije, no moguća je i sekundarna bakterijska infekcija koju je potrebno liječiti antibioticima (29). Osim antibiotika čija je upotreba često neindicirana, terapijske opcije akutnog rinosinuitisa uključuju nazalnu primjenu kortikosteroida, zatim nazalnu ili oralnu primjenu dekongestiva, sistemsku primjenu antihistaminika te primjenu paracetamola ili nesteroidnih protuupalnih lijekova za olakšavanje boli (29). Nefarmakološke mjere liječenja akutnog rinosinuitisa uzrokovanog virusom obične

prehlade obuhvaćaju ispiranje nosne sluznice fiziološkom otopinom, inhaliranje i laganu tjelovježbu (29), dok probiotici, vitamin C, cink i pripravci crvene rudbekije (*Ehinacea purpurea* (L.) Moench) spadaju u dodatke prehrani s mogućim pozitivnim učinkom na simptome akutnog rinosinuitisa. Nijedna od navedenih opcija nema snažne dokaze o učinkovitosti. U slučaju akutnog postviralnog rinosinuitisa, moguća je primjena i sistemskih kortikosteroida (29).

Kronični rinosinuitis zahvaća 5 – 12 % svjetske populacije i značajno smanjuje kvalitetu života pacijenta te predstavlja globalni zdravstveni problem (29). Za dijagnozu rinosinuitisa pomoću subjektivnih simptoma potrebno je postojanje upale nosne sluznice i paranazalnih sinusa uz prisustvo barem još dva simptoma, jedan od kojih mora biti nazalna kongestija ili curenje nosa, uz osjećaj boli ili pritiska u licu i smanjenja osjeta njuha, u trajanju više od 12 tjedana (29). Rinosinuitis može biti dijagnosticiran i prema endoskopskim znakovima nosnih polipa, mukopurulentnog iscjetka primarno iz srednje nosne školjke ili edema sluznice srednje nosne školjke te prema promjenama na sluznici turbinatne regije i/ili na sluznici sinusa, što može biti vidljivo na snimci dobivenoj računalnom tomografijom (engl. *computerized tomography,* CT) (29). Nosni polipi su izrasline nastale kao posljedica hipertrofije srednje nosne školjke proizašle uslijed upalnih procesa sluznice nosa i paranazalnih sinusa (30,31). Brojni čimbenici utječu na razvoj i progresiju polipa, primjerice anatomski poremećaji, genska predispozicija, virusne, bakterijske i gljivične infekcije, zatim astma, alergijski rinitis te nealergijski iritansi (31).

Iako je glavni simptom kroničnog rinosinuitisa i nosne polipoze nazalna opstrukcija, pacijenti kao vodeći simptom koji im narušava kvalitetu života navode hiposmiju ili anosmiju (32). Anosmija (grč. *an-*, odsutan i *-osmē,* miris) je nemogućnost osjećanja mirisa, odnosno gubitak osjeta njuha, dok je hiposmija smanjen osjet njuha (33). Narušavanje osjetila njuha može biti uzrokovano različitim čimbenicima kao što su upala nosne sluznice i sinusa, opstrukcija olfaktorne regije nosnim polipima, oštećenje mozga i olfaktornih vlakana, korištenje raznih lijekova, lokalna trauma, genski poremećaji, starenje i neurodegenerativne bolesti poput Parkinsonove ili Alzheimerove bolesti (33,34). U zadnje vrijeme anosmija je najčešće spomenuta kao simptom bolesti Covid-19, pri čemu je najčešće praćena ageuzijom, odnosno gubitkom osjeta okusa (34).

Nazalna primjena kortikosteroida predstavlja prvu liniju liječenja kroničnog rinosinuitisa i nosne polipoze (29,35–38). Iako su simptomi kroničnog rinosinuitisa bez nosnih polipa blaži,

bez adekvatnog liječenja nastupa pogoršanje upalnog procesa, daljnje zadebljanje sluznice te razvoj polipa (31). U slučaju nedovoljne učinkovitosti terapije lokalnim kortikosteroidima, ostale terapijske opcije uključuju sistemske kortikosteroide, kratkotrajnu i dugotrajnu primjenu antibiotika, zatim primjenu dekongestiva, antihistaminika, antileukotriena, antimikotika te kapsaicina (29,32). U nefarmakološke mjere spadaju ispiranje nosne šupljine fiziološkom ili hipertoničnom otopinom te otopinama mukolitika ili blagih surfaktanata (29). Potreba za primjenom oralnih kortikosteroida u pacijenata s nazalnim polipima pokazuje prostor za poboljšanje učinkovitosti lokalne terapije (39).

1.2.4. Nosna šupljina i Covid-19

Nazalni put primjene odnedavno se intenzivno istražuje kao perspektivni put primjene za prevenciju ili liječenje bolesti Covid-19 uzorkovane virusom SARS-CoV-2 (40–42). Angiotenzin konvertirajući enzim 2, jedan od značajnih receptora za virus SARS-CoV-2, nalazi se u stanicama nazalnog epitela. Posebno velika količina nalazi se u olfaktornom epitelu, što je mogući razlog razvoja hiposmije i anosmije u pacijenata s bolesti Covid-19 (40). Trenutna istraživanja uloge nosne šupljine u borbi protiv bolesti Covid-19 obuhvaćaju razvoj nazalnih cjepiva za prevenciju bolesti, zatim nazalnu primjenu protutijela, dušikovog oksida, lipopeptida koji inhibira fuziju virusne membrane s membranom stanice domaćina, antimikrobnih i/ili mukoadhezivnih polimera koji sprječavaju adheriranje virusa za epitel nazalne sluznice te raznih antimikrobnih i protuupalnih djelatnih tvari koje imaju potencijal olakšavanja ili skraćenja simptoma bolesti, uključujući ivermektin, klorokin, niklozamid, povidon jod, hipokloritnu kiselinu i kortikosteroide (40).

1.3. Kortikosteroidi za nazalnu primjenu

Kortikosteroidi su učinkoviti protuupalni lijekovi. Djelovanje kortikosteroidnih lijekova, odnosno glukokortikoida, ostvaruje se vezanjem na steroidne receptore u citoplazmi stanice (43). Nakon apsorpcije, kortikosteroid u krvi veže se na globulin koji veže kortikosteroide (engl. *corticosteroid-binding globulin,* CBG), od kojeg se odvaja prije ulaska u stanicu pasivnom difuzijom. Unutarstanični steroidni receptor vezan je sa stabilizirajućim proteinima, proteinima toplinskog šoka (engl. *heat shock protein,* Hsp90) te je kao takav neaktivan. Stereospecifično vezanje kortikosteroida na receptor rezultira konformacijskom promjenom receptora, on se odvaja od šaperona Hsp90 te nastaje receptorski dimer koji se premješta u jezgru (43). Kompleks se veže na element odgovora glukokortikoida (engl. *glucocorticoid response element*, GRE) i inhibira transkripciju gena za proupalne, a povećava za protuupalne molekule

te smanjuje migraciju proupalnih stanica (44). Uz njihovu učinkovitost, prilikom sistemske primjene kortikosteroida postoji znatni rizik razvoja blažih, ali i ozbiljnijih nuspojava, kao što su intolerancija glukoze, krhkost kože, atrofija mišića, Cushingov sindrom, osteoporoza i zaostajanje u rastu (44). Stoga je nazalna primjena kortikosteroida prva linija liječenja bolesti nosne sluznice i paranazalnih sinusa koje nastaju kao posljedica upale (29), a nedavno je predložena i kao učinkovita strategija za kontrolu neuroupalnih procesa u bolesnika s teškim oblikom bolesti Covid-19 (45).

Nazalni pripravci kortikosteroida odobreni u Europskoj uniji (EU) vodene su suspenzije za primjenu u obliku kapi ili spreja (46). U pojedinim državama EU odobrena je i otopina natrijevog deksametazonfosfata (47) te jedan praškasti farmaceutski oblik kortikosteroida budezonida za nazalnu primjenu (48).

1.3.1. Flutikazonpropionat

Flutikazon je potentni kortikosteroid druge generacije, za koje su karakteristični netopljivost u vodi, visoki afinitet vezanja i visoka selektivnost za steroidni receptor, zatim visoka potentnost te mala sistemska raspoloživost (27,36,37,44). U pripravcima za nazalnu primjenu dolazi u obliku estera flutikazonfuroata ili flutikazonpropionata (27). U Republici Hrvatskoj (RH) većina nazalnih pripravaka flutikazona sadržava flutikazonpropionat, čija je struktura prikazana na Slici 2 (49–53). Pripravci flutikazonpropionata u obliku spreja za nos u pravilu su u RH odobreni za profilaksu i ublažavanje simptoma sezonskog i cjelogodišnjeg alergijskog rinitisa (49–52), dok su kapi za nos odobrene u liječenju nosnih polipa i povezanih simptoma nosne opstrukcije (53).

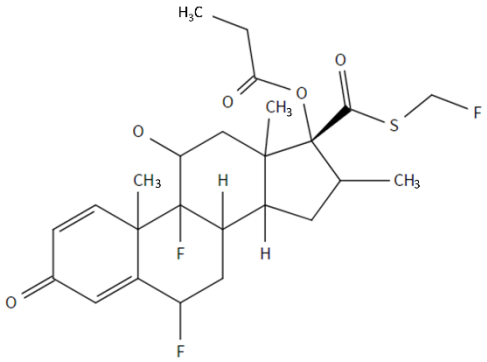

Slika 2. Struktura flutikazonpropionata

1.3.2. Natrijev deksametazonfosfat

Deksametazon je snažan, dugodjelujući kortikosteroidni lijek. Natrijev deksametazonfosfat je esterski prolijek deksametazona. Njegova struktura prikazana je na Slici 3. Topljiv je u vodi, što omogućava njegovo oblikovanje u otopine za parenteralnu i topikalnu primjenu te otopine inhalata (54,55). Na tržištu RH natrijev deksametazonfosfat nalazi se u otopini za injekciju/infuziju, te u kapima i gelu za oko (56). Na njemačkom, američkom i japanskom tržištu postoje pripravci deksametazona za nazalnu primjenu indicirani za liječenje alergijskog rinitisa (46,57), dok je nazalna primjena visokih doza natrijevog deksametazonfosfata ispitivana i u svrhu poboljšanja lokalne terapije kroničnog rinosinuitisa s nosnim polipima (58).

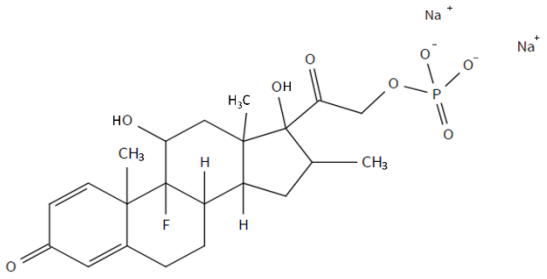

Slika 3. Struktura natrijevog deksametazonfosfata

1.4. Izazovi u nazalnoj primjeni lijekova

Usprkos brojnim prednostima, potencijal nazalne primjene lijekova nije u potpunosti iskorišten. Za djelotvornu nazalnu primjenu lijeka potrebna je njegova dostava u turbinatno područje, odnosno područje iza nosne valvule, te dovoljno dugo zadržavanje na mjestu djelovanja za postizanje učinka (13,59). Izazovi u nazalnoj primjeni lijekova usko su povezani s anatomskim i fiziološkim značajkama nosne šupljine, o kojima ovisi depozicija lijeka u ciljnoj regiji (19,60,61).

Jedan od glavnih ograničavajućih čimbenika u ciljanoj dostavi lijeka u nosnu šupljinu vezan je uz nosnu valvulu. Ona limitira pristup nosnoj šupljini te ograničava dostupnost primijenjene doze lijeka za djelovanje (60). Tijekom udisanja, s povećanjem protoka zraka, nosna valvula se sužava. Prilikom izdisaja, nosna valvula usporava protok zraka i produljuje trajanje izdisaja, što daje dovoljno vremena za izmjenu plinova u alveolama pluća te za zadržavanje tekućine i topline iz toplog, zasićenog zraka koji se izdiše (19,62). Mala površina

nosne valvule, njezin oblik te dodatno sužavanje prilikom udaha predstavljaju značajne prepreke za učinkovitu dostavu lijeka u nos (19).

Značajne poteškoće u nazalnoj dostavi lijekova proizlaze i iz fiziološke funkcije mukocilijarnog mehanzima čišćenja. Iako je prvenstveno namijenjen uklanjanju štetnih tvari, mukocilijarni klirens uklanja i nazalno primijenjeni lijek u vrlo kratkom vremenu te tako onemogućuje dulji kontakt lijeka i nazalnog epitela te ograničava lokalni i/ili sistemski učinak lijeka (13). Iz tog razloga je u središtu istraživanja razvoj mukoadhezivnih formulacija za nazalnu primjenu koje omogućuju produljeno zadržavanje lijeka na mjestu primjene, a bez pretjeranog narušavanja fiziološke funkcije cilija (63).

Protok zraka također utječe na depoziciju lijeka u nosnoj šupljini. Stoga se prilikom razvoja nazalnog lijeka i uređaja za nazalnu dostavu lijeka može uzeti u obzir i nazalni ciklus koji utječe na dinamiku i protok zraka u području nosne valvule (19).

1.5. Inovativni farmaceutski oblici za nazalnu primjenu

S ciljem nadilaženja navedenih ograničenja nazalne primjene, razvijaju se inovativni farmaceutski oblici čija je svrha osigurati ciljanu dostavu lijeka u područje od interesa, dulje zadržavanje na mjestu primjene te prilagođeno oslobađanje djelatne tvari, smanjujući tako učestalost primjene i/ili varijabilnost terapijskog ishoda (64).

1.5.1. Tekući in situ gelirajući oblici

Postoje razni načini poboljšavanja zadržavanja formulacije na mjestu primjene, jedan od kojih je razvoj *in situ* gelirajućih sustava. To su najčešće polimerne otopine koje pod utjecajem nekog od fizioloških čimbenika pri dodiru sa sluznicom ili kožom stvaraju umreženu strukturu, odnosno formiraju gel. Gelirani sustav osigurava dulji kontakt sa sluznicom ili kožom te prikladni profil oslobađanja lijeka (63). Fiziološki čimbenici koji potiču stvaranje gela mogu biti odgovarajuća koncentracija iona, temperatura ili pH (64). Polimeri izbora za razvoj *in situ* gelirajućih sustava najčešće su prirodni biokompatibilni polimeri, kao što su pektin, gelan guma, poloksamer, a kombiniraju se s natrijevim hijaluronatom, kitozanom, hipromelozom i drugim polimerima, koji redom pokazuju mukoadhezivna svojstva (63,65). *In situ* gelirajući sustavi primjenjuju se kao otopine, osiguravajući točnost primijenjene doze, a nakon kontakta s ciljnim mjestom stvaraju gel osiguravajući produljeno zadržavanje, kontrolirano oslobađanje te poboljšanu raspoloživost na mjestu primjene (63,66). Pomoću takvih sustava moguće je

postići i lokalni i sistemski učinak lijeka, a korisni su i kao nosači za nano- i mikroterapijske sustave (67).

Geliranje potaknuto promjenom temperature

Za sustave koji geliraju ovisno o temperaturi poželjno je da temperatura geliranja bude u rasponu od 25 do 37 °C, ovisno o ciljnom putu primjene (68,69). Najčešće korišteni termoosjetljivi polimeri su poloksameri. Ovisno o koncentraciji polimera i temperaturi, stvaraju se micele koje se orijentiraju ovisno o interakciji desolvatiranih polimernih lanaca. Geliranje potaknuto promjenom temperature, osim poloksamera, iskazuju i prirodni polimeri kao što su ksiloglukani i kitozani, ali i sintetski derivati prirodnih polimera kao što je, primjerice, trimetilkitozan (63).

Geliranje potaknuto prisustvom iona

Mehanizam geliranja potaknutog prisustvom iona uključuje ionsku interakciju negativno nabijenih polimernih lanaca s kationima, pogotovo ionima kalcija, koja uzrokuje stvaranje uređene trodimenzionalne mreže koja čini strukturu gela (63). Najčešće korišteni polimeri u farmaceutskoj tehnologiji s takvim mehanizmom geliranja su anionski polisaharidi iz prirodnih izvora, primjerice pektin, gelan guma, alginat i ksantan guma (67). Pektin i alginat u kontaktu s ionima kalcija tvore strukturu nalik na kutiju jaja (engl. *egg box model*) (68).

Geliranje potaknuto promjenom pH

Sustavi koji geliraju ovisno o pH medija najčešće su slabe kiseline koje pri povećanoj pH vrijednosti otpuštaju vodikov ion. Time najstaje veliki broj negativno nabijenih karboksilnih skupina na polimernom lancu koje se međusobno odbijaju uzrokujući strukturiranje polimernih lanaca u trodimenzionalnu strukturu gela (70). Takvi polimeri su polimeri poliakrilne kiseline (karbopoli) te aminopolisaharid kitozan (70).

U razvoju *in situ* gelirajućih sustava za nazalnu primjenu najčešće se koriste polimeri koji geliraju pod utjecajem temperature ili u prisustvu iona (63). U Europskoj uniji odobren je *in situ* gelirajući tekući oblik opioidnog analgetika fentanila za nazalnu primjenu (PecFent®), temeljen na pektinu (71).

1.5.2. Praškasti sustavi za nazalnu primjenu

Novija istraživanja usmjerena su na razvoj praškastih farmaceutskih oblika za nazalnu primjenu (72). Praškasti sustavi osiguravaju veću kemijsku i mikrobiološku stabilnost od

tekućih oblika te omogućuju uklapanje veće doze lijeka (73). Iako postoji mogućnost izravne nazalne primjene same djelatne tvari, većinom ju je potrebno formulirati u farmaceutski oblik koji uključuje i pomoćne tvari. Kao i kod tekućih *in situ* gelirajućih sustava za nazalnu primjenu, i u razvoju praškastih sustava većinom se koriste *in situ* gelirajući i/ili mukoadhezivni polimeri koji pri kontaktu s nosnom sluznicom bubre stvarajući gelastu strukturu koja osigurava dulje zadržavanje i prilagođeno oslobađanje lijeka na mjestu primjene (72). Također, razvijaju se i praškasti sustavi koji uključuju fizičko miješanje djelatne tvari s punilom kao što su vodotopljive tvari poput laktoze, manitola, sorbitola, ali i netopljivi prašci poput kalcijevog karbonata, talka te barijevog sulfata (72). Najčešće korišteni polimeri u izradi praškastih sustava za nazalnu primjenu su kitozan, pektin, hipromeloza i natrijev hijaluronat (72,74–76). Uz navedene sustave, istražuju se i polimerni praškasti sustavi s uklopljenom djelatnom tvari koji se pomoću mješača prašaka miješaju s inertnim nosačima (77).

1.5.2.1. Sušenje raspršivanjem

Jedna od najčešće korištenih metoda priprave praškastih sustava za nazalnu primjenu je metoda sušenja raspršivanjem (72). Sušenje raspršivanjem metoda je uklanjanja disperzijskog sredstva iz tekućeg uzorka s ciljem priprave suhih čestica točno određenih svojstava (78). Radi se o procesu koji se odvija u jednom koraku te je jednostavan za prijenos iz laboratorijskog u industrijsko mjerilo (79). Uzorak za sušenje raspršivanjem može biti otopina, suspenzija ili emulzija (80,81). Uređaj za sušenje raspršivanjem sastoji se od sapnice, komore za sušenje, posude za sakupljanje tekućeg uzorka u slučaju curenja, ciklona, posude za sakupljanje suhog produkta i odvodne cijevi za medij za sušenje (najčešće zrak ili dušik) (Slika 4). Uzorak se peristaltičkom pumpom dovodi do sapnice gdje se, ovisno o vrsti sapnice, pod utjecajem visokog tlaka, ultrazvuka, centrifugalne sile ili kinetičke energije, tekući uzorak raspršuje u sitne kapljice koje se suše u dodiru sa zagrijanim medijem za sušenje (79). Ovisno o tipu otapala (disperzijskog sredstva), sušenje raspršivanjem može se provoditi u otvorenom (engl. *open loop*) i zatvorenom (engl. *closed loop*) sustavu. Sušenje u otvorenom sustavu koristi se kada se suši uzorak koji sadrži vodu, a kao medij za sušenje najčešće se koristi atmosferski zrak. Zatvoreni sustav, s ukapljivačem uklonjenog otapala, upotrebljava se za rad u aseptičkim uvjetima te pri sušenju uzoraka koji sadrže organska otapala. Za sušenje takvih sustava se umjesto zraka često koristi inertni plin poput dušika kako bi se smanjio rizik od eksplozije organskog otapala pri visokim temperaturama (78). Osušene kapljice, odnosno suhe čestice povučene podtlakom aspiratora spojenog na odvodnu cijev za medij za sušenje, odlaze u ciklon gdje se odvajaju od medija za sušenje te se nakupljaju u posudi za sakupljanje suhog produkta

(78). Čimbenici koji utječu na svojstva produkta u procesu sušenja raspršivanjem mogu se svrstati u formulacijske i procesne parametre. Formulacijski parametri podrazumijevaju svojstva tekućeg uzorka za sušenje, a uključuju vrstu i koncentraciju dispergiranih tvari te vrstu korištenog otapala. Procesni parametri vezani su uz izvedbu samog uređaja za sušenje raspršivanjem, a uključuju protok uzorka, energiju atomizacije, protok medija za sušenje i ulaznu temperaturu (78). Variranjem navedenih parametara moguće je utjecati na iskorištenje procesa, građu, morfologiju i površinska svojstva čestica, raspodjelu veličine čestica i sadržaj vlage (82), što sve može utjecati na svojstva raspršivanja praška bitna za nazalnu primjenu (72). Zbog velikog broja parametara koji utječu na svojstva produkta, u istraživanjima se koristi statistički dizajn eksperimenta za optimiranje procesa sušenja, a s obzirom na svojstva čestica suhog produkta (83–85).

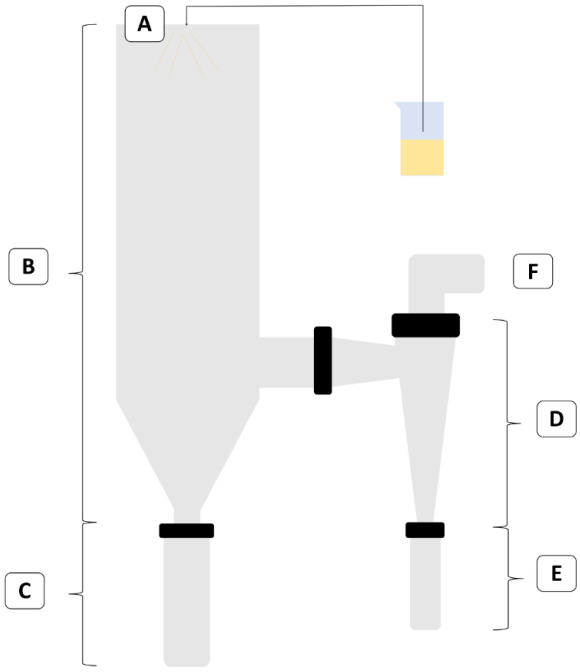

Slika 4. Shema uređaja za sušenje raspršivanjem. Na slici su prikazani: sapnica (A), komora za sušenje (B), posuda za sakupljanje tekućeg uzorka u slučaju curenja (C), ciklon (D), posuda za sakupljanje produkta (E) i odvodna cijev za medij za sušenje (F).

1.5.3. Nanokristali

Nanonizacija, odnosno usitnjavanje čestica do nanometarskog raspona dimenzija posljednjih je godina često upotrebljavana tehnika u oblikovanju djelatnih tvari teško topljivih u vodi (86). Pripravom nanokristala povećava se specifična površina čestica, što prema Noyes-Whitneyevoj jednadžbi znači i veću brzinu otapanja (87), a može rezultirati i većom topljivošću (88).

Navedene promjene mogu omogućiti povećanje (bio)raspoloživosti djelatne tvari, uklanjanje učinka hrane na bioraspoloživost pri oralnoj primjeni te posljedično smanjenje terapijske doze i bolji sigurnosni profil lijeka (86). Iako se nanokristali većinom pripravljaju s ciljem povećanja sistemske raspoloživosti lijekova, mogu biti korisni i u optimiranju lokalne nazalne terapije, omogućujući smanjenje primijenjene doze i/ili bolju mukoadhezivnost, posebice u kombinaciji s prikladnim polimerima (89,90).

Metode izrade nanokristala dijele se na metode smanjenja veličine čestica (engl. *top-down methods*), u kojima se krutina većih dimenzija usitnjava na nanometarski raspon dimenzija (primjerice mljevenjem), i na metode povećanja veličine čestica (engl. *bottom-up methods*), gdje je tvar otopljena u prikladnom otapalu, a povećanje do nanometarske veličine postiže se taloženjem, najčešće uz antiotapalo (91,92). Metode smanjenja veličine čestica uključuju vlažno mljevenje (engl. *wet media milling*) koje može biti nisko- i visokoenergetsko, zatim metodu visokotlačne homogenizacije te kombinirane postupke (92).

1.5.3.1. *Metoda vlažnog mljevenja*

Priprava nanokristala slabo topljivih djelatnih tvari metodom vlažnog mljevenja značajno je zastupljena u farmaceutskoj tehnologiji (93). Postupak niskoenergetskog vlažnog mljevenja moguće je provesti u laboratorijskom mjerilu. U grubu disperziju djelatne tvari s jednom ili više stabilizirajućih tvari dodaju se kuglice za mljevenje te magnetski mješači. Kao kuglice za mljevenje najčešće se koriste kuglice od polistirena ili itrijem stabiliziranog cirkonijevog oksida (91). Čestice u disperziji izložene su smičnom naprezanju uslijed kojeg se veće čestice „razbijaju“ na manje i tako usitnjavaju do nanometarskog raspona veličina (91).

1.6. Svojstva *in situ* gelirajućih farmaceutskih oblika za nazalnu primjenu

Najprihvatljiviji nazalni farmaceutski oblik s obzirom na jednostavnost rukovanja i primjene je sprej za nos, koji može biti tekući i praškasti. Na učinkovitost dostave nazalno primijenjenog lijeka u ciljnu regiju pomoću spreja utječu reološka svojstva, veličina raspršenih kapljica/čestica i kut raspršenja formulacije (94) te profil oslobađanja djelatne tvari.

1.6.1. Reološka svojstva tekućih in situ gelirajućih sustava

U razvoju tekućih *in situ* gelirajućih sustava za nazalnu primjenu nužno je provesti temeljitu reološku karakterizaciju, što obuhvaća rotacijske i oscilacijske reološke testove kojima se određuje ponašanje sustava u ovisnosti o reološkim parametrima, prije i nakon geliranja. Rotacijskim testovima određuje se viskoznost pri mirovanju i u ovisnosti o brzini smicanja, dok

oscilacijski testovi služe za promatranje ponašanja viskoelastičnih modula u ovisnosti o smičnoj deformaciji, kutnoj frekvenciji te vremenu ili temperaturi (95).

1.6.1.1. *Viskoznost*

Povećanje viskoznosti pripravaka te razvoj *in situ* gelirajućih sustava za nazalnu primjenu prepoznati su kao formulacijski pristupi za postizanje produljenog zadržavanja lijeka na nosnoj sluznici jer otežavaju kretanje cilija (90,96–98). Za formulacije koje se primjenjuju u obliku spreja bitno je iskazivanje pseudoplastičnog ponašanja (engl. *shear thinning behaviour*), odnosno smanjenje viskoznosti porastom brzine smicanja (99). Poželjno je da su takvi sustavi tiksotropni, odnosno da im se s porastom brzine smicanja narušava struktura i posljedično smanjuje viskoznost, dok se prilikom naknadnog smanjenja brzine smicanja sustav restrukturira, uz posljedično povećanje viskoznosti (100). Brzina smicanja prilikom raspršivanja iz nazalne sprej pumpice iznosi oko 10^5 s^{-1} (95), što omogućuje primjenu tiksotropnih sustava veće viskoznosti, uzimajući u obzir da im se prilikom raspršivanja viskoznost smanji te se vrati na početnu nakon depozicije u nosnoj šupljini (100).

1.6.1.2. *Viskoelastičnost sustava*

Tekući *in situ* gelirajući sustavi spadaju u viskoelastične sustave. To su sustavi koji iskazuju komponente viskoznog i elastičnog ponašanja, odnosno imaju svojstva idealno viskoznih (Newtonovih) tekućina i idealno elastičnih tijela (95). Reološko ponašanje viskoelastičnih sustava opisuje se viskoznim i elastičnim modulom. Elastični modul, ili modul pohrane (G'), prikazuje elastičnu komponentu sustava, odnosno težnju sustava da se ponaša kao krutina, dok viskozni modul, ili modul gubitka (G''), opisuje viskoznu komponentu sustava, odnosno njegovo ponašanje kao tekućine (95). Omjer modula gubitka i modula pohrane (G''/G') naziva se faktorom gubitka, tan δ. Ukoliko je modul pohrane veći od modula gubitka (tan $\delta < 1$), radi se o viskoelastičnoj krutini koja se najčešće naziva gelom, dok je u suprotnom slučaju (tan $\delta > 1$) riječ o viskoelastičnoj tekućini (95). Prema Winteru i Chambonu, točka geliranja je trenutak ili temperatura pri kojima se krivulje faktora gubitka pri različitim kutnim frekvencijama sijeku, odnosno točka u kojoj je faktor gubitka neovisan o frekvenciji (101), no u literaturi se kao indikator točke geliranja često uzima sjecište krivulja na grafu ovisnosti modula pohrane i gubitka o vremenu ili temperaturi (95,102–104).

1.6.1.3. *Linearno viskoelastično područje*

Linearno viskoelastično područje (engl. *linear viscoelastic range,* LVE) je raspon smičnih deformacija, odnosno amplituda, pod utjecajem kojih se struktura uzorka ne narušava, odnosno

nema promjena modula pohrane i gubitka (105). Određuje se pomoću reometra testom promjene amplitude, gdje sustav oscilira sve većim amplitudama, pri konstantnoj kutnoj frekvenciji (95). Sva ostala oscilacijska reološka mjerenja potrebno je izvoditi pri amplitudi iz LVE područja. Primjerice, promatranje modula pohrane i gubitka u ovisnosti o kutnoj frekvenciji vrši se pri konstantnoj amplitudi (95). Test promjene frekvencije daje informaciju o kratkoročnoj i dugoročnoj stabilnosti viskoelastičnog sustava (95).

1.6.1.4. *Vrijeme geliranja*

Za *in situ* gelirajuće sustave koji se umrežavaju u trodimenzionalnu strukturu pod utjecajem iona, važno je odrediti vrijeme geliranja. Poželjno je da ono bude što kraće, odnosno da sustav gelira odmah nakon kontakta sa stimulansom, primjerice ionima kalcija na nosnoj sluznici (63). Određivanje vremena geliranja *in situ* gelirajućih sustava provodi se oscilacijskim testom vremena geliranja pomoću reometra. Prati se ovisnost modula pohrane i gubitka, faktora gubitka i kompleksne viskoznosti o vremenu pri konstantnoj smičnoj deformaciji (iz LVE područja) te konstantnoj kutnoj frekvenciji i temperaturi. U opisanom testu, točku geliranja predstavlja sjecište krivulja na grafu ovisnosti modula pohrane i gubitka o vremenu (95).

1.6.2. Reološka svojstva praškastih sustava

U razvoju praškastih sustava za nazalnu primjenu iznimno su važna njihova reološka svojstva odnosno svojstva tečenja. Ona ovise o veličini čestica, gustoći tvari, obliku i površinskim svojstvima čestica praška (106). Određivanje svojstava tečenja prašaka uključuje određivanje nasipne gustoće prije i nakon protresivanja, iz čega se računaju Hausnerov omjer i Carrov indeks (indeks kompresibilnosti), zatim određivanje brzine istjecanja kroz otvor i nasipnog kuta (sipkosti) te reološka mjerenja pomoću smične ćelije za praške (engl. *powder shear* cell) na reometru (107). Za navedena svojstva (osim metode sa smičnom ćelijom za praške) Europska farmakopeja klasificira raspon vrijednosti i prema tome karakterizira prašak s obzirom na svojstva tečenja od praška vrlo, vrlo lošeg tečenja do praška izvrsnog tečenja (Ph. Eur. 10). Polimerne mikrosfere pripravljene sušenjem raspršivanjem često imaju nepovoljna svojstva tečenja (107). Nadvladavanje tog problema postiže se miješanjem mikosfera s (inertnim) nosačem odgovarajućih svojstava tečenja i adsorptivnog kapaciteta (108).

1.6.3. Veličina raspršenih kapljica/čestica

Veličina raspršenih kapljica/čestica jedno je od ključnih svojstava nazalnih sprejeva s utjecajem na depoziciju u nosnoj šupljini. Prema smjernicama Europske agencije za lijekove (engl. *European Medicines Agency*, EMA), karakterizacija nazalnih sprejeva mora uključivati

određivanje raspodjele veličine raspršenih kapljica ili čestica. Prikladnom raspodjelom veličina čestica za nazalnu primjenu smatra se ona pri kojoj glavnina čestica ima promjer veći od 10 μm, čime se osigurava njihova depozicija unutar nosne šupljine (94). U slučaju praškastih farmaceutskih oblika promjera čestica manjeg od 10 μm, navedeni zahtjev može se ispuniti uslijed kohezije manjih čestica ili adhezije manjih čestica na čestice inertnog nosača odgovarajuće veličine (72), kao što je spomenuto u poglavlju *1.5.2. Praškasti sustavi za nazalnu primjenu*. Praškaste čestice promjera 10 do 50 μm smatraju se optimalnima za nazalnu primjenu (72,106). Najkorištenija metoda analize veličine raspršenih kapljica i veličine čestica je metoda laserske difrakcije (109).

1.6.4. Oblik i geometrija raspršenog oblaka

Oblik (engl. *spray pattern*) i geometrija raspršenog oblaka također su značajke nazalnog spreja od iznimne važnosti za njegovu usmjerenu dostavu i učinkovitost (110). Oblik raspršenog oblaka karakteriziraju najmanji (D_{min}) i najveći (D_{max}) promjer oblaka, zatim njegova ovalnost (D_{max}/D_{min}) te površina, dok je geometrija oblaka karakterizirana kutom raspršenja i širinom raspršenog oblaka (111,112). Oblik i geometrija raspršenog oblaka ovise o svojstvima formulacije, uređaju za nazalnu dostavu lijeka te o parametrima primjene (60,110). Kut raspršenja prepoznat je kao parametar s izraženim utjecajem na depoziciju formulacije u nosnoj šupljini; većinom sa smanjenjem kuta raspršenja raste udio lijeka koji dospije do turbinatne regije, odnosno prođe nosnu valvulu (112). Uži kut raspršenja imaju tekući sustavi veće viskoznosti (110). Međutim, preuski kut raspršenja može izazvati nelagodu prilikom primjene (61). Određivanje kuta raspršenja i geometrije raspršenog oblaka uključuje tehnike velike brzine snimanja raspršenog oblaka (engl. *high-speed imaging*) i tehnike velike brzine snimanja raspršenog oblaka laserom (engl. *high-speed laser imaging*) te naknadnu analizu slike (110).

1.6.5. Oslobađanje lijeka in vitro

Određivanje profila oslobađanja djelatne tvari preduvjet je za predviđanje potencijala razvijanih *in situ* gelirajućih sustava za nazalnu primjenu. Gelirani polimerni matriks može osigurati produljeno ili odgođeno oslobađanje lijeka, ovisno o željenom učinku i mjestu dostave (63). Kinetika oslobađanja ovisi i o topljivosti uklopljenog lijeka u vodi, s obzirom na ograničeni volumen nosnog fluida koji prekriva sluznicu. Produljeno oslobađanje lijeka u kombinaciji s mukoadhezivnošću i produljenim zadržavanjem farmaceutskog oblika na nosnoj sluznici pružaju potencijal poboljšane raspoloživosti lijeka na mjestu učinka. Najčešće

korištena aparatura za ispitivanje oslobađanja lijeka iz in situ gelirajućih tekućih i praškastih sustava je Franzova difuzijska ćelija koja se sastoji od donorskog i receptorskog odjeljka koji su odijeljeni polupropusnom membranom (113,114). Uzorak se nanosi na površinu membrane te je putem nje u kontaktu s prikladnim medijem za oslobađanje djelatne tvari (115).

1.6.6. Biofarmaceutska karakterizacija in situ gelirajućih farmaceutskih oblika za nazalnu primjenu

Usmjereni razvoj tekućih i praškastih *in situ* gelirajućih sustava za nazalnu primjenu uključuje i ispitivanje biokompatibilnosti, permeabilnosti i mukoadhezivnosti korištenjem relevantnih modela biološke barijere od interesa (116).

Calu-3 stanice izolirane su iz adenokarcinoma pluća čovjeka. Prema fenotipu, dijele se na stanice koje izlučuju sluz i stanice s cilijarnim kretanjem (117). Stoga Calu-3 stanična linija predstavlja široko korišteni i prikladni model respiratornog epitela u ispitivanju biokompatibilnosti nazalnih farmaceutskih oblika te permeacije uklopljenog lijeka (116). Pokazana je i dobra korelacija između permeacije lijeka kroz Calu-3 stanični monosloj i rezultata farmakokinetičkih ispitivanja *in vivo*, potvrđujući prikladnost Calu-3 stanične linije kao modela epitela nazalne sluznice u procjeni permeacije lijeka iz različitih farmaceutskih oblika (otopine, suspenzije) nakon nazalne primjene (118).

Nazalna sluznica svinje, zbog fiziološke i histološke sličnosti s ljudskom sluznicom, odgovarajući je model za ispitivanje mukoadhezivnosti nazalnih farmaceutskih oblika (119,120).

1.7. Ispitivanja depozicije lijeka u nosnoj šupljini

Depozicija *in situ* gelirajućih tekućih i praškastih farmaceutskih oblika u nosnoj šupljini od ključnog je značaja za terapijski ishod. Usprkos tome, ispitivanje nazalne depozicije samo je u nekoliko studija uključeno u razvoj farmaceutskog oblika za nazalnu primjenu (121–123). Na profil depozicije u nosnoj šupljini mogu utjecati formulacijski i procesni parametri u izradi farmaceutskog oblika (72,112) te parametri primjene (60).

Formulacijski parametri

Kao što je ranije navedeno, vrsta i koncentracija djelatne(ih) i pomoćnih tvari (primjerice biokompatibilnih i mukoadhezivnih polimera) te korištena otapala u tekućem sustavu formulacijski su parametri koji utječu na viskoznost, površinsku napetost, kut raspršenja i

veličinu raspršenih kapljica, zatim i na depoziciju u nosnoj šupljini te profil oslobađanja lijeka (110). Viskoznost sustava može se prilagoditi dodatkom različitih polimera prikladnih za nazalnu primjenu, primjerice mukoadhezivnih i/ili *in situ* gelirajućih polimera poput kitozana, hipromeloze, pektina i gelan gume te polimera s biološkim učinkom na samu sluznicu, poput natrijevog hijaluronata (63). U slučaju praškastih sustava, odabir pomoćnih tvari i otapala utječe na svojstva sušene otopine/disperzije koja pak utječu na svojstva suhog produkta kao što su uspješnost uklapanja djelatne tvari te veličina, morfologija i površinska svojstva mikrosfera. Omjer sastavnica utječe na kohezivnost/adhezivnost samog praška, a time i na njegovo ponašanje prilikom primjene (77). Odabir i koncentracija sastavnica *in situ* gelirajućih sustava parametri su koji definiraju biokompatibilnost formulacije te njen utjecaj na permeaciju uklopljene djelatne tvari preko biološke barijere.

Procesni parametri

U slučaju složene priprave nazalnih farmaceutskih oblika, sam proces utječe na njihova konačna svojstva pa posljedično i na nazalnu depoziciju. Sušenje raspršivanjem primjer je takvog procesa. Naime, promjena parametara sušenja može značajno utjecati na svojstva čestica suhog produkta, a time i na profil depozicije te ponašanje u kontaktu s nosnom sluznicom (122). Procesni i formulacijski parametri te njihovi utjecaji na svojstva suhog produkta prikazani su u Tablici 1. Kod priprave nanokristala vlažnim mljevenjem, dimenzije kuglica za mljevenje, omjeri kuglica različitih veličina, omjer kuglica i uzorka za mljevenje te trajanje i brzina miješanja neki su od parametara koji utječu na svojstva produkta (92).

Tablica 1. Utjecaj formulacijskih i procesnih parametara na svojstva čestica pripravljenih metodom sušenja raspršivanjem

Svojstvo čestica	**Procesni parametri**			**Formulacijski parametri**	
	Protok uzorka ↑	Protok medija za sušenje ↑	Ulazna temperatura ↑	Koncentracija dispergiranih tvari ↑	Udio organskog otapala ↑
Iskorištenje procesa	↑↓ (ovisi)	↑	↑	↑	↑
Sadržaj vlage (ostatnog otapala)	↑	↑	↓	↓	-
Veličina čestica	↑	-	↑	↑	↑

Parametri primjene

Način primjene farmaceutskog oblika značajno utječe na njegovu depoziciju u nosnoj šupljini (60,77). U novije vrijeme brojna istraživanja su usmjerena na ispitivanje utjecaja različitih parametara primjene na profil nazalne depozicije (60,77,110,112,124). Najčešće ispitivani parametri nazalne primjene lijeka su kut primjene u odnosu na horizontalnu ravninu, kut primjene u odnosu na vertikalnu ravninu, odnosno septum i protok udahnutog zraka (60).

Ključni čimbenik u određivanju parametara nazalne primjene lijeka je njegov željeni učinak, odnosno ciljna regija u nosnoj šupljini. Lijekove koji trebaju djelovati lokalno ili se apsorbirati sistemski potrebno je dostaviti u respiratorno, odnosno turbinatno područje nosne šupljine, dok je za izravnu dostavu lijeka u središnji živčani sustav, odnosno mozak, potrebno ciljati olfaktornu regiju (125). Ovisno o ciljanoj regiji i vrsti farmaceutskog oblika, optimalni parametri primjene lijeka u nos mogu varirati. Primjerice, uočeno je da se učinkovitija dostava tekućih sustava u turbinatnu regiju može postići primjenom nazalnog spreja pri manjim kutovima u odnosu na horizontalnu ravninu (npr. kut od 30 °; (126)), dok su za iste sustave pri ciljanju olfaktorne regije bolji veći kutovi primjene u odnosu na horizontalnu ravninu (npr. kut od 75 °) (127). Ipak, nazalna primjena praška već pri kutu od 45 ° može rezultirati znatnom depozicijom u olfaktornoj regiji (74).

Važnost pravilne primjene nazalnog pripravka razvidna je i iz uputa o lijeku sprejeva za nos s kortikosteroidima prisutnih na tržištu RH, gdje su navedene precizne upute kako primijeniti

sprej. Za lijekove Tafen® (budezonid) i Avamys™ (flutikazonfuroat) u Uputi o lijeku navedeno je da je potrebno sprej pumpicu usmjeriti prema lateralnoj stijenki nosne šupljine, odnosno od septuma (128,129). Takva primjena nazalnog spreja može biti učinkovita ne samo zbog preciznijeg ciljanja respiratornog područja nosne šupljine, već i zbog izbjegavanja dostave lijeka u Kiesselbachovo područje te smanjenja pojavnosti epistakse (29). Protok udahnutog zraka također može povoljno utjecati na depoziciju u nosnoj šupljini, ovisno o primijenjenom farmaceutskom obliku (110,130). Za sve kortikosteroidne nazalne sprejeve navedeno je da se primjenjuju uz udah, a većina sadrži i uputu o zatvaranju druge nosnice te o položaju glave koja mora biti lagano nagnuta prema naprijed (49–52,128,129,131–135). Ipak, dio istraživanja pokazuje izostanak utjecaja protoka zraka na nazalnu depoziciju (110,126,136), a u literaturi je opisano i smanjenje frakcije lijeka dostavljene u turbinatno i/ili olfaktorno područje pri primjeni nazalnog spreja uz simulaciju udaha, što je posebice pokazano kod praškastih sustava za nazalnu primjenu (76,77).

Osim navedenih parametara koji utječu na depoziciju, veliki utjecaj na ishod liječenja čine interindividualne razlike u nazalnoj anatomiji i fiziologiji (59,60). Navedeni izazovi jasan su pokazatelj da je razmatranje depozicije farmaceutskog oblika u nosnoj šupljini potrebno uvrstiti u rane faze razvoja.

1.7.1. Metode ispitivanja nazalne depozicije lijeka

Razvoj metoda za određivanje nazalne depozicije lijeka iznimno je zahtjevan i složen proces. U novijim istraživanjima zastupljeni su komercijalno dostupni modeli nosne šupljine, 3D printani modeli nosne šupljine izrađeni prema CT snimkama glave pacijenta te tehnike računalne simulacije dinamike fluida (engl. *computational fluid dinamics*, CFD) (125). Od komercijalno dostupnih modela, u istraživanjima su najzastupljeniji transparentni silikonski model Koken (Koken Co. Ltd., Japan) (112,121,123,130,137,138) i model Bespak (139–141). 3D printani modeli nosne šupljine najčešće se izrađuju iz više dijelova koji odgovaraju anatomskim segmentima nosne šupljine (60,110,127). Tehnika 3D printanja omogućava razvoj modela nosne šupljine sa specifičnim značajkama, ovisno namjeni i planiranim ispitivanjima. Primjerice, tehnika 3D printanja omogućava odabir materijala za izradu modela nosne šupljine pa tako gotovo cijeli model može biti transparentan i rigidan, dok se sam vanjski nos može izraditi iz mekšeg materijala koji omogućava manipulaciju pumpicom spreja te vjernije simulira stvarnu situaciju.

S ciljem simulacije protoka zraka, odnosno fiziološkog disanja, koriste se vakuum pumpe s mogućom prilagodbom protoka zraka (60,110,126,127,142) te respiratorna pumpa koje omogućuje relevantniju simulaciju disanja nudeći mogućnost prilagodbe volumena udahnutog zraka, omjera udaha i izdaha te frekvencije, odnosno broja udaha po minuti (76,112,136).

1.8. Dizajn eksperimenta u razvoju farmaceutskih oblika za nazalnu primjenu

Uzevši u obzir velik broj čimbenika koje treba razmatrati pri razvoju novog farmaceutskog oblika, a s ciljem smanjenja troškova i poboljšanja učinkovitosti, u takva istraživanja sve više se uvodi statistički dizajn eksperimenta (engl. *Design of Experiments,* DoE). Njime se postiže kakvoća utemeljena kroz dizajn (engl. *Quality by Design*, QbD), definirana kao sustavni pristup razvoju formulacije temeljen na znanstvenim otkrićima i upravljanju rizicima, s unaprijed definiranim ciljevima i naglaskom na razumijevanju proizvoda te kontroli procesa (143). Takav pristup omogućuje usmjereni razvoj farmaceutskog oblika za nazalnu primjenu, optimiranog profila depozicije i povoljnih biofarmaceutskih svojstava (144).

U razvoju nazalnih farmaceutskih oblika DoE omogućuje potrebnu implementaciju sveobuhvatnog pristupa koji uključuje ispitivanje formulacijskih, procesnih i parametara primjene te njihovih utjecaja na promatrana svojstva. U nazalnoj primjeni, do sada je DoE najčešće primjenjivan za optimiranje svojstava mikročestica dobivenih sušenjem raspršivanjem (74,122,145,146).

2. Innovative sprayable *in situ* gelling fluticasone suspension: Development and optimization of nasal deposition

International Journal of Pharmaceutics 563 (2019) 445–456

Contents lists available at ScienceDirect

International Journal of Pharmaceutics

journal homepage: www.elsevier.com/locate/ijpharm

Innovative sprayable *in situ* gelling fluticasone suspension: Development and optimization of nasal deposition

Laura Nižić[a], Ivo Ugrina[b], Drago Špoljarić[c], Vesna Saršon[d], Maša Safundžić Kučuk[d], Ivan Pepić[a], Anita Hafner[a,*]

[a] University of Zagreb, Faculty of Pharmacy and Biochemistry, Department of Pharmaceutical Technology, Zagreb, Croatia
[b] University of Split, Faculty of Science, Department of Mathematics, Split, Croatia
[c] Intellomics d.o.o., Zagreb, Croatia
[d] Jadran-galenski laboratorij d.d., Rijeka, Croatia

ARTICLE INFO

Keywords:
Fluticasone
Pectin
Gellan gum
Sodium hyaluronate
In situ gelling
Nasal deposition

ABSTRACT

The aim of this study was to develop an innovative *in situ* gelling suspension for effective nasal delivery of fluticasone. Pectin, gellan gum and sodium hyaluronate were used as gelling/thickening agents, and Tween 80 as a suspending agent. The influence of the formulation and/or administration parameters on formulation sprayability and nasal deposition was explored with an appropriate experimental design with the range for parameters in the design obtained from previous research and domain knowledge. All formulations exhibited appropriate sprayability and instant gelation upon mixing with simulated nasal fluid exhibiting weak gel properties convenient for nasal delivery. Targeted turbinate deposition depended on administration and formulation parameters, including their interactions. Decrease in the administration angle from horizontal plane, increase in inspiratory flow and presence of sodium hyaluronate significantly increased deposition in turbinate region. Parameters in interactions included concentration of polymers, surfactant and fluticasone, as well as administration angle. Selected formulations with high turbinate deposition exhibited significant increase in viscosity upon gelation, showing potential to prolong the drug retention at the nasal mucosa. The highest effect on the gel viscosity, strength and fluticasone release profile was observed for gellan gum, thus recognised as crucial parameter for the optimisation of overall therapeutic effect.

1. Introduction

Nasal application of corticosteroids is widespread in the treatment of nasal inflammatory disorders such as allergic and non-allergic rhinitis, chronic rhinosinusitis and nasal polyposis. By anti-inflammatory action, corticosteroids relieve related symptoms, decrease the polyp size and prevent their recurrence after surgical therapy (Del Río-Navarro et al., 2009). Although oral corticosteroids are effective, they are associated with well-known side effects including adrenal suppression, alteration in bone metabolism, hyperglycaemia, gastrointestinal bleeding, hypocalcaemia, insomnia, hypertension, cataracts and glaucoma. Therefore, nasal delivery of corticosteroids is recommended as the first-line treatment of such inflammatory conditions (Fokkens and Reitsma, 2018; Martino et al., 2015).

Superior effect of systemic over local corticosteroids shows that there is room for improvement of local corticosteroid delivery. The relatively low efficiency of conventional topical corticosteroid sprays in patients with nasal polyps has been attributed to the limited delivery of the drug to the regions posterior to the nasal valve, i.e. where the polyps occur. Thus, current interests focus on the innovative exhalation nasal delivery device with the potential to ensure more effective corticosteroid delivery to the site of inflammation (Fokkens and Reitsma, 2018). Nonetheless, great potential to improve the nasal corticosteroid efficiency lies also in the innovative formulation platforms that can prolong the residence time and availability of the drug at the site of action, thus reducing the frequency of administration and/or the variability of the therapeutic outcome (Altuntaş and Yener, 2017; Pandey et al., 2017). Hence, it is reasonable to expect that innovative formulation benefits in conjunction with the effective nasal deposition could significantly improve the overall therapeutic effect of locally administered corticosteroid.

In situ gelling system offers unique advantages in nasal drug delivery. It can be easily sprayed as a liquid formulation in the nasal cavity and ensure prolonged contact time with nasal mucosa due to

* Corresponding author at: A. Kovačića 1, 10000 Zagreb, Croatia.
E-mail address: ahafner@pharma.hr (A. Hafner).

https://doi.org/10.1016/j.ijpharm.2019.04.015
Received 30 December 2018; Received in revised form 18 March 2019; Accepted 6 April 2019
Available online 06 April 2019
0378-5173/

rapid gelation that reduces post-nasal drip, anterior leakage and mucociliary clearance of the administered drug. Depending on the gel structure, such system can hinder the drug release and permeation, minimising its systemic absorption, which is important for locally acting drugs (Jurišić Dukovski et al., 2017).

As rapid clearance has been generally recognised as one of the most critical factors in relation to nasal delivery, many literature reports are focused on the development of polymeric *in situ* gelling systems able to ensure prolonged drug retention at the nasal mucosa due to sol-gel phase transition triggered by physiological factors upon nasal administration. However, information on their sprayability and deposition within the nasal cavity, although crucial for the treatment outcome, are very scarce. There are only few literature reports focused on the applicability of *in situ* gelling technology in the preparation of nasal formulations that deal with the aspect of their nasal deposition. Castile and co-workers (Castile et al., 2013) investigated the deposition pattern using a nasal cavity model to evaluate the ability of PecSys® *in situ* nasal gelling technology to reduce nasal run-off and drip. Lungare et co-workers developed the thermoresponsive hydrogel for nasal delivery of anti-Parkinsonian drug amantadine and assessed the deposition in the olfactory region, but only in relation to the administration parameters (Lungare et al., 2016).

In this work, we propose the development of innovative sprayable *in situ* gelling fluticasone suspension with the consideration of its nasal deposition included in the early phase of its development.

For the preparation of *in situ* gelling fluticasone suspensions, pectin, gellan gum and sodium hyaluronate were used as polymeric constituents, while Tween 80 was used as a fluticasone suspending agent. Pectin and gellan gum are well known gelling agents that form dispersions which undergo ion-triggered sol-gel phase transition in contact with nasal mucosa (Karavasili and Fatouros, 2016). Sodium hyaluronate was selected as a gel-structuring and bioactive formulation constituent, since it plays an important role in healing process and repair of mucosal surfaces. When given as a supplement to nasal corticosteroids, sodium hyaluronate showed the potential of decreasing the severity of symptoms and discomfort associated with allergic and non-allergic rhinitis (Gelardi et al., 2013) as well as chronic rhinosinusitis with polyps (Cantone and Iengo, 2016). Quality by Design (QbD) principles were employed in order to optimise the formulation (concentration of constituents) and/or administration parameters (angle of administration, inspiratory flow rate), elucidating their influence (including also their possible interactions) on the formulation gelation time, sprayability, and nasal deposition. The leading formulations were further characterised in terms of rheological properties upon gelation and *in vitro* drug release kinetics, with the aim to select the formulation with the highest overall therapeutic potential.

2. Materials and methods

2.1. Materials

Micronised fluticasone propionate (pharma grade; further denoted as fluticasone) was purchased from Carbosynth Ltd., UK. Low methylester amidated pectin CF 025 (degree of esterification 23–28%; degree of amidation 22–25%) was kindly donated by Herbstreith&Fox, Germany. Gellan gum Phytagel was obtained from Sigma-Aldrich, USA. Sodium hyaluronate (Molecular weight 0.8 MDa) was purchased from Contipro, Czech Republic. Tween 80 was obtained from Sigma-Aldrich, USA and mannitol from BDH Prolabo, UK. Simulated Nasal Fluid (SNF) was prepared as an aqueous solution containing NaCl (150.0 mM; Kemig, Croatia), KCl (40.0 mM; Kemig, Croatia) and $CaCl_2{\cdot}2H_2O$ (5.3 mM; Sigma-Aldrich, Germany) (Jurišić Dukovski et al., 2017). Water indicating paste Sar-Gel® was purchased from Arkema Inc., Sartomer Americas, USA. All other reagents were of analytical grade and purchased from Kemika, Croatia and Sigma-Aldrich, Germany.

2.2. Experimental design

In order to optimise the formulation and administration parameters for effective nasal deposition/delivery of fluticasone by means of simple *in situ* gelling system, Quality by Design (QbD) principles were employed. The influence of seven parameters at two or three levels was studied with a custom experimental design obtained with JMP 14.0 statistical software (JMP®, Version 14.0, SAS Institute Inc., Cary, NC, 1989–2007). The design included fluticasone, pectin, gellan-gum, sodium hyaluronate and Tween 80 concentration as formulation parameters, while the angle of administration from the horizontal plane and inspiratory flow rate were investigated as administration parameters (Table 1). Preliminary experiments were performed to determine appropriate values for low, medium and high settings of parameters. Sprayability (zero shear viscosity, droplet size distribution, spray cone angle), gelation time and nasal turbinate deposition were investigated as responses. The analyses related to the responses were performed in duplicate or triplicate. Design of experiments and data analyses were performed with the statistical software JMP 14.0 (JMP®, Version 14.0, SAS Institute Inc., Cary, NC, 1989–2007).

Table 1
Parameters considered in the experimental design and their levels.

Parameter	High (+1)	Medium (0)	Low (−1)
Fluticasone concentration, F (%, *w/w*)	0.100	0.075	0.050
Tween 80 concentration, Tw (%, *w/w*)	0.05	0.03	0.01
Pectin concentration, P (%, *w/w*)	0.7	0.6	0.5
Gellan gum concentration, GG (%, *w/w*)	0.2	0.1	0
Sodium hyaluronate concentration, SH (%, *w/w*)	0.05	–	0
Angle of administration from the horizontal plane, AA (°)	75°	52.5°	30°
Inspiratory flow, IF (L min^{-1})	60	30	0

2.3. Preparation of in situ gelling fluticasone suspensions

For the preparation of *in situ* gelling fluticasone suspensions pectin, gellan gum and sodium hyaluronate were dissolved separately in the distilled water at concentration of 1.4%, 0.6% and 0.5% (*w/w*), respectively. Pectin and sodium hyaluronate solutions were prepared under stirring conditions at room temperature, while gellan gum was heated at 80 °C and dissolved under stirring conditions (Hao et al., 2016). Pectin, gellan gum and sodium hyaluronate solutions were then mixed in appropriate weight ratio and the mixture was diluted with distilled water in order to obtain the final polymer concentrations as set within the individual runs of the experimental design (Table 2). Fluticasone was thoroughly mixed with the suspending agent Tween 80 in the weight ratio ranging from 10:1 to 1:1 (Table 2). The final polymers' solution mixture was then gradually added to the fluticasone/Tween 80 mixture under constant agitation, resulting in fine drug suspension with the appropriate drug concentration ranging between 0.05 and 0.1%, *w/w* (Table 2). Finally, mannitol as an isotonicity agent was dissolved in the prepared drug suspension at a concentration of 4%. The value of pH of the formulations was adjusted to 6.0 with the addition of 0.1 M NaOH. Osmolality of the formulations mixed with SNF in volume ratio 1:1 was measured using osmometer Osmomat 030-D (Gonotec, Germany).

2.4. Particle size determination

Size of suspended fluticasone particles was determined by a microscopic imaging analysis technique using Olympus BH-2 microscope equipped with a camera (CCD Camera ICD-42E; Ikegami Tsushinki Co., Tokyo, Japan) and computer-controlled image analysis system

Table 2
Sample sequence from design of experiment and corresponding zero shear viscosity (η_0), droplet size distribution (Dv10, Dv50, Dv90), cone angle (CA) and turbinate deposition (TD).

	F% (*w/w*)	Tw% (*w/w*)	P% (*w/w*)	GG% (*w/w*)	SH% (*w/w*)	AA* (°)	IF* (l/min)	η_0 (mPas)	Dv10 (μm)	Dv50 (μm)	Dv90 (μm)	CA (°)	TD (%)
1	0.050	0.01	0.5	0	0.05	30	60	8.33 ± 0.03	27.5 ± 0.8	88.5 ± 3.1	204.3 ± 9.3	32.6 ± 1.3	92.5 ± 3.4
2	0.050	0.01	0.5	0.2	0.05	30	0	91.55 ± 0.51	30.5 ± 1.9	97.3 ± 7.5	203.0 ± 10.5	27.6 ± 1.2	81.8 ± 1.2
3A	0.050	0.01	0.5	0.2	0.05	75	60	91.32 ± 2.21	37.5 ± 7.0	121.7 ± 18.6	242.7 ± 32.1	29.7 ± 1.3	37.4 ± 0.1
3B	0.050	0.01	0.5	0.2	0.05	75	60	83.07 ± 1.14	35.1 ± 2.1	118.3 ± 3.9	247.9 ± 1.6	30.8 ± 1.4	35.5 ± 0.8
4	0.050	0.01	0.5	0.2	0	30	60	55.50 ± 2.60	21.9 ± 2.4	59.9 ± 10.0	142.4 ± 17.5	43.1 ± 1.2	81.7 ± 3.0
5A	0.050	0.01	0.7	0	0	75	0	5.64 ± 0.01	16.7 ± 1.0	38.3 ± 2.6	99.0 ± 4.0	56.5 ± 0.4	6.9 ± 0.2
5B	0.050	0.01	0.7	0	0	75	0	5.92 ± 0.42	16.5 ± 0.6	36.2 ± 1.8	86.9 ± 5.5	57.4 ± 0.9	4.6 ± 1.6
6	0.050	0.01	0.7	0.1	0	30	30	25.75 ± 1.70	19.7 ± 2.0	47.6 ± 6.4	110.3 ± 13.1	41.0 ± 1.4	49.8 ± 5.3
7	0.050	0.01	0.7	0.2	0.05	30	60	107.76 ± 2.58	40.6 ± 1.9	132.1 ± 6.3	280.6 ± 30.9	30.3 ± 1.0	98.8 ± 0.8
8	0.050	0.01	0.7	0.2	0.05	75	0	106.25 ± 0.65	32.7 ± 3.9	103.9 ± 9.0	207.4 ± 12.9	28.5 ± 0.6	33.8 ± 3.5
9	0.050	0.03	0.5	0	0	75	30	3.98 ± 0.04	17.1 ± 1.9	38.5 ± 5.3	94.2 ± 5.3	57.1 ± 1.0	54.1 ± 1.8
10	0.050	0.03	0.6	0.2	0	75	60	67.61 ± 0.60	20.5 ± 0.3	55.3 ± 2.9	139.5 ± 9.5	47.4 ± 2.6	84.4 ± 3.0
11	0.050	0.03	0.7	0	0.05	30	0	11.16 ± 0.10	24.5 ± 0.6	74.5 ± 3.3	166.8 ± 4.1	33.1 ± 0.8	90.0 ± 0.5
12	0.050	0.05	0.5	0	0.05	75	0	8.34 ± 0.10	24.7 ± 2.2	73.9 ± 9.4	166.0 ± 13.6	29.3 ± 1.0	0.5 ± 0.5
13	0.050	0.05	0.5	0	0	30	0	3.98 ± 0.00	17.1 ± 1.1	37.5 ± 3.5	90.4 ± 4.2	53.8 ± 1.7	96.4 ± 3.5
14	0.050	0.05	0.5	0.2	0.05	30	60	83.16 ± 0.93	32.4 ± 2.7	110.1 ± 9.0	233.3 ± 14.8	26.9 ± 0.2	96.5 ± 0.4
15	0.050	0.05	0.5	0.2	0	75	0	50.61 ± 0.33	20.0 ± 0.3	48.2 ± 1.1	165.1 ± 3.6	38.1 ± 0.8	6.5 ± 4.0
16A	0.050	0.05	0.7	0	0	52.5	60	5.72 ± 0.02	18.5 ± 1.2	44.5 ± 3.3	110.6 ± 7.8	51.6 ± 0.4	54.0 ± 4.0
16B	0.050	0.05	0.7	0	0	52.5	60	5.81 ± 0.14	18.2 ± 0.5	42.1 ± 1.9	104.7 ± 3.7	52.6 ± 0.3	58.1 ± 4.0
17	0.050	0.05	0.7	0.1	0.05	75	30	37.31 ± 0.30	32.8 ± 2.2	113.6 ± 8.4	241.9 ± 13.1	29.1 ± 0.8	58.3 ± 2.8
18	0.050	0.05	0.7	0.2	0	30	0	77.46 ± 0.84	20.9 ± 0.7	52.5 ± 2.6	154.0 ± 3.5	39.8 ± 1.3	72.4 ± 2.5
19	0.075	0.01	0.5	0	0	52.5	0	5.24 ± 0.10	17.5 ± 0.5	40.5 ± 1.1	146.5 ± 8.0	52.6 ± 1.3	49.3 ± 0.5
20A	0.075	0.01	0.7	0	0.05	75	60	10.12 ± 0.24	32.0 ± 1.7	114.4 ± 7.4	252.9 ± 17.4	48.5 ± 0.8	56.6 ± 4.4
20B	0.075	0.01	0.7	0	0.05	75	60	9.91 ± 0.08	32.7 ± 2.6	112.4 ± 8.0	239.1 ± 11.6	47.0 ± 0.2	49.0 ± 0.6
21	0.075	0.03	0.7	0.2	0	52.5	0	84.49 ± 3.80	21.8 ± 1.1	56.0 ± 4.6	160.3 ± 6.4	45.1 ± 0.9	38.9 ± 0.5
22A	0.075	0.05	0.5	0.1	0	75	60	15.21 ± 0.89	19.1 ± 0.9	41.7 ± 3.2	97.9 ± 7.8	50.0 ± 0.6	27.7 ± 0.4
22B	0.075	0.05	0.5	0.1	0	75	60	13.74 ± 0.04	18.2 ± 0.2	43.4 ± 0.7	107.9 ± 2.6	50.9 ± 1.1	25.8 ± 3.4
23A	0.075	0.05	0.6	0	0	30	30	4.75 ± 0.07	18.4 ± 0.9	44.3 ± 2.6	110.1 ± 5.3	52.4 ± 0.4	70.4 ± 3.5
23B	0.075	0.05	0.6	0	0	30	30	4.74 ± 0.09	18.7 ± 1.4	45.7 ± 4.6	112.0 ± 10.0	52.3 ± 0.7	69.1 ± 2.0
24	0.100	0.01	0.5	0	0.05	75	0	8.67 ± 0.24	26.1 ± 1.2	78.5 ± 5.3	192.4 ± 6.5	34.6 ± 0.6	44.8 ± 0.3
25	0.100	0.01	0.5	0	0	75	60	3.84 ± 0.01	16.4 ± 0.6	35.9 ± 1.2	90.3 ± 3.0	55.9 ± 0.7	32.9 ± 3.9
26	0.100	0.01	0.5	0.2	0.05	30	60	109.47 ± 10.64	35.3 ± 2.3	117.2 ± 4.6	246.5 ± 4.5	27.1 ± 1.2	98.6 ± 1.0
27	0.100	0.01	0.5	0.2	0	75	0	55.10 ± 0.13	21.3 ± 1.9	54.4 ± 7.9	161.0 ± 5.9	41.9 ± 0.5	17.8 ± 0.6
28A	0.100	0.01	0.6	0.1	0.05	52.5	60	31.69 ± 0.46	28.3 ± 1.1	92.6 ± 7.2	203.9 ± 19.0	28.3 ± 1.0	81.5 ± 0.9
28B	0.100	0.01	0.6	0.1	0.05	52.5	60	31.85 ± 0.28	30.8 ± 0.8	104.2 ± 0.5	227.9 ± 10.6	28.8 ± 0.4	70.2 ± 4.4
29A	0.100	0.01	0.6	0.2	0	30	0	74.81 ± 6.00	18.3 ± 0.4	42.5 ± 1.0	106.6 ± 1.9	44.9 ± 2.9	73.6 ± 4.5
29B	0.100	0.01	0.6	0.2	0	30	0	69.30 ± 1.14	18.4 ± 0.9	42.5 ± 2.5	107.5 ± 5.9	45.7 ± 1.5	78.5 ± 0.9
30	0.100	0.01	0.7	0	0.05	30	0	11.18 ± 0.10	22.5 ± 0.3	62.63 ± 2.0	148.6 ± 5.3	30.0 ± 1.1	87.7 ± 1.8
31	0.100	0.01	0.7	0	0	30	60	5.70 ± 0.03	17.8 ± 0.5	43.34 ± 0.4	110.5 ± 1.3	39.9 ± 0.4	89.3 ± 2.2
32	0.100	0.01	0.7	0.2	0	75	30	87.76 ± 0.42	19.9 ± 0.6	51.90 ± 2.8	128.0 ± 5.1	34.4 ± 1.5	18.1 ± 2.1
33	0.100	0.03	0.5	0.1	0	30	0	15.46 ± 0.36	18.6 ± 0.3	45.77 ± 1.9	118.1 ± 7.9	42.7 ± 0.2	87.7 ± 4.7
34	0.100	0.05	0.5	0	0.05	30	0	8.43 ± 0.05	24.1 ± 0.4	70.56 ± 2.9	162.2 ± 5.6	31.6 ± 0.7	67.7 ± 2.2
35	0.100	0.05	0.5	0	0.05	75	60	8.40 ± 0.06	24.0 ± 0.7	70.19 ± 3.5	160.5 ± 6.8	37.0 ± 0.7	40.6 ± 3.5
36	0.100	0.05	0.5	0.2	0.05	75	0	88.83 ± 4.52	24.7 ± 0.5	74.59 ± 1.9	168.8 ± 3.3	33.4 ± 1.3	0.1 ± 0.05
37	0.100	0.05	0.5	0.2	0	52.5	30	52.40 ± 0.22	19.7 ± 0.2	48.21 ± 1.8	119.3 ± 7.3	49.7 ± 0.7	35.5 ± 4.4
38A	0.100	0.05	0.7	0	0.05	30	60	10.54 ± 0.02	24.4 ± 1.1	73.47 ± 4.8	166.4 ± 4.8	30.3 ± 0.5	95.3 ± 2.1
38B	0.100	0.05	0.7	0	0.05	30	60	10.66 ± 0.04	24.6 ± 0.8	72.83 ± 3.7	162.6 ± 6.8	30.2 ± 1.2	95.9 ± 1.1
39A	0.100	0.05	0.7	0	0	75	0	5.65 ± 0.02	18.3 ± 1.1	42.01 ± 2.7	105.3 ± 3.5	55.7 ± 0.9	32.6 ± 0.3
39B	0.100	0.05	0.7	0	0	75	0	5.78 ± 0.04	17.4 ± 0.3	40.11 ± 1.0	106.1 ± 7.4	55.3 ± 0.8	25.1 ± 2.8
40	0.100	0.05	0.7	0.2	0.05	30	0	113.46 ± 0.69	24.0 ± 0.4	71.23 ± 1.5	162.9 ± 2.0	27.6 ± 0.9	92.9 ± 2.8
41	0.100	0.05	0.7	0.2	0.05	75	60	127.16 ± 4.32	39.7 ± 7.5	128.32 ± 22.9	251.4 ± 32.3	28.2 ± 0.4	71.7 ± 1.9
42	0.100	0.05	0.7	0.2	0	30	60	84.83 ± 4.62	29.6 ± 1.5	95.42 ± 4.0	201.5 ± 4.0	47.4 ± 0.7	91.1 ± 1.1

F = fluticasone propionate concentration; Tw = Tween 80 concentration; P = pectin concentration; GG = gellan gum concentration; SH = sodium hyaluronate concentration; AA = administration angle in relation to horizontal plane; IF = inspiratory flow.
Values for the responses are mean ± SD, n ≥ 2.
For all formulations gelation occurred instantly upon mixture with simulated nasal fluid in volume ratio of 1:1.
* Parameters related only to turbinate deposition.

(Optomax V, Cambridge, UK). In all measurements a minimum of 3000 particles was examined.

2.5. Droplet size distribution

The droplet size distribution (DSD) was measured by laser diffraction using Malvern Spraytec® (Malvern Instruments, UK). Preservative-free spray pump system (Spray Pump 3 K, 140 μl, Aeropump, Germany) was primed by several actuations sent to waste, followed by one test actuation at 90° from the horizontal plane. The tip of the spraying device was placed 3 cm below the laser diffraction measurement zone. The focal distance from the lens was 300 mm. Actuation was performed manually in order to simulate the real clinical situation as closely as possible. Each formulation was tested three times. The data were analysed using Malvern Spraytec 3.20 software. Volume diameters defined by 10%, 50% and 90% of the cumulative volume undersize were determined (Dv10, Dv50, and Dv90, respectively). Span was expressed as (Dv90 - Dv10)/Dv50 (Dayal et al., 2004).

2.6. Spray cone angle determination

For each formulation the spray cone angle was measured by a

virtual protractor after spraying against a dark background, employing the same spraying device and actuation conditions as for DSD analysis. The emitted plume was recorded by a camera Panasonic Lumix DMC-FZ1000 (Panasonic, Japan) of 120 frames per second and subsequently analysed for the spray cone angle. Each formulation was tested in triplicate.

2.7. Assessment of the deposition pattern

Deposition pattern was assessed using an anatomically accurate transparent silicone nasal cavity model (Koken Co. Ltd., Japan), according to Kundoor and Dalby (2010) and Pu et al. (2014). The nose model was positioned on a stand and connected to Respiratory Pump Model 613 (Harvard Apparatus, USA), simulating breathing at different inspiratory flow rates (0–60 l/min; Table 1) (Blomgren et al., 2003; Ottaviano et al., 2006). The volumetric flow rate was measured by a nasal inspiratory flow meter In-Check Nasal (Clement Clarke International Ltd., UK). During inspiration with one nostril blocked, *in situ* gelling formulation was manually actuated with Spray Pump 3 K, 140 µl, (Aeropump, Germany) to the other nostril of the nasal cavity model, at an actuation angle ranging between 30 and 75° (Table 1) from the horizontal plane, 20° from the vertical plane, and at a nostril insertion depth of 5 mm. In order to visualize the spray deposition, the inner surface of the nasal cavity model was previously uniformly covered with Sar-Gel®, a water-indicating paste that turns purple in contact with water. Fractional spray deposition pattern within the nasal cavity was determined by gravimetric analysis using an electronic scale (Mettler Toledo 0.01 mg precision, Switzerland) measuring the fraction of the sprayed dose deposited in the nasal vestibule (anterior region) and turbinate region of the nasal cavity. Two replicate assessments of deposition pattern were conducted for each formulation.

2.8. Rheological characterisation

The rheological characterisation of *in situ* gelling systems before and after mixing with SNF was performed using Modular Compact Rheometer MCR 102 (Anton Paar GmbH, Austria) equipped with either cone (1°)-plate (diameter 50 mm, CP50) or parallel-plate (diameter 50 mm, PP50) measuring system, and an air cooled Peltier temperature control system with an accuracy of 0.01 °C. Oscillatory strain/stress sweeps were performed at 34 °C to establish linear viscoelastic range (LVE range) at 6.28 rad s^{-1} angular frequency. Data were calculated by rheometer software RheoCompass TM Light (Anton Paar).

2.8.1. Measurement of gelation time

Oscillation time sweep test was performed to determine the gelation time of *in situ* gelling systems upon mixing with SNF in volume ratio of 1:1, measuring the changes in storage (G′) and loss modulus (G″) over time. Intersection of G′ and G″ curves was used as the indicator of gel point. The time sweep test was performed at 34 °C using PP50 measuring system. The gap was set at 0.500 mm. Angular frequency was fixed at 6.28 rad s^{-1} and strain applied at 0.5%, ensuring the linear viscoelastic domain during the measurements. All measurements were done in triplicate.

2.8.2. Zero shear viscosity

Zero shear viscosity at 25 °C of *in situ* gelling systems was determined by creep test using CP50 measuring system. The gap was set at 0.102 mm. Samples were equilibrated at 25 °C for 3 min. A fixed shear stress (0.1 Pa) was applied to the sample and the resultant shear strain was monitored for a predetermined amount of time (300 s). The stress was applied for duration long enough for the deformation to reach a constant value, which corresponds to steady state flow. Zero shear viscosity was calculated by the RheoCompass software by fitting the shear stress versus shear rate data and calculating regression with 3 retardation times on creep measuring data. The measurement for each of the samples was performed in triplicate.

2.8.3. Viscosity curve determination

Shear viscosity profiles of *in situ* gelling systems before and after mixing with SNF were determined by means of rotational test using CP50 measuring system. The gap was set at 0.102 mm. Samples were equilibrated at 34 °C for 3 min. The viscosity of the sample was measured as a function of shear rate in the range of 0.01 s^{-1}–1000 s^{-1}. Three replicate measurements were conducted for each formulation.

2.8.4. Frequency sweep analysis

In situ gelling systems upon mixing with SNF were subjected to frequency sweep test using PP50 measuring system. Sample was placed carefully on the lower plate of rheometer and equilibrated for 15 min at 34 °C. Gap was set to 0.500 mm. The strain applied was in the linear viscoelastic (LVE) range (at 0.5%) while the angular frequencies were in the range of 0.1–100 rad s^{-1}. The elastic modulus (G′) and viscous modulus (G″) were recorded.

2.9. In vitro release studies

Fluticasone release from *in situ* gelling systems was assessed under sink conditions using a Franz diffusion cell apparatus. A water-permeable polyamide membrane with 0.45 µm pore size (Sartolon polyamide, Sartorius Stedim Biotech GmbH, Germany) was placed between the donor and the receiver compartment. The receiver compartment was filled with the mixture of SNF and ethanol in the volume ratio 1:1. The receiver medium was continuously stirred and thermostated at 34 °C. *In situ* gelling systems or suspension (used as control) containing 0.4 mg of fluticasone were placed on the membrane in the donor compartment. At scheduled time intervals, the aliquots (0.5 ml) were withdrawn from the receiver compartment and replaced with an equal volume of fresh receiver medium. The withdrawn samples were analysed for fluticasone content by HPLC method described below. All release experiments were performed in triplicate.

2.10. Quantitave determination of fluticasone

The quantitative determination of fluticasone was performed by high performance liquid chromatography (HPLC) using Agilent 1100 instrument with Diode Array (DAD detector) (Agilent, USA). The chromatographic separation of fluticasone was done on column Kinetex C18, 4.6x50 mm, 2.6 µm, 100 Å (Phenomenex, USA). Isocratic HPLC method was used with the mobile phase consisting of 40% 10 mM phosphate buffer pH 3.5 and 60% acetonitrile (*v/v*). The column temperature was set at 45 °C. The injection volume was 80 µl. The flow rate of the mobile phase was 1.0 ml/min and detection was at 236 nm wavelength.

3. Results and discussion

This study focused on development of *in situ* gelling platform for effective nasal delivery of corticosteroids, employing Quality by Design approach. All formulation compounds are selected based on their known safety profile related to nasal and/or oral route of administration. Namely, Tween 80 is commonly used suspending agent in the approved conventional fluticasone propionate suspensions. Pectin has long been used in pharmaceutical and food industry, and is denoted as “generally recognised as safe” (Watts et al., 2009). Low methoxy pectin represents *in situ* gelling component in PecSys™ technology used in approved nasal fentanyl formulation PecFent® (Watts et al., 2013). Gellan gum (E 418) is authorised as a food additive in the European Union (Younes et al., 2018) and is commonly used in food and pharmaceutical industry. Gellan gum based structures are nowadays investigated as injectable carriers for various autologous cells (Osma et al., 2014). Sodium hyaluronate is used as excipient in conventional

nasal sprays as a humectant to moisturize nasal mucosa. It plays a significant role in both homeostasis and healing process of nasal mucosa, showing no allergizing or immunogenic properties (Casale et al., 2015).

In situ gelling system represents an intelligent solution for nasal drug delivery. It combines the advantages of liquid formulations such as ease of administration and precise dosing, with the advantages of gels which provide prolonged retention of the formulation within the nasal cavity and prolonged drug release. Zaki et al. performed *in vivo* study in rats to assess nasal mucociliary transport time of control solution, non-mucoadhesive (poloxamer P407) *in situ* gel, and mucoadhesive (hydroxypropyl cellulose or PVA or Carbopol 994P – containing) P407-based *in situ* gels. The results obtained clearly indicated significant increase in retention time of *in situ* gelling formulation when compared to solution, exclusively due to *in situ* gelling phenomenon. Further increase in retention time was achieved by introducing mucoadhesive polymers in the formulation (Zaki et al., 2007). Since all three polymers used in our study are known for their mucoadhesivness (Jurišić Dukovski et al., 2019; Mahdi et al., 2015; Xu et al., 2014), notable prolongation of retention time could be expected, too. Gel-related formulation properties that emerge upon the formulation contact with nasal mucosa can improve drug therapeutic effect, reduce the side effects, and eliminate the drawbacks related to the bad taste that occurs if formulation reaches the back of the throat (Salunke and Patil, 2016). However, the overall therapeutic potential greatly depends on the deposition pattern of the formulation within the nasal cavity and thus needs to be considered in the early phase of formulation development.

3.1. Experimental design: analysis of results

Experimental design helped in the process of fine tuning of formulation and administration parameters for effective nasal deposition/delivery of fluticasone by means of simple *in situ* gelling system. DSD analysis performed on preliminary samples enabled the selection of the appropriate delivery device that was further used throughout the study (data not shown). Samples prepared according to the design matrix (Table 2) represented fine fluticasone suspensions with mean suspended particle diameter ranging between 2.03 ± 0.05 µm and 2.28 ± 0.10 µm. Osmolality was in range from 292 ± 1 mOsm kg^{-1} to 318 ± 5 mOsm kg^{-1} indicating suitability for nasal application (Bitter et al., 2011). Formulations were further characterised in terms of gelation time, zero shear viscosity, droplet size distribution, spray cone angle and nasal deposition pattern (Table 2).

Regression modelling (with linear effects, quadratic effects and interactions between linear components where applicable) was applied to derive an insight into which formulation and/or administration parameters as well as their interactions are important to precisely estimate evaluated responses. Covariates were standardized through centering and scaling to intervals [−1,1] as is customary in the experimental design modelling (Goos and Jones, 2011). Equations in the rest of the text contain regression coefficients on standardized covariates.

Regression modelling approach revealed the parameters with the greatest influence on the responses, the existence of interactions between those parameters, and the optimized parameter values that yielded desired values of the responses.

3.2. Gelation time

In the early phase of this study, preliminary experiments were performed to determine appropriate values for settings of formulation parameters in order to ensure instant formulation gelation upon the contact with nasal mucosa. Nonetheless, the gelation time was verified for each sample defined by experimental design. Gelling time of the *in situ* gelling fluticasone suspensions was determined by oscillatory time sweep test performed at physiological temperature of the nasal mucosa upon mixing with SNF. The intersection of storage (G′) and loss modulus (G″) curves was taken as the indicator of gel point. More general and reliable method for identification of sol-gel transition is based on Winter-Chambon criterion defining the gel point as the point at which tan δ (loss factor) becomes independent of the frequency and thus corresponds to the intersection of tan δ curves obtained at different angular frequencies (Winter and Chambon, 1986). Although the two aforementioned intersection points might not exactly coincide, G′/G″ intersection is considered a useful descriptor of gelation time and is often used in rheological characterization of drug delivery systems (Mezger, 2006; Moura et al., 2007; Ta et al., 2009; Ye et al., 2016).

Fluticasone *in situ* gelling suspensions were mixed with SNF in volume ratio of 1:1, in order to simulate the conditions *in vivo* regarding the concentration of ions at the nasal mucosa and the ratio of volume dose to be applied to volume of the nasal epithelial lining (Jurišić Dukovski et al., 2017). For all the samples storage modulus was higher than loss modulus during the entire measurement period ($t \geq 0$) indicating that gelation occurred instantly upon mixture with SNF. All formulations upon gelling exhibited typical weak gel properties with G′ approximately one order of magnitude higher than G″. Such rheological behaviour has been found convenient for nasal delivery systems such as nasal sprayable gels (Mahdi et al., 2015).

3.3. Zero shear viscosity

Zero shear viscosity of *in situ* gelling systems defined by experimental design ranged between 3.84 ± 0.01 and 127.16 ± 4.62 mPa s (Table 2). The model obtained from the regression modelling exhibited a good fit (R-squared 0.98, RMSE 4.81, Press R-squared 0.98 and Press RMSE 5.25) and is given by the following equation:

$$\eta_0 = 6.52 * P + 39.31 * GG + 8.98 * SH + 5.98 * P * GG + 7.23 * GG * SH + 19.90 * GG^2 + 26.64$$

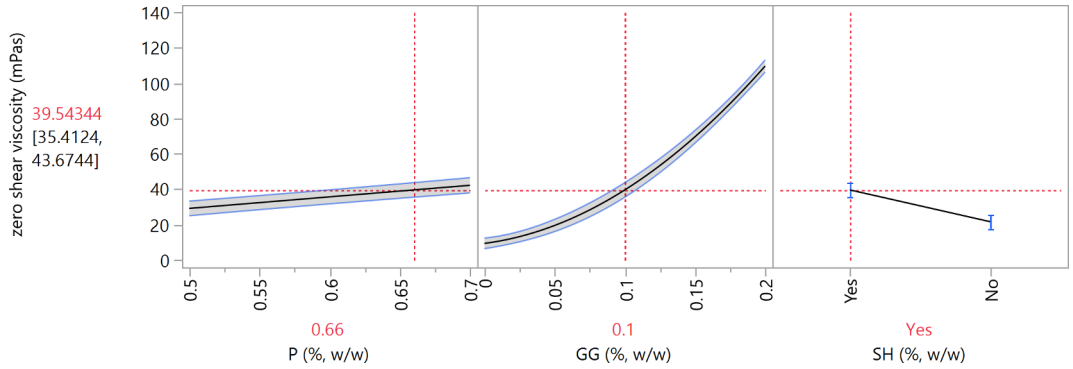

Fig. 1. Prediction of zero shear viscosity in relation to pectin concentration (P), gellan gum concentration (GG) and the presence of sodium hyaluronate (SH; 0 (NO) or 0.05% (YES), *w/w*) in the *in situ* gelling fluticasone suspension. Values in brackets refer to 95% confidence interval.

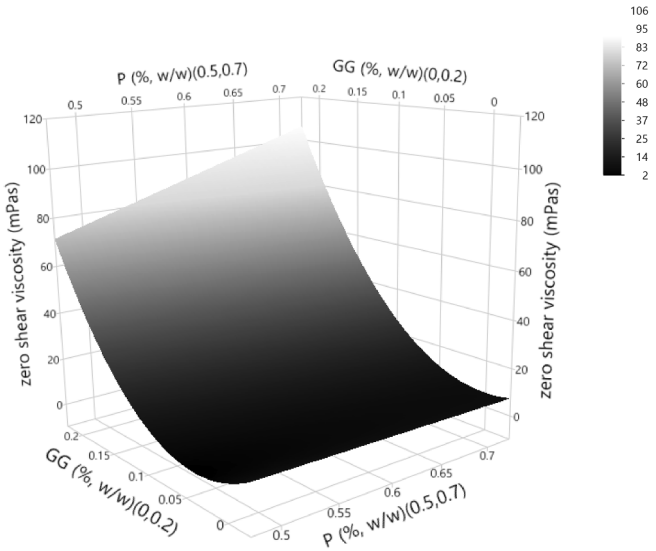

Fig. 2. Response surface as a function of concentration of gellan gum (GG) and pectin (P) in the presence of sodium hyaluronate (SH; 0.05% *w/w*) on zero shear viscosity.

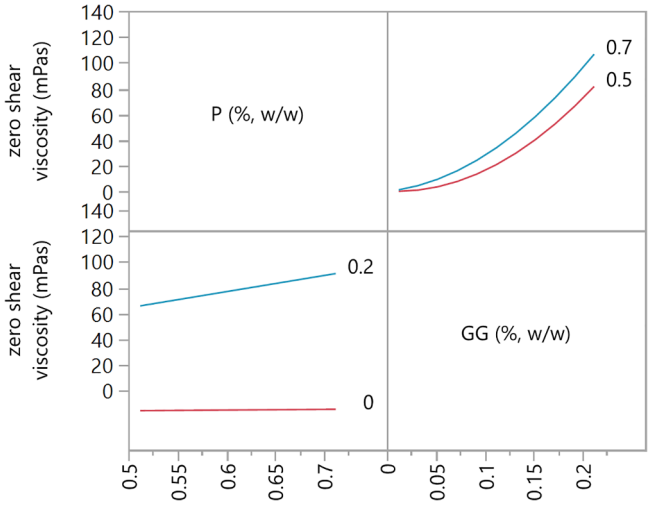

Fig. 3. Interaction profiler for zero shear viscosity regression model showing that highest concentration of gellan gum (GG set to 0.2%, *w/w*) potentiated the positive effect of pectin on the zero shear viscosity of *in situ* gelling fluticasone suspension.

where the value of sodium hyaluronate concentration (SH) is equal to 1 if it is included in the formulation and −1 otherwise.

Increase in polymer concentration, as expected, resulted in increase in zero shear viscosity as can be seen in Figs. 1 and 2. Except for the individual parameters, interactions between polymer concentrations were also included in the obtained model. Namely, the presence of gellan gum in the system at the highest investigated concentration (0.2%, *w/w*) potentiated the positive effect of pectin on the zero shear viscosity of the system (Figs. 2 and 3), which can be ascribed to the entanglement and hydrodynamic interactions among polymer chains in the solution (Kaneda, 2017).

Fluticasone *in situ* gelling suspensions showed viscosity related settling behaviour. Higher values of viscosity at zero shear provided the greater suspension stability as viscous medium hindered the particle settling due to gravity. Furthermore, all formulations showed appropriate resuspendibility. During 6-month storage at 4 °C particle size in the recovered suspension remained unchanged in relation to freshly prepared suspension. Such behaviour can be ascribed to the (i) effect of suspending agent that prevented particle aggregation and (ii) increased viscosity of the system owing to the presence of constitutive polymers that hindered the particle settling (Aulton and Taylor, 2013). This behaviour is in line with approved conventional nasal fluticasone formulations, encompassing suspensions with Tween 80 as suspending agent and cellulose derivatives as viscosifying polymers.

3.4. Droplet size distribution

Results on droplet size analysis for all samples defined by experimental design are presented in Table 2. Values for Dv10, Dv50 and Dv90 ranged between 16.4 ± 0.6–40.6 ± 1.9 µm, 35.9 ± 1.2–132.1 ± 6.3 µm and 86.9 ± 5.5–280.6 ± 30.9 µm, respectively. Span, as the measure of DSD broadness, varied over the range of 1.69 ± 0.05 and 3.20 ± 0.28. The obtained droplet size distribution met current requirements for localised nasal delivery, i.e. deposition within the nasal cavity (Guideline on the Pharmaceutical Quality of Inhalation and Nasal Products, 2006).

Models obtained through regression modelling exhibited a good fit: Dv90 (R-squared 0.83, RMSE 24.45, Press R-squared 0.74 and Press RMSE 27.26); Dv50 (R-squared 0.84, RMSE 12.68, Press R-squared 0.77 and Press RMSE 14.11); Dv10 (R-squared 0.83, RMSE 2.98, Press R-squared 0.75 and Press RMSE 3.3). The following equations present the obtained models:

$$Dv90 = -5.4 * F - 5.91 * Tw + 4.87 * P + 21.26 * GG + 43.15 * SH + 7.78 * Tw * P - 6.66 * Tw * SH - 24.99 * F^2 + 185.04$$

$$Dv50 = -3.02 * F - 2.59 * Tw + 3.55 * P + 10.71 * GG + 24.17 * SH + 3.12 * Tw * P - 3.89 * Tw * SH - 9.1 * F^2 + 78.80$$

$$Dv10 = -0.72 * F - 0.53 * Tw + 0.81 * P + 2.75 * GG + 5.27 * SH - 0.72 * Tw * P - 0.98 * Tw * SH - 1.86 * F^2 + 26.02$$

As can be noticed from models obtained for Dv10, Dv50 and Dv90 and Fig. 4, concentration of sodium hyaluronate (followed by gellan gum) had the highest influence on the droplet size distribution. Higher polymer concentration resulted in larger droplet size, which can be related to higher formulation viscosity (Dayal et al., 2004).

Regression models obtained for Dv10, Dv50 and Dv90 also revealed slight increase in droplet size distribution with the increase of pectin concentration. Similarly, there was a trend of particle size decreasing with the increase in content of Tween 80 (Fig. 4). The observed trend may be assigned to the decrease in surface tension (Guo et al., 2008). The concentration of fluticasone showed nonlinear effect to the droplet size distribution, meaning that higher values are expected in the middle of design space, while at the edge of design space lower DSD values are expected (Fig. 4).

Combinations of parameters were also included in the obtained fitted models for Dv90, Dv50 and Dv10. Namely, at the highest Tween 80 concentration (0.05%, *w/w*), the increase in pectin concentration resulted in increase in DSD values, pointing to their possible hydrophobic interaction (Joshi et al., 2016) that reduced the sprayability of the prepared systems. Interaction between Tween 80 and sodium hyaluronate was also part of all DSD regression models. Lowering the concentration of Tween 80 exhibited increase in DSD values in the presence of sodium hyaluronate. Study on sodium hyaluronate/surfactant interactions in aqueous media revealed no aggregation phenomena (Yin et al., 2005).

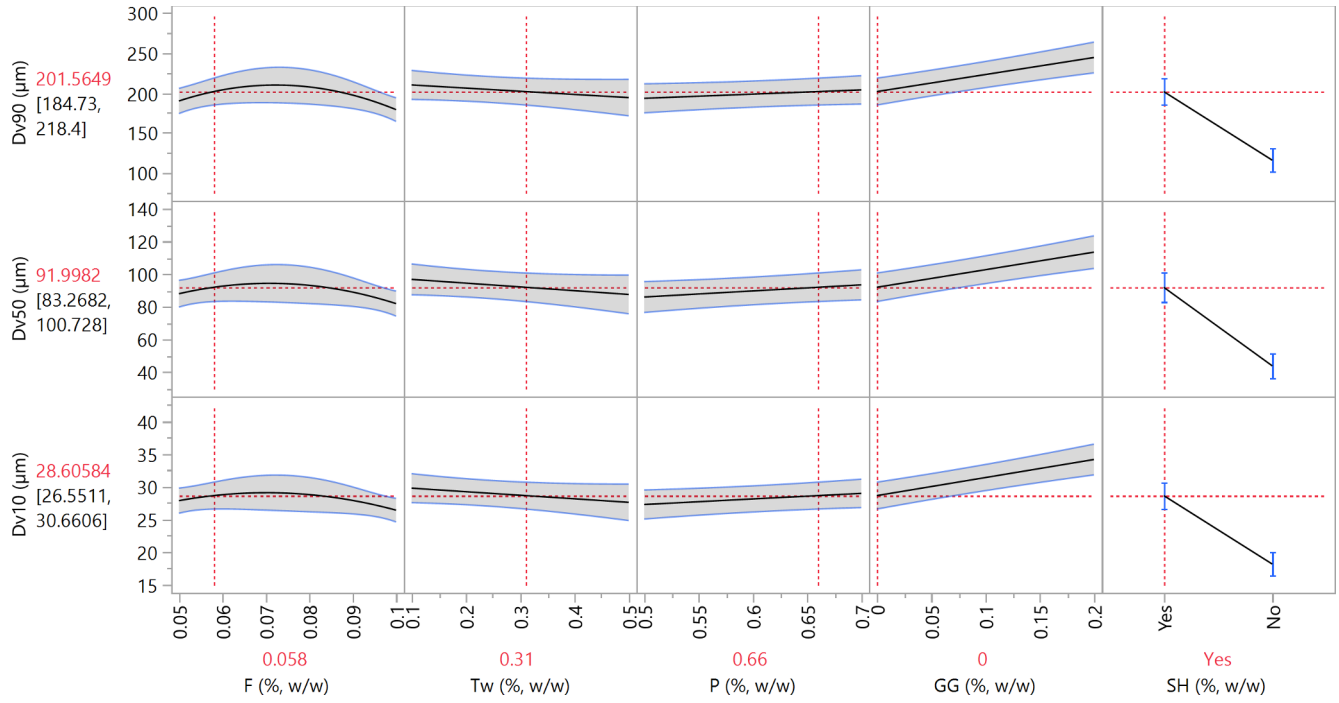

Fig. 4. Prediction of Dv10, Dv50 and Dv90 in relation to fluticasone concentration (F), Tween 80 concentration (Tw), pectin concentration (P), gellan gum concentration (GG) and the presence of sodium hyaluronate (SH; 0 (NO) or 0.05% (YES), *w/w*) in the *in situ* gelling fluticasone suspension. Values in brackets refer to 95% confidence interval.

3.5. Spray cone angle

Spray cone angles of the *in situ* gelling formulations defined within experimental design ranged between 26.9 ± 0.2° and 57.4 ± 0.9° (Table 2).

Model obtained from regression modelling exhibited a good fit (R-squared 0.80, RMSE 4.75, Press R-squared 0.77 and Press RMSE 4.90). The following equation presents the obtained model:

$$CA = -4.04 * GG - 8.30 * SH + 39.82$$

Spray cone angle decreased with the increase in polymer concentration (Fig. 5), with higher impact of sodium hyaluronate in comparison to gellan gum (Fig. 6). Narrower cone angles have already been demonstrated to result in higher turbinate deposition lowering the chances of early impaction in the anterior area of nasal cavity (Cheng et al., 2001; Foo et al., 2007; Pu et al., 2014). It has been recently shown that, apart from the concentration of polymeric constituents, spray cone angle is also influenced by the inspiratory air flow (Moraga-Espinoza et al., 2018). Namely, increase in airflow rate was shown to decrease the spray cone angle. Therefore, in the further section of this study deposition pattern was investigated as a function of both, concentration of formulation constituents and administration parameters including inspiratory air flow. In addition, narrower plume geometry has also been recognised as a promising strategy for individualization of nasal therapy by means of adjusting the administration angle, making it a desirable property of nasal formulations (Warnken et al., 2018).

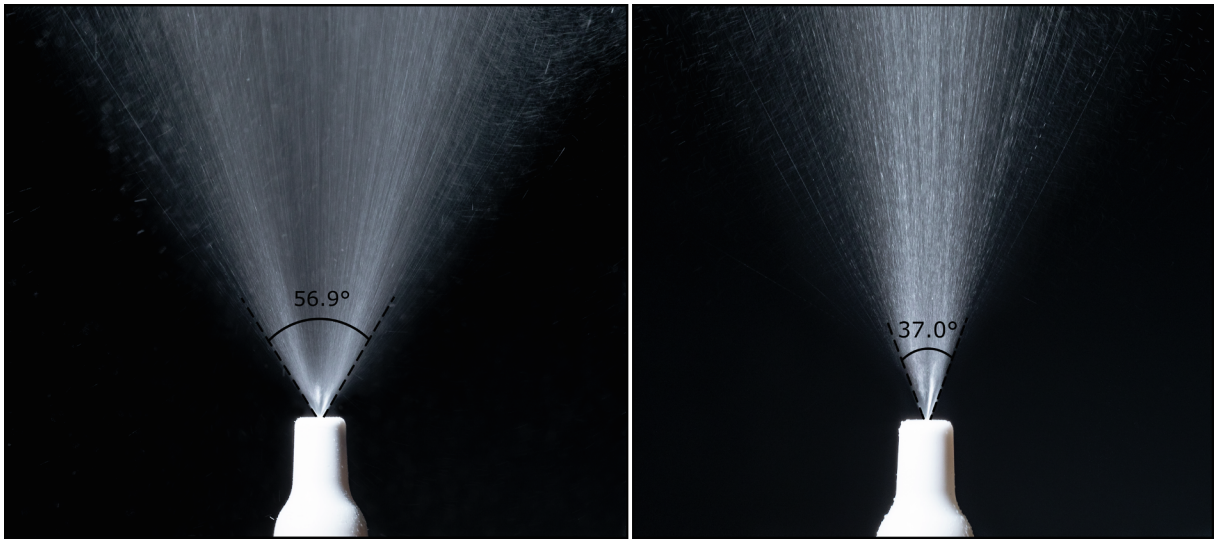

Fig. 5. Spray cone angles of *in situ* gelling fluticasone (0.05%, *w/w*) suspensions prepared with (a) pectin (0.5%, *w/w*; sample 9) and (b) pectin and gellan gum (0.5% and 0.2%, *w/w*, respectively; sample 15).

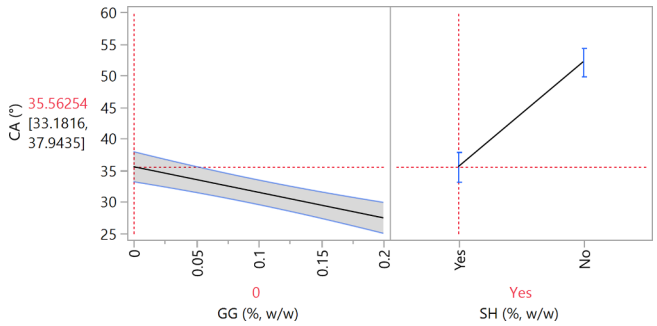

Fig. 6. Prediction of spray cone angle (CA) in relation to gellan gum concentration (GG) and the presence of sodium hyaluronate (SH; 0 (NO) or 0.05% (YES), *w/w*) in the *in situ* gelling fluticasone suspension. Values in brackets refer to 95% confidence interval.

the deposition in the turbinate region (Fig. 7). Even though comfortable use of nasal sprays is limited to angles between 55° and 75° (Kimbell et al., 2007), the results obtained showed that angles below the comfortable range should be considered with the aim to increase the deposition beyond the nasal valve (Warnken et al., 2018). Effective turbinate deposition of sprays with small cone angles administered at angle of 30° from the horizontal plane was already reported in the literature (Foo et al., 2007). In this study, for administration angle of 30°, predominant deposition in the lower part of turbinate region was observed, which is in agreement with results of Moraga-Espinoza et al. on the deposition pattern of nasal spray administered at angle of 30°, under inspiratory flow rate of 45 l min^{-1} with one nostril closed, studied using human nasal airway replica casts of 48 year old male. However, results they obtained in other airway replica nasal casts showed that turbinate subregion deposition varied with age (Moraga-Espinoza et al., 2018).

Within this study inspiratory flow rate resulted in increase in tur-

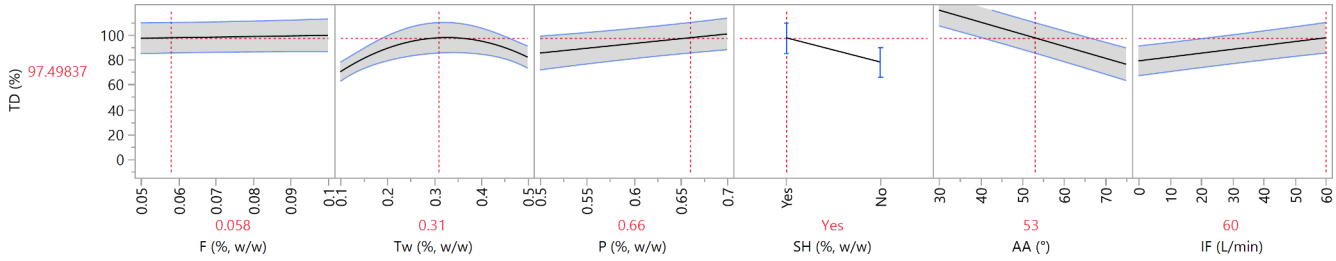

Fig. 7. Prediction of turbinate deposition (TD) in relation to formulation parameters – fluticasone concentration (F), Tween 80 concentration (Tw), pectin concentration (P) and presence of sodium hyaluronate (SH; 0 (NO) or 0.05% (YES), *w/w*), and administration parameters – angle of administration (AA) and inspiratory flow (IF).

3.6. Nasal deposition

Nasal deposition was explored using a nasal cavity cast model allowing simulations of breath airflow. There are some literature reports on investigation of formulation nasal deposition in animal models (Hoekman and Ho, 2011), e.g. rats, however, due to the substantial interspecies variability in the nasal anatomy, direct result extrapolation from animals to humans is not feasible (Corley et al., 2012; Xi et al., 2018, 2016).

Deposition pattern of *in situ* gelling formulations was evaluated after manual spray actuation under breathing conditions (i.e. during the inspiration phase), with one nostril closed. This is in agreement with the instructions given for the majority of FDA approved nasal sprays, which include inhalation during administration, in most cases with one nostril closed. This particularly refers to nasal corticosteroids (Moraga-Espinoza et al., 2018). EMA-approved corticosteroid nasal sprays such as Avamys and Flixonase are also instructed to be used under breathing conditions, with pointing the end of the nozzle slightly outwards and closing one nostril, respectively. Closing of one nostril results in increase in the velocity of the inspiratory air passing through the nasal cavity, while airflow rate is kept constant (Moraga-Espinoza et al., 2018).

Fraction of the sprayed dose deposited in the turbinate region for all runs within the experimental design ranged between 0.5 ± 0.5 and 98.8 ± 0.8% (Table 2).

Model obtained from the regression modelling exhibited a good fit (R-squared 0.89, RMSE 11.09, Press R-squared 0.80 and Press RMSE 13.18) and is given by the following equation:

$$TD = 1.34 * F + 0.26 * Tw + 2.33 * P + 6.71 * SH - 24.66 * AA + 9.28 * IF - 3.71 * F * Tw + 5.22 * Tw * P + 4.97 * P * SH + 4.84 * P * AA - 21.21 * Tw^2 + 78.28$$

The administration parameters showed the pronounced impact on the deposition pattern. Decreasing the angle of administration from horizontal plane within the range of 75 to 30° significantly increased

binate region deposition (Fig. 7). Moraga-Espinoza et al. summarized previously performed studies (Foo et al., 2007; Guo et al., 2005) that showed no or scarce effect of breathing conditions on nasal deposition pattern, explaining such results with relatively low flow rates or both nostrils open during the tests performed (Moraga-Espinoza et al., 2018). In our study, it was generally observed that increase in inspiratory flow rate resulted in deposition more distally beyond the nasal valve.

Among the individual formulation parameters, sodium hyaluronate showed the largest influence on the deposition pattern (Fig. 7). In general, the addition of sodium hyaluronate resulted in increase in turbinate deposition. This observation could be related to the cone angle narrowing effect of sodium hyaluronate confirmed within the experimental design. The influence of gellan gum on the deposition pattern was not found to be significant.

Several interactions between the investigated parameters have shown a significant influence on the deposition pattern (see model equation above). The parameters in interactions include concentration of polymers, surfactant and fluticasone, as well as administration angle. Such interactions have not been observed in the models for droplet size and spray cone angle and could be the consequence of the difference in spray device orientation when comparing DSD and spray cone measurements with nasal spray administration. The orientation of spray device might influence the characteristics and mechanisms of droplet deformation, breakup and collision, known to affect the droplet shape (Ghaemi et al., 2009), and thus might influence the nasal deposition pattern.

3.7. Verification of the models and final formulation adjustment

With the aim of verification of the models and the final formulation adjustments, set of six formulations (A–F) with high turbinate deposition were derived, differing in parameters that might affect rheological properties and *in vitro* release profile (i.e. presence of sodium hyaluronate, concentration of gellan gum and surfactant concentration; Table 3). Drug concentration was set at 0.058% (*w/w*). The selected

Table 3
Statistical model-derived formulations with predicted high turbinate deposition.

Sample	F% (*w/w*)	Tw% (*w/w*)	P% (*w/w*)	SH% (*w/w*)	GG% (*w/w*)	AA (°)	IF (L/min)
A	0.058	0.031	0.66	0.05	0	53	60
B	0.058	0.031	0.66	0	0	33	60
C	0.058	0.031	0.66	0.05	0.1	45	36
D	0.058	0.031	0.66	0.05	0.2	53	60
E	0.058	0.010	0.66	0.05	0	30	60
F	0.058	0.050	0.66	0.05	0	30	39

drug concentration in conjunction with the dosing volume of 140 µl ensured the delivery of the fluticasone dose comparable to the lowest efficient dose used in the recent randomized double-blind trial of the exhalation delivery system with fluticasone for nasal polyposis (Leopold et al., 2018).

Derived formulations were first characterised in terms of all responses included in the experimental design with the aim to assess the accuracy of the models obtained. Developed models exhibited suitable fit between experimental and predicted values of all responses (Table 4), verifying their applicability in the well-directed formulation development. Turbinate deposition obtained reflected the formulation and administration parameters (Fig. 8a–c), as discussed in the Section 3.6. The angle of administration had the most pronounced effect on the distribution of deposited spray between upper and lower part of the turbinate region. Furthermore, higher viscosity and lower inspiratory flow rate reduced the deposition area within the turbinate region (Fig. 8c).

For the final formulation adjustment, derived formulations were subjected to in depth rheological and *in vitro* release characterisation.

Shear viscosity profiles of derived *in situ* gelling formulations revealed their shear thinning behaviour (Fig. 9), reaching constant viscosity value of ≤ 11.4 mPa s above shear rate of $1\ s^{-1}$, which assured appropriate sprayability. All derived formulations exhibited significant increase in viscosity upon mixing with SNF, verifying their potential to prolong the drug retention time at the nasal mucosa. Among the parameters investigated, the most pronounced effect on the gel viscosity was observed for gellan gum (Fig. 9) which undergoes cation-induced gelling process at physiological ion concentration (Cao et al., 2009). Varying the surfactant concentration (samples E and F) and omitting sodium hyaluronate from the formulation (sample B) induced no significant change in shear viscosity profile in relation to gel A (data not shown). The viscosity of the formed gels gradually decreased with increase in the shear rate showing typical shear thinning behaviour. However, the viscosities of the gels were significantly higher than viscosities of *in situ* gelling fluticasone suspensions over entire shear related profile, which confirmed their potential to provide increased retention time under physiological shear stress resulting from the nasal mucociliary swing and air flow. Shear-thinning behaviour and the moderate reduction in viscosity of the formed gels could be beneficial in regards of their easier spreading within the targeted area (Hao et al., 2016).

With the aim of thorough characterization of viscoelastic properties, formulations A–F were subjected to frequency sweep analysis upon mixing with SNF, under strain previously determined to be within LVE range in which stress is directly proportional to strain. Fig. 10 presents the G′ and G″ curves for the obtained gels in relation to angular frequency. For all of the systems G′ was higher than G″ indicating

Table 4
Experimental and predicted values of zero shear viscosity (η_0), droplet size distribution (Dv10, Dv50 and Dv90), cone angle (CA) and turbinate deposition (TD) of statistical model-derived formulations. Values in brackets refer to 95% confidence interval.

Sample		η_0 (mPa s)	Dv10 (µm)	Dv50 (µm)	Dv90 (µm)	CA (°)	TD (%)
A	Experimental	10.11 ± 0.15	30.7 ± 1.5	106.6 ± 2.4	232.4 ± 6.4	33.0 ± 0.8	90.6 ± 2.3
	Predicted	9.32 [6.28, 12.36]	28.61 [25.55, 30.66]	92 [83.27, 100.73]	202.95 [185.08, 220.82]	35.6 [33.18, 37.94]	97.5 [85.23, 100]
B	Experimental	5.48 ± 0.12	16.6 ± 1.5	40.5 ± 4.0	103.5 ± 2.5	52.6 ± 1.5	88.4 ± 1.6
	Predicted	5.82 [3.05, 8.59]	18.16 [16.39, 19.93]	44.05 [36.54, 51.56]	115.49 [100.11, 130.86]	52.2 [49.92, 54.39]	97.45 [85.01, 100]
C	Experimental	40.00 ± 3.00	31.5 ± 1.5	109.1 ± 3.3	236.5 ± 3.5	32.1 ± 0.7	92.8 ± 0.5
	Predicted	39.54 [35.41, 43.67]	31.36 [29.36, 33.36]	102.71 [94.21, 111.21]	225.26 [207.87, 242.65]	31.5 [29.57, 33.47]	97.8 [86.14, 100]
D	Experimental	102.28 ± 1.03	34.1 ± 1.2	116.1 ± 1.5	238.8 ± 1.4	28.5 ± 0.7	91.4 ± 3.0
	Predicted	109.58 [106.12, 113.04]	34.11 [31.76, 36.46]	113.42 [103.44, 123.4]	247.57 [227.14, 267.99]	27.5 [25.02, 29.93]	97.5 [85.23, 100]
E	Experimental	10.26 ± 0.06	25.8 ± 1.0	85.0 ± 5.0	195.7 ± 10.5	35.9 ± 0.3	93.8 ± 3.3
	Predicted	9.32 [6.28, 12.36]	29.74 [27.52, 31.95]	96.83 [87.43, 106.24]	208.86 [189.62, 228.11]	35.6 [33.18, 37.94]	92.38 [83.39, 100]
F	Experimental	10.67 ± 0.21	25.6 ± 2.1	79.9 ± 5.2	186.8 ± 5.2	33.2 ± 0.6	96.8 ± 1.2
	Predicted	9.32 [6.28, 12.36]	27.58 [24.8, 30.36]	87.62 [75.81, 99.44]	197.6 [173.42, 221.78]	35.6 [33.18, 37.94]	97.7 [88.51, 100]

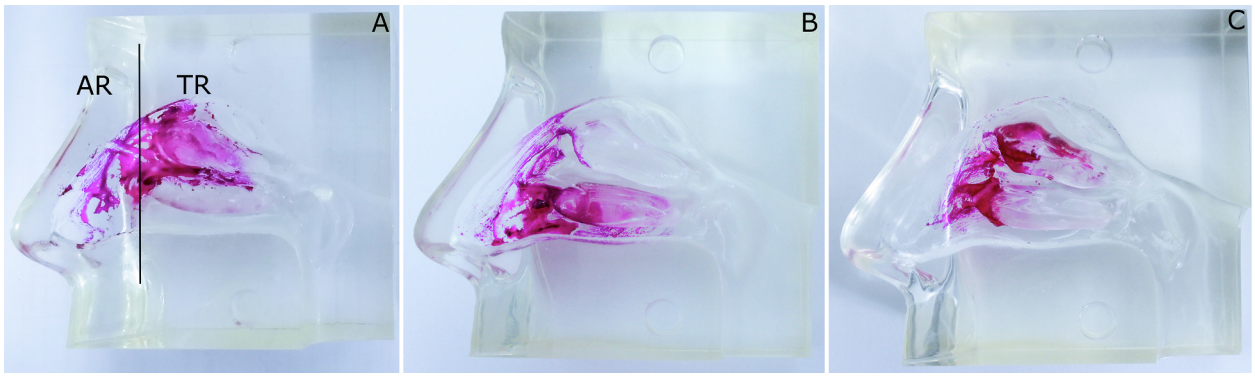

Fig. 8. Turbinate deposition of *in situ* gelling fluticasone suspensions (0.058% fluticasone, 0.31% Tween 80) prepared with pectin and sodium hyaluronate (A), pectin (B), and pectin, sodium hyaluronate and gellan gum (C). Pectin, sodium hyaluronate and gellan gum concentrations were 0.66%, 0.05% and 0.1%, respectively. Administration angles and inspiratory flow rates were as follows: 53° and 60 l/min, respectively (A), 33° and 60 l/min, respectively (B), and 45° and 36 l/min, respectively (C). AR and TR denote anterior and turbinate region, respectively.

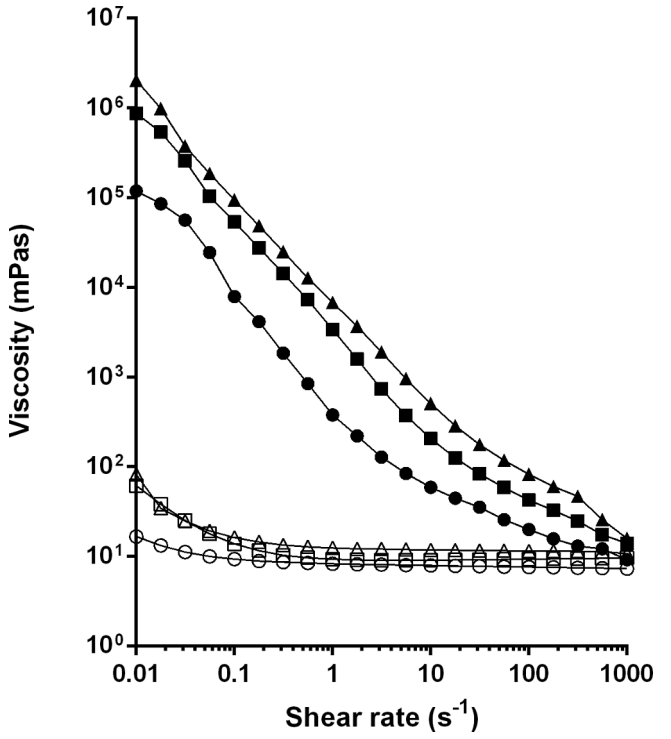

Fig. 9. Shear viscosity profiles of *in situ* gelling fluticasone suspensions prepared with 0.058% fluticasone, 0.031% Tween 80, 0.66% pectin, 0.05% sodium hyaluronate and: no addition of gellan gum (circle; sample A); 0.1% of gellan gum (rectangle; sample C), and 0.2% of gellan gum (triangle; sample D), before (open symbols) and upon (filled symbols) mixing with SNF.

appropriate gel stability. The values of tan δ at angular frequency of 1 rad s^{-1} for selected samples (A–F) ranged between 0.073 and 0.108, while at angular frequency of 10 rad s^{-1} tan δ ranged between 0.080 and 0.112. The influence of sodium hyaluronate on the gel strength was found to be negligible (Fig. 10a). On the contrary, the presence of gellan gum resulted in significantly increased G′ and G″ values indicating higher gel strength (Fig. 10b). G′ modulus represents the measure of the energy that is stored and recovered from deformation per cycle, thus indicating the elastic behaviour of the system (Hao et al., 2016). The greater elasticity of the *in situ* gels indicates the greater potential of the formulation to prolong drug retention at the administration site and to provide its prolonged release (Hao et al., 2016). Increase in Tween 80 concentration up to 0.05%, *w/w*, decreased the gel strength (Fig. 10c). Occurrence of fragile pectin based gels at high nonionic surfactants concentrations (c > > cmc) was already reported in the literature (Joshi et al., 2016).

Fluticasone release profiles from *in situ* gelling formulations were determined using Franz diffusion cell apparatus with SNF/ethanol mixture (1:1, *v/v*) as the receptor medium, triggering the gelation process and assuring sink conditions throughout the experiment. The profile of fluticasone release from the aqueous suspension prepared with Tween 80 at concentration of 0.031% (*w/w*) was also determined and served as control. Gellan gum free *in situ* gelling formulation containing sodium hyaluronate (sample A) provided moderate reduction in fluticasone release rate in comparison to suspension (Fig. 11a). Modulation of drug release due to diffusion through gel matrix may decrease the rate of systemic absorption and hence reduce the systemic side effects (Watts et al., 2009). Omitting sodium hyaluronate (sample B; Fig. 11a), adding gellan-gum at lower concentration (0.1%, *w/w*; sample C, Fig. 11b) and varying the surfactant concentration in the formulation (samples E and F; Fig. 11c) induced no significant change in release profile in relation to gel A. However, more pronounced reduction in release rate was achieved by the formulation containing

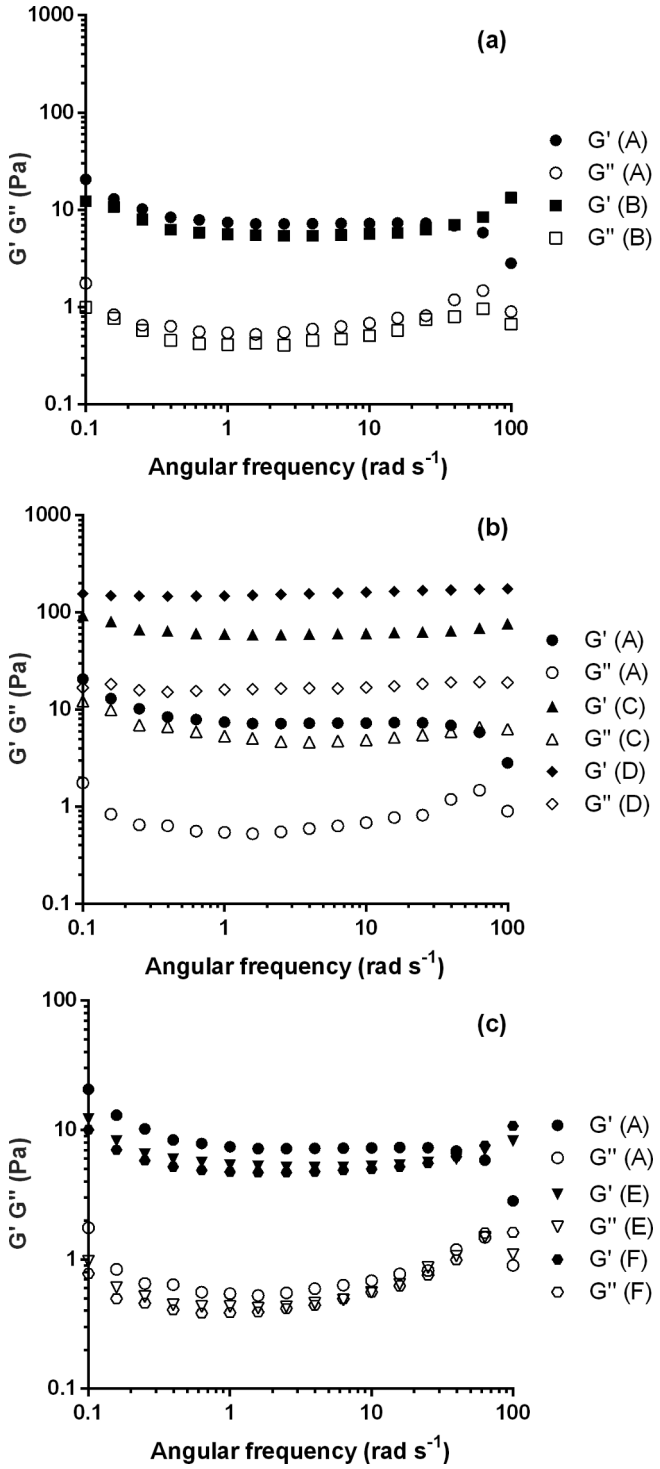

Fig. 10. Elastic (G′; filled symbol) and viscous (G″; open symbol) modulus as a function of angular frequency of *in situ* gelling fluticasone suspensions mixed with SNF. Fluticasone suspensions differed in: sodium hyaluronate (a; sample B), gellan gum (b; samples C and D) and Tween 80 (c; samples E and F) concentration from the reference suspension prepared with 0.058% fluticasone, 0.031% Tween 80, 0.66% pectin and 0.05% sodium hyaluronate (sample A).

gellan gum at the concentration of 0.2% (*w/w*), which is in line with the highest gel strength observed for the mentioned formulation. Considering low solubility of fluticasone, extensive reduction in its release rate could be unfavourable as it could impair the therapeutic effect (Jurišić Dukovski et al., 2017). Therefore, inclusion of gellan gum in the formulation at the concentration of 0.1% is proposed, revealing the

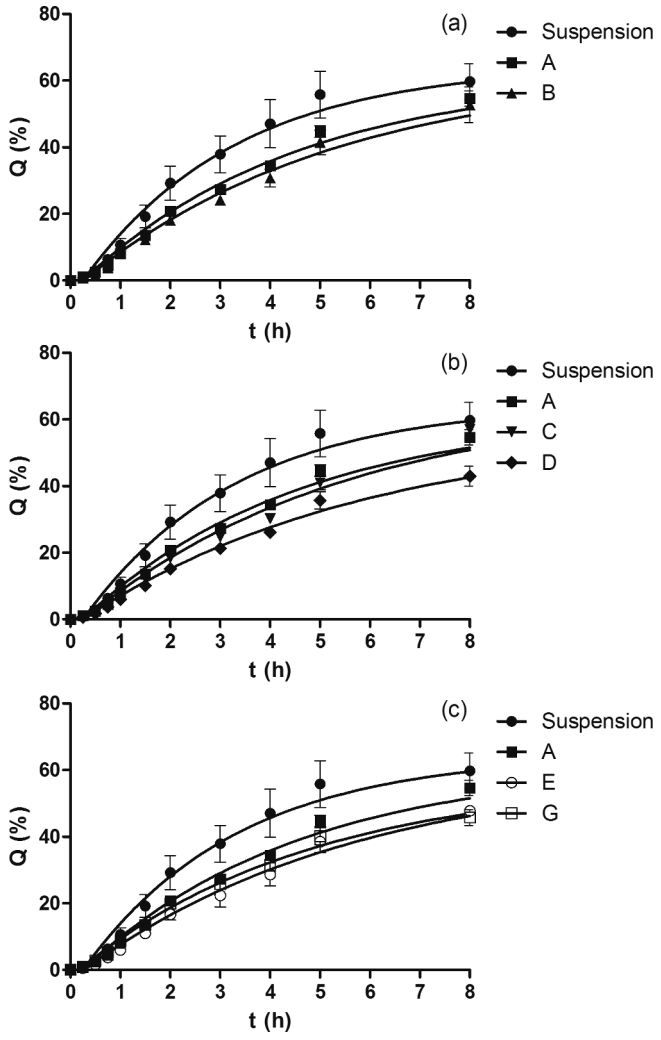

Fig. 11. *In vitro* release profiles of fluticasone from *in situ* gelling fluticasone suspensions determined using Franz diffusion cell and SNF/ethanol mixture in volume ratio 1:1 as a receptor medium. Fluticasone suspensions differed in: sodium hyaluronate (a; sample B), gellan gum (b; samples C and D) and Tween 80 (c; samples E and F) concentration from the reference suspension prepared with 0.058% fluticasone, 0.031% Tween 80, 0.66% pectin and 0.05% sodium hyaluronate (sample A). The release profile of fluticasone from aqueous suspension prepared with 0.058% fluticasone and 0.031% Tween 80 is also presented. Q represents the cumulative amount of drug released at time t. Data are expressed as the mean ± SD (n = 3).

formulation C to have the highest overall therapeutic potential. The leading formulation (C) is also in favour due to convenient administration parameters including administration angle of 45° and moderate inspiratory air flow (Table 3).

4. Conclusion

Herein, we propose the development of nasal *in situ* gelling fluticasone suspension considering the optimisation of deposition pattern in the early phase of formulation development. Regression models developed for investigated responses related to formulation sprayability and turbinate deposition exhibited suitable fit between experimental and predicted values, verifying their applicability in the well-designed formulation development. Further characterisation revealed gellan gum to be the crucial parameter for the optimisation of gel strength and fluticasone *in vitro* release, setting the basis for fine tuning of the overall formulation therapeutic potential to be conducted in the next phase of this study.

Declaration of interests

The authors declare that they have no known competing financial interests.

Acknowledgement

This work has been supported in part by Croatian Science Foundation under the project UIP-2017-05-4592.

References

Guideline on the Pharmaceutical Quality of Inhalation and Nasal Products, 2006. In: Committee for Medicinal Products for Human Use (CHMP), pp. 27. https://www.ema.europa.eu/en/documents/scientific-guideline/guideline-pharmaceutical-quality-inhalation-nasal-products_en.pdf; accessed December 28, 2019.

Altuntaş, E., Yener, G., 2017. Formulation and evaluation of thermoreversible in situ nasal gels containing mometasone furoate for allergic rhinitis. AAPS PharmSciTech 18, 2673–2682. https://doi.org/10.1208/s12249-017-0747-8.

Aulton, M.E., Taylor, K.M.G., 2013. Aulton's Pharmaceutics The Design and Manufacture of Medicines, fourth ed. Elsevier Ltd.

Bitter, C., Suter-Zimmermann, K., Surbera, C., 2011. Nasal drug delivery in humans. Curr. Probl. Dermatol. 40, 20–35.

Blomgren, K., Simola, M., Hytönen, M., Pitkäranta, A., 2003. Peak nasal inspiratory and expiratory flow measurements-practical tools in primary care? Rhinology 41, 206–210.

Cantone, E., Iengo, M., 2016. Effect of sodium hyaluronate added to topical corticosteroids in chronic rhinosinusitis with nasal polyposis. Am. J. Rhinol. Allergy 30, 340–343. https://doi.org/10.2500/ajra.2016.30.4344.

Cao, S. Lei, Ren, X. Wei, Zhang, Q. Zhi, Chen, E., Xu, F., Chen, J., Liu, L.C., Jiang, X. Guo, 2009. In situ gel based on gellan gum as new carrier for nasal administration of mometasone furoate. Int. J. Pharm. 365, 109–115. https://doi.org/10.1016/j.ijpharm.2008.08.042.

Casale, M., Moffa, A., Sabatino, L., Pace, A., Oliveto, G., Vitali, M., Baptista, P., Salvinelli, F., 2015. Hyaluronic acid: perspectives in upper aero-digestive tract. A systematic review. PLoS One 1, 1–17. https://doi.org/10.1371/journal.pone.0130637.

Castile, J., Cheng, Y.H., Simmons, B., Perelman, M., Smith, A., Watts, P., 2013. Development of in vitro models to demonstrate the ability of PecSys®, an in situ nasal gelling technology, to reduce nasal run-off and drip. Drug Dev. Ind. Pharm. 39, 816–824. https://doi.org/10.3109/03639045.2012.707210.

Cheng, Y.S., Holmes, T.D., Gao, J., Guilmette, R.A., Li, S., Surakitbanharn, Y., Rowlings, C., 2001. Characterization of nasal spray pumps and deposition pattern in a replica of the human nasal airway. J. Aerosol Med. 14, 267–280. https://doi.org/10.1089/08942680152484199.

Corley, R.A., Kabilan, S., Kuprat, A.P., Carson, J.P., Minard, K.R., Jacob, R.E., Timchalk, C., Glenny, R., Pipavath, S., Cox, T., Wallis, C.D., Larson, R.F., Fanucchi, M.V., Postlethwait, E.M., Einstein, D.R., 2012. Comparative computational modeling of airflows and vapor dosimetry in the respiratory tracts of rat, monkey, and human. Toxicol. Sci. 128, 500–516. https://doi.org/10.1093/toxsci/kfs168.

Dayal, P., Shaik, M.S., Singh, M., 2004. Evaluation of different parameters that affect droplet-size distribution from nasal sprays using the Malvern Spraytec®. J. Pharm. Sci. 93, 1725–1742. https://doi.org/10.1002/jps.20090.

Del Río-Navarro, B.E., Ito-Tsuchiya, F.M., Zepeda-Ortega, B., 2009. Rhinitis, sinusitis and allergy. Rev. Alerg. Mex. 56, 200–212. https://doi.org/10.1016/j.jaci.2009.12.989.

Fokkens, W., Reitsma, S., 2018. New delivery forms of nasal corticosteroids. J. Allergy Clin. Immunol. https://doi.org/10.1016/j.jaci.2018.10.037.

Foo, M.Y., Cheng, Y.-S., Su, W.-C., Donovan, M.D., 2007. The influence of spray properties on intranasal deposition. J. Aerosol Med. 20, 495–508. https://doi.org/10.1089/jam.2007.0638.

Gelardi, M., Iannuzzi, L., Quaranta, N., 2013. Intranasal sodium hyaluronate on the nasal cytology of patients with allergic and nonallergic rhinitis. Int. Forum Allergy Rhinol. 3, 807–813. https://doi.org/10.1002/alr.21193.

Ghaemi, S., Rahimi, P., Nobes, D.S., 2009. Assessment of parameters for distinguishing droplet shape in a spray field using image-based techniques. At. Sprays 19, 809–831.

Goos, P., Jones, B., 2011. Optimal Design of Experiments, first ed. .

Guo, C., Stine, K.J., Kauffman, J.F., Doub, W.H., 2008. Assessment of the influence factors on in vitro testing of nasal sprays using Box-Behnken experimental design. Eur. J. Pharm. Sci. 35, 417–426. https://doi.org/10.1016/j.ejps.2008.09.001.

Guo, Y., Laube, B., Dalby, R., 2005. The effect of formulation variables and breathing patterns on the site of nasal deposition in an anatomically correct model. Pharm. Res. 22, 1871–1878. https://doi.org/10.1007/s11095-005-7391-9.

Hao, J., Zhao, J., Zhang, S., Tong, T., Zhuang, Q., Jin, K., Chen, W., Tang, H., 2016. Fabrication of an ionic-sensitive in situ gel loaded with resveratrol nanosuspensions intended for direct nose-to-brain delivery. Colloids Surf. B: Biointerfaces 147, 376–386. https://doi.org/10.1016/j.colsurfb.2016.08.011.

Hoekman, J.D., Ho, R.J.Y., 2011. Effects of localized hydrophilic mannitol and hydrophobic nelfinavir administration targeted to olfactory epithelium on brain distribution. AAPS PharmSciTech 12, 534–543. https://doi.org/10.1208/s12249-011-9614-1.

Joshi, N., Rawat, K., Bohidar, H.B., 2016. Influence of structure, charge, and concentration on the pectin-calcium-surfactant complexes. J. Phys. Chem. B 120, 4249–4257. https://doi.org/10.1021/acs.jpcb.6b00016.

Jurišić Dukovski, B., Mrak, L., Winnicka, K., Szekalska, M., Juretić, M., Filipović-grčić, J., Pepić, I., Lovrić, J., Winnicka, K., Szekalska, M., Lovric, J., Hafner, A., 2019. Spray-dried nanoparticle-loaded pectin microspheres for dexamethasone nasal delivery. Dry. Technol. 1–11. https://doi.org/10.1080/07373937.2018.1545783.

Jurišić Dukovski, B., Plantić, I., Čunčić, I., Krtalić, I., Juretić, M., Pepić, I., Lovrić, J., Hafner, A., 2017. Lipid/alginate nanoparticle-loaded in situ gelling system tailored for dexamethasone nasal delivery. Int. J. Pharm. 533, 480–487. https://doi.org/10.1016/j.ijpharm.2017.05.065.

Kaneda, I., 2017. Rheology of Biological Soft Matter.

Karavasili, C., Fatouros, D.G., 2016. Smart materials: in situ gel-forming systems for nasal delivery. Drug Discov. Today 21, 157–166. https://doi.org/10.1016/j.drudis.2015.10.016.

Kimbell, J.S., Segal, R.A., Asgharian, B., Wong, B.A., Schroeter, J.D., Southall, J.P., Dickens, C.J., Brace, G., Miller, F.J., 2007. Characterization of deposition from nasal spray devices using a computational fluid dynamics model of the human nasal passages. J. Aerosol Med. 20, 59–74. https://doi.org/10.1089/jam.2006.0531.

Kundoor, V., Dalby, R.N., 2010. Assessment of nasal spray deposition pattern in a silicone human nose model using a color-based method. Pharm. Res. 27, 30–36. https://doi.org/10.1007/s11095-009-0002-4.

Leopold, D.A., Elkayam, D., Messina, J.C., Kosik-Gonzalez, C., Djupesland, P.G., Mahmoud, R.A., 2018. NAVIGATE II: randomized, double-blind trial of the exhalation delivery system with fluticasone for nasal polyposis. J. Allergy Clin. Immunol. https://doi.org/10.1016/j.jaci.2018.06.010.

Lungare, S., Bowen, J., Badhan, R., 2016. Development and evaluation of a novel intranasal spray for the delivery of amantadine. J. Pharm. Sci. 105, 1209–1220. https://doi.org/10.1016/j.xphs.2015.12.016.

Mahdi, M.H., Conway, B.R., Smith, A.M., 2015. Development of mucoadhesive sprayable gellan gum fluid gels. Int. J. Pharm. 488, 12–19. https://doi.org/10.1016/j.ijpharm.2015.04.011.

Martino, B.J., Church, C.A., Seiberling, K.A., 2015. Effect of intranasal dexamethasone on endogenous cortisol level and intraocular pressure. Int. Forum Allergy Rhinol. 5, 605–609. https://doi.org/10.1002/alr.21514.

Mezger, T.G., 2006. The Rheology Handbook For Users of Rotational and Oscillatory Rheometers, second ed. Vincentz Network, Hanover, Germany.

Moraga-Espinoza, D., Warnken, Z., Moore, A., Williams, R.O., Smyth, H.D.C., 2018. A modified USP induction port to characterize nasal spray plume geometry and predict turbinate deposition under flow. Int. J. Pharm. 548, 305–313. https://doi.org/10.1016/j.ijpharm.2018.06.058.

Moura, M.J., Figueiredo, M.M., Gil, M.H., 2007. In: Rheological Study of Genipin Cross-Linked Chitosan Hydrogels, pp. 3823–3829.

Osma, T., Froelich, A., Tasarek, S., 2014. Application of gellan gum in pharmacy and medicine. Int. J. Pahrm. https://doi.org/10.1016/j.ijpharm.2014.03.038.

Ottaviano, G., Scadding, G.K., Coles, S., Lund, V.J., 2006. Peak nasal inspiratory flow; normal range in adult population. Rhinology 44, 32–35. https://doi.org/10.1021/cm300881t.

Pandey, P., Cabot, P.J., Wallwork, B., Panizza, B.J., Parekh, H.S., 2017. Formulation, functional evaluation and ex vivo performance of thermoresponsive soluble gels – a platform for therapeutic delivery to mucosal sinus tissue. Eur. J. Pharm. Sci. 96, 499–507. https://doi.org/10.1016/j.ejps.2016.10.017.

Pu, Y., Goodey, A.P., Fang, X., Jacob, K., 2014. A comparison of the deposition patterns of different nasal spray formulations using a nasal cast. Aerosol Sci. Technol. 48, 930–938. https://doi.org/10.1080/02786826.2014.931566.

Salunke, S.R., Patil, S.B., 2016. Ion activated in situ gel of gellan gum containing salbutamol sulphate for nasal administration. Int. J. Biol. Macromol. 87, 41–47. https://doi.org/10.1016/j.ijbiomac.2016.02.044.

Ta, H.T., Han, H., Larson, I., Dass, C.R., Dunstan, D.E., 2009. Chitosan-dibasic orthophosphate hydrogel: a potential drug delivery system. Int. J. Pharm. 371, 134–141. https://doi.org/10.1016/j.ijpharm.2009.01.018.

Warnken, Z.N., Smyth, H.D.C., Davis, D.A., Weitman, S., Kuhn, J.G., Williams, R.O., 2018. Personalized medicine in nasal delivery: the use of patient-specific administration parameters to improve nasal drug targeting using 3D-printed nasal replica casts. Mol. Pharm. 15, 1392–1402. https://doi.org/10.1021/acs.molpharmaceut.7b00702.

Watts, P., Smith, A., Perelman, M., 2013. Nasal delivery of fentanyl. Drug Deliv. Transl. Res. 75–83. https://doi.org/10.1007/s13346-012-0078-y.

Watts, P., Smith, A., Watts, P., Smith, A., 2009. PecSys : in situ gelling system for optimised nasal drug delivery. Expert Opin Drug Deliv 5247. https://doi.org/10.1517/17425240902939135.

Winter, H.H., Chambon, F., 1986. Analysis of linear viscoelasticity of a crosslinking polymer at the gel point analysis of linear viscoelasticity of a crosslinking polymer at the gel point. J. Rheol. 367. https://doi.org/10.1122/1.549853.

Xi, J., Kim, J.W., Si, X.A., Corley, R.A., Zhou, Y., 2016. Modeling of inertial deposition in scaled models of rat and human nasal airways: towards in vitro regional dosimetry in small animals. J. Aerosol Sci. 99, 78–93. https://doi.org/10.1016/j.jaerosci.2016.01.013.

Xi, J., Wang, Z., Si, X.A., Zhou, Y., 2018. Nasal dilation effects on olfactory deposition in unilateral and bi-directional deliveries: in vitro tests and numerical modeling. Eur. J. Pharm. Sci. 118, 113–123. https://doi.org/10.1016/j.ejps.2018.03.027.

Xu, X., Shen, Y., Wang, W., Sun, C., Li, C., Xiong, Y., Tu, J., 2014. Preparation and in vitro characterization of thermosensitive and mucoadhesive hydrogels for nasal delivery of phenylephrine hydrochloride. Eur. J. Pharm. Biopharm. 5–11. https://doi.org/10.1016/j.ejpb.2014.08.015.

Ye, X., Li, X., Shen, Y., Chang, G., Yang, J., Gu, Z., 2016. Self-healing pH-sensitive cytosine- and guanosine-modified hyaluronic acid hydrogels via hydrogen bonding. Polymer. https://doi.org/10.1016/j.polymer.2016.11.063.

Yin, D.S., Yang, W.Y., Ge, Z.Q., Yuan, Y.J., 2005. A fluorescence study of sodium hyaluronate/surfactant interactions in aqueous media. Carbohydr. Res. 340, 1201–1206. https://doi.org/10.1016/j.carres.2005.01.017.

Younes, M., Aggett, P., Aguilar, F., Crebelli, R., Filipic, M., Frutos, M.J., Galtier, P., Gott, D., Gundert-remy, U., Kuhnle, G.G., Leblanc, J., Lillegaard, I.T., Moldeus, P., Mortensen, A., Oskarsson, A., Stankovic, I., Waalkens-berendsen, I., Woutersen, R.A., Wright, M., Brimer, L., Mosesso, P., Christodoulidou, A., Cascio, C., Tard, A., Lodi, F., Dusemund, B., 2018. In: Re-evaluation of gellan gum (E 418) as food additive, pp. 16. https://doi.org/10.2903/j.efsa.2018.5296.

Zaki, N.M., Awad, G.A., Mortada, N.D., Abd, S.S., 2007. Enhanced bioavailability of metoclopramide HCl by intranasal administration of a mucoadhesive in situ gel with modulated rheological and mucociliary transport properties. Eur. J. Pharm. Sci. 2, 296–307. https://doi.org/10.1016/j.ejps.2007.08.006.

3.A Dry Powder Platform for Nose-To-Brain Delivery of Dexamethasone: Formulation Development and Nasal Deposition Studies

pharmaceutics

MDPI

Article

A Dry Powder Platform for Nose-To-Brain Delivery of Dexamethasone: Formulation Development and Nasal Deposition Studies

Laura Nižić Nodilo [1], Ivo Ugrina [2], Drago Špoljarić [3], Daniela Amidžić Klarić [1], Cvijeta Jakobušić Brala [1], Mirna Perkušić [1], Ivan Pepić [1], Jasmina Lovrić [1], Vesna Saršon [4], Maša Safundžić Kučuk [4], Dijana Zadravec [5], Livije Kalogjera [6] and Anita Hafner [1,*]

[1] Faculty of Pharmacy and Biochemistry, University of Zagreb, 10000 Zagreb, Croatia; lnizic@pharma.hr (L.N.N.); damidzic@pharma.hr (D.A.K.); cjakobus@pharma.hr (C.J.B.); mperkusic@pharma.hr (M.P.); ipepic@pharma.hr (I.P.); jlovric@pharma.hr (J.L.)
[2] Faculty of Science, University of Split, 21000 Split, Croatia; iugrina@pmfst.hr
[3] Visage Technologies d.o.o., 10000 Zagreb, Croatia; drago.spoljaric@visagetechnologies.com
[4] Jadran-Galenski Laboratorij d.d., 51000 Rijeka, Croatia; vesna.sarson@jgl.hr (V.S.); masa.safundzic@jgl.hr (M.S.K.)
[5] Department of Diagnostic and Interventional Radiology, University Hospital Center "Sestre milosrdnice", University of Zagreb, 10000 Zagreb, Croatia; zadravec@sfzg.hr
[6] ORL/HNS Department, Zagreb School of Medicine, University Hospital Center "Sestre milosrdnice", University of Zagreb, 10000 Zagreb, Croatia; kalogjera@sfzg.hr
* Correspondence: anita.hafner@pharma.unizg.hr

Citation: Nižić Nodilo, L.; Ugrina, I.; Špoljarić, D.; Amidžić Klarić, D.; Jakobušić Brala, C.; Perkušić, M.; Pepić, I.; Lovrić, J.; Saršon, V.; Safundžić Kučuk, M.; et al. A Dry Powder Platform for Nose-To-Brain Delivery of Dexamethasone: Formulation Development and Nasal Deposition Studies. *Pharmaceutics* **2021**, *13*, 795. https://doi.org/10.3390/pharmaceutics13060795

Academic Editor: Piroska Szabó-Révész

Received: 30 March 2021
Accepted: 20 May 2021
Published: 26 May 2021

Abstract: Nasal route of administration offers a unique opportunity of brain targeted drug delivery via olfactory and trigeminal pathway, providing effective CNS concentrations at lower doses and lower risk for adverse reactions compared to systemic drug administration. Therefore, it has been recently proposed as a route of choice for glucocorticoids to control neuroinflammation processes in patients with severe Covid-19. However, appropriate delivery systems tailored to enhance their efficacy yet need to emerge. In this work we present the development of sprayable brain targeting powder delivery platform of dexamethasone sodium phosphate (DSP). DSP-loaded microspheres, optimised employing Quality-by-Design approach, were blended with soluble inert carriers (mannitol or lactose monohydrate). Powder blends were characterized in terms of homogeneity, flow properties, sprayability, in vitro biocompatibility, permeability and mucoadhesion. Nasal deposition studies were performed using 3D printed nasal cavity model. Mannitol provided better powder blend flow properties compared to lactose. Microspheres blended with mannitol retained or enlarged their mucoadhesive properties and enhanced DSP permeability across epithelial model barrier. DSP dose fraction deposited in the olfactory region reached 17.0% revealing the potential of developed powder platform for targeted olfactory delivery. The observed impact of nasal cavity asymmetry highlighted the importance of individual approach when aiming olfactory region.

Keywords: dexamethasone sodium phosphate; nose-to-brain delivery; spray-dried microspheres; pectin; hypromellose; mannitol; 3D nasal cavity model; in vitro nasal deposition

1. Introduction

The nasal route of administration offers a variety of therapeutic opportunities, including local-, systemic- and brain-targeted drug delivery. Currently it is attracting increasing scientists' attention as a promising route of drug delivery in Covid-19 patients [1,2], particularly in severe cases presenting with central nervous system manifestations [3]. In particular nasally delivered drugs can easily access the CNS via the olfactory and trigeminal nerves bypassing the blood-brain barrier, thus providing effective CNS concentrations at lower doses and at lower risk for adverse reactions compared to systemic drug administration [4].

Nasal delivery of glucocorticoids has been proposed as an effective strategy to control neuroinflammation processes in patients with severe Covid-19, avoiding problems related to systemic application of high glucocorticoid doses [5]. Previously it was shown that nasally applied dexamethasone resulted in more efficient control of lipopolysaccharide-induced murine neuroinflammation when compared to intravenous administration of dexamethasone at the same dose [6]. Furthermore, nasal delivery of corticosteroids targeting olfactory region can be considered in the treatment of anosmia and hyposmia, frequently seen in Covid-19 patients [7].

The extent of direct nose-to-brain drug delivery greatly depends on the properties of drug delivery system and ability to reach targeted regions of nasal cavity [8]. Nasal powders offer important advantages over liquid formulations, including increased stability without the use of preservatives, prolonged residence time and higher drug concentration at nasal mucosa [9,10]. Powder formulations were previously shown as promising platforms for nose-to-brain drug delivery, as evidenced by animal studies [11–15]. However, the potential for nose-to-brain delivery in man cannot be easily drawn from data obtained in animal models due to discrepancy in their anatomical features [4].

In this work we present the development of nasal powder delivery platform for dexamethasone sodium phosphate (DSP), including consideration of nasal deposition in the early phase of formulation development. To our best knowledge, up to now there were no studies related to development of delivery system intended for nose-to-brain delivery of dexamethasone or its derivatives.

DSP is an ester prodrug of dexamethasone, freely soluble in water. When formulated in the dry powder form, it is expected to rapidly dissolve in contact with nasal fluid and to provide high drug concentration on the surface of the nasal epithelium, favouring drug absorption. On the other hand, due to its anionic nature, DSP is less permeable than dexamethasone base. Generally, for drugs with high solubility and low permeability, the rate limiting step in absorption process is the permeation across the nasal epithelium and in such cases, increase in nasal retention time is expected to augment the absorption the most [10]. Furthermore, absorption of phosphate ester prodrugs is promoted by their conversion to more permeable form by phosphatases that are present in human olfactory and respiratory nasal mucosa [16–18]. Antunes Viegas and co-workers demonstrated bioconversion of phosphate ester fosphenytoin to more permeable phenytoin by phosphatases in nasal porcine mucosa and nasal mucus from healthy human volunteers. In addition, they demonstrated nasal permeation potential of fosphenytoin itself. Recent study on fosphenytoin administration in mice proved the applicability of phosphate esters as useful strategy in nose-to-brain delivery of poorly soluble drugs [17,19].

Herein we propose a powder system consisting of spray-dried DSP-loaded pectin/hypromellose microspheres blended with mannitol or lactose monohydrate as inert carrier. Blending of microspheres with an inert carrier represents effective strategy to improve powder applicability. In optimised systems, drug-loaded microspheres as fine particles adhere to coarse carrier particles resulting in highly homogenous blend with improved dispersibility and nasal deposition profile [20,21].

A microsphere matrix composed of mucoadhesive polymers hypromellose and pectin is aimed to provide optimal swelling and drug release in contact with nasal fluid, ensuring prolonged retention at the deposition site and adequate rate and extent of drug delivery [22]. Furthermore, cellulose powder is well known gel forming (i.e., mechanical barrier forming) inert substance that is being used for the management and prevention of allergic rhinitis protecting mucosa from contact with allergens [23–25]. In that sense, it is reasonable to expect that the same concept might be applied to prevent the contact with airborne viruses, lowering the chance for viral respiratory co-infections.

In this study DSP-loaded microspheres were prepared by a spray drying method. The quality-by-design concept was applied to optimise the formulation (DSP and hypromellose concentration in the spray-drying feed) and process parameters (inlet air temperature and feed flow rate) in relation to microspheres' physico-chemical properties, including process

yield, DSP entrapment efficiency, residual moisture content, microsphere size and swelling properties. Optimised microspheres blended with inert carrier at different ratios were further characterised in terms of powder blend homogeneity, sprayability/flow properties, behaviour in contact with simulated nasal fluid, biocompatibility and DSP permeability across in vitro model of respiratory epithelial barrier. Nasal deposition pattern of the powder blend at various administration parameters was studied using 3D printed nasal cavity model, complementing the screening of its potential to ensure desired therapeutic effect.

2. Materials and Methods

2.1. Materials

DSP was purchased from Carbosynth Ltd. (Compton, UK). Low methoxy amidated pectin (CF 005, degree of esterification 35%; degree of amidation 15%; further denoted as pectin) was kindly donated by Herbstreith & Fox (Neuenbürg, Germany). Hypromellose (Metolose® SH 4000) was obtained by courtesy of Shin-Etsu Chemical Co., Ltd., Tokyo, Japan. Lactose monohydrate (GranuLac® 200; further denoted as lactose) was obtained from Meggle (Wasserburg am Inn, Germany). Mannitol was purchased from BDH Prolabo (Lutterworth, UK). Simulated Nasal Fluid (SNF) was prepared by dissolving NaCl (150.0 mM; Kemig, Zagreb, Croatia), KCl (40.0 mM; Kemig) and $CaCl_2 \times H_2O$ (5.3 mM; Sigma-Aldrich, Munich, Germany) in distilled water.

For cell biocompatibility and permeability studies in vitro, Hank's balanced salt solution with 5.3 mM Ca^{2+} (HBSS-Ca^{2+}; pH 7.4) was prepared by dissolving KCl (5.4 mM), $NaHCO_3$ (4.2 mM), NaCl (136.9 mM), D-glucose monohydrate (5.6 mM) (all purchased from Kemig), KH_2PO_4 (0.4 mM; Kemika, Zagreb, Croatia), $Na_2HPO_4 \times 2H_2O$ (0.3 mM; Fluka Chemie AG, Buchs, Switzerland) and $CaCl_2 \times 2H_2O$ (5.3 mM) (Sigma-Aldrich) in distilled water.

2.2. Statistical Design of Experiments

In order to optimise the formulation and process parameters for effective preparation of DSP-loaded microspheres suitable for nasal delivery, quality by design (QbD) principles were employed. The influence of four parameters at three levels was studied with a custom D-optimal experimental design that included varying formulation parameters such as the concentration of DSP and hypromellose and process parameters such as inlet air temperature and feed flow rate (Supplementary Materials; Table S1). To properly define design space i.e., lower and upper limits for parameter intervals from which corresponding parameter values in design will be chosen, preliminary experiments were performed. Spray drying process yield, drug loading (DL), entrapment efficiency (EE), particle size distribution, moisture content (MC) and swelling properties were investigated as responses. The analyses related to the responses were performed in triplicates, except for MC which was measured in duplicate. Design of experiments and data analyses were performed with the statistical software JMP 14.0 (JMP®, Version 14.0, SAS Institute Inc., Cary, NC, USA, ©1989–2007).

2.3. Preparation of Microspheres

DSP-loaded microspheres were prepared by spray drying of aqueous solutions of DSP and polymers—pectin and hypromellose. Firstly, concentrated aqueous solution of pectin (1.4%, *w*/*w*) and another of hypromellose (1.2%, *w*/*w*) were prepared. Pectin was dissolved at room temperature under stirring conditions for 24 h. Hypromellose solution was obtained after heating the water at 80–90 °C, followed by 24-h stirring at room temperature and storage in the refrigerator afterwards. DSP was dissolved in distilled water at concentrations of 1.0 and 10.0% (*w*/*w*). Spray-drying feed sample was prepared by mixing pectin and hypromellose solutions in suitable ratios, followed by addition of DSP solution, and distilled water when needed. Concentrations of polymers and DSP in feed solutions are shown in Table 1.

Table 1. Sample sequence from design of experiment and corresponding spray drying process yield, microspheres drug loading (DL), drug entrapment efficiency (EE), particle size distribution (*D*v10, *D*v50, *D*v90 and *D*[4,3]), residual moisture content (MC) and swelling properties expressed as volume of SNF (V_{SNF}) and water (V_{water}) absorbed per mg of microspheres in the swelling process.

	HPMC (%; *w*/*w*)	DSP (%; *w*/*w*)	T_{inlet} (°C)	FFR (g min^{-1})	Yield (%)	DL (%)	EE (%)	*D*v10 (μm)	*D*v50 (μm)	*D*v90 (μm)	*D*[4,3] (μm)	MC (%)	V_{SNF} (μL mg^{-1})	V_{water} (μL mg^{-1})
1	0.2	0.20	120	4.5	48.2	32.4 ± 0.5	97.2 ± 1.6	1.6 ± 0.0	2.7 ± 0.0	5.8 ± 0.1	3.3 ± 0.0	6.9 ± 0.6	13.6 ± 2.9	26.2 ± 4.2
2	1.0	0.20	160	4.5	52.4	14.6 ± 0.0	101.9 ± 0.3	1.9 ± 0.0	5.0 ± 0.0	17.7 ± 0.4	7.7 ± 0.1	4.7 ± 0.2	15.5 ± 1.4	22.4 ± 1.0
3	0.2	0.02	120	2.5	58.5	5.1 ± 1.6	97.9 ± 10.1	1.4 ± 0.0	2.2 ± 0.0	4.9 ± 0.0	2.0 ± 1.2	6.2 ± 0.4	11.7 ± 1.8	37.0 ± 2.0
4	0.6	0.11	140	3.5	63.5	11.7 ± 0.15	97.1 ± 1.2	1.6 ± 0.0	2.9 ± 0.0	8.1 ± 0.0	4.0 ± 0.0	5.0 ± 0.1	16.5 ± 2.6	20.7 ± 3.2
5	0.6	0.11	140	3.5	65.2	11.7 ± 0.15	97.1 ± 1.3	1.6 ± 0.0	3.0 ± 0.0	11.4 ± 0.4	5.0 ± 0.1	5.0 ± 0.1	16.1 ± 0.7	24.5 ± 0.4
6	0.2	0.02	120	4.5	50.7	4.3 ± 0.2	91.3 ± 3.2	1.4 ± 0.0	2.2 ± 0.0	4.4 ± 0.0	2.7 ± 0.0	5.7 ± 1.4	17.5 ± 2.2	39.2 ± 3.4
7	1.0	0.02	120	2.5	38.8	1.5 ± 0.0	91.8 ± 0.4	1.8 ± 0.0	3.3 ± 0.0	12.3 ± 0.1	5.4 ± 0.0	3.6 ± 0.5	16.3 ± 3.7	27.9 ± 2.0
8	1.0	0.20	120	4.5	25.2	13.2 ± 0.0	96.6 ± 5.8	1.8 ± 0.0	7.3 ± 0.9	36.6 ± 2.4	13.6 ± 0.3	3.2 ± 0.8	9.7 ± 1.4	16.0 ± 1.6
9	0.2	0.02	160	2.5	56.9	4.7 ± 0.0	98.6 ± 0.6	1.4 ± 0.0	2.2 ± 0.0	6.3 ± 0.0	3.6 ± 0.0	6.9 ± 0.5	14.8 ± 1.6	40.6 ± 4.0
10	0.2	0.20	160	4.5	68.6	31.7 ± 0.3	95.1 ± 1.0	1.6 ± 0.0	2.6 ± 0.0	5.1 ± 0.1	3.0 ± 0.0	6.6 ± 0.1	8.8 ± 1.0	24.8 ± 0.8
11	1.0	0.20	120	2.5	55.0	13.8 ± 0.3	99.4 ± 4.6	1.9 ± 0.0	4.1 ± 0.0	13.5 ± 0.3	6.9 ± 0.2	6.6 ± 0.0	15.0 ± 1.1	15.0 ± 3.7
12	0.2	0.02	160	4.5	53.2	4.6 ± 0.1	97.1 ± 1.6	1.4 ± 0.0	2.2 ± 0.0	4.4 ± 0.0	2.6 ± 0.0	7.7 ± 0.2	14.7 ± 2.9	41.6 ± 3.4
13	1.0	0.02	160	4.5	59.2	1.3 ± 0.0	85.2 ± 4.8	1.7 ± 0.0	3.6 ± 0.0	15.3 ± 0.3	5.4 ± 0.0	5.9 ± 0.0	14.3 ± 0.5	23.9 ± 1.0
14	0.2	0.20	160	4.5	66.6	31.7 ± 0.3	95.1 ± 1.0	1.7 ± 0.0	2.9 ± 0.0	6.0 ± 0.0	3.4 ± 0.0	6.6 ± 0.1	9.4 ± 1.0	21.9 ± 0.7
15	1.0	0.02	160	2.5	55.1	1.5 ± 0.0	97.6 ± 8.7	1.6 ± 0.0	3.1 ± 0.0	12.9 ± 0.0	5.4 ± 0.0	4.5 ± 1.9	23.5 ± 1.9	32.7 ± 0.5
16	1.0	0.02	120	2.5	65.9	1.5 ± 0.0	91.8 ± 0.6	2.0 ± 0.0	4.0 ± 0.0	10.8 ± 0.2	5.3 ± 0.1	3.6 ± 0.5	13.8 ± 2.7	30.2 ± 1.7
17	1.0	0.20	160	2.5	46.6	14.3 ± 0.1	101.6 ± 1.6	2.2 ± 0.1	13.7 ± 0.5	21.4 ± 0.9	13.3 ± 0.6	5.1 ± 0.1	19.5 ± 2.8	24.2 ± 2.2
18	0.2	0.20	120	2.5	56.7	32.9 ± 0.2	92.3 ± 8.9	1.5 ± 0.0	2.4 ± 0.0	4.8 ± 0.0	2.8 ± 0.0	9.1 ± 0.2	21.5 ± 1.4	35.7 ± 3.8
19	0.2	0.02	120	4.5	32.8	4.6 ± 0.4	96.7 ± 8.8	1.5 ± 0.0	2.2 ± 0.0	3.7 ± 0.0	2.4 ± 0.0	5.7 ± 1.4	14.7 ± 0.7	37.9 ± 3.0
20	0.2	0.02	160	4.5	51.7	4.6 ± 0.1	97.1 ± 1.6	1.5 ± 0.0	2.7 ± 0.0	7.1 ± 0.3	3.9 ± 0.2	7.7 ± 0.2	20.2 ± 2.9	32.1 ± 2.7
21	1.0	0.02	120	4.5	30.9	1.6 ± 0.1	100.4 ± 6.4	2.3 ± 0.0	12.7 ± 0.1	42.9 ± 0.6	18.0 ± 0.2	4.1 ± 0.4	9.9 ± 2.1	18.3 ± 0.4
22	1.0	0.20	120	4.5	13.9	13.2 ± 0.0	87.4 ± 7.2	2.0 ± 0.0	5.1 ± 0.2	34.0 ± 4.0	11.4 ± 0.3	3.2 ± 0.8	9.7 ± 1.4	16.0 ± 1.6
23	0.6	0.11	140	3.5	62.8	11.7 ± 0.2	97.1 ± 1.3	1.6 ± 0.0	2.8 ± 0.0	9.2 ± 0.4	4.4 ± 0.2	6.0 ± 0.2	6.1 ± 1.6	17.0 ± 3.3
24	0.2	0.20	160	2.5	57.0	33.5 ± 0.4	100.6 ± 1.3	1.5 ± 0.0	2.9 ± 0.0	8.2 ± 0.2	4.3 ± 0.1	8.7 ± 0.3	7.4 ± 2.1	23.6 ± 1.1
25	0.6	0.11	140	3.5	60.4	11.7 ± 0.2	97.1 ± 1.3	1.6 ± 0.0	2.7 ± 0.0	9.8 ± 0.3	4.7 ± 0.2	6.0 ± 0.2	9.4 ± 1.9	20.6 ± 0.9
26	0.2	0.20	120	4.5	42.8	32.4 ± 0.5	97.2 ± 1.6	1.7 ± 0.0	2.8 ± 0.0	5.3 ± 0.0	3.2 ± 0.0	6.9 ± 0.6	16.0 ± 0.6	23.8 ± 1.5
27	1.0	0.20	160	4.5	59.4	13.8 ± 0.2	96.6 ± 1.2	2.5 ± 0.0	6.5 ± 0.1	14.8 ± 0.6	7.7 ± 0.2	4.7 ± 0.2	15.5 ± 1.4	22.4 ± 1.0
28	1.0	0.02	120	4.5	25.9	1.6 ± 0.1	100.4 ± 6.4	1.7 ± 0.0	3.5 ± 0.0	36.0 ± 1.1	12.2 ± 0.4	4.1 ± 0.4	13.5 ± 0.7	22.5 ± 0.9
29	1.0	0.02	160	4.5	67.3	1.5 ± 0.1	93.9 ± 9.1	1.9 ± 0.0	3.9 ± 0.0	12.7 ± 0.1	5.8 ± 0.0	5.9 ± 0.0	14.3 ± 0.5	23.9 ± 1.0
30	0.2	0.20	120	2.5	57.5	32.9 ± 0.2	96.5 ± 3.0	1.5 ± 0.0	2.6 ± 0.0	6.3 ± 0.1	3.8 ± 0.1	9.1 ± 0.2	21.5 ± 1.4	35.7 ± 3.8
31	1.0	0.20	120	2.5	43.3	13.8 ± 0.3	96.4 ± 1.9	2.3 ± 0.0	14.9 ± 3.4	36.7 ± 7.8	18.5 ± 3.8	6.6 ± 0.0	13.4 ± 0.9	17.3 ± 0.9
32	1.0	0.20	160	2.5	55.6	14.3 ± 0.1	99.2 ± 1.9	2.6 ± 0.3	14.8 ± 2.0	26.7 ± 0.1	13.8 ± 0.0	5.1 ± 0.1	14.1 ± 0.5	19.4 ± 1.6

HPMC = hypromellose concentration in the spray drying solution; DSP = dexamethasone sodium phosphate concentration in the spray drying solution; T_{inlet} = inlet air temperature; FFR = feed flow rate. Values for the responses are mean ± SD, n = 3 (except for MC where n = 2).

DSP-loaded microspheres were obtained by spray-drying using a Büchi Mini Spray Dryer B–190 (Büchi, Flawil, Switzerland) equipped with a standard 0.7 mm nozzle. Two of the process parameters (aspirator capacity and compressed airflow) were constant, while inlet air temperature and feed flow rate varied between 120 and 160 °C and 2.5 and 4.5 g min^{-1}, respectively. The process yield of each experiment was calculated as the ratio between the weight of obtained microspheres and the weight of DSP and polymers used for the preparation of the solution to be spray-dried.

2.4. Determination of Entrapment Efficiency and DSP Loading

The amount of DSP entrapped within the spray-dried microspheres was determined by the high performance liquid chromatography (HPLC) method as described in the Section 2.20. Microspheres (20 mg) were dispersed in distilled water and stirred for 24 h. Dispersion was filtered (0.2 µm) and analysed for DSP content. Each formulation was analysed in triplicate. Entrapment efficiency (EE) was determined as follows (Equation (1)):

$$\text{EE } (\%) = Q_a / Q_t \times 100 \quad (1)$$

where Q_a is the actual drug content in the examined amount of microspheres and Q_t is theoretical drug content in the examined amount of microspheres.

Drug loading (DL) was calculated using the following equation (Equation (2)):

$$\text{DL } (\%) = Q_a / Q_m \times 100 \quad (2)$$

where Q_m is the examined amount of microspheres.

2.5. Particle Size Distribution Measurement

Particle size distribution was determined by laser diffraction using a Malvern Mastersizer 3000 (Malvern Instruments Ltd., Malvern, UK), with a focal length of 300 mm, equipped with Hydro MV sample cell equipped with a magnetic stirrer. Approximately 5 mg of microspheres were dispersed in about 10 mL of ethanol (96%) by sonication in an ultrasonic bath until the suspension was homogeneous. Prior to the measurement, a background reading was made and the microsphere suspension was added to the Hydro MV cell until a 10–30% obscuration was reached. Before starting the measurement, the samples were equilibrated for 10 s. Each sample was analysed in triplicate. The results were expressed as volume diameters *D*v10, *D*v50 and *D*v90 and volume-weighted mean diameter *D*[4,3].

2.6. Moisture Content Determination

The moisture content in microspheres was analysed by thermogravimetric analysis using TGA Q500 (TA Instruments, New Castle, DE, USA). A small amount of microspheres was heated under dynamic nitrogen atmosphere of 25 mL min^{-1} to 150 °C at a rate of 10 °C min^{-1}. Each sample was tested in duplicate. Moisture content was calculated using the following equation (Equation (3)):

$$\text{MC } (\%) = \frac{m_0 - m_e}{m_0} \times 100 \quad (3)$$

where m_0 and m_e are the weights of the powder at the beginning and at the end of experiment, respectively.

2.7. Swelling Study

Swelling properties of microspheres were analysed by an indirect method previously developed by our research group that includes using a Franz diffusion cell [22,26]. Microspheres were weighed (10 mg) directly on the polyamide membrane with 0.45 µm pore size (Sartorius Stedim Biotech GmbH, Goettingen, Germany), covering evenly the membrane surface. The receiver compartment was filled up with SNF or distilled water

thermostated at 34 °C. At predetermined time intervals (3, 6, 9, 12 and 15 min), the receiver compartment was filled with fresh medium up to the initial level that lowered due to SNF/water uptake of the powder samples, using graduated microliter syringe (Hamilton, Bonaduz, Switzerland). Swelling properties of formulations were expressed as a volume of the medium uptaken by milligram of the microspheres. Three replicate measurements were performed for each sample.

2.8. Zeta-Potential Analysis

Zeta-potential of the microspheres was determined using Zetasizer Nano ZSP (Malvern Instruments) upon dispersion in 10 mM NaCl. All measurements were carried out at 25 °C. Each sample was analysed in triplicate.

2.9. In Vitro *Release Study*

In vitro DSP release study was performed using a Franz diffusion cell apparatus (25 mm: 20 mL volume, PermeGear, Hellertown, PA, USA) in which the receiver compartment was filled up with SNF and thermostated at 34 °C. In preliminary experiments, DSP was proven to be stable in SNF, at both 25 °C and 34 °C for 24 h. Sink conditions were provided during the whole experiment. The receiving medium was magnetically stirred during the whole experiment. The amount of (microspheres) powder sample containing 1.5 mg of DSP was weighed on the polyamide membrane (0.45 µm pore size) inserted between the donor and the receiver compartment. At scheduled time intervals, the samples (0.5 mL) were withdrawn from the receiver compartment and replaced with fresh medium in the total duration of 3 h. DSP content in the taken samples was determined by HPLC method as described in the Section 2.20. Each experiment was performed in triplicate.

2.10. Preparation of Powder Blends

Lactose and mannitol powders with particle size ranging between 45 and 63 µm were used as carriers. This powder fraction was separated using a laboratory sieve shaker (Vibratory Sieve Shaker AS 200, Retsch, Haan, Germany) equipped with 20 cm diameter sieves (Retsch®; nominal aperture 63 and 45 µm). The system was vibrated for 10 min at an amplitude of 50%. Powder blends were prepared by mixing microsphere and carrier powder at 1:9 and 1:19 weight ratios. After premixing for 5 min using MX-S vortex mixer (1250 rpm; DLAB Scientific Co. Ltd., Beijing, China) in 50 mL centrifuge tube (Falcon®, Corning Costar Inc. Tewksbury, MA, USA), microspheres and carrier were transferred in 1.5 mL centrifuge tube (Eppendorf, Hamburg, Germany) and mixed using a Turbula® shaker mixer (WAB Group, Muttenz, Switzerland) operating for 10 min at 70 rpm.

Homogeneity of microspheres/carrier blends was evaluated based on the analysis of drug content in the powder samples (10 mg) taken from the top, centre and bottom of the centrifuge tube. Powder samples were dissolved in 10.0 mL of distilled water. After filtering (pore size 0.2 µm), the solutions were analysed for DSP content by the HPLC method as described in the Section 2.20. All samples were taken in triplicate.

Adequate homogeneity was assumed for the powder blends that showed mean percentage ratio of experimentally determined and theoretical mass of DSP in the analysed samples within the range of 100.0 ± 5.5%, with a relative standard deviation (RSD) value ≤5.5% [27].

2.11. Scanning Electron Microscopy

The morphology and surface of the microspheres and microspheres/carrier powder blends was observed by scanning electron microscopy (SEM) using a VEGA3 microscope (TESCAN, Brno, Czech Republic) operating at an acceleration voltage of 20 kV. The powder samples were placed on a metal stub using a double-sided adhesive tape and were coated with a thin layer of gold and palladium applying a Quorum SC7620 sputter coater (Emitech, London, UK) under 0.01 mbar vacuum and inert argon atmosphere.

2.12. Powder Flow Properties

Powder flow properties were determined by indirect method by measuring tapped and bulk density of the powders. The experiment was performed according to Kaialy et al. [28] with slight modifications. Powder (200 mg) was weighed and filled in a 5 mL syringe and the volume was recorded. Then, the syringe was tapped until there was no change in the powder volume (around 100 times) and the new volume was recorded. Hausner ratio was calculated according to the formula (Equation (4)):

$$Hausner\ ratio = \frac{Tapped\ density}{Bulk\ density} \quad (4)$$

2.13. Spray Cone Angle Determination

Spray cone angle was measured by a virtual protractor after spraying the powder samples against a dark background [29]. Powder samples (15 mg) were weighed in a hypromellose capsule (Vcaps® Plus, size 3, kindly donated by Capsugel, Lonza, Basel, Switzerland). The capsule was placed in Miat® monodose nasal insufflator (Miat S. p. A., Milan, Italy), pierced and the powder sample was actuated by squeezing a rubber bulb to generate airflow. The emitted plume was recorded using a camera Panasonic Lumix DMCFZ1000 (Panasonic, Osaka, Japan) of 120 frames per second and afterwards analysed for the spray cone angle. Each formulation was tested in triplicate.

2.14. In Vitro *Mucoadhesion Test*

Nasal mucosa was isolated from porcine heads obtained from a local abattoir following procedure described by Fachel et al. [30]. The head was split in two halves by longitudinal incision exposing septum and conchae in the nasal cavities. The mucosa was carefully separated from the underlying tissue and stored at −20 °C until use. Mucoadhesive properties of microspheres and their blends with lactose or mannitol were determined according to the slightly modified method of Jurišić Dukovski et al. [31] using TA.XT Plus Texture Analyser (Stable Micro Systems, Godalming, UK) equipped with the Mucoadhesion Rig. Briefly, nasal porcine mucosa was cut into circular sections with a 10 mm diameter, which were then fixed to the upper probe with a cyanoacrylate glue. The amount of 5 mg of powder samples was weighed onto the lower platform of the mucoadhesion rig and was moisturized with SNF (20 µL) for 30 s. The mucosal section on the upper probe was soaked in SNF thermostated at 34 °C for 30 s prior to measurement. The settings of the test were as follows: pre-test speed 0.5 mm s^{-1}, test speed 0.1 mm s^{-1}, contact time 30 s, applied force 0.1 N and post-test speed 0.1 mm s^{-1}. All experiments were performed in triplicate. The maximum detachment force (F_{max}) and the work of adhesion (W_{adh}) were used as a measure of mucoadhesive properties. The work of adhesion was calculated according to the following equation (Equation (5)):

$$W_{adh} = A \times 0.1 \times 1000 \quad (5)$$

where A corresponds to the area under the force-distance plot, 0.1 represents the conversion of the time measurement to distance (the sample was raised at 0.1 mm s^{-1}), and multiplication by 1000 serves to express the values in µJ.

2.15. Cell Culture Conditions

Calu-3 cell line (ATCC® HTB-55™) was obtained from ATCC (Manassas, VA, USA). The cells were cultured in DMEM-F12 cell culture medium (Sigma Aldrich, St. Louis, MO, USA), supplemented with penicillin/streptomycin (1% *v*/*v*; Lonza) and foetal bovine serum (FBS; 10% *v*/*v*; Sigma Aldrich). The cell cultures were maintained in the incubator (Sanyo CO_2, Nagasaki, Japan) at 37 °C, 5% CO_2. The culture medium was changed every 2–3 days and the cells were passaged when 70–90% confluence was reached. The cells were detached from the flasks by trypsin/EDTA (0.25%/0.02% in phosphate-buffered saline,

PBS, respectively). The cells were split in ratios from 1:3 to 1:6. The passages used for biocompatibility and permeation studies were 13–15 and 13, 19 and 23, respectively.

2.16. In Vitro *Biocompatibility Studies*

The cells were seeded in 96 well plates (Corning Costar, Corning, NY, USA) at density of 4×10^4 cells per well and were used for biocompatibility studies after 48 h of culturing. Microspheres and microspheres/carrier powder blends were homogeneously dispersed in distilled water at DSP concentration ranging from 0.9 to 3.68 mg mL^{-1}, and corresponding inert carrier concentration range from 25.4 to 214.4 mg mL^{-1}. DSP, mannitol and lactose solutions at concentrations equal to those in powder sample dispersions were used as controls. The dispersions and solutions were mixed with HBSS-Ca^{2+} (pH 7.4) in volume ratio 1:1, reaching the final concentration in the range of 0.45–1.8 mg mL^{-1} for DSP and 12.7 to 107.2 mg mL^{-1} for lactose or mannitol per well. Before the treatment, cell culture medium was withdrawn, cells were washed with HBSS-Ca^{2+} and exposed to the prepared dispersions or solutions for 2 h at 37 °C. Cells incubated in HBSS-Ca^{2+} were used as a negative control. After the treatment, the cells were washed twice with HBSS-Ca^{2+} and the biocompatibility test was performed. Cell viability was determined by colorimetric MTT (3-[4,5-dimethylthiazol-2-yl]-2,5-diphenyl tetrazolium bromide, Sigma-Aldrich) assay. The reagent was prepared by dissolving MTT (2.5 mg mL^{-1}) in PBS (Lonza), followed by the addition of DMEM-F12 cell medium to obtain the concentration of 0.5 mg mL^{-1}. In each well 100 µL of the MTT solution was added, after which the cells were incubated for 30 min at 37 °C. Afterwards, the medium was removed, the cells were lysed and the formazan crystals dissolved by the addition of 100 µL of isopropanol per well. The amount of formazan was determined spectrophotometrically at 570 nm (1420 Multilabel counter VICTOR3, Perkin Elmer, Waltham, MA, USA). Metabolic activity was expressed as relative to control (untreated cells incubated in HBSS-Ca^{2+}) according to the following equation (Equation (6)):

$$\text{Viability } (\%) = \frac{A_{sample} - A_{ipr}}{A_c - A_{ipr}} \times 100 \quad (6)$$

where A_{sample} is the absorbance of a solution of formazan crystals formed in cells treated with tested samples, A_{c} is the absorbance of a solution of formazan crystals formed in untreated cells (exposed to HBSS-Ca^{+}) and A_{ipr} is the absorbance of pure isopropanol.

2.17. In Vitro *Permeability through Epithelial Model Barrier*

In vitro permeability studies of DSP were performed using Calu-3 cell monolayer according to procedure described by Matilainen et al. [32]. Calu-3 epithelial cells were seeded onto the polycarbonate 12-well Transwell® inserts (0.4 µm mean pore size, 1.12 cm^2 surface area; Corning Costar Inc.) at a density of 5.5×10^5 cells per well. The cells were cultured with the cell culture medium volume of 0.5 mL in the apical and 1.5 mL in the basolateral compartment. After 48 h, cell culture medium was removed from the apical compartment to create an air interface and the cells were grown with 800 µL of culture medium in the basolateral compartment. The cell culture medium in basolateral compartment was changed every other day and 24 h prior to the permeability experiment. The transepithelial electrical resistance (TEER) of the monolayers was measured using epithelial volt/ohm meter EVOM equipped with STX-2 chopstick electrode (WPI Inc., Sarasota, FL, USA) to determine the formation of the monolayers and their integrity. The cells were grown on Transwell® membranes for 12–14 days, until the plateau of TEER values was reached (above 1000 Ω cm^2). Permeability studies were carried out in HBSS-Ca^{2+}. In order to determine permeation profile of DSP and dexamethasone base (DB) across Calu-3 monolayer from isoosmotic solution, DSP and DB were dissolved in HBSS-Ca^{2+} at concentration of 0.9 mg mL^{-1} and 0.075 mg mL^{-1}, respectively. Other samples for permeability experiments were prepared by dissolving/dispersing the appropriate amount of DSP, DSP-MS and DSP-MS/carrier in distilled water obtaining DSP concentration of 1.8 mg mL^{-1}. In addition, solutions of DB and DB/carrier in distilled water at DB concentration of 0.15 mg mL^{-1} were also prepared.

Aqueous solutions/dispersions were then mixed with HBSS-Ca^{2+} in 1:1 ratio, reaching the final DSP concentration of 0.9 mg mL^{-1} or final DB concentration of 0.075 mg mL^{-1}. Concentration of mannitol in the test samples containing mannitol was 54.5 mg mL^{-1}. HBSS-Ca^{2+} was used as negative control for TEER values and cell viability. Osmolality of all test samples was measured using OsmoTECH® Single-Sample Micro-Osmometer (Advanced Instruments, Norwood, MA, USA).

Prior to the experiment, the monolayers were washed with HBSS-Ca^{2+} and HBSS-Ca^{2+} was placed into the apical (0.5 mL) and basolateral (1.5 mL) compartments. The cell monolayers were then incubated for 20 min at 37 °C, 5% CO_2. At the beginning of the experiment, the apical compartment was emptied and 0.5 mL of the tested sample or HBSS-Ca^{2+} was added. Samples (0.5 mL) were taken from the basolateral compartment at regular time intervals over 120 min and replaced with the same volume of fresh thermostated HBSS-Ca^{2+} (37 °C). During the permeability experiment, monolayers were incubated at 37 °C and 50 rpm on a horizontal orbital shaker. The TEER values were measured before, during and after the permeation experiments to check the cell layer integrity. At the end of the experiment, the samples from the apical compartments were also collected. All experiments were done in triplicate. Samples were analysed for drug content using HPLC (Section 2.20). The apparent permeability coefficient (P_{app}) was calculated according to the following equation (Equation (7)):

$$Papp = \frac{dQ}{dt} \times \frac{1}{AC_0} \quad (7)$$

where dQ/dt is the permeability rate, A is the surface area of the permeation barrier and C_0 is the initial concentration of drug in the apical compartment [33].

The biocompatibility of the formulations by MTT assay was also examined on Calu-3 cell monolayer grown on Transwell® plates 24 h after the permeability assay. A 5 μg mL^{-1} MTT (3-[4,5-dimethylthiazol-2-yl]-2,5-diphenyl tetrazolium bromide, Sigma-Aldrich) solution was prepared in PBS and diluted with DMEM-F12 cell medium to a final MTT concentration of 0.5 mg mL^{-1}. MTT solution (0.7 mL) was added to both the basolateral and apical compartment. Treated cells were incubated for 30 min at 37 °C. After 30 min, the medium was removed and 0.7 mL of isopropanol was added to both the apical and basolateral compartment. The Transwell® plate was placed on an orbital shaker at room temperature to facilitate the dissolution of the formed formazan crystals. The plate was covered with aluminium foil for protection from light. After dissolving formazan, solutions from the apical and basolateral compartments were combined and stirred, and 100 μL of the solution for each sample was transferred to a 96-well plate in triplicate. Absorbance was measured at a wavelength of 570 nm (Victor, PerkinElmer, Waltham, MA, USA). Cell viability was expressed as relative to control as described in the Section 2.15.

2.18. Development of Nasal Cavity Model

Multi-sectional nasal cavity model was developed based on anonymized Computed Tomography (CT) scan of a 62-year old patient, obtained from Sisters of Charity Hospital database. The patient had healthy nasal airway passages, as confirmed by a specialist. Reconstruction, design and 3D print of a nasal cavity model was performed by CATEH d.o.o., Zagreb, complying with ISO 13485 standards. InVesalius 3.1 software was used to segment CT and reconstruct the nasal cavity model while Rhinocheros® 7 was used to design the nasal cavity model in multiple separate pieces. Nasal cavity model was fragmented into anterior region, turbinate region with detachable olfactory segment, septum with detachable olfactory segment and posterior region/nasopharynx equipped with a connector for respiratory pump used to produce adequate inspiration pattern. The model also includes paranasal sinuses with openings into the nasal cavity. Bar pins with 6.4 and 2.0 mm diameter and 6.0 and 4.0 mm height and transverse coupling were used to ensure proper assembly and alignment of the model segments.

The model was produced by stereolithography using 3D Systems®ProX 800 (3D Systems, Inc., Rock Hill, SC, USA). It was printed in transparent rigid plastic Accura ClearVue, with the resolution of 10 µm layer thickness. In order to enable appropriate nasal device insertion into the nostrils, anterior region was printed in flexible material (DigitalMaterial FLX 9850, 60 ShoreA TangoBlackPlus and VeroWhitePlus) at a resolution of 30 µm layer thickness using Stratasys Connex 350 printer (Stratasys Ltd, Rehovot, Israel).

2.19. Assessment of the Deposition Profile within the Nasal Cavity In Vitro

The nasal cavity model was placed on a stand and connected to Respiratory Pump Model 613 (Harvard Apparatus, Holliston, MA, USA), simulating breathing at inspiratory flow rate of 0 L min^{-1} (no breathing) or 20 L min^{-1} (representing moderately deep inspiration of the patient) [21]. Volumetric flow rate was checked by nasal inspiratory flow meter In-Check Nasal (Clement Clarke International Ltd., Harlow, UK). During inspiration with one nostril blocked, powder formulation was sprayed with Miat® device to the free nostril of the nasal cavity model at a nostril insertion depth of 5 mm, at actuation angle 0° from the vertical plane, and 60 or 75° from the horizontal plane. Fractional spray deposition pattern was quantitatively determined after thorough rinsing of each segment of the nasal cavity with distilled water. Eluates were characterised in terms of drug content by the HPLC method described in the Section 2.20. Drug deposited in each region was expressed in relation to total dose. For determination of total dose recovery, the fraction of the dose retained in the capsule after device actuation was also evaluated. Three replicate assessments of deposition pattern were conducted for each formulation.

2.20. Quantitative Determination of DSP and DB

Quantitative determination of DSP and DB was performed by HPLC. The chromatographic system consisted of an autosampler, system controller, pump, degasser, an UV–VIS detector, a column oven, all Series 200 (PerkinElmer). TotalChrome Navigator software for data processing was used for all chromatographic analyses. Satisfactory separation was achieved on Kinetex C18 (100 × 4.6 mm, 2.6-µm particle size) reverse-phase column with suitable guard column, both obtained by Phenomenex (Torrance, CA, USA). The chromatographic conditions were a modification of those by Jurišić Dukovski et al. [31]. The mobile phase consisted of 68% 5 mM acetate buffer (pH 4.5) and 32% acetonitrile (v/v). The isocratic elution was carried out at a flow rate of 0.7 mL min^{-1} and the column was thermostatically controlled to a temperature of 55 °C. The injection volume was 20 µL. The detection wavelength for each analyte was at 241 nm. The corresponding concentrations were determined from the integrated peak area using the appropriate calibration curves. The proposed method was validated based on the International Conference on Harmonization (ICH) guideline Q2 (R1) [34]. Validation of the method was carried out for selectivity, linearity, range, accuracy, repeatability, intermediate precision, limit of detection (LOD) and limit of quantification (LOQ) (Table S2, Figure S1).

2.21. Statistical Analysis

Statistical data analyses were performed on all data using a one-way ANOVA followed by a Tukey's post hoc test with $p < 0.05$ set as the minimal level of significance. Calculations were performed using JMP 14.0 software (JMP®, Version 14.0, SAS Institute Inc., Cary, NC, USA, 1989–2007).

To evaluate the correlation between two variables (i.e., percentage of the dose retained within the capsule vs. Hausner ratio and spray cone angle vs. Hausner ratio), Pearson's (parametric) correlation coefficient was determined using the same statistical software. Significance level was set to 0.05.

3. Results and Discussion

This study focused on the development of dry powder platform for brain targeted dexamethasone delivery consisting of DSP-loaded pectin/hypromellose microspheres prepared by spray drying and mannitol or lactose as inert carrier.

DSP is a water-soluble sodium phosphate salt of dexamethasone, suitable for formulation procedures such as aqueous solution spray drying. Apart from enabling the administration of higher drug doses and achieving high drug bioavailability owing to permeation and/or conversion to diffusible active form in vivo, water-soluble phosphate ester prodrugs are easy to formulate with no need for potentially toxic excipients [19]. Pectin and hypromellose are biocompatible and mucoadhesive polymers already used as constituents in approved liquid nasal formulations, such as PecFent (approved by the European Medicines Agency) and Astelin (approved by The United States Food and Drug Administration, FDA). Hypromellose presented a polymer of choice in several studies aimed at development of nasal powders intended for CNS drug delivery [13,15]. Hypromellose showed mucoadhesive properties and provided appropriate drug release profile in relation to route of administration [15]. Our group previously demonstrated that combining hypromellose with pectin improved polymer matrix properties ensuring moderate swelling in contact with nasal fluid, due to pectin crosslinking in the presence of calcium ions [22]. For each API to be incorporated in pectin/hypromellose matrix it is important to optimise pectin to hypromellose and API to polymers weight ratios in the spray dried solution.

Both selected inert carriers (lactose and mannitol) are listed in the FDA database of inactive ingredients for nasal or respiratory use [35]. Pharmaceuticals and Medicals Devices Agency of Japan approved nasal powder formulation of dexamethasone cipecilate as dexamethasone ester prodrug for the treatment of allergic rhinitis (Erizas®), comprising active pharmaceutical ingredient and lactose as an additive. Mannitol is a chemically inert highly water-soluble pharmaceutical excipient that has been considered as a bulking (matrix forming) agent and/or carrier in development of various nasal powders such as vaccine formulations [36], systemic [37] and nose-to-brain drug delivery platforms [11]. Mannitol has been demonstrated to alter mucosal permeability by osmotic effect [38,39]. In addition, lactose and mannitol are expected to provide beneficial effect on the polymer network hydration status of the swollen microspheres. Namely, the moisturising effect of carriers is known to prevent drying out of the gel and formation of the polymeric crusty layer that might irritate mucosa [40].

3.1. Experimental Design: Analysis of the Results

Within this work, experimental design was employed for fine tuning of the formulation and process parameters with the aim to optimise microspheres' physicochemical properties.

Drug/polymers solution spray drying following the design matrix (Table 1) resulted in dry powder product for every experimental run approving the appropriateness of the formulation and process parameter settings within the design of experiment.

Microspheres prepared were characterised in terms of drug entrapment efficiency, drug loading, particle size and particle size distribution, residual moisture content and swelling ability in water and SNF (Table 1).

Before the statistical analysis of the obtained results, the input parameters were normalized to the unitless interval [−1,1]. This approach is customary in the experimental design modelling [41] and the analysis in the rest of the paper will be presented in the normalized terms (standardized covariates) to simplify obtained model equations which describe specific response variables.

Regression modelling (with linear effects and two-way interactions where applicable) was applied to derive an insight into which formulation and/or process parameters as well as their interactions are important to precisely estimate evaluated responses.

3.1.1. Process Yield

Spray drying yield ranged between 13.9% and 68.6% (Table 1). The model obtained by the regression analysis exhibited a good fit (R-squared 0.67, RMSE 8.52 and Press RMSE 9.19) and can be presented by the following equation (Equation (8)):

$$\text{Yield} = 52.27 - 4.06 \times \text{HPMC} + 6.6 \times \text{T\_inlet-4.13} \times \text{FFR} + 2.91 \times \text{HPMC} \times \text{T\_inlet} + 6.4 \times \text{IT} \times \text{FFR} \quad (8)$$

The yield increased with the increase of inlet temperature and decrease of feed flow rate (Figure 1). These are commonly seen effects related to improved drying and decreased particle adhesiveness [42–44]. It was also noted that the process yield decreased with the increase of hypromellose concentration in the drying feed. Reduction of yield at higher hypromellose concentration may be related to the higher particle adherence on drying chamber walls resulting from the hydrophilic character of the polymer [45].

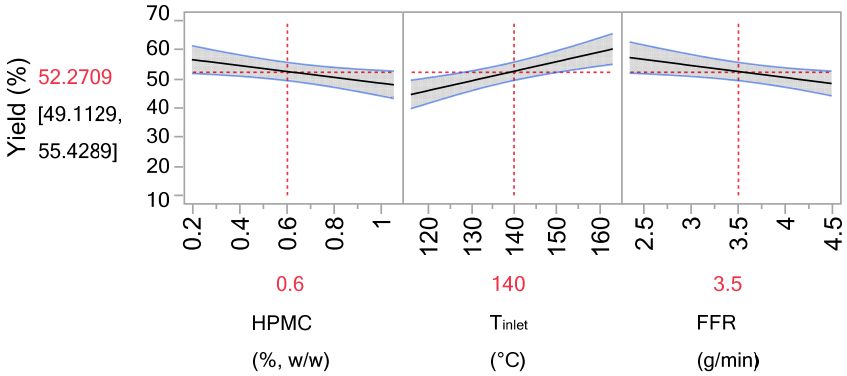

Figure 1. Prediction of yield in relation to hypromellose concentration (HPMC), inlet air temperature (T_{inlet}) and feed flow rate (FFR). Values in brackets refer to 95% confidence interval.

Interaction between inlet temperature and feed flow rate has shown a significant influence on the process yield (Figure 2). At T_{inlet} of 120 °C, the yield decreased with the increase in FFR, which was not observed at T_{inlet} of 160 °C due to better drying efficiency at higher temperature.

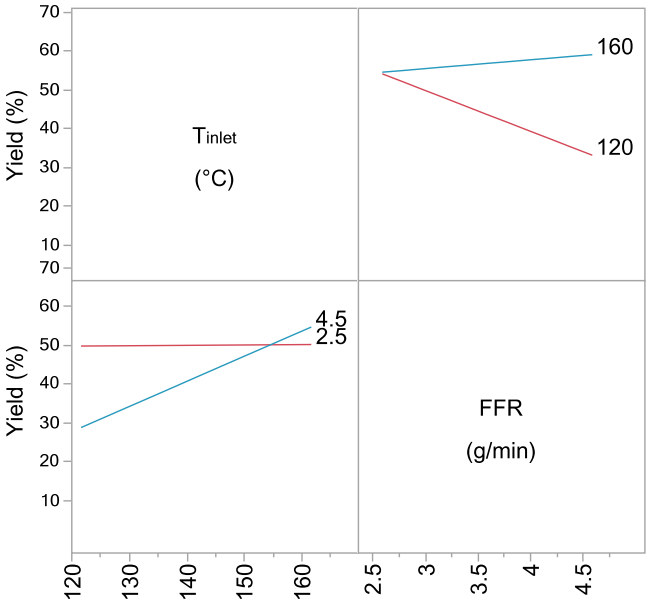

Figure 2. Interaction profiler illustrates the interaction effect between inlet air temperature (T_{inlet}) and feed flow rate (FFR).

3.1.2. Entrapment Efficiency and Drug Loading

All microspheres were characterised by high DSP entrapment efficiency (85.2 ± 4.8–101.9 ± 0.3%, Table 1) that was shown not to be correlated with inspected process and formulation parameters. Drug loading ranged between 1.4% and 33.5% being increased by increase of DSP concentration and decreased by hypromellose concentration increase in the feed solution. The model for drug content obtained by regression analysis exhibited a good fit (R-squared 1, RMSE 0.69 and Press RMSE 0.72) and is given by the following equation (Equation (9)):

$$DL = 12.87 - 5.3 \times HPMC + 9.98 \times DSP - 3.79 \times HPMC \times DSP \quad (9)$$

3.1.3. Particle Size

Results of microsphere size analysis for each experimental run are presented in Table 1. Values for *D*v10, *D*v50 and *D*v90 ranged between 1.4 ± 0.0–2.6 ± 0.3 µm, 2.2 ± 0.0–14.9 ± 3.4 µm and 3.7 ± 0.0–42.9 ± 0.6 µm, respectively. Values for *D*[4,3] ranged between 2.0 ± 1.2–18.5 ± 3.8 µm.

Models obtained by regression analysis exhibited a good fit for *D*v90 (R-squared 0.8, RMSE 5.83 and Press RMSE 6.99) and Dv10 (R-squared 0.68, RMSE 0.19 and Press RMSE 0.21) while *D*v50 (R-squared 0.46, RMSE 2.92 and Press RMSE 3.12) fit was not as good. Obtained models are presented by the following equations (Equations (10)–(12)):

$$Dv10 = 1.73 + 0.24 \times HPMC + 0.11 \times DSP + 0.02 \times T_{inlet} + 0.07 \times DSP \times T_{inlet} \quad (10)$$

$$Dv50 = 4.46 + 2.22 \times HPMC + 1.14 \times DSP + 0.9 \times HPMC \times DSP \quad (11)$$

$$Dv90 = 13.2 + 8.67 \times HPMC + 2.26 \times DSP - 2.03 \times T_{inlet} + 2.08 \times FFR - 3.49 \times HPMC \times T_{inlet} - 2.33 \times DSP \times FFR - 3.32 \times FFR \times T_{inlet} \quad (12)$$

Models for *D*v10, *D*v50 and *D*v90 reveal the highest impact of hypromellose concentration in the feed solution on the microsphere size distribution. Increase in hypromellose concentration resulted in larger microsphere sizes, which can be explained by higher viscosity of feed solution. Namely, for a given amount of energy available for atomisation process, increase in feed solution viscosity results in atomisation into larger droplets than in the case of less viscous feed, leading to larger size of dry particles [43]. Furthermore, increase in DSP concentration in the feed solution was shown to increase *D*v10, *D*v50 and *D*v90. This could be ascribed to increase in the solid content in the droplets to be dried. Except for the individual parameters, derived model for *D*v90 also included interactions between formulation and process parameters showing their interdependent effect on particle formation process [46].

Model obtained by regression analysis for *D*[4,3] (R-squared 0.62, RMSE 3.05 and Press RMSE 3.36) was given by the following equation (Equation (13)):

$$D[4,3] = 6.13 + 3.49 \times HPMC + 1.25 \times DSP + 0.3 \times FFR - 1.24\ DSP \times FFR \quad (13)$$

The model confirmed hypromellose and DSP concentrations in the feed solution as parameters with the highest impact on microsphere size distribution.

3.1.4. Residual Moisture Content

Residual moisture content (MC) in the microspheres prepared following designed experiments, ranged between 3.2 ± 0.8–9.1 ± 0.2%. The model obtained by regression analysis exhibited a relatively good fit (R-squared 0.57, RMSE 1.08 and Press RMSE 1.14; Figure 3) and is given by the following equation (Equation (14)):

$$MC = 5.9 - 1.23 \times HPMC + 0.33 \times DSP \quad (14)$$

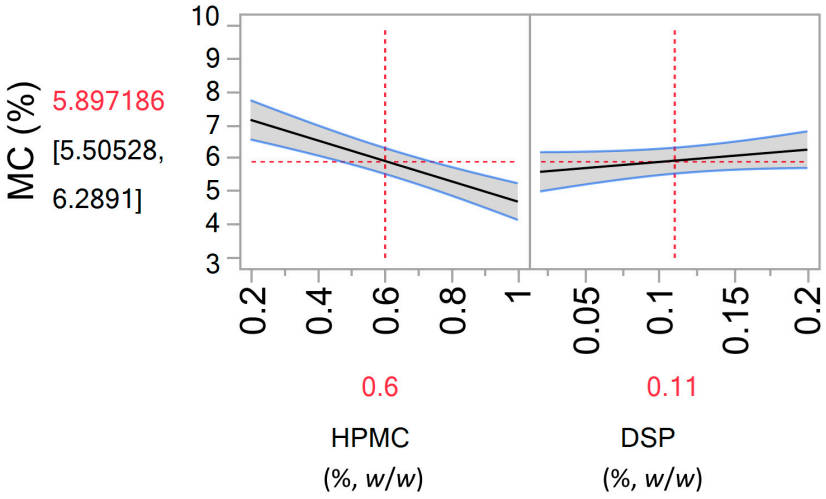

Figure 3. Prediction of moisture content (MC) in relation to hypromellose (HPMC) and DSP concentrations. Values in brackets refer to 95% confidence interval.

Residual moisture is shown to increase with the decrease in hypromellose and increase in DSP concentration in the feed solution. However, the values up to 10% of residual moisture content are acceptable for dry powder formulation based on hydrophilic polymers [47]. Decreasing hypromellose concentration in the feed solution led to microsphere matrix with higher pectin content as its concentration was kept constant in the feed solution. Thus, noted influence of hypromellose can be explained by higher hygroscopicity of pectin in relation to hypromellose, as confirmed by results on dynamic vapour sorption of polymers used reported in the literature [48]. The impact of DSP on residual moisture content in the microspheres can also be related to its hygroscopic nature [49].

3.1.5. Swelling of the Microspheres

During the swelling process microspheres generally absorbed lower volumes of SNF (6.1 ± 1.6–23.5 ± 1.9 µL mg^{-1}) when compared to purified water (6.7 ± 2.7–41.6 ± 3.4 µL mg^{-1}). That can be explained by crosslinking of the pectin chains with calcium ions present in the SNF. Model obtained for swelling of microspheres in contact with water (V_{water}) exhibited a good fit (R-squared 0.62, RMSE 4.96 and Press RMSE 5.18) and is given by the following equation (Equation (15)):

$$V_{water} = 26.67 - 5.05 \times HPMC - 4.17 \times DSP \quad (15)$$

Volume of absorbed water decreased with the increase of hypromellose and DSP concentration in the feed solution. Increasing hypromellose and DSP concentration in the feed solution led to microsphere matrix with lower content of pectin. This is in agreement with previously shown better swelling properties of pectin in contact with water compared to hypromellose [22]. Higher content of drug entrapped reduced the amount of swellable polymers in the microsphere matrix.

Swelling of the microspheres in contact with SNF could not be adequately described by a regression model including inspected formulation and process parameters and their interactions. Such an observation leads to the conclusion that crosslinking of pectin with calcium ions present in SNF was the main factor governing the swelling behaviour.

Swelling of the microspheres in contact with nasal mucosa presents a prerequisite for exhibiting mucoadhesion properties and triggers release of the drug entrapped. Furthermore, microsphere swelling can cause dehydration of epithelial cells, leading to reversible widening of tight junctions and increase in the paracellular absorption for drugs [12]. However, excessive hydration of mucoadhesive polymers can result in slippery mucilage formation and reduction of adhesive strength [50]. Therefore, swelling behaviour moder-

ated by means of pectin chains crosslinking with calcium ions is favourable for attaining prolonged residence time at nasal mucosa and adequate rate and extent of drug release.

3.1.6. Selection of the Leading DSP-Loaded Microspheres

Models obtained through regression modelling revealed optimised process and formulation parameters in the production of DSP-loaded microspheres. Namely, spray drying of aqueous solution of DSP (0.2%, *w/w*), hypromellose (0.2%, *w/w*) and pectin (0.2%, *w/w*) at inlet temperature of 160 °C and feed flow rate of 2.5 g min^{-1} was identified as optimal for the production of moderately swelling DSP-loaded microspheres (sample 24; Table 1; further denoted as DSP-MS). Employed settings of inlet temperature (160 °C), feed flow rate (2.5 g min^{-1}) and hypromellose concentration (0.2%, *w/w*) are linked to high process yield. In addition, selected hypromellose concentration was favourable as it resulted in particle size distribution shifted towards smaller particles. Namely, within the observed size range (Table 1), smaller particles are expected to exhibit stronger adhesion to coarse carrier particles as there is higher possibility for them to fit into irregularities of rough carrier surface which were previously shown to increase the attachment [21]. High DSP concentration (0.2%, *w/w*) in the spray drying feed is advantageous as it leads to the formation of microspheres with high drug content, leaving open the possibility of mixing the microspheres with inert carrier while not compromising the administration of therapeutic dose in the applicable amount of powder (up to 25 mg per nostril; [9]).

Observed residual moisture content in the selected microspheres was found not to influence the stability of incorporated drug, as drug loading within the microspheres stored in sealed containers at 4 °C for 12 months decreased for less than 2% (i.e., from 33.5 ± 0.4% to 31.9 ± 0.8%). Furthermore, microsphere size distribution upon 12 months of storage remained unchanged, as values of *D*v10, *D*v50, *D*v90 and *D*[4,3] (1.1 ± 0.0 µm, 3.2 ± 0.0 µm, 7.6 ± 0.0 µm and 4.1 ± 0.0 µm, respectively) were comparable to corresponding parameters determined immediately after microsphere preparation (1.5 ± 0.0 µm, 2.9 ± 0.0 µm, 8.2 ± 0.2 µm and 4.3 ± 0.1 µm, respectively; Table 1). Surface charge of microspheres was taken as another stability indicator: the values of zeta-potential measured immediately after microsphere preparation and upon 12 months of storage were −23.1 ± 1.4 mV and −22.0 ± 2.2 mV, respectively, confirming adequate microspheres' stability profile. Moisture within the dry powder induces capillary forces at particle interfaces contributing to cohesive and adhesive forces in powder blends [51,52]. Thus, parameters of mixing of microspheres with inert carrier need to be matched with their properties in order to effectively disjoin microsphere agglomerates and produce homogenous adhesive powder blend [53].

3.1.7. In vitro Release of DSP from Microspheres

The in vitro release profiles of DSP from microspheres in SNF were assessed under sink conditions using vertical Franz diffusion cell. The setup of the method allowed microspheres' hydrating and gelling in conditions similar to ones at nasal mucosa [54]. It was observed that microspheres swelled in contact with SNF turning into gel. The formulation retained gel structure by the end of in vitro release study. Polymeric microspheres ensured prolonged DSP release in comparison to the pure drug powder (Figure 4). Two phases of drug release from microspheres could be recognised: rapid initial release (around 50% in 30 min) followed by a slower release (around 100% in 90 min) with ultimately resuming a plateau. Considering further formulation development that comprises blending of the selected microspheres with inert carrier, DSP release from microspheres in the presence of mannitol was also evaluated (Figure 4; graph insert). It was observed that DSP release rate from DSP-MS/mannitol blend (1:9, *w/w*) was increased in relation to that from DSP-MS alone. Similarly, shorter time-period was needed for complete dissolution of DSP from DSP/mannitol blend than from the pure DSP powder (Figure 4).

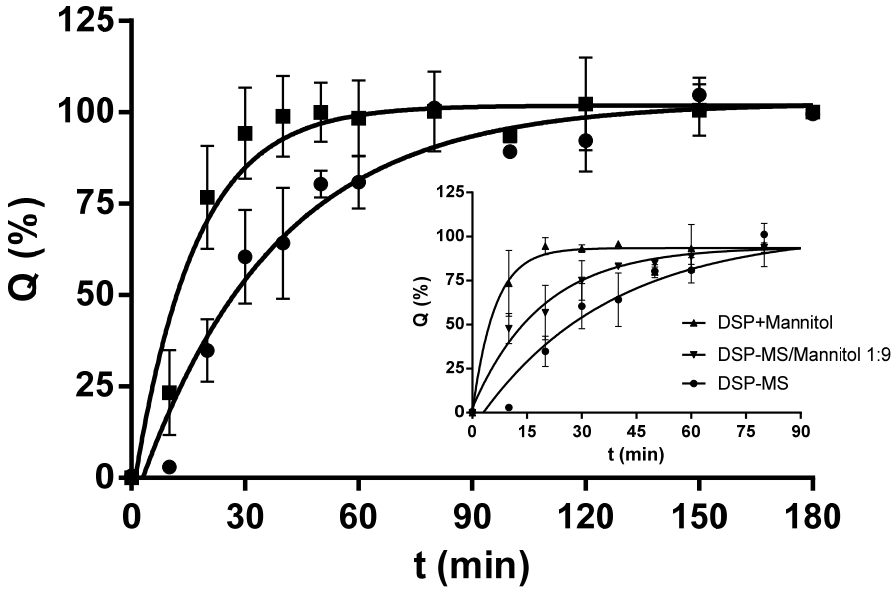

Figure 4. In vitro release profile of DSP from DSP-MS microspheres (circle) compared to dissolution of pure DSP powder (square). Graph insert: DSP in vitro release profile from DSP-MS microspheres blended with inert carrier (DSP-MS/Mannitol 1:9, *w/w*; reversed triangle) compared to dissolution of DSP from corresponding DSP/inert carrier blend (DSP + Mannitol; triangle). *Q* represents cumulative percentage of DSP released at time *t*. Data are expressed as the mean ± SD (n = 3).

This effect might be related to osmotic activity of mannitol that increased powder wetting rate [9]. However, drug diffusion control by the swollen polymeric matrix of microspheres is evident from significantly slower DSP release from DSP-MS/mannitol blend in relation to DSP dissolution from corresponding DSP/mannitol blend. In contact with SNF, the inert carrier got dissolved and hydrophilic pectin and hypromellose in microspheres hydrated quickly forming a swollen hydrogel crosslinked with calcium ions which allowed adequate diffusion of drug molecules. The formulation retained gel structure by the end of in vitro release study. The observed release profile fit the needs for nasal DSP delivery showing the potential to initially provide high drug concentration at nasal mucosa favouring absorption and to ensure complete drug release within expected residence time of microspheres at nasal mucosa [9,22,55].

3.2. Properties of DSP-MS/Inert Carrier Blends

Powder blends were prepared by mixing of DSP-MS with lactose or mannitol at weight ratios of 1:9 and 1:19 using fraction of carrier particles in the size range from 45 to 63 μm, selected as optimal for nasal powder application [9,21].

SEM micrographs of DSP-MS and DSP-MS/inert carrier blends at ratio 1:9 (*w/w*) are shown in Figure 5. DSP-MS microspheres were spherical in shape with smooth and corrugated surface. A corrugated particle morphology was previously reported to reduce cohesiveness between the particles [56] which is beneficial for the production of homogenous DSP-MS/inert carrier blends. Carrier particles were characterised by irregular shape and rough surface. SEM micrographs of DSP-MS/inert carrier blends revealed DSP-MS adhered to mannitol or lactose particles, evenly covering their rough surface and fitting into the surface irregularities. It has previously been assumed that microparticles adhere better to rough carrier surfaces [21]. Such a phenomenon is beneficial for nasal powders since microspheres should stay attached to the carrier particles upon administration, co-depositing at the nasal mucosa. Rapid dissolution of carrier particles in nasal fluid liberates the microspheres enabling their intimate contact with nasal epithelium [21].

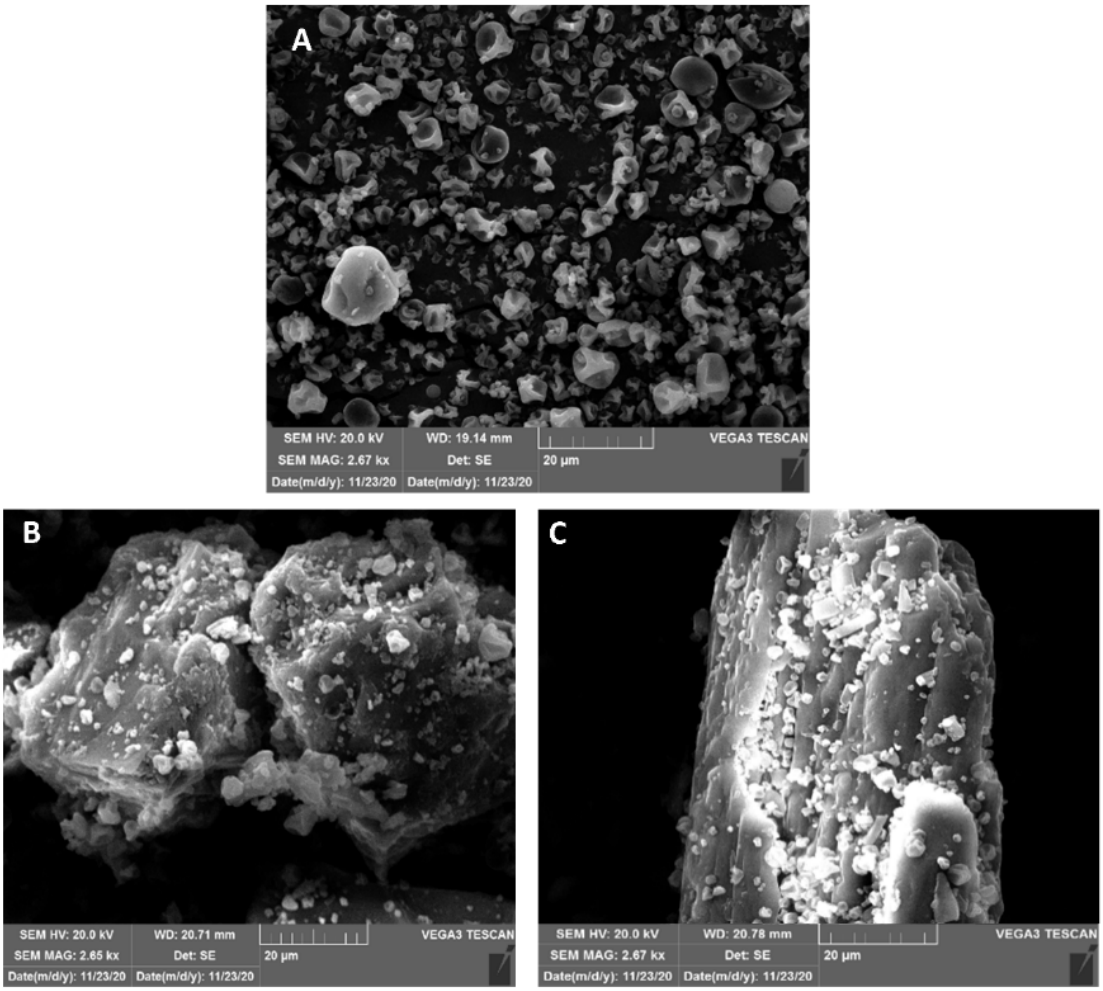

Figure 5. SEM micrographs of DSP-MS (**A**), DSP-MS/lactose blend (**B**) and DSP-MS/mannitol blend (**C**) with DSP-MS to inert carrier ratio 1:9, *w/w*.

Homogeneity, flowability and sprayability of DSP-MS/inert carrier blends are presented in Table 2. Powder blends of DSP-MS with inert carrier (lactose or mannitol) at weight ratios of 1:9 and 1:19 were shown to be homogenous as mean values of percent amount of DSP to nominal dose in the taken powder blend samples (from bottom, medium and upper part of cuvettes) were in range of 100 ± 5.5%, with relative standard deviation (RSD) ≤ 5.5 [57]. The results obtained confirmed the effectiveness of mixing procedure employed and delivery of uniform dosage units. Apart from the mixing procedure, evolution of the blend state is influenced by the size and morphology of the carriers in a way that irregular and larger carriers favour deagglomeration of fine particles and their adhesion to open pores [58]. Namely, the carrier particles need to provide sufficient force to break up agglomerates of small particles during the mixing process [20].

Hausner ratios for DSP-MS, inert carriers and DSP-MS/inert carrier blends ranged between 1.14 ± 0.00 and 1.96 ± 0.18, as presented in Table 2. According to the Hausner ratio-based classification given in Ph. Eur. 10, the flowability of the investigated powders was denoted as good (for inert carrier) to very, very poor (for DSP-MS). Although Hausner ratio is not precisely predictive for non-freely flowable powder (e.g., spray-dried powder) behaviour, it certainly may show a trend in flow properties [59]. Thus, values of Hausner ratio obtained in this study clearly indicated that mixing of DSP-MS with inert carrier significantly improved powder flow properties (Table 2).

Table 2. Properties of powder blends prepared with DSP-loaded microspheres (DSP-MS) and inert carrier (lactose or mannitol) at weight ratios of 1:9 and 1:19.

Powder Sample	Homogeneity		Flowability		Spray Properties
	D (%)	RSD (%)	Hausner Ratio	Powder Retention within Capsule (%)	CA (°)
DSP-MS	/	/	1.96 ± 0.18	14.8 ± 2.8	26.5 ± 0.3
DSP-MS/Lactose 1:9	100.2	4.6	1.43 ± 0.00	6.3 ± 1.7	22.0 ± 0.5
DSP-MS/Lactose 1:19	102.1	1.6	1.43 ± 0.10	6.0 ± 4.0	21.3 ± 0.4
DSP-MS/Mannitol 1:9	96.9	4.1	1.33 ± 0.00	1.7 ± 0.0	20.6 ± 0.2
DSP-MS/Mannitol 1:19	100.3	3.2	1.32 ± 0.07	1.7 ± 1.7	19.6 ± 1.0
Lactose	/	/	1.31 ± 0.10	5.5 ± 0.4	20.5 ± 0.6
Mannitol	/	/	1.14 ± 0.00	0.0 ± 0.0	18.7 ± 0.5

D = mean percentage ratio of experimentally determined and theoretical mass of DSP in the analysed samples (n = 6); RSD = relative standard deviation (n = 6); CA = spray cone angle. All values except for D and RSD are mean ± SD, n = 3.

Powder retention within the capsule upon device activation decreased with the decrease in Hausner ratio (Table 2) and served as a valuable and realistic indicator of powder flow behaviour. Statistical analysis performed on data for DSP-MS, mannitol, lactose and DSP-MS blends with mannitol or lactose at weight ratios of 1:19 and 1:9 revealed clear correlation of these variables described by Pearson's coefficient of 0.9517 (Figure 6, left). Namely, percentage of the dose retained within the capsule for DSP-MS/inert carrier blends (1.7–6.3%; Table 2.) was significantly lower than in case of DSP-MS alone (14.8%; Table 2). The same parameter indicated better flow properties of DSP-MS powder blends with mannitol in comparison to blends with lactose, reflecting delivery of almost 98% of the dose contained in the capsule. The difference in flow properties of DSP-MS powder blends with mannitol and lactose can be explained by the difference in the carriers' particle morphology. Namely, mannitol particles were characterised by more pronounced surface roughness which might lead to stronger DSP-MS adherence [21]. No significant difference in percentage of dose retained within the capsule was noted between powder blends prepared at two different DSP-MS to inert carrier weight ratios (1:9 vs. 1:19).

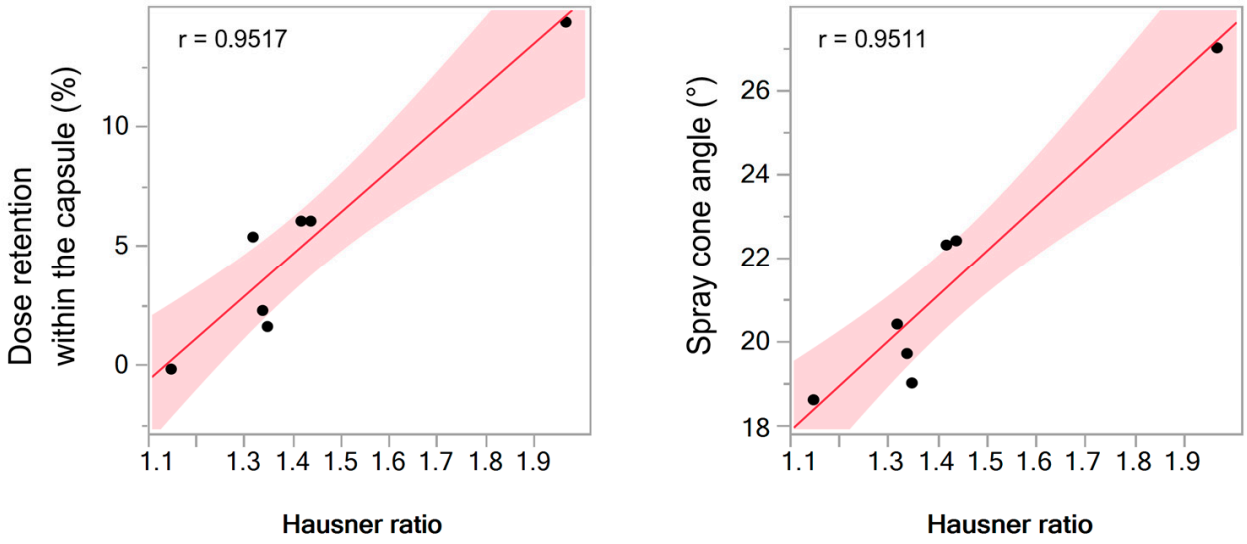

Figure 6. Correlation between dose percentage retained within the capsule and Hausner ratio (**left**; Pearson's coefficient of 0.9517) and between spray cone angle and Hausner ratio (**right**; Pearson's coefficient of 0.9511) established based on statistical analysis of data for DSP-MS, mannitol, lactose and DSP-MS blends with mannitol or lactose at weight ratios of 1:19 and 1:9.

The spray cone angle for all investigated powders ranged between 19.6 ± 1.0° and 26.5 ± 0.3° (Figure 7). Mixing of DSP-MS with inert carrier resulted in decrease in spray cone angle in relation to DSP-MS alone. Spray cone angle was shown to be related to powder flow properties as it decreased with the decrease in Hausner ratio. Statistical analysis performed on data for DSP-MS, mannitol, lactose and DSP-MS blends with mannitol or lactose at weight ratios of 1:19 and 1:9 revealed linear relationship between inspected variables, with Pearson's coefficient of 0.9511 (Figure 6, right). The results obtained indicated smaller spray cone angle for DSP-MS blends with mannitol in relation to those with lactose which is advantageous as, generally, smaller spray cone angles increase the chance for drug delivery beyond the nasal valve [29].

Figure 7. Spray cone of DSP-MS/Mannitol 1:9 upon aerosolisation with Miat® insufflator.

3.3. In Vitro *Mucoadhesion Studies*

Mucociliary clearance has been recognised as one of the major limiting factors in nasal drug delivery since it reduces the time available for drug absorption to occur. Ciliated epithelial cells that provide mucus transport by the coordinated cilia beating are found in respiratory mucosa. However, mucociliary clearance also occurs in the olfactory region due to the presence of patches and islets of respiratory mucosa in the olfactory mucosa.

Active clearance in olfactory region is also supported by Bowman's glands secretion and gravitational forces reducing the time available for drug uptake to occur [60].

Mucoadhesive drug delivery systems bear the potential to ensure improved drug therapeutic effect by prolonging its residence time at nasal mucosa and thus increasing its brain uptake [12,56]. Herein we investigated mucoadhesive properties of DSP-MS and DSP-MS/inert carrier powder blends using excised nasal porcine mucosa that was selected for this study due to its high similarity in histology and physiology with human nasal mucosa [61,62]. Mucoadhesion of powders was expressed as maximum detachment force and work of adhesion, as presented in Figure 8.

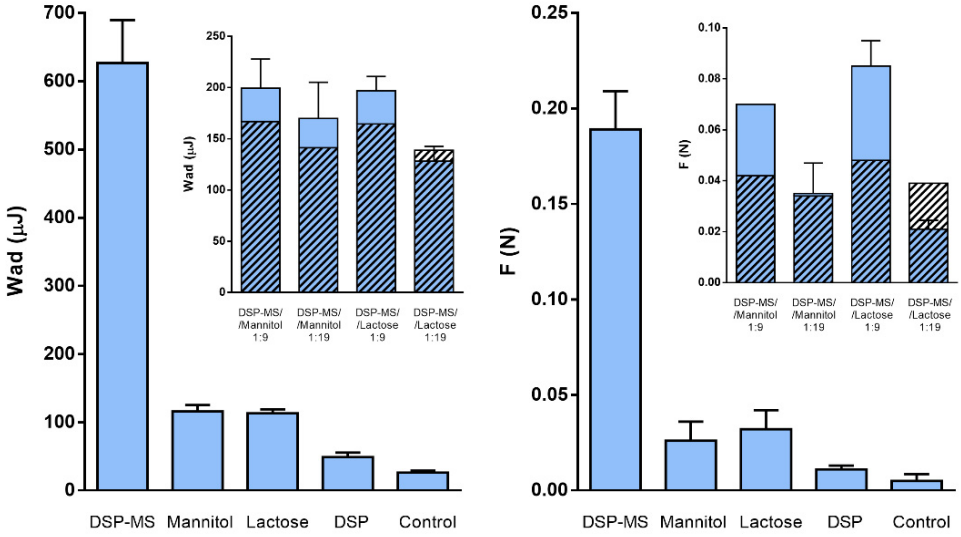

Figure 8. Work of adhesion (W_{ad}; **left**) and maximum detachment force (F; **right**) of DSP-MS microspheres, inert carriers (mannitol and lactose) and pure drug powder compared to control (filter paper). Graph insert: Work of adhesion (W_{ad}; **left**) and maximum detachment force (F; **right**) for DSP-MS/inert carrier blends at ratios 1:9 and 1:19 (*w/w*). For all graphs, bars coloured in blue represent measured values W_{ad} (**left**) and F (**right**) for 5 mg of each tested powder. Shaded bars represent theoretical values for W_{ad} (**left**) and F (**right**) calculated based on weight ratios and individual parameter values of powder blend constituents presented in the main graph. Data are expressed as the mean ± SD (n = 3).

DSP-MS microspheres were characterised by prominent mucoadhesive properties, presenting 19 fold higher maximum detachment force and 12.8 fold higher work of adhesion in relation to pure drug powder.

Both pectin and hypromellose show mucoadhesive properties. Their adhesion to mucus layers is based on the interpenetration with mucin chains and hydrogen bond formation [63,64]. Hypromellose is a water-soluble electroneutral cellulose derivative that has a great number of hydroxyl groups available for interaction with the mucin glycoproteins [64]. Pectin bears carboxylic acid groups that are negatively charged at physiologic pH value, as indicated by overall negative zeta-potential of pectin/hypromellose DSP-MS microspheres (−23.1 ± 1.4 mV). The electrostatic repulsion between negatively charged pectin and mucin may contribute to uncoiling of polymer chains and facilitate their entanglement as well as hydrogen bond formation [63].

Mucoadhesive properties of DSP-MS microspheres are closely related to their swelling behaviour enabling interpenetration of polymer and mucin chains [65]. Excessive swelling that might lead to poor mucoadhesion has been avoided due to the presence of pectin in the polymer matrix that became crosslinked with the calcium ions present in SNF [22]. Measured W_{ad} and F for DSP-MS/inert carrier blends were significantly lower than that of DSP-MS alone. This was expected since microspheres presented only 5% or 10% of total quantity of examined powder blend. Therefore, in order to define the influence of inert

carriers on DSP-MS mucoadhesive properties, we compared measured and theoretical values of W_{ad} and F for DSP-MS/inert carrier blends. Theoretical values were calculated based on weight ratios and individual W_{ad} or F values measured for powder blend constituents (Figure 8). Such an approach revealed that DSP-MS, when blended with inert carrier, retained or even enlarged their mucoadhesive properties in all inspected powder blends except for the blend with lactose at 1:19 weight ratio. The observed increase in mucoadhesive properties can be explained by the state of homogenous powder blends in which larger carrier particles induced deagglomeration of microspheres in the mixing procedure and promoted their adhesion to open pores.

When such a powder gets in contact with simulated nasal fluid the carrier particles rapidly dissolve [21], liberating microspheres that interact with the nasal mucosa more efficiently (i.e., with larger total surface area) than in case of DSP-MS alone that might be agglomerated. DSP-MS blend with lactose at 1:19 weight ratio (i.e., higher lactose content compared to 1:9 ratio) failed to retain or enlarge microsphere mucoadhesive properties, probably due to slower dissolution of lactose in relation to mannitol.

3.4. Biocompatibility of DSP-MS/Inert Carrier Blends

Biocompatibility of investigated powder delivery systems was evaluated in vitro using human airway epithelial Calu-3 cell line. The viability of cells exposed to DSP-MS/mannitol and DSP-MS/lactose powder blends at DSP concentration ranging from 0.45 mg mL^{-1} to 1.8 mg mL^{-1} and corresponding carrier concentration ranging from 12.7 mg mL^{-1} to 107.2 mg mL^{-1}, was above 80% in relation to control. The results obtained suggested appropriate biocompatibility profile of all constituents of powder blends in concentration range tested.

Based on thorough characterisation of DSP-MS/inert carrier blends and recognised advantages of mannitol compared to lactose in the role of the carrier for DSP-MS microspheres, powder blends with mannitol were selected for further studies. Prior to in vitro permeability and nasal deposition studies, DSP-MS/mannitol blends were proven to be homogenous upon three months of storage in the sealed containers at 4 °C. Adequate powder blend homogeneity upon storage was confirmed by mean percentage ratio of experimentally determined and theoretical mass of DSP in the analysed samples of 99.0% and 99.4% and RSD value of 3.8% and 1.3% for DSP-MS/mannitol 1:9 and 1:19 blends, respectively.

3.5. In Vitro *DSP Permeability Studies*

DSP permeability studies were performed using immortalized Calu-3 cells grown at air-liquid interface as a model of the nasal epithelial barrier [66,67]. Such a model has been used in number of studies screening the potential of innovative nasal formulations intended for brain targeted drug delivery [68–70]. Air-liquid interface culturing of Calu-3 cells was previously shown to provide closer simulation of in vivo airway epithelia properties including monolayer ultrastructure, secretory function (i.e., mucus production) and barrier integrity, compared to liquid-liquid culturing [71].

In general, immortalized cell lines are characterized by easy maintenance, high throughput capacity as well as high reproducibility and genetic homogeneity [72,73], thus being convenient for the evaluation of different drug formulations in terms of drug permeation profile. The suitability of the Calu-3 cells for nasal epithelial barrier modelling has been proven by comprehensive permeability study on wide range of model drugs chosen from high to low permeability categories. The study revealed excellent correlation with the fully differentiated 3D human nasal epithelial model (MucilAir™) and good correlation with the human nasal epithelial cell line RPMI 2650 [72]. Finally, Calu-3 cell monolayer grown at air-liquid interface was recently shown to correctly predict the outcome of pharmacokinetic studies and indicate the (non)equivalence of different formulations for two first-generation intranasal corticosteroids with relatively high aqueous solubility [74].

In this study Calu-3 cell monolayer was used to investigate the influence of developed powder delivery platform on DSP permeability across the epithelial barrier. DSP-

MS/mannitol powder blend at weight ratio of 1:19 was selected for this study in order to ensure both, hypertonic conditions in the donor compartment (expected in vivo) and sink conditions in the receiver compartment throughout the experiment. Table 3 presents all relevant test samples used to elucidate the key factors influencing DSP permeability across Calu-3 monolayer. DB solutions were also included in the study to prove the applicability of the barrier model employed.

Table 3. Permeation of DSP across Calu-3 monolayer from DSP-MS suspension and DSP solution in the presence and absence of mannitol. Corresponding DB solutions were also included in the study. Apparent permeability coefficients (P_{app}) of DSP and DB were presented in relation to osmolality of the test sample and TEER drop of the Calu-3 cell monolayer during permeability study.

–	Medium	Osmolality (mOsm kg^{-1})	TEER % of Initial Value in the Period 30–120 min of Experiment	P_{app} (10^{-6} cm s^{-1})
DSP-MS/Mannitol 1:19	HBSS-Ca^{2+}/water	613 ± 4	63 ± 2–94 ± 5	0.65 ± 0.12 ‡
DSP-MS	HBSS-Ca^{2+}/water	160 ± 3	16 ± 2–22 ± 3	3.03 ± 0.01 ‡
DSP/Mannitol	HBSS-Ca^{2+}/water	470 ± 1	53 ± 5–93 ± 5	0.39 ± 0.01
DSP	HBSS-Ca^{2+}/water	162 ± 1	17 ± 1–20 ± 2	3.43 ± 0.62‡
DSP *	HBSS-Ca^{2+}	304 ± 1	97 ± 4–103 ± 8	0.38 ± 0.06
DB/Mannitol	HBSS-Ca^{2+}/water	460 ± 2	48 ± 6–73 ± 9	17.94 ± 1.61
DB	HBSS-Ca^{2+}/water	161 ± 10	9 ± 1–13 ± 2	26.46 ± 2.94 †
DB *	HBSS-Ca^{2+}	298 ± 1	102 ± 4–104 ± 12	18.65 ± 1.92

Concentration of DSP, DB and mannitol (where applicable) in the test samples was equal to 0.9 mg mL^{-1}, 0.075 mg mL^{-1} and 54.5 mg mL^{-1}, respectively. Data are expressed as the mean ± SD (n = 3). ‡ statistically significant difference with respect to DSP/Mannitol and DSP * ($p < 0.05$). † statistically significant difference with respect to DB/Mannitol and DB * ($p < 0.05$).

Table 3 summarises P_{app} values for DSP and DB for all tested samples including their osmolalities and Calu-3 cell monolayer TEER drop during permeability studies.

P_{app} values for DB and DSP isoosmotic solutions in HBSS-Ca^{2+} across Calu-3 cell monolayer were determined to be 18.65 × 10^{-6} cm s^{-1} and 0.38 × 10^{-6} cm s^{-1}, respectively, verifying the cell model capacity to differentiate between drugs with high and moderate permeability. Sibinovska and co-workers tested 22 model drugs with high, moderate and low permeability (defined according to the values of the orally absorbed fraction) in the air/liquid Calu-3 cell model. The P_{app} value for DB obtained in this study is in line with P_{app} values reported by Sibinovska et al. for highly permeable drugs (1.0 × 10^{-5} to 1.7 × 10^{-5} cm s^{-1}). P_{app} value for DSP is within the P_{app} range the same group of authors obtained for drugs with moderate permeability (0.2 × 10^{-6} to 0.6 × 10^{-6} cm s^{-1}) [72].

DB is a lipophilic drug that permeates biological barriers by transcellular pathway [31]. On the contrary, DSP is expected to permeate Calu-3 monolayer by paracellular route. This was evidently shown in our study as a 9-fold increase in P_{app} of DSP across Calu-3 cell monolayer was observed with the decrease in TEER that was induced by exposing the cell monolayer to hypoosmotic stress (Table 3; samples DSP and DSP-MS). Similar profound drop in TEER (to 29.2 ± 3.4% of initial TEER value) after apical cell exposure to hypotonic solution with osmolarity of 150 mOsmol was previously observed in case of Caco-2 cell monolayer [75]. At these conditions, a 12- and 8-fold increase in paracellular transport of hydrophilic model compounds (fluorescein-Na and fluorescein-isothiocyanate-labeled dextran, respectively) was reported. However, hypoosmotic stress induced no change in cell viability [75].

DSP/mannitol solution with osmolality of 470 mOsm kg^{-1} was characterised by DSP permeation across Calu-3 monolayer similar to that of isotonic DSP solution. DSP-MS/mannitol blend increased P_{app} value of DSP 1.7 fold in relation to corresponding DSP/mannitol solution suggesting the potential of developed microspheres to increase drug uptake by paracellular transport. The observed permeation enhancing effect of DSP-MS/mannitol powder blend was found to be statistically significant ($p < 0.05$) and, coupled with (i) prolonged drug release through swollen microsphere polymeric matrix and (ii) mucoadhesive properties (the benefit of which cannot be encompassed by static

permeability model used), suggests that developed powder platform might increase overall DSP permeation across the olfactory epithelium in vivo.

As previously elaborated, DSP is a water-soluble sodium phosphate salt of dexamethasone that enables the administration of higher drug doses easily formulated in mucoadhesive powder delivery system with prolonged retention at the site of delivery. The approach suggested in this study has the potential to ensure double benefit, since based on the recent reports related to bioconversion of phosphate esters to more permeable forms by phosphatases present in nasal mucosa [17,19], it is reasonable to expect that the significant portion of the applied DSP dose will be absorbed in the form of dexamethasone base.

Viability of cells in Calu-3 cell monolayers used in permeability studies ranged between 88.2 ± 0.3 and 103.1 ± 2.9% in relation to cell monolayer exposed to HBSS-Ca^{2+} (Figure 9). Biocompatibility of the formulations was also confirmed by complete TEER recovery 22 h after permeability studies, showing that formulation effect on TEER was transient and reversible.

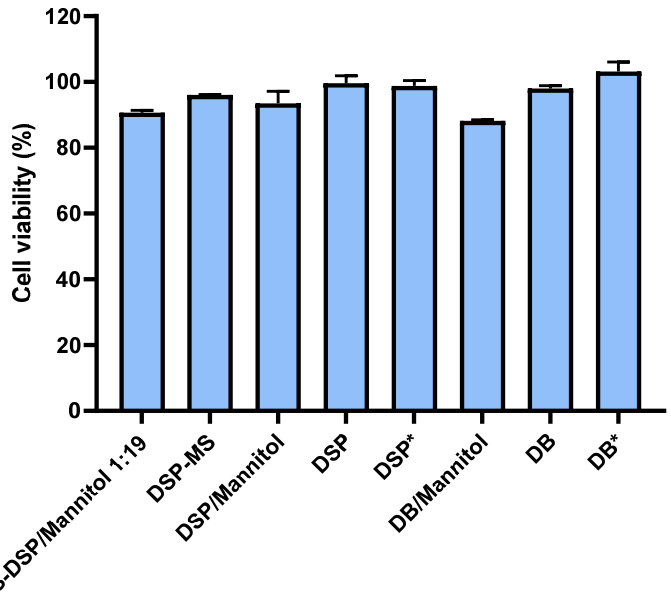

Figure 9. Viability of cells (MTT test) in Calu-3 cell monolayers used in permeability studies of DSP from DSP-MS suspensions and DSP solutions with and without mannitol. Corresponding DB solutions were also included in the study (see Table 3). Concentration of DSP, DB and mannitol (where applicable) in the test samples was equal to 0.9 mg mL^{-1}, 0.075 mg mL^{-1} and 54.5 mg mL^{-1}, respectively. Data are expressed as mean ± SD (n = 3). DSP * ($p < 0.05$); DB * ($p < 0.05$).

3.6. Nasal Deposition Profile of DSP Powder Formulations

Nasal deposition studies in vitro represent indispensable part of drug delivery system characterisation that complements the screening of its potential to ensure desired therapeutic effect. Owing to the efficiency in the treatment of neuroinflammatory processes, excessive first pass metabolism and systemic adverse reactions [76], dexamethasone represents the candidate for direct nose-to-brain delivery, which allows for reduction of the administered drug dose and systemic exposure. In case of dexamethasone, it might reduce the risk for systemic adverse reactions and decrease the extent of interaction with other drugs that are metabolized by CYP3A4, such as antiviral drug indinavir [77] investigated as a potential drug for the treatment of COVID-19 [78].

The direct nose-to-brain pathways start in olfactory and respiratory regions of the nasal cavity (via olfactory and trigeminal nerves, respectively). Olfactory pathway presents the most important route in this regard [8]. However, broader distribution to the respiratory mucosa innervated by the trigeminal nerve may also contribute to the brain targeted drug delivery [4,79].

In this work deposition studies were performed using a multi-sectional nasal cavity model (Figure 10A) developed using the CT scan of a patient with healthy nasal airways passages, with length of a nasal cavity (measured from the nostril to the end of the turbinates; [80]) of 92.1 mm (Figure 10B), and smallest vertical cross-sectional areas (valve region) of 141.3/98.4 mm^2 (right/left, respectively; Figure 10C) fitting into the 'normative' mean (range) of 85 mm^2 (20–160 cm^2) [81]. The multi-sectional nasal cavity model enabled precise determination of drug deposited in the regions of interest, namely, olfactory region (superior turbinate with small portion of the middle turbinate and the corresponding segment of the nasal septum [82]) and respiratory region (the rest of turbinates innervated by trigeminal nerve and septum that are covered by respiratory epithelium).

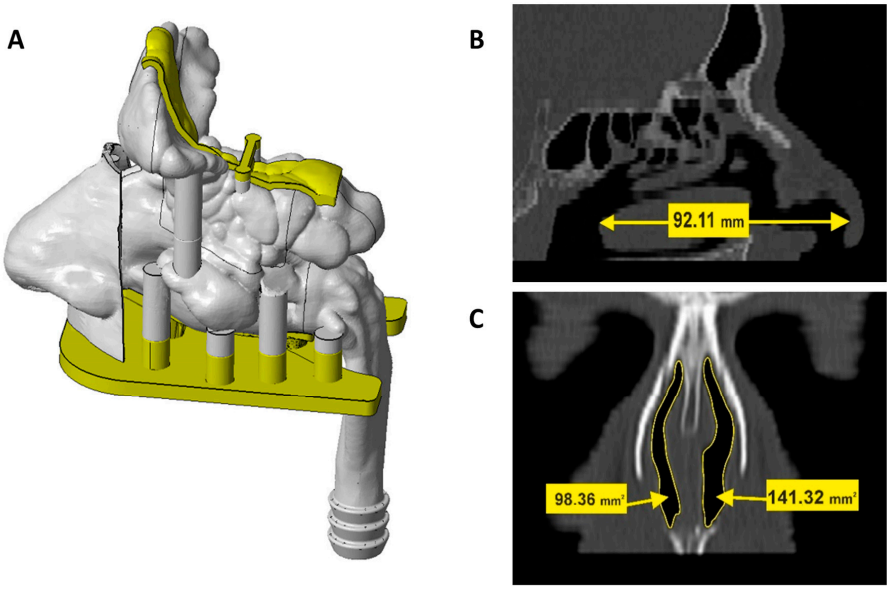

Figure 10. Schematic presentation of a 3D-printed nasal cavity model (**A**) and nasal geometry measurements including length of a nasal cavity (92.11 mm; (**B**) and smallest vertical cross-sectional areas (left: 98.36 mm^2/right 141.32 mm^2; (**C**).

Preliminary studies on nasal deposition of DSP-MS microspheres performed at administration angle of 60° and inspiratory air flow of 0 L min^{-1} confirmed inappropriate nasal DSP delivery by means of pure microsphere powder. This was related to poor DSP-MS flow properties leading to high powder retention within the capsule (Table 2), as well as to the loss of the sprayed powder at the entrance to the nasal cavity (visible during powder administration) and significant deposition outside the nasal cavity owing to small particle size. Blending of the microspheres with mannitol resulted in improved powder performance. As there was no crucial difference in the observed properties between DSP-MS/mannitol blends at 1:9 and 1:19 weight ratios (Table 2, Figure 8), nasal deposition was studied with the powder blend at higher drug dose (1:9, *w/w*).

The selected powder blend was shown to be homogenous upon 12 months of storage in sealed container at 4 °C, as mean percentage ratio of experimentally determined and theoretical mass of DSP in the analysed sample was 95.8%, with RSD value of 3.4%.

The deposition in olfactory region (superior turbinate with a small portion of the middle turbinate and corresponding segment of the nasal septum) and the rest of turbinates innervated by trigeminal nerve upon administration of the powder blend at different angles from horizontal plane (60 and 75°) and inspiratory air flows (0 and 20 L min^{-1}) are shown in Figure 11.

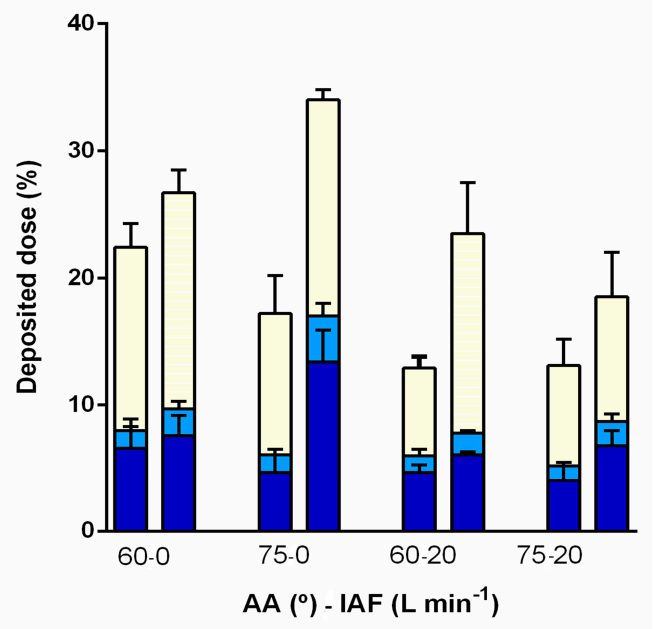

Figure 11. Nasal deposition of DSP-MS/Mannitol 1:9 in olfactory region (superior turbinate with a small portion of the middle turbinate (■) and corresponding segment of the nasal septum (■)) and the rest of turbinates innervated by trigeminal nerve (■) at various administration parameters in left and right half of 3D printed nasal cavity model (left and right bar, respectively). Administration parameters include angle of administration from horizontal plane (AA) and inspiratory airflow (IAF). All values are mean ± SD, n = 3.

The fraction of the DSP dose deposited in the olfactory region ranged between 5.1 ± 0.9 and 17.0 ± 1.6% revealing the potential of developed powder platform for targeted olfactory delivery. For the comparison, available studies on nasal deposition of nebulised liquid formulation of albuterol sulphate as the model drug report less than 5% deposition in the olfactory region, for both, unilateral and bidirectional delivery [83], and even when different levels of nasal passage dilations were employed [84].

The highest fraction of the dose deposited in the olfactory region (17.0 ± 1.6%) and the highest total dose recovery (87.4 ± 2.1%) were obtained for powder blend administration at AA of 75° and breath hold (inspiratory airflow of 0 L min^{-1}). Inspiratory airflow of 20 L min^{-1} was shown to reduce deposited DSP fraction in all regions of nasal cavity, resulting in low dose recovery (34.7 ± 1.5 to 50.3 ± 0.6%). Such observation is probably related to particle de-agglomeration enhanced by inspiratory airflow, leading to increased deposition outside the nasal cavity [21,22]. Favourable drug insufflation at breath hold is also advantageous from the patient's point of view as it simplifies the mode of administration avoiding problems related to (i) coordination of breathing with powder actuation and (ii) producing adequately deep breath if drug should be administered under breathing conditions.

For all inspected administration parameters, fraction of the dose deposited in the turbinate region innervated by trigeminal nerve was relatively limited and ranged between 6.9 ± 0.9 and 17.0 ± 1.8% of the total dose. This fraction may contribute to direct nose-to-brain drug delivery via trigeminal pathway, however, it is also available for systemic absorption due to high vascularisation of nasal respiratory mucosa [69]. Therefore, moderate drug delivery to this region might be beneficial in the light of reducing the possibility for systemic drug effects. The fraction of the dose that is also available for systemic absorption is the one found on the septum outside the segment corresponding to olfactory region, and it ranged between 5.3 ± 0.6 to 12.6 ± 1.3%.

Fraction of the dose deposited in olfactory (and respiratory) region was higher when powder was administered to the right nostril of the 3D nasal cavity model, as right half was characterised by higher vertical cross-sectional area of valve region. This finding opens the

possibility to adjust the administration strategy to individual patient nasal geometry when aiming olfactory region.

Conclusively, the fraction deposited in the olfactory region (up to 17.0%) can be considered as relatively large. Namely, direct nose-to-brain delivery implies avoidance of first pass effect as well as avoidance of dilution due to distribution and protein binding, therefore, the dose that needs to be delivered to the olfactory region to be absorbed by neuronal pathway may be as low as 0.01–1% of orally administered dose [85]. In this work, the highest fraction of the DSP dose (0.08 mg) delivered to the olfactory region (by single nasal administration of powder blend with DSP dose of 0.475 mg) represents 1% of dexamethasone oral daily dose (6 mg) recommended for the treatment of patients with severe and critical COVID-19 [86], clearly fitting to declared range.

4. Conclusions

QbD approach enabled rational design of spray-dried DSP-loaded polymeric microspheres. Optimised microspheres/mannitol powder blend showed favourable biopharmaceutical and sprayability properties considering the proposed route of administration. Nasal deposition studies revealed the potential of strategy employed for efficient delivery of DSP to the olfactory region of nasal cavity. The obtained results present a firm base for extending the study to an appropriate in vivo model needed for the final proof-of-concept.

Supplementary Materials: The following are available online at https://www.mdpi.com/article/10.3390/pharmaceutics13060795/s1, Table S1. Parameters and their levels included in experimental design., Table S2. Validation parameters of HPLC method employed for DSP and DB analysis., Figure S1. Chromatogram of (**A**) standard dexamethasone sodium phosphate (DSP) and dexamethasone base (DB) solution (both at 2 μg mL^{-1}), (**B**) sample of receptor medium taken during DSP permeability study form DSP powder formulation across Calu-3 cell monolayer, (**C**) eluate obtained by rinsing of the nasal cavity segment within nasal deposition studies of DSP powder formulation. All chromatograms were recorded at wavelength of 241 nm.

Author Contributions: Conceptualization, A.H., L.N.N., D.Š., L.K.; Methodology, A.H., L.N.N., D.Š., I.U., D.A.K., C.J.B., I.P., J.L., V.S., M.S.K., D.Z., L.K.; Validation, L.N.N., M.P. A.H.; Formal Analysis, L.N.N., D.Š., I.U., D.A.K., C.J.B., M.P., V.S., A.H.; Investigation, L.N.N., I.P., D.A.K., C.J.B., M.P., V.S.; Resources, A.H., M.S.K., D.Z., L.K.; Data Curation, L.N.N., I.P., J.L., D.Š., I.U., A.H.; Writing—original draft, A.H., L.N.N., D.Š., I.U.; Writing—Review & Editing, L.N.N., D.Š., I.U., D.A.K., C.J.B., M.P., I.P., J.L., V.S., M.S.K., D.Z., L.K., A.H.; Visualization, L.N.N., D.Š., I.U., A.H.; Supervision, A.H.; Project Administration, A.H.; Funding Acquisition, A.H. All authors have read and agreed to the published version of the manuscript.

Funding: This work has been supported in part by Croatian Science Foundation under the project UIP-2017-05-4592, European Social Fund under the Croatian Science Foundation project DOK-2020-01-2473 and Strengthening the scientific research and innovation capacities of the Faculty of Pharmacy and Biochemistry, University of Zagreb (FarmInova; project number KK.01.1.1.02.0021), financed from the European Regional Development Fund, Operational Program Competitiveness and Cohesion for the period 2014–2020.

Institutional Review Board Statement: Development of nasal cavity model based on a CT scan of a patient was carried out following the rules of the Declaration of Helsinki. The protocol was approved by the Ethics Committee of Sisters of Charity Hospital (Project identification code: EP-9941/19-3) and Ethics Committee of University of Zagreb Faculty of Pharmacy and Biochemistry (Class: 643-02/19-01/02; Registry number: 251-62-03-19-43).

Informed Consent Statement: The patient gave informed consent for inclusion before exporting data for the reconstruction of the nasal cavity and 3D printing.

Data Availability Statement: Not applicable.

Acknowledgments: The authors thank Miodrag Katalenić and Mladen Šercer (Cateh d.o.o., Zagreb) for help in the production of 3D nasal cavity model, and Matija Gretić, (University of Zagreb Faculty of Chemical Engineering and Technology, Zagreb, Croatia) for help with SEM analysis of the powder samples.

Conflicts of Interest: The authors declare no conflict of interest.

References

1. Higgins, T.S.; Wu, A.W.; Illing, E.A.; Sokoloski, K.J.; Weaver, B.A.; Anthony, B.P.; Hughes, N.; Ting, J. Intranasal antiviral drug delivery and Coronavirus disease 2019 (COVID-19): A State of the Art Review. *Otolaryngol. Head Neck Surg.* **2020**, *163*, 682–694. [CrossRef]
2. Basu, S.; Holbrook, L.T.; Kudlaty, K.; Fasanmade, O.; Wu, J.; Burke, A.; Langworthy, B.W.; Farzal, Z.; Mamdani, M.; Bennett, W.D.; et al. Numerical evaluation of spray position for improved nasal drug delivery. *Sci. Rep.* **2020**, *10*, 1–18. [CrossRef]
3. Siddiqui, R.; Khan, N.A. Proposed intranasal route for drug administration in the management of central nervous system manifestations of COVID-19. *ACS Chem. Neurosci.* **2020**, *11*, 1523–1524. [CrossRef] [PubMed]
4. Djupesland, P.G.; Messina, J.C.; Mahmoud, R.A. The nasal approach to delivering treatment for brain diseases: An anatomic, physiologic, and delivery technology overview. *Ther. Deliv.* **2014**, *5*, 709–733. [CrossRef] [PubMed]
5. Cárdenas, G.; Torres-García, D.; Cervantes-Torres, J.; Rosales-Mendoza, S.; Fleury, A.; Fragoso, G.; Laclette, J.P.; Sciutto, E. Role of Systemic and Nasal Glucocorticoid Treatment in the Regulation of the Inflammatory Response in Patients with SARS-Cov-2 Infection. *Arch. Med. Res.* **2020**, *52*, 143–150. [CrossRef] [PubMed]
6. Meneses, G.; Gevorkian, G.; Florentino, A.; Bautista Marcel, A.; Espinosa, A.; Acero, G.; Díaz, G.; Fleury, A.; Pérez Osorio, I.N.; Del Rey, A.; et al. Intranasal delivery of dexamethasone efficiently controls LPS-induced murine neuroinflammation. *Clin. Exp. Immunol.* **2017**, *190*, 304–314. [CrossRef] [PubMed]
7. Vroegop, A.V.; Eeckels, A.-S.; Van Rompaey, V.; Vanden Abeele, D.; Schiappoli, M.S.; Alobid, I.; Hummel, T.; Dorlodot, C.D.; Levie, P.; Huart, C.; et al. COVID-19 and olfactory dysfunction—An ENT perspective to the current COVID-19 pandemic. *B-ENT* **2020**, *16*, 81–85. [CrossRef]
8. Martins, P.P.; Smyth, H.D.C.; Cui, Z. Strategies to facilitate or block nose-to-brain drug delivery. *Int. J. Pharm.* **2019**, *570*, 118635. [CrossRef] [PubMed]
9. Fasiolo, L.T.; Manniello, M.D.; Tratta, E.; Buttini, F.; Rossi, A.; Sonvico, F.; Bortolotti, F.; Russo, P.; Colombo, G. Opportunity and challenges of nasal powders: Drug formulation and delivery. *Eur. J. Pharm. Sci.* **2018**, *113*, 2–17. [CrossRef]
10. Tanaka, A.; Furubayashi, T.; Tomisaki, M.; Kawakami, M.; Kimura, S.; Inoue, D.; Kusamori, K.; Katsumi, H.; Sakane, T.; Yamamoto, A. Nasal drug absorption from powder formulations: The effect of three types of hydroxypropyl cellulose (HPC). *Eur. J. Pharm. Sci.* **2017**, *96*, 284–289. [CrossRef]
11. Giuliani, A.; Balducci, A.G.; Zironi, E.; Colombo, G.; Bortolotti, F.; Lorenzini, L.; Galligioni, V.; Pagliuca, G.; Scagliarini, A.; Calzà, L.; et al. In vivo nose-to-brain delivery of the hydrophilic antiviral ribavirin by microparticle agglomerates. *Drug Deliv.* **2018**, *25*, 376–387. [CrossRef] [PubMed]
12. Rassu, G.; Soddu, E.; Cossu, M.; Brundu, A.; Cerri, G.; Marchetti, N.; Ferraro, L.; Regan, R.F.; Giunchedi, P.; Gavini, E.; et al. Solid microparticles based on chitosan or methyl-β-cyclodextrin: A first formulative approach to increase the nose-to-brain transport of deferoxamine mesylate. *J. Control. Release* **2015**, *201*, 68–77. [CrossRef] [PubMed]
13. Belgamwar, V.S.; Patel, H.S.; Joshi, A.S.; Agrawal, A.; Surana, S.J.; Tekade, A.R. Design and development of nasal mucoadhesive microspheres containing tramadol HCl for CNS targeting. *Drug Deliv.* **2011**, *18*, 353–360. [CrossRef]
14. Rassu, G.; Ferraro, L.; Pavan, B.; Giunchedi, P.; Gavini, E.; Dalpiaz, A. The role of combined penetration enhancers in nasal microspheres on in vivo drug bioavailability. *Pharmaceutics* **2018**, *10*, 206. [CrossRef] [PubMed]
15. Gavini, E.; Rassu, G.; Ferraro, L.; Beggiato, S.; Alhalaweh, A.; Velaga, S.; Marchetti, N.; Bandiera, P.; Giunchedi, P.; Dalpiaz, A. Influence of polymeric microcarriers on the in vivo intranasal uptake of an anti-migraine drug for brain targeting. *Eur. J. Pharm. Biopharm.* **2013**, *83*, 174–183. [CrossRef]
16. Picher, M.; Burch, L.H.; Hirsh, A.J.; Spychala, J.; Boucher, R.C. Ecto 5′-nucleotidase and nonspecific alkaline phosphatase: Two AMP-hydrolyzing ectoenzymes with distinct roles in human airways. *J. Biol. Chem.* **2003**, *278*, 13468–13479. [CrossRef] [PubMed]
17. Antunes Viegas, D.; Rodrigues, M.; Francisco, J.; Falcão, A.; Alves, G.; Santos, A.O. Development and application of an ex vivo fosphenytoin nasal bioconversion/permeability evaluation method. *Eur. J. Pharm. Sci.* **2016**, *89*, 61–72. [CrossRef] [PubMed]
18. Bourne, G.H. Alkaline Phosphatase in Taste Buds and Nasal Mucosa. *Nature* **1948**, *161*, 445–446. [CrossRef] [PubMed]
19. Pires, P.C.; Santos, L.T.; Rodrigues, M.; Alves, G.; Santos, A.O. Intranasal fosphenytoin: The promise of phosphate esters in nose-to-brain delivery of poorly soluble drugs. *Int. J. Pharm.* **2021**, *592*, 120040. [CrossRef] [PubMed]
20. Fransén, N.; Björk, E.; Nyström, C. Development and characterisation of interactive mixtures with a fine-particulate mucoadhesive carrier for nasal drug delivery. *Eur. J. Pharm. Biopharm.* **2007**, *67*, 370–376. [CrossRef] [PubMed]
21. Trows, S.; Scherließ, R. Carrier-based dry powder formulation for nasal delivery of vaccines utilizing BSA as model drug. *Powder Technol.* **2016**, *292*, 223–231. [CrossRef]
22. Nižić, L.; Potaś, J.; Winnicka, K.; Szekalska, M.; Erak, I.; Gretić, M.; Jug, M.; Hafner, A. Development, characterisation and nasal deposition of melatonin-loaded pectin/hypromellose microspheres. *Eur. J. Pharm. Sci.* **2020**, *141*, 105–115. [CrossRef]

23. Popov, T.A.; Åberg, N.; Emberlin, J.; Josling, P.; Ilyina, N.I.; Nikitin, N.P.; Church, M. Methyl-cellulose powder for prevention and management of nasal symptoms. *Expert Rev. Respir. Med.* **2017**, *11*, 885–892. [CrossRef] [PubMed]
24. Åberg, N.; Ospanova, S.T.; Nikitin, N.P.; Emberlin, J.; Dahl, Å. A nasally applied cellulose powder in seasonal allergic rhinitis in adults with grass pollen allergy: A double-blind, randomized, placebo-controlled, parallel-group study. *Int. Arch. Allergy Immunol.* **2014**, *163*, 313–318. [CrossRef] [PubMed]
25. Chen, X.; Guan, W.-J.; Sun, S.-X.; Zheng, P.-Y.; Sun, L.-H.; Chen, D.-H.; Wang, D.-D.; Chen, C.; Sun, B.-Q.; Zhang, X.-H.D. Effects of Intranasal Cellulose Powder on Asthma Control in Children with Mild-to-Moderate Perennial Allergic Rhinitis: A Randomized, Placebo-Controlled Trial. *Am. J. Rhinol. Allergy* **2019**, *33*, 184–193. [CrossRef] [PubMed]
26. Martinac, A.; Filipović-Grčić, J.; Perissutti, B.; Voinovich, D.; Pavelić, Ž. Spray-dried chitosan/ethylcellulose microspheres for nasal drug delivery: Swelling study and evaluation of in vitro drug release properties. *J. Microencapsul.* **2005**, *22*, 549–561. [CrossRef] [PubMed]
27. Kaialy, W.; Alhalaweh, A.; Velaga, S.P.; Nokhodchi, A. Influence of lactose carrier particle size on the aerosol performance of budesonide from a dry powder inhaler. *Powder Technol.* **2012**, *227*, 74–85. [CrossRef]
28. Kaialy, W.; Martin, G.P.; Ticehurst, M.D.; Momin, M.N.; Nokhodchi, A. The enhanced aerosol performance of salbutamol from dry powders containing engineered mannitol as excipient. *Int. J. Pharm.* **2010**, *392*, 178–188. [CrossRef]
29. Nižić, L.; Ugrina, I.; Špoljarić, D.; Saršon, V.; Kučuk, M.S.; Pepić, I.; Hafner, A. Innovative sprayable in situ gelling fluticasone suspension: Development and optimization of nasal deposition. *Int. J. Pharm.* **2019**, *563*, 445–456. [CrossRef] [PubMed]
30. Fachel, F.N.S.; Medeiros-Neves, B.; Prá, M.D.; Schuh, R.S.; Veras, K.S.; Bassani, V.L.; Koester, L.S.; Henriques, A.T.; Braganhol, E.; Teixeira, H.F. Box-Behnken design optimization of mucoadhesive chitosan-coated nanoemulsions for rosmarinic acid nasal delivery—In vitro studies. *Carbohydr. Polym.* **2018**, *199*, 572–582. [CrossRef] [PubMed]
31. Dukovski, B.J.; Mrak, L.; Winnicka, K.; Szekalska, M.; Juretić, M.; Filipović-Grčić, J.; Pepić, I.; Lovrić, J.; Hafner, A. Spray-dried nanoparticle-loaded pectin microspheres for dexamethasone nasal delivery. *Dry Technol.* **2019**, *39*, 1–11. [CrossRef]
32. Matilainen, L.; Toropainen, T.; Vihola, H.; Hirvonen, J.; Järvinen, T. In vitro toxicity and permeation of cyclodextrins in Calu-3 cells. *J. Control. Release* **2008**, *126*, 10–16. [CrossRef] [PubMed]
33. Hafner, A.; Lovrić, J.; Voinovich, D.; Filipović-Grčić, J. Melatonin-loaded lecithin/chitosan nanoparticles: Physicochemical characterisation and permeability through Caco-2 cell monolayers. *Int. J. Pharm.* **2009**, *381*, 205–213. [CrossRef] [PubMed]
34. European Medicines Agency. *Validation of Analytical Procedures: Text and Methodology Q2(R1)*; European Medicines Agency: London, UK, 2005. Available online: https://database.ich.org/sites/default/files/Q2%28R1%29Guideline.pdf (accessed on 5 May 2021).
35. Food and Drug Administration. *Inactive Ingredients in Approved Drug Products*; Food and Drug Administration: Silver Spring, MD, USA, 2021.
36. Scherließ, R.; Mönckedieck, M.; Young, K.; Trows, S.; Buske, S.; Hook, S. First in vivo evaluation of particulate nasal dry powder vaccine formulations containing ovalbumin in mice. *Int. J. Pharm.* **2015**, *479*, 408–415. [CrossRef] [PubMed]
37. Balducci, A.G.; Ferraro, L.; Bortolotti, F.; Nastruzzi, C.; Colombo, P.; Sonvico, F.; Russo, P.; Colombo, G. Antidiuretic effect of desmopressin chimera agglomerates by nasal administration in rats. *Int. J. Pharm.* **2013**, *440*, 154–160. [CrossRef] [PubMed]
38. Bálint, Z.; Krizbai, I.A.; Wilhelm, I.; Farkas, A.E.; Párducz, Á.; Szegletes, Z.; Váró, G. Changes induced by hyperosmotic mannitol in cerebral endothelial cells: An atomic force microscopic study. *Eur. Biophys. J.* **2007**, *36*, 113–120. [CrossRef] [PubMed]
39. Hirsh, A.J. Altering airway surface liquid volume: Inhalation therapy with amiloride and hyperosmotic agents. *Adv. Drug Deliv. Rev.* **2002**, *54*, 1445–1462. [CrossRef]
40. Dreijer-vander Glas, S.; Hafner, A. Nose. In *Practical Pharmaceutics*; Bouwman-Boer, Y., Fenton-May, V., Le Brun, P., Eds.; Springer: London, UK, 2015; pp. 139–152.
41. Goos, P.; Jones, B. *Optimal Design of Experiments*, 1st ed.; Wiley: Hoboken, NJ, USA, 2011.
42. Focaroli, S.; Mah, P.; Hastedt, J.; Gitlin, I.; Oscarson, S.; Fahy, J.; Healy, A. A Design of Experiment (DoE) approach to optimise spray drying process conditions for the production of trehalose/leucine formulations with application in pulmonary delivery. *Int. J. Pharm.* **2019**, *562*, 228–240. [CrossRef]
43. Ziaee, A.; Albadarin, A.B.; Padrela, L.; Femmer, T.; O'Reilly, E.; Walker, G. Spray drying of pharmaceuticals and biopharmaceuticals: Critical parameters and experimental process optimization approaches. *Eur. J. Pharm. Sci.* **2019**, *127*, 300–318. [CrossRef]
44. Magri, G.; Franzé, S.; Musazzi, U.M.; Selmin, F.; Cilurzo, F. Data on spray-drying processing to optimize the yield of materials sensitive to heat and moisture content. *Data Brief* **2019**, *23*, 4–7. [CrossRef] [PubMed]
45. Rodriguez, C.A.B.; Bassani, V.L.; Castellanos, L.; Rodríguez, F.A.R.; Baena, Y. Development of an oral control release system from Physalis peruviana L. fruits extract based on the co-spray-drying method. *Powder Technol.* **2019**, *354*, 676–688. [CrossRef]
46. Singh, A.; Van den Mooter, G. Spray drying formulation of amorphous solid dispersions. *Adv. Drug Deliv. Rev.* **2016**, *100*, 27–50. [CrossRef] [PubMed]
47. Shahin, H.I.; Vinjamuri, B.P.; Mahmoud, A.A.; Shamma, R.N.; Mansour, S.M.; Ammar, H.O.; Ghorab, M.M.; Chougule, M.B.; Chablani, L. Design and evaluation of novel inhalable sildenafil citrate spray-dried microparticles for pulmonary arterial hypertension. *J. Control. Release* **2019**, *302*, 126–139. [CrossRef]
48. Trenkel, M.; Scherließ, R. Nasal Powder Formulations: In-Vitro characterisation of the impact of powders on nasal residence time and sensory effects. *Pharmaceutics* **2021**, *13*, 385. [CrossRef] [PubMed]

49. Drugbank. Available online: https://www.drugbank.com (accessed on 15 January 2021).
50. Smart, J.D. The basics and underlying mechanisms of mucoadhesion. *Adv. Drug Deliv. Rev.* **2005**, *57*, 1556–1568. [CrossRef] [PubMed]
51. Yang, J.; Wu, C.Y.; Adams, M. DEM analysis of particle adhesion during powder mixing for dry powder inhaler formulation development. *Granul. Matter* **2013**, *15*, 417–426. [CrossRef]
52. Cai, X.; Yang, Y.; Xie, X.; Yu, F.; Yang, Y.; Yang, Z.; Zhang, T.; Mei, X. Preparation, characterization and pulmonary pharmacokinetics of a new inhalable zanamivir dry powder. *Drug Deliv.* **2016**, *23*, 1962–1971. [CrossRef] [PubMed]
53. Selvam, P.; Marek, S.; Truman, C.R.; McNair, D.; Smyth, H.D.C. Micronized drug adhesion and detachment from surfaces: Effect of loading conditions. *Aerosol Sci. Technol.* **2011**, *45*, 81–87. [CrossRef]
54. Jug, M.; Hafner, A.; Lovrić, J.; Kregar, M.L.; Pepić, I.; Vanić, Ž.; Cetina-Čižmek, B.; Filipović-Grčić, J. An overview of in vitro dissolution/release methods for novel mucosal drug delivery systems. *J. Pharm. Biomed. Anal.* **2018**, *147*, 350–366. [CrossRef] [PubMed]
55. Soane, R.J.; Hinchcliffe, M.; Davis, S.S.; Illum, L. Clearance characteristics of chitosan based formulations in the sheep nasal cavity. *Int. J. Pharm.* **2001**, *217*, 183–191. [CrossRef]
56. Yarragudi, S.B.; Richter, R.; Lee, H.; Walker, G.F.; Clarkson, A.N.; Kumar, H.; Rizwan, S.B. Formulation of olfactory-targeted microparticles with tamarind seed polysaccharide to improve nose-to-brain transport of drugs. *Carbohydr. Polym.* **2017**, *163*, 216–226. [CrossRef]
57. Lee, H.-J.; Lee, H.-G.; Kwon, Y.-B.; Kim, J.-Y.; Rhee, Y.-S.; Chon, J.; Park, E.-S.; Kim, D.-W.; Park, C.-W. The role of lactose carrier on the powder behavior and aerodynamic performance of bosentan microparticles for dry powder inhalation. *Eur. J. Pharm. Sci.* **2018**, *117*, 279–289. [CrossRef]
58. Rudén, J.; Frenning, G.; Bramer, T.; Thalberg, K.; An, J.; Alderborn, G. Linking carrier morphology to the powder mechanics of adhesive mixtures for dry powder inhalers via a blend-state model. *Int. J. Pharm.* **2019**, *561*, 148–160. [CrossRef] [PubMed]
59. Jüptner, A.; Scherließ, R. Spray dried formulations for inhalation—Meaningful characterisation of powder properties. *Pharmaceutics* **2020**, *12*, 14. [CrossRef]
60. Gänger, S.; Schindowski, K. Tailoring formulations for intranasal nose-to-brain delivery: A review on architecture, physico-chemical characteristics and mucociliary clearance of the nasal olfactory mucosa. *Pharmaceutics* **2018**, *10*, 116. [CrossRef]
61. Yang, J.; Dai, L.; Yu, Q.; Yang, Q. Histological and anatomical structure of the nasal cavity of Bama minipigs. *PLoS ONE* **2017**, *12*, e0173902. [CrossRef] [PubMed]
62. Ladel, S.; Schlossbauer, P.; Flamm, J.; Luksch, H.; Mizaikoff, B.; Schindowski, K. Improved in vitro model for intranasal mucosal drug delivery: Primary olfactory and respiratory epithelial cells compared with the permanent Nasal cell line RPMI 2650. *Pharmaceutics* **2019**, *11*, 367. [CrossRef] [PubMed]
63. Joergensen, L.; Klösgen, B.; Simonsen, A.C.; Borch, J.; Hagesaether, E. New insights into the mucoadhesion of pectins by AFM roughness parameters in combination with SPR. *Int. J. Pharm.* **2011**, *411*, 162–168. [CrossRef] [PubMed]
64. Mašková, E.; Kubová, K.; Raimi-Abraham, B.T.; Vllasaliu, D.; Vohlídalová, E.; Turánek, J.; Mašek, J. Hypromellose—A traditional pharmaceutical excipient with modern applications in oral and oromucosal drug delivery. *J. Control. Release* **2020**, *324*, 695–727. [CrossRef]
65. Jiang, L.; Gao, L.; Wang, X.; Tang, L. The application of mucoadhesive polymers in nasal drug delivery. *Drug Dev. Ind. Pharm.* **2010**, *36*, 323–336. [CrossRef]
66. Furubayashi, T.; Inoue, D.; Nishiyama, N.; Tanaka, A.; Yutani, R.; Kimura, S.; Katsumi, H.; Yamamoto, A.; Sakane, T. Comparison of various cell lines and three-dimensional mucociliary tissue model systems to estimate drug permeability using an in vitro transport study to predict nasal drug absorption in rats. *Pharmaceutics* **2020**, *12*, 79. [CrossRef] [PubMed]
67. Inoue, D.; Furubayashi, T.; Tanaka, A.; Sakane, T.; Sugano, K. Quantitative estimation of drug permeation through nasal mucosa using in vitro membrane permeability across Calu-3 cell layers for predicting in vivo bioavailability after intranasal administration to rats. *Eur. J. Pharm. Biopharm.* **2020**, *149*, 145–153. [CrossRef]
68. Salade, L.; Wauthoz, N.; Deleu, M.; Vermeersch, M.; De Vriese, C.; Amighi, K.; Goole, J. Development of coated liposomes loaded with ghrelin for nose-to-brain delivery for the treatment of cachexia. *Int. J. Nanomed.* **2017**, *12*, 8531–8543. [CrossRef] [PubMed]
69. Salade, L.; Wauthoz, N.; Vermeersch, M.; Amighi, K.; Goole, J. Chitosan-coated liposome dry-powder formulations loaded with ghrelin for nose-to-brain delivery. *Eur. J. Pharm. Biopharm.* **2018**, *129*, 257–266. [CrossRef]
70. Zhang, L.; Du, S.Y.; Lu, Y.; Liu, C.; Tian, Z.H.; Yang, C.; Wu, H.C.; Wang, Z. Puerarin transport across a Calu-3 cell monolayer—An in vitro model of nasal mucosa permeability and the influence of paeoniflorin and menthol. *Drug Des. Dev. Ther.* **2016**, *10*, 2227–2237. [CrossRef] [PubMed]
71. Ong, H.X.; Traini, D.; Young, P.M. Pharmaceutical applications of the Calu-3 lung epithelia cell line. *Expert Opin. Drug Deliv.* **2013**, *10*, 1287–1302. [CrossRef]
72. Sibinovska, N.; Žakelj, S.; Roškar, R.; Kristan, K. Suitability and functional characterization of two Calu-3 cell models for prediction of drug permeability across the airway epithelial barrier. *Int. J. Pharm.* **2020**, *585*, 19484. [CrossRef] [PubMed]
73. Pepić, I.; Lovrić, J.; Cetina-Čižmek, B.; Reichl, S.; Filipović-Grčić, J. Toward the practical implementation of eye-related bioavailability prediction models. *Drug Discov. Today* **2014**, *19*, 31–44. [CrossRef] [PubMed]
74. Sibinovska, N.; Božič, D.; Ribarski, M.B.; Kristan, K. Prediction of pharmacokinetic studies outcome for locally acting nasal sprays by using different in vitro methods. *Int. J. Pharm.* **2021**. [CrossRef] [PubMed]

75. Noach, A.B.; Sakai, M.; Blom-Roosemalen, M.C.; de Jonge, H.R.; de Boer, A.G.; Breimer, D.D. Effect of anisotonic conditions on the transport of hydrophilic model compounds across monolayers of human colonic cell lines. *J. Pharmacol. Exp. Ther.* **1994**, *270*, 1373–1380. [PubMed]
76. Brophy, T.R.O.R.; Mccafferty, J.; Tyrer, J.H.; Eadie, M.J. Bioavailability of Oral Dexamethasone During High Dose Steroid Therapy in Neurological Patients. *Eur. J. Clin. Pharmacol.* **1983**, *24*, 103–108. [CrossRef] [PubMed]
77. Crixivan Summary of Product Characteristics. Available online: https://www.ema.europa.eu (accessed on 25 February 2021).
78. Indu, P.; Rameshkumar, M.R.; Arunagirinathan, N.; Al-Dhabi, N.A.; Valan Arasu, M.; Ignacimuthu, S. Raltegravir, Indinavir, Tipranavir, Dolutegravir, and Etravirine against main protease and RNA-dependent RNA polymerase of SARS-CoV-2: A molecular docking and drug repurposing approach. *J. Infect. Public Health* **2020**, *13*, 1856–1861. [CrossRef] [PubMed]
79. Djupesland, P.G. Nasal drug delivery devices: Characteristics and performance in a clinical perspective—A review. *Drug Deliv. Transl. Res.* **2013**, *3*, 42–62. [CrossRef] [PubMed]
80. Warnken, Z.N.; Smyth, H.D.C.; Davis, D.A.; Weitman, S.; Kuhn, J.G.; Williams, R.O. Personalized medicine in nasal delivery: The use of patient-specific administration parameters to improve nasal drug targeting using 3D-printed nasal replica casts. *Mol. Pharm.* **2018**, *15*, 1392–1402. [CrossRef] [PubMed]
81. Djupesland, P.G.; Mahmoud, R.A. Role of nasal casts for in vitro evaluation of nasal drug delivery and quantitative evaluation of various nasal casts. *Ther. Deliv.* **2020**, *11*, 485–495. [CrossRef] [PubMed]
82. Choi, R.; Goldstein, B.J. Olfactory epithelium: Cells, clinical disorders, and insights from an adult stem cell niche. *Laryngoscope Investig. Otolaryngol.* **2018**, *3*, 35–42. [CrossRef] [PubMed]
83. Xi, J.; Wang, Z.; Nevorski, D.; White, T.; Zhou, Y. Nasal and olfactory deposition with normal and bidirectional intranasal delivery techniques: In vitro tests and numerical simulations. *J. Aerosol Med. Pulm. Drug Deliv.* **2016**, *29*, 118–131.
84. Xi, J.; Wang, Z.; Si, X.A.; Zhou, Y. Nasal dilation effects on olfactory deposition in unilateral and bi-directional deliveries: In vitro tests and numerical modeling. *Eur. J. Pharm. Sci.* **2018**, *118*, 113–123. [CrossRef] [PubMed]
85. Erdő, F.; Bors, L.A.; Farkas, D.; Bajza, Á.; Gizurarson, S. Evaluation of intranasal delivery route of drug administration for brain targeting. *Brain Res. Bull.* **2018**, *143*, 155–170. [CrossRef] [PubMed]
86. European Medicines Agency. *Assessment Report on Dexamethasone in Hospitalized Patients with Covid-19*; European Medicines Agency: Amsterdam, The Netherlands, 2020; Volume 5.

4. *In situ* gelling nanosuspension as an advanced platform for fluticasone propionate nasal delivery

European Journal of Pharmaceutics and Biopharmaceutics 175 (2022) 27–42

Contents lists available at ScienceDirect

European Journal of Pharmaceutics and Biopharmaceutics

journal homepage: www.elsevier.com/locate/ejpb

In situ gelling nanosuspension as an advanced platform for fluticasone propionate nasal delivery

Laura Nižić Nodilo [a], Mirna Perkušić [a], Ivo Ugrina [b], Drago Špoljarić [c], Cvijeta Jakobušić Brala [a], Daniela Amidžić Klarić [a], Jasmina Lovrić [a], Vesna Saršon [d], Maša Safundžić Kučuk [d], Dijana Zadravec [e], Livije Kalogjera [f], Ivan Pepić [a,*], Anita Hafner [a,*]

[a] University of Zagreb, Faculty of Pharmacy and Biochemistry, Zagreb, Croatia
[b] University of Split, Faculty of Science, Split, Croatia
[c] Visage Technologies d.o.o, Zagreb, Croatia
[d] Jadran-galenski laboratorij d.d, Rijeka, Croatia
[e] Department of Diagnostic and Interventional Radiology, Sestre milosrdnice University Hospital Center, University of Zagreb, Zagreb, Croatia
[f] ENT Department, Zagreb School of Medicine, University Hospital Center "Sestre milosrdnice", Zagreb, Croatia

ARTICLE INFO

Keywords:
In situ gelling
Nanosuspension
Fluticasone propionate
Nasal drug delivery
3D printed nasal cavity model
Chronic rhinosinusitis

ABSTRACT

In this work we present the development of *in situ* gelling nanosuspension as advanced form for fluticasone propionate nasal delivery. Drug nanocrystals were prepared by wet milling technique. Incorporation of drug nanocrystals into polymeric *in situ* gelling system with pectin and sodium hyaluronate as constitutive polymers was fine-tuned attaining appropriate formulation surface tension, viscosity and gelling ability. Drug nanonisation improved the release profile and enhanced formulation mucoadhesive properties. QbD approach combining formulation and administration parameters resulted in optimised nasal deposition profile, with 51.8% of the dose deposited in the middle meatus, the critical region in the treatment of rhinosinusitis and nasal polyposis. Results obtained in biocompatibility and physico-chemical stability studies confirmed the leading formulation potential for safe and efficient nasal corticosteroid delivery.

1. Introduction

Chronic rhinosinusitis is a chronic inflammatory disease of sinonasal mucosa with cardinal symptoms including nasal obstruction or congestion, nasal discharge, reduction or loss of smell, as well as facial pain and pressure. It affects relatively high proportion of the global population (5–12%) and significantly decreases patient's quality of life, thus presenting a global health concern. In addition, chronic rhinosinusitis has a great economic impact. It is associated with huge indirect costs owing to workplace productivity reduction and absenteeism, as majority of patients with chronic rhinosinusitis are of working age [1].

Nasal administration of corticosteroids presents the first-line treatment of chronic rhinosinusitis with or without nasal polyps. Local delivery of new-generation corticosteroids results in negligible systemic drug exposure and thus presents the viable option for the treatment of local inflammatory processes [2]. The main limitations of such an approach comprise complex nasal geometry that hinders drug delivery to the targeted regions of nasal cavity, and mucocilliary clearance that reduces the drug residence time at nasal mucosa. Currently, new formulation and delivery technologies are aimed at increasing the efficiency of nasal corticosteroid therapy, by prolonging the drug contact with nasal mucosa and increasing the fraction delivered to the site of inflammation. The final aim is to reduce the need for oral corticosteroid administration that is more effective but also linked with diverse systemic side effects [3].

One of the promising formulation strategies is the development of *in situ* gelling drug delivery platforms. They represent the low-viscous liquid forms that can be easily administered in the form of spray, while in contact with the nasal mucosa they turn into gel providing prolonged drug retention at the deposition site [4]. In our recent study on nasal *in situ* gelling fluticasone propionate suspension, we demonstrated the importance of concomitant consideration of formulation and administration parameters to ensure well guided development process, addressing the issue of nasal deposition in the early phase of formulation

* Corresponding authors at: A. Kovačića 1, 10000 Zagreb, Croatia.
E-mail addresses: ivan.pepic@pharma.unizg.hr (I. Pepić), anita.hafner@pharma.unizg.hr (A. Hafner).

https://doi.org/10.1016/j.ejpb.2022.04.009
Received 27 December 2021; Received in revised form 23 March 2022; Accepted 24 April 2022
Available online 27 April 2022

development [3].

The basic study has now been extended towards development of nasal *in situ* gelling system tailored to efficiently deliver fluticasone propionate nanocrystals as advanced form of highly lipophilic drug.

Nanonisation of the drug crystals represent effective approach to enhancement of solubility and dissolution rate of poorly water-soluble drugs [5]. In nasal delivery, nanosuspensions may offer a rapid onset of drug action that is followed by prolonged drug release owing to limited volume of nasal fluid available for drug dissolution, as seen in pulmonary delivery [5]. Nasal conventional or *in situ* gelling nanosuspensions have been mainly studied for their potential in the systemic [6,7] and brain targeted drug delivery [8–11]. However, combined strategy of incorporation of drug nanocrystals into *in situ* gelling formulation is worth evaluating for enhanced efficacy of locally acting poorly water-soluble drugs. Increased saturation solubility induced by nanonisation is expected to increase the passive drug diffusion to the site of action, opening the possibility for the reduction of the applied dose. Similarly, cyclodextrin/budesonide inclusion complex spray drying was recently employed to increase the solubility of locally acting budesonide intended for nasal delivery [12]. Finally, local use of nasal ivermectin mucoadhesive nanosuspension was shown to be effective and safe in the treatment of patients with mild COVID-19 [13]. Drug particles in nanometre size range allows for more precise drug dosing, even distribution and improved diffusion efficiency at the site of administration and ensures enhanced adhesion to the cell membrane compared to unprocessed drug particles [5,14]. Moreover, in the study performed by Alshweiat et al. [7], the addition of drug nanocrystals to mucoadhesive nasal polymer solutions further increased their mucoadhesive properties [7].

From the formulation point of view, comprehensive approach to development of *in situ* gelling nanosuspension is essential, taking into consideration nanocrystal impact on the formulation surface tension, viscosity and gelling ability, as these are the key attributes influencing formulation sprayability, deposition and performance at the nasal mucosa.

Within this work, fluticasone propionate nanocrystals have been prepared by wet milling technique. *In situ* gelling nanosuspensions comprised pectin and/or sodium hyaluronate as constitutive polymers, polysorbate 80 as a suspending agent and mannitol as a tonicity agent. Quality by design approach was employed to optimise formulation (fluticasone propionate, polysorbate 80 and sodium hyaluronate concentration) and/or administration parameters (inspiratory airflow, angle of administration from horizontal plane, angle of administration from vertical plane) according to the key responses, including nanoparticle size and zeta potential, surface tension, viscosity, gelation time, droplet size distribution, spray cone angle, and nasal deposition profile.

For the deposition studies, a 3D printed nasal cavity model based on the CT scan of a patient with chronic rhinosinusitis has been newly developed. Apart from total turbinate deposition, the issue of fluticasone propionate delivery to the middle meatus (i.e. middle turbinate region) has been specifically addressed. Namely, in patients with rhinosinusitis, oedema/mucosal obstruction and nasal polyps primarily occur in middle meatus [1], thus presenting the critical region of nasal cavity in the treatment of rhinosinusitis and nasal polyposis [15–17].

The leading formulation with optimised nasal deposition profile was further characterised in terms of gel behaviour, fluticasone propionate *in vitro* release, mucoadhesive properties, biocompatibility and physicochemical stability, to get a deeper insight into its potential for safe and efficient nasal corticosteroid delivery.

2. Materials and methods

2.1. Materials

Fluticasone propionate (micronised, pharma grade; further denoted as FP) was obtained from Carbosynth Ltd, UK. Polysorbate 80 (Tween 80; further denoted as P80) was purchased from Sigma Aldrich, Germany. Pectin CF 025 (degree of esterification and amidation 23 – 28% and 22 – 25%, respectively) was kindly donated by Herbstreith&Fox, Germany. Sodium hyaluronate (molecular weight 0.8 Da; further denoted as SH) was obtained from Contipro, Czech Republic. Mannitol was purchased from VWR International, Ltd. Simulated nasal fluid (SNF) was prepared as an aqueous solution of NaCl (150.0 mM; Kemig, Croatia), KCl (40.0 mM; Kemig, Croatia) and $CaCl_2{\cdot}2H_2O$ (5.3 mM; Sigma Aldrich, Germany). Hank's balanced salt solution with 5.3 mM Ca^{2+} (HBSS-Ca^{2+}; pH = 7.4)) for *in vitro* biocompatibility and permeability studies was prepared by dissolving KCl (5.4 mM), $NaHCO_3$ (4.2 mM), NaCl (136.9 mM), D-glucose monohydrate (5.6 mM) (all purchased from Kemig, Croatia), KH_2PO_4 (0.4 mM; Kemika, Croatia), $Na_2HPO_4{\cdot}2H_2O$ (0.3 mM; Fluka Chemie AG, Switzerland) and $CaCl_2{\cdot}2H_2O$ (5.3 mM) (Sigma Aldrich, Germany) in distilled water. Sargel® indicator paste was purchased from Arkema, France.

2.2. Design of experiments (DoE)

With the aim to optimise formulation and administration parameters for effective nasal delivery of fluticasone *in situ* gelling nanosuspension, quality by design (QbD) principles were employed. Three formulation (concentration of FP, polysorbate 80 and sodium hyaluronate) and three administration (inspiratory flow rate and angles of administration from the vertical and horizontal plane) parameters were included in the definitive screening experimental design developed with JMP 14.0 statistical software (JMP®, Version 14.0, SAS Institute Inc., Cary, NC, 1989–2007). After thorough preliminary studies, appropriate values for upper and lower limits of parameters were determined (Table 1). Nanoparticle size and zeta potential, gelation time, zero shear viscosity, droplet size distribution, surface tension, spray cone angle, deposition in the turbinate region and, more specifically, in the middle turbinate region of nasal cavity were studied as responses. All experiments related to the responses were performed in duplicate or triplicate. Data analysis was performed using the statistical software JMP 14.0.

2.3. Preparation of in situ gelling FP nanosuspensions

To obtain FP nanosuspensions, wet media milling technique as described in [18] was used. Briefly, concentrated aqueous suspension of FP in the presence of P80 was milled in round vial which contained five cylindrical magnetic stirrers (size 6 × 10 mm), and a mixture of yttrium stabilized zirconium oxide beads of 3 different diameter ranges (0.1 mm, 0.2 mm and 0.4 to 0.6 mm), each present in the same amount (0.5 g). The stirring was performed during 24 h at 350 rpm on a magnetic stirrer (MIX eco 15, Germany). Afterwards, the nanosuspension was mixed with the solutions of pectin (1.4%, *w/w*), SH (0.5%, *w/w*) and with distilled water to obtain the final substance concentrations listed in Table 1. Mannitol (4%, *w/w*) was added as a tonicity agent, and pH was adjusted to 6.0 ± 0.1 with NaOH (1 M), measured by pH meter (Mettler Toledo, Switzerland). Osmolality of the *in situ* gelling nanosuspensions mixed with SNF, as well as with HBSS-Ca^{2+}, in volume ratio 1:1 was determined using OsmoTECH® Single-Sample Micro-Osmometer

Table 1
Parameters considered in the experimental design and their levels.

Parameter	High (+1)	Medium (0)	Low (−1)
Fluticasone propionate concentration, FP (%, *w/w*)	0.060	0.045	0.030
Polysorbate 80 concentration, P80 (%, *w/w*)	0.060	0.045	0.030
Sodium hyaluronate concentration, SH (%, *w/w*)	0.050	0.035	0.020
Angle of administration from the horizontal plane, AAH (°)	75	60	45
Angle of administration from the vertical plane, AAV (°)	20	10	0
Inspiratory flow, IF (L min^{-1})	60	30	0

(Advanced Instruments, USA).

2.4. Particle size and zeta-potential measurement

Mean particle diameter, polydispersity index and zeta-potential were determined by photon correlation spectroscopy using Zetasizer Ultra (Malvern Panalytical Ltd, UK) at 25 °C. Particle size was measured by diluting 0.1 ml of *in situ* gelling nanosuspensions up to 1 ml with of polysorbate 80 solution equal to the tested nanosuspension in polysorbate 80 concentration (0.03–0.06%, *w/w*). For zeta-potential measurements, the undiluted samples were placed in an electrophoretic cell. All measurements were performed in triplicate.

2.5. Rheological characterisation

Rheological characterisation was performed according to methods described previously by our research group, with slight modifications (3). Rotational and oscillatory rheological tests were performed using a modular compact rheometer MCR 102 (Anton Paar GmbH, Austria) equipped with an air-cooled Peltier temperature control system and cone-plate (cone slope 1°, diameter 50 mm; CP50) or parallel plate (diameter 50 mm; PP50) measuring system. All data were analysed using RheoCompass TM Light (Anton Paar GmbH, Austria).

2.5.1. Zero-shear viscosity determination

Zero-shear viscosity of *in situ* gelling fluticasone nanosuspensions at 25 °C was determined by rotational creep test using CP50 measuring system at a fixed gap of 0.102 mm from the lower plate. The sample was equilibrated at 25 °C for 3 min. Shear stress of 0.1 Pa was applied to the sample and maintained for 5 min, while the shear strain was recorded as a function of time. Zero-shear viscosity was calculated by RheoCompass software. Each measurement was performed in triplicate.

2.5.2. Determination of linear viscoelastic range

Linear viscoelastic range (LVE range) of samples was determined by amplitude sweep test. Prior to measurement, *in situ* gelling samples were mixed with SNF in volume ratio 1:1. The test was performed at the angular frequency of 6.28 rad s^{-1}, at the temperature of 34 °C and in the amplitude range of 0.1–100%. Limit of LVE range was calculated by RheoCompass software.

2.5.3. Gelation time measurement

SNF was added to *in situ* gelling fluticasone nanosuspension at the ratio of 1:1 (*v/v*) and was stirred on a magnetic stirrer for 1 min prior to rheological measurement. Gelation time was determined at 34 °C by time sweep test using PP50 measuring system. The gap from the lower plate was set at 0.500 mm. Shear strain was set at 0.1% (from the LVE range). To determine the gel point according to [19], the test was performed at three angular frequencies (1, 6.28 and 10 rad s^{-1}). Storage (*G*') and loss moduli (*G*'') versus time plot were recorded. Three replicate measurements were performed at each of the frequencies.

2.6. Droplet size distribution determination

Droplet size distribution (DSD) was determined by Spraytec® (Malvern Panalytical Ltd) using laser diffraction technique, according to [3]. Briefly, the measurements were performed using a preservative-free spray pump system (Spray Pump 3 K, 140 µl, Aeropump, Germany) actuated at an angle of 90° from the horizontal plane, with 300 mm focal distance from the lens. The tip of the spray pump was 3 cm below the laser diffraction measurement zone. All actuations were performed manually and in triplicate after priming the spray pump by 4 actuations sent to waste. The data were analysed using Malvern Spraytec 3.20 software and expressed as volume diameters D_v10, D_v50, D_v90 and span as described in literature [20].

2.7. Surface tension determination

Surface tension of *in situ* gelling fluticasone nanosuspensions was measured using Krüss K-100C tensiometer (Krüss, Germany), employing Du Noüy ring method. The instrument was calibrated using distilled water, where the surface tension of 70.62 ± 0.67 mN m^{-1} at 25 °C was considered as accurately standardized [21,22]. All measurements were performed at 25 °C in triplicate. Each sample was equilibrated for 30 min in the measurement cell before initialising the measurement.

2.8. Spray cone angle measurement

Spray cone angle was measured after spraying the sample against a dark background under the same conditions employed for DSD determination. The spray plume was recorded using a digital camera Lumix MC-FZ1000 (Panasonic, Japan) with 120 frames per second. The images were afterwards analysed and the angle was determined using a virtual protractor. Three replicate measurements were performed for each formulation.

2.9. Development of the representative nasal cavity model

Multi-sectional nasal cavity model was developed according to an anonymised Computer Tomography (CT) scan of a 28-year-old patient, obtained from Sisters of Charity Hospital database. The patient had chronic rhinosinusitis without nasal polyps, as confirmed by a specialist. Reconstruction, design and 3D print of a nasal cavity model was performed by CATEH d.o.o., Zagreb, complying with ISO 13485 standards. InVesalius 3.1 software was used to segment CT and reconstruct the nasal cavity model while Rhinocheros® 7 was used to design the nasal cavity model in multiple separate pieces. Nasal cavity model was segmented into anterior region, upper, medium and lower turbinate regions, septum and posterior region/nasopharynx which had a connector for respiratory pump used for simulating breathing conditions. Paranasal sinuses with openings into the nasal cavity are also included in the nasal cavity model. The model was produced by Stratasys Connex 350 and printed in flexible material DM 9850 combination materials TangoBlack+ and VeroWhite+ at a thickness of layer 0.030 mm to ensure optimal fit of the segments and to enable adequate insertion of the atomizer tip inside the nostril.

2.10. Assessment of the deposition profile in the nasal cavity in vitro

To accurately assess fractional nasal deposition, 3D printed nasal cavity model was placed on a stand and connected to a respiratory pump (model 613; Harvard Apparatus, USA), which simulated breathing in the airflow range from 0 L min^{-1} (representing breath hold) to 60 L min^{-1} (representing moderately strong inspiration by the patient; Table 1; [3,23]. The inhalation flow rate was measured by In-Check Nasal inspiratory flow meter (Clement Clarke International Ltd, UK). Relative air humidity was 40 ± 2%. Prior to formulation administration, Sargel® indicator paste was evenly applied onto the segments of nasal cavity model to visualise deposition pattern and prevent formulation dripping. *In situ* gelling nanosuspensions were administered to one nostril of the nasal cavity using Spray Pump 3 K (Aeropump) at an insertion depth of 5 mm under various angles from the horizontal (45−75°) and vertical (0−20°) plane (Table 1). The administration was performed with the other nostril closed. The fractional deposition in the nasal cavity model was determined by weighing each segment before and after formulation administration, using an electronic balance (precision 0.01 mg; Mettler Toledo, Switzerland). Two replicate assessments of deposition pattern were conducted for each formulation.

2.11. Preparation and characterisation of the leading formulation

Optimal formulation and administration parameters for nasal

delivery of FP in the form of *in situ* gelling nanosuspension were generated by DoE analysis. Leading *in situ* gelling FP nanosuspension was prepared employing generated formulation parameters and was initially characterised the same way as the formulations included in DoE. Then, the leading formulation was subjected to further characterisation in terms of gel behaviour, FP *in vitro* release, mucoadhesive properties, biocompatibility and physico-chemical stability. Corresponding *in situ* gelling FP microsuspension as well as conventional FP nano and microsuspension were used as controls where appropriate. *In situ* gelling FP microsuspension was prepared following the same procedure as for the preparation of *in situ* gelling FP nanosuspensions, omitting wet media milling. Conventional microsuspension was prepared by dispersing FP with P80 in distilled water at concentration of 0.041% and 0.03% (*w/w*), respectively. Conventional nanosuspension was prepared by dispersing FP and P80 in distilled water at concentration of 0.328% and 0.24% (*w/w*), respectively, which was further subjected to wet media milling as described in section *2.3. Preparation of in situ gelling FP nanosuspensions*. The prepared concentrated nanosuspension was diluted with distilled water to final FP and P80 concentration of 0.041% and 0.03% (*w/w*), respectively.

2.11.1. Drug content determination

Drug content of leading *in situ* gelling FP nanosuspension was determined after mixing the systems with ethanol in volume ratio 1:9. The mixture was sonicated for 5 min and centrifuged for 5 min at 4000 rpm. Supernatant was diluted, filtered (0.2 μm) and analysed for FP concentration using HPLC method described in section *2.12. Quantitative determination of fluticasone propionate*. Drug content was expressed in relation to theoretical drug content.

2.11.2. Transmission electron microscopy (TEM)

Leading *in situ* gelling FP nanosuspension was pipetted on a flat surface and a Formvar®/Carbon copper grid with a mesh size 100 (Emtec GmbH, Germany) was immersed in the droplet and left to dry at ambient conditions. The morphological evaluation of the particles in nanosuspension was performed by TEM Morgagni 268 (FEI, USA) operating at 70 kV.

2.11.3. Gel expansion determination

Determination of gel expansion coefficient was performed according to [9] with slight modifications. The leading *in situ* gelling FP nanosuspension (1 ml) was placed in a plugged graduated syringe and 1 ml of SNF was added. The syringe was thermostated at 34 °C and total volume in the syringe was noted (V_T).

The volume expansion coefficient (VEC) was calculated from the following expression (Eq. (1)):

$$VEC = (V_T - 2ml) \times 100 \quad (1)$$

Corresponding *in situ* gelling FP microsuspension was characterised by the same procedure and served as control.

2.11.4. In vitro release study

The release profile of fluticasone from the leading *in situ* gelling FP nanosuspension was determined using an automated Franz diffusion cells testing system Phoenix™ RDS (Teledyne Hanson, USA). The system consisted of six Franz diffusion cells (nominal volume of 16 ml) placed in a Peltier heating block. The cells were filled with a mixture of SNF and ethanol in the ratio 1:1 (*v/v*). The system was thermostated at 34 °C with constant stirring. Formulation was pipetted in the donor compartment. Aliquots (0.4 ml) from the receiver compartment were taken at predetermined time intervals during a total of 8 h. Taken samples were replaced with fresh medium. The aliquots were filtered and analysed for drug content using a previously developed HPLC method (Section *2.12. Quantitative determination of fluticasone propionate*). The content of the drug remained in donor compartment was also analysed. Each experiment was performed in triplicate. Corresponding *in situ* gelling FP microsuspension as well as conventional FP nano and microsuspension were used as controls.

2.11.5. Saturation solubility determination

FP saturation solubility was determined according to the method by Hong et al. [24], with slight modifications. Conventional FP micro and nanosuspension (prepared at FP and P80 concentrations equal to those in leading *in situ* gelling nanosuspension) were mixed with SNF in ratio 1:1 (*v/v*). The mixtures were incubated at 34 °C for 48 h and shaken constantly at 120 rpm using thermostated orbital shaker (Biosan, Latvia). After 48 h, removed aliquots were centrifuged, supernatant was filtered (0.22 μm) and analysed for FP content using the method described in section *2.12. Quantitative determination of fluticasone propionate*. The measurements were performed in triplicate.

2.11.6. In vitro mucoadhesion test

To determine mucoadhesive properties of the leading *in situ* gelling FP nanosuspension, porcine nasal mucosa was obtained from a local abattoir and isolated according to [25]. Porcine heads were longitudinally split in half. Nasal mucosa was meticulously separated from the septum and conchae and stored at – 20 °C until use. Mucoadhesiveness of the formulation was measured using a texture analyser TA.XT Plus (Stable Micro Systems, UK) equipped with the mucoadhesion rig by modifying the method of [26]. The nasal mucosa was cut in disks with 10 mm diameter and was attached to the upper probe using a cyanoacrylate glue (Fig. 1). The formulation was mixed with SNF in 1:1 ratio (*v/v*). The mixture (0.5 ml) was pipetted onto the lower platform and thermostated at 34 °C. The mucosal section on the upper probe was also soaked in SNF thermostated at 34 °C for 30 s prior to measurement. Test settings were as follows: pre-test speed 0.5 mm s^{-1}, test speed 0.1 mm s^{-1}, contact time 120 s, applied force 0.1 N and post-test speed 0.1 mm s^{-1}. Three replicate measurements were performed for each sample. The maximum detachment force (F_{max}) and the work of adhesion (W_{adh}, calculated from the force-distance plot; [26] were used as measures of mucoadhesive properties. Corresponding *in situ* gelling FP microsuspension as well as conventional FP nano and microsuspension were used as controls.

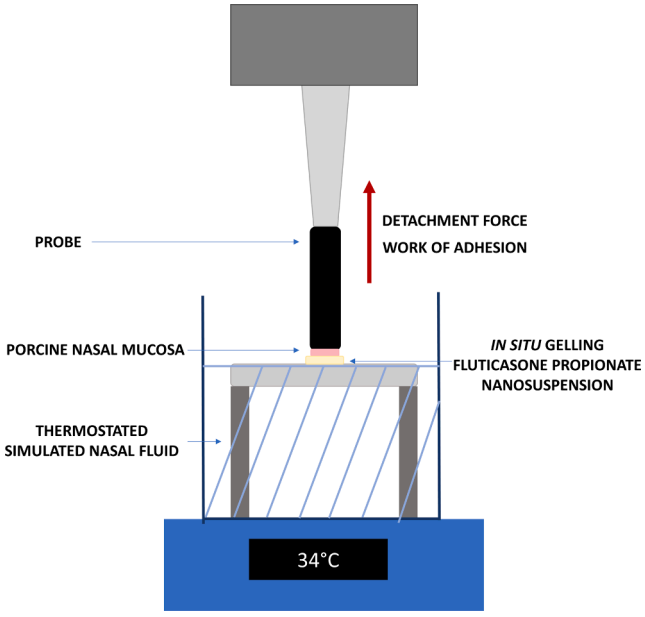

Fig. 1. Schematic presentation of mucoadhesion measurement. Probe elevation is accompanied with measurement of time-dependent detachment force and distance. Texture analyser is connected to software which calculates corresponding work of adhesion.

2.11.7. Cell culture conditions

Calu-3 cell line (ATCC® HTB-55™; ATCC, USA) was used for *in vitro* biocompatibility study. The cells were cultured in DMEM-F12 cell culture medium (Sigma Aldrich, USA) containing 1% penicillin and streptomycin (*v/v*; Lonza, Switzerland) and 10% foetal bovine serum (*v/v*, Sigma Aldrich). The cell cultures were kept in an incubator (Sanyo CO_2, Japan) at 37 °C, 5% CO_2 and 95% relative humidity. The cell medium was changed every 2–3 days, and the cells were split in ratios from 1:3 to 1:6 after reaching 70–90% confluence. The cells were detached from the flasks by trypsin/EDTA mixture (0.25%/0.02% in phosphate-buffered saline, PBS, Lonza, Switzerland; respectively).

2.11.8. In vitro biocompatibility study

In vitro biocompatibility of the leading *in situ* gelling FP nanosuspension and corresponding *in situ* gelling FP microsuspension was determined by MTT assay. The cells were seeded in 96-well plates at a density of 4×10^4 cells per well. After 48 h, the cells were washed with HBSS-Ca^{2+} and treated with formulations mixed with HBSS-Ca^{2+} in volume ratio 1:1 for 2 h at 37 °C. Pure HBSS-Ca^{2+} was used as a negative control. Each formulation was tested in pentaplicate. Afterwards, the formulations were removed from the wells, the cells were rinsed with HBSS-Ca^{2+} and incubated with cell medium. Cell viability was determined after 24 h by MTT (3-[4,5-dimethylthiazol-2-yl]-2,5-diphenyl tetrazolium bromide; Sigma-Aldrich, Germany) colorimetric assay. MTT was dissolved in PBS (2.5 mg ml^{-1}) and was further diluted by DMEM-F12 to the final concentration of 0.5 mg ml^{-1}. The cells were exposed to MTT reagent (100 µl per well) for 30 min, after which the reagent was removed, the cells were lysed and the formazan crystals were dissolved in isopropanol (100 µl per well). The amount of formazan was determined spectrophotometrically by 1420 Multilabel Counter Victor3 (PerkinElmer, USA) at 570 nm wavelength. Cell viability was calculated in relation to control (cells incubated in HBSS-Ca^{2+}) according to the following expression (Eq. (2)):

$$Cell\ viability(\%) = \frac{A_{sample} - A_{ipr}}{A_{control} - A_{ipr}} \times 100 \quad (2)$$

where A_{sample} is the absorbance of formazan solution from the cells treated with tested formulations, $A_{control}$ is the absorbance of formazan solution from untreated cells (incubated with HBSS-Ca^{2+}), and A_{ipr} is the absorbance of pure isopropanol at the same wavelength.

2.11.9. Frequency sweep test

Frequency sweep test of the leading *in situ* gelling FP nanosuspension and corresponding *in situ* gelling FP microsuspension after mixing with SNF was performed at 34 °C using PP50 measuring system, with a 0.500 mm gap. The sample was equilibrated for 15 min. Storage and loss moduli were recorded in the range of angular frequencies from 0.1 to 100 rad s^{-1}, with the applied shear strain of 0.1% (within the LVE range). Corresponding *in situ* gelling FP microsuspension was used as control. The measurements were performed in triplicate.

2.12. Quantitative determination of fluticasone propionate

Quantitative determination of fluticasone propionate was performed by high performance liquid chromatography (HPLC) using a PerkinElmer Series 200 chromatographic system consisting of an autosampler, system controller, pump, degasser, a column oven, and an UV–VIS detector (PerkinElmer, USA). The chromatographic conditions were a modification of those from European Pharmacopoeia [27]. Separation was performed on Kinetex C18 column (100 × 4.6 mm, 2.6 µm, 100 Å) with suitable guard column, both obtained by Phenomenex (USA). The mobile phase consisted of 10 mM phosphate buffer (pH 3.5) and acetonitrile in volume ratio 40:60, respectively. The isocratic elution was carried out and flow of the mobile phase was set to 1.0 ml min^{-1}. The column was thermostated at 45 ± 0.1 °C during the analysis and the injection volume was set to 80 µl. Fluticasone was monitored at the wavelength of 236 nm. The corresponding concentrations were determined from the integrated peak area using the appropriate calibration curves. The proposed method was validated based on the International Conference on Harmonization (ICH) guideline Q2 (R1) [28].

2.13. Stability studies

Stability tests were performed upon 8-week storage in an impermeable container at 4 °C/RH 65%, following ICH guidelines on stability testing of new drug products stored in impermeable containers, in terms of stability criteria including [29]: drug content, formulation appearance, physical attributes, and functionality tests (colour, phase separation, resuspendibility, particle size, polydispersity index, zeta potential and gelation properties employing time and frequency oscillatory tests). The selected stability indicators are in line with recent literature reports on stability testing of (*in situ* gelling) nanosuspensions [7,30,31]. All measurements were done in triplicate.

2.14. Statistical analysis

For all statistical analyses, $p < 0.05$ was set as the minimal level of significance. Statistical analysis of data obtained in the scope of DoE was performed using JMP 14.0 software (JMP®, Version 14.0, SAS Institute Inc., USA, 1989–2007.) Comparison of *in vitro* release profiles was performed by calculating the similarity factor (f2), as described previously [32]. The mean cumulative amount of drug released of the two formulations were compared at each time point. The release profiles were considered similar when $f2 > 50$ [33]. Analysis of mucoadhesiveness and formulation stability was performed using GraphPad Prism (trial version), employing a one-way analysis of variance (ANOVA) followed by a Tukey's post hoc test.

3. Results and discussion

The purpose of this study is to develop nasal *in situ* gelling FP nanosuspension with the potential to increase the efficiency of local corticosteroid delivery in the treatment of chronic rhinosinusitis. Combined strategy of drug nanonisation and incorporation into *in situ* gelling platform is aimed towards increasing drug bioavailability at the site of action, with the possibility of reducing the applied dose. Namely, nanosized drug particles are characterised by improved solubility, diffusivity and adhesive properties when compared to micron-sized drug particles. Formulation attribute of sol-gel transition in contact with nasal mucosa is embedded to prevent the leakage, prolong retention and adjust the drug release at the nasal mucosa. Formulation issues are supplemented with nasal deposition studies targeting FP delivery beyond the nasal valve, and, specifically, to the middle turbinate region regions where oedema/mucosal obstruction and nasal polyps primarily occur [1].

3.1. Experimental design – analysis of the results

Development of *in situ* gelling FP nanosuspension included QbD approach that coupled consideration of formulation and administration parameters to optimise FP nasal delivery efficiency. Namely, three formulation and three administration parameters were included in the DoE (Table 1), with FP nanosuspension particle size, zeta-potential, gelation time, zero shear viscosity, surface tension, droplet size distribution, spray cone angle, total turbinate deposition and middle turbinate deposition analysed as responses. The parameters (covariates) were standardised to unitless interval [−1, 1]. This approach is widely used in experimental design modelling [34] and equations in the rest of the paper are presented in normalized terms. Regression modelling (with linear effects and two-way interactions where applicable) was applied to enlighten the formulation and/or administration parameters as well as

their interactions that are significant in estimation of evaluated responses. ANOVA results for statistical models fitted to results of designed experiments are shown in Table 2. All *in situ* gelling FP nanosuspensions defined by the experimental design were successfully prepared. The pH value was adjusted to 6.0 ± 0.1. The osmolality of *in situ* gelling FP nanosuspensions upon mixing with SNF in 1:1 vol ratio was 320.0 ± 1.0–342.3 ± 4.7 mOsm kg^{-1}, falling within the suitable range for nasal formulations (290 – 500 mOsm kg^{-1}) [35].

3.1.1. FP nanoparticle size

Efficacy of wet media milling for the preparation of *in situ* gelling FP nanosuspension was evaluated in relation to resulting FP nanoparticle size and polydispersity. Laboratory-scale wet media milling has recently been receiving a lot of attention as an effective particle size reduction technique [18,36–41]. It is based on suspended particles colliding with each other and the grinding medium, such as small glass pearls or ceramic beads in a liquid medium [42]. In this work, FP nanosuspensions were successfully prepared by wet media milling, as evidenced by FP mean nanoparticle diameter of 133.0 ± 0.8 – 160.7 ± 3.6 nm and polydispersity index (PDI) of 0.227 ± 0.027 – 0.273 ± 0.011 (Table 3). All the formulations had PDI lower than 0.3, indicating monodisperse size distribution [43]. The model obtained from regression modelling showed a good fit (R-squared 0.78, RMSE 3.73, PRESS R-squared 0.51, and PRESS RMSE 4.5), as shown in the Eq. (3) (Eq. (3)):

$$d_{mean} = 143.29 + 3.69 \times P80 + 0.11 \times SH - 4.26 \times FP - 2.67 \times P80 \times SH + 5.90 \times FP^2 \quad (3)$$

Mean particle diameter, i.e. particle size was positively influenced by the P80 and SH concentration increase. The observed effect could be ascribed to polymer adhesion to the nanoparticle surface as previously reported in literature [7,44].

3.1.2. Zeta-potential

In situ gelling FP nanosuspensions prepared according to the DoE were characterised by nanoparticle zeta-potential ranging between −93.1 ± 0.6 and −77.2 ± 3.7 mV (Table 3). The model obtained from the regression modelling exhibited a good fit (R-squared 0.78, RMSE 2.62, PRESS R-squared 0.62, and PRESS RMSE 2.99) and is given by the following equation (Eq. (4)):

$$\zeta = -82.67 + 3.36 \times P80 - 2.66 \times SH + 2.18 \times P80 \times SH \quad (4)$$

Zeta-potential decreased (absolute value increased) with the increase in SH concentration. Similar observation has already been reported in literature [7,45,46]. Hydrophobic SH regions adhere to the surface of FP nanoparticles [47], ensuring sterical stabilisation. Decrease in zeta-potential is related to the negative charge of SH polymeric chains which causes electrostatic repulsion, contributing to formulation stability [45]. Generally, nanosuspensions are considered stable with zeta-potential absolute values above 30 mV [48,49], while the absolute values above 60 mV indicate excellent stability [49].

The increase in P80 concentration resulted in an increase in zeta-potential, i.e. in the reduction of the negative zeta-potential value. P80 is a non-ionic suspending agent widely used in nanosuspension preparation and stabilisation, ensuring physical barrier for the agglomeration of nanoparticles [50–55]. Decrease of negative zeta-potential value after addition of P80 has been reported in literature [54,55]. Due to its relatively large structure, once it is adsorbed on the nanoparticle surface, P80 can mask the electrostatic repulsion caused by ionic polymers or surfactants, causing a decrease in the potential between the particle surface and the dispersion medium [51]. This premise is supported by the regression model since the interaction between P80 and SH has also shown positive influence on zeta-potential (Eq. (4)).

3.1.3. Gelation time

To ensure instant gelation, concentration of ion-responsive *in situ* gelling polymer, as well as concentrations of other compounds in the formulations need to be carefully selected. High and low levels for the concentration of pectin, SH, P80 and FP (Table 1) were determined based on thorough preliminary experiments, with the aim to ensure instant gel forming after contact with the nasal mucosa for all the

Table 2
ANOVA results for statistical models fitted to results of designed experiments.

DoE response	Analysis of Variance					
	Source	DF	Sum of Squares	Mean Square	F Ratio	Prob > F
Fluticasone propionate nanoparticle size	Model	5	553.29947	110.660	7.9579	0.0022
	Error	11	152.96288	13.906		
	C. Total	16	706.26235			
Zeta-potential	Model	3	313.77182	104.591	15.2066	0.0002
	Error	13	89.41373	6.878		
	C. Total	16	403.18555			
Zero shear viscosity	Model	4	25.801338	6.45033	26.5418	<0.0001
	Error	12	2.916310	0.24303		
	C. Total	16	28.717647			
D_v10	Model	5	186.22119	37.2442	27.5001	<0.0001
	Error	11	14.89762	1.3543		
	C. Total	16	201.11881			
D_v50	Model	5	4540.6841	908.137	31.6493	<0.0001
	Error	11	315.6311	28.694		
	C. Total	16	4856.3152			
D_v90	Model	5	16528.458	3305.69	23.0261	<0.0001
	Error	11	1579.193	143.56		
	C. Total	16	18107.651			
Spray cone angle	Model	3	591.01571	197.005	31.4611	<0.0001
	Error	13	81.40429	6.262		
	C. Total	16	572.42000			
Total turbinate deposition	Model	7	8678.1981	1239.74	18.0972	<0.0001
	Error	9	616.5407	68.50		
	C. Total	16	9294.7388			
Middle turbinate deposition	Model	8	1997.7268	249.716	3.8284	0.0376
	Error	8	521.8120	65.227		
	C. Total	16	2519.5388			

DF = degrees of freedom; D_v10, D_v50, D_v90 = parameters of volume size distribution of aerosolised droplets.

Table 3
Sample sequence from design of experiment and corresponding mean nanoparticle diameter (d_{mean}), polydispersity (PDI), zeta-potential (ζ), zero shear viscosity (η_0), droplet size distribution (D_v10, D_v50, D_v90), span, surface tension (σ), cone angle (CA), total turbinate deposition (TD) and middle turbinate deposition (MTD).

	FP% (*w*/*w*)	P80% (*w*/*w*)	SH% (*w*/*w*)	AAH* (°)	AAV* (°)	IF* (L min^{-1})	d_{mean} (nm)	PDI	ζ (mV)	η_0 (mPa s)	D_v10 (μm)	D_v50 (μm)	D_v90 (μm)	Span	σ (mN m^{-1})	CA (°)	TD (%)	MTD (%)
1	0.060	0.030	0.020	75	0	0	133.0 ± 0.8	0.240 ± 0.015	−83.7 ± 0.6	10.7 ± 0.2	19.3 ± 3.0	49.3 ± 11.7	121.9 ± 22.3	2.10 ± 0.22	37.39 ± 0.19	36.2 ± 0.5	24.9 ± 6.7	10.2 ± 1.6
2	0.060	0.030	0.020	45	20	60	144.0 ± 7.6	0.262 ± 0.006	−79.3 ± 3.4	10.2 ± 0.3	20.3 ± 0.8	52.6 ± 3.8	123.3 ± 7.7	1.96 ± 0.02	36.30 ± 0.13	34.8 ± 0.6	25.8 ± 3.8	1.6 ± 1.8
3	0.030	0.030	0.020	75	10	60	145.2 ± 5.3	0.237 ± 0.007	−81.1 ± 3.2	9.7 ± 0.3	22.8 ± 0.5	65.6 ± 3.4	147.8 ± 5.7	1.91 ± 0.02	35.89 ± 0.19	25.9 ± 1.3	26.3 ± 6.6	1.9 ± 1.7
4	0.030	0.030	0.035	45	20	0	153.7 ± 2.3	0.273 ± 0.011	−88.5 ± 1.2	10.5 ± 0.1	25.8 ± 3.8	82.5 ± 18.0	178.6 ± 30.0	1.86 ± 0.08	37.05 ± 0.07	30.5 ± 1.0	71.5 ± 1.9	2.4 ± 3.4
5	0.045	0.030	0.050	75	20	0	142.3 ± 1.7	0.258 ± 0.006	−89.9 ± 0.9	12.4 ± 0.2	26.6 ± 1.9	85.9 ± 8.7	186.1 ± 14.3	1.86 ± 0.04	37.22 ± 0.07	21.0 ± 0.9	42.6 ± 3.5	40.3 ± 2.6
6	0.060	0.030	0.050	45	0	30	146.7 ± 4.0	0.246 ± 0.004	−88.2 ± 2.2	11.9 ± 0.1	30.4 ± 8.4	100.7 ± 30.3	209.9 ± 49.0	1.81 ± 0.13	37.02 ± 0.16	17.0 ± 0.7	82.7 ± 4.6	1.8 ± 1.8
7	0.030	0.030	0.050	60	0	60	149.9 ± 2.6	0.263 ± 0.003	−93.1 ± 0.6	12.1 ± 0.0	24.1 ± 3.8	76.3 ± 19.6	170.4 ± 34.2	1.93 ± 0.09	37.89 ± 0.18	26.0 ± 2.4	57.2 ± 7.8	37.1 ± 6.0
8	0.030	0.045	0.020	45	0	0	153.6 ± 3.5	0.237 ± 0.005	−78.5 ± 4.8	10.0 ± 0.2	21.2 ± 2.6	58.9 ± 12.5	137.2 ± 20.9	1.98 ± 0.11	35.66 ± 0.14	32.1 ± 0.7	79.0 ± 2.6	13.2 ± 0.7
9	0.045	0.045	0.035	60	10	30	141.8 ± 2.2	0.228 ± 0.006	−78.9 ± 1.7	9.7 ± 0.1	20.4 ± 1.4	54.7 ± 7.1	129.5 ± 12.2	2.00 ± 0.06	36.03 ± 0.08	24.2 ± 0.3	59.3 ± 6.2	1.7 ± 0.4
10	0.060	0.045	0.050	75	20	60	141.9 ± 2.4	0.227 ± 0.027	−87.5 ± 3.5	11.3 ± 0.3	25.5 ± 4.0	78.5 ± 18.7	173.1 ± 30.1	1.90 ± 0.14	35.86 ± 0.10	20.7 ± 2.6	42.6 ± 6.2	0.1 ± 0.1
11	0.060	0.060	0.020	60	20	0	151.0 ± 1.3	0.237 ± 0.003	−78.5 ± 1.3	9.9 ± 0.3	16.9 ± 0.4	38.7 ± 1.1	98.2 ± 3.0	2.10 ± 0.03	37.51 ± 0.19	35.7 ± 0.4	73.6 ± 3.9	3.6 ± 4.1
12	0.030	0.060	0.020	75	20	30	160.7 ± 3.6	0.274 ± 0.025	−81.8 ± 2.4	9.7 ± 0.2	20.1 ± 2.0	50.1 ± 8.7	120.2 ± 15.9	2.01 ± 0.07	37.28 ± 0.15	35.7 ± 0.6	24.6 ± 8.1	1.1 ± 0.4
13	0.045	0.060	0.020	45	0	60	151.1 ± 1.8	0.240 ± 0.005	−79.0 ± 2.2	9.3 ± 0.3	20.9 ± 2.5	51.2 ± 1.1	120.2 ± 18.2	1.95 ± 0.06	36.20 ± 0.06	32.8 ± 0.5	42.7 ± 0.5	20.9 ± 3.5
14	0.060	0.060	0.035	75	0	60	144.3 ± 2.5	0.233 ± 0.011	−77.2 ± 3.7	10.5 ± 0.2	21.6 ± 1.1	59.0 ± 5.1	140.8 ± 10.0	2.02 ± 0.03	36.80 ± 0.07	25.5 ± 0.3	21.5 ± 4.9	9.2 ± 0.5
15	0.060	0.060	0.050	45	10	0	150.9 ± 1.8	0.279 ± 0.013	−84.1 ± 2.5	12.8 ± 0.1	28.9 ± 1.6	94.4 ± 6.0	219.3 ± 45.3	2.00 ± 0.34	37.27 ± 0.11	17.5 ± 0.4	84.4 ± 2.0	2.8 ± 0.2
16	0.030	0.060	0.050	75	0	0	153.3 ± 2.4	0.263 ± 0.002	−77.4 ± 1.5	13.0 ± 0.3	23.7 ± 3.9	70.6 ± 17.5	159.6 ± 27.5	1.95 ± 0.17	37.30 ± 0.30	23.1 ± 1.7	27.2 ± 10.3	19.0 ± 2.2
17	0.030	0.060	0.050	45	20	60	155.1 ± 0.8	0.268 ± 0.007	−78.8 ± 1.6	13.4 ± 0.1	23.2 ± 0.7	66.8 ± 3.9	152.6 ± 8.6	1.94 ± 0.01	37.42 ± 0.21	23.7 ± 0.2	83.9 ± 3.7	2.5 ± 0.5

FP = fluticasone propionate concentration; P80 = polysorbate 80 concentration; SH = sodium hyaluronate concentration;
AAH = administration angle in relation to horizontal plane; AAV = administration angle in relation to vertical plane; IF = inspiratory flow.
*Parameters related only to total and middle turbinate deposition.
Values for the responses are mean ± SD, n = 3, except for TD and MTD where n = 2. For all formulations gelation occurred instantly upon mixture with simulated nasal fluid in volume ratio of 1:1.

formulations planned by DoE. The relation between storage (G') and loss (G'') moduli describe the state of the system: G' > G'' indicates that the elastic component prevails over viscous component, hence, the system is a viscoelastic gel [56]. Values of loss factor (tan δ) for gels must be less than 1. According to Winter and Chambon [19], gel point is the moment at which tan δ curves obtained at different angular frequencies intersect, implying that tan δ became independent of frequency [19]. In order to verify instant gelation of formulations prepared within DoE following Winter-Chambon criteria, gelation time test for each formulation was performed at three different angular frequencies: 1, 6.28 and 10 rad s^{-1}. For all tested formulations, G' was higher than G'' immediately upon mixing with SNF and intersection of tan δ curves obtained at different angular frequencies was not observed during the measuring time period, indicating quick gel formation. Values of tan δ for all the formulations were about 0.1, demonstrating weak gel properties, shown to be favourable for nasal sprayable gels [3,57].

3.1.4. Zero shear viscosity

Zero shear viscosity of prepared formulations was in the range from 9.3 ± 0.3 mPa s to 13.4 ± 0.1 mPa s (Table 3). The model obtained from regression modelling showed an excellent fit (R-squared 0.90, RMSE 0.49, PRESS R-squared 0.82, and PRESS RMSE 0.56) and is given in Eq. (5).

$$\eta_0 = 10.20 + 0.07 \times P80 + 1.24 \times SH + 0.39 \times P80 \times SH + 0.96 \times SH^2 \quad (5)$$

The increase in SH concentration resulted in an increase in zero shear viscosity of *in situ* gelling FP nanosuspensions, which was in accordance with literature reports [3,7]. SH concentration exhibited both linear and quadratic influence on zero shear viscosity.

Zero shear viscosity showed positive dependence on P80 concentration. Increase in viscosity caused by an increase in P80 concentration has previously been demonstrated [20,58]. P80 and SH chains may form weak interactions which influence the formulation properties, namely its viscosity. However, no aggregation due to the P80-SH interactions was noticed in aqueous medium [59].

Viscosity is one of the most crucial properties that needs to be considered in development of nasal formulation, as it may significantly impact its sprayability [58], deposition in the nasal cavity [60,61] and formulation retention time at the nasal mucosa [62,63]. Relatively low viscosity of *in situ* gelling FP nanosuspensions prepared within this experimental design contributes to its simple application by spraying, while the *in situ* gelling mechanism is expected to provide prolonged drug retention at the deposition site [3].

3.1.5. Droplet size distribution

Results on droplet size distribution (DSD) for each experimental run are listed in Table 3. Values for D_v10, D_v50 and D_v90 ranged between 16.9 ± 0.4 – 30.4 ± 8.4 μm, 38.7 ± 1.1 – 100.7 ± 30.3 μm and 98.2 ± 3.0 – 219.3 ± 45.3 μm, respectively, while span was in the range from 1.81 ± 0.13 to 2.10 ± 0.03. Regression models obtained by statistical analysis exhibited a great fit for all three volume diameters: D_v10 (R-squared 0.93, RMSE 1.16, PRESS R-squared 0.82, and PRESS RMSE 1.47), D_v50 (R-squared 0.94, RMSE 5.36, PRESS R-squared 0.83, and PRESS RMSE 6.95) and D_v90 (R-squared 0.91, RMSE 11.98, PRESS R-squared 0.76, and PRESS RMSE 16.03). The models are presented by Eq. (6), (7) and (8):

$$D_v10 = 20.89 - 1.02 \times P80 + 2.91 \times SH + 0.14 \times FP + 2.62 \times P80^2 + 2.22 \times SH \times FP \quad (6)$$

$$D_v50 = 57.58 - 5.86 \times P80 + 14.77 \times SH + 0.17 \times FP + 11.21 \times P80^2 + 9.69 \times SH \times F \quad (7)$$

$$D_v90 = 134.06 - 9.08 \times P80 + 28.73 \times SH + 1.44 \times FP + 22.12 \times P80^2 + 18.81 \times SH \times FP \quad (8)$$

DSD for all the formulations was in accordance with EMA and FDA guidelines for nasal drug delivery, requesting that volume diameter of majority of nasal spray droplets/particles must be above 10 μm [64,65]. High correlation coefficients (R-squared = 0.91–0.94) indicated excellent predictive values of the obtained regression models for all three volume diameters. While FP concentration showed minor influence on DSD, the increase in SH concentration resulted in pronounced increase of volume diameters. Similar findings have previously been reported by our research group (Nižić 2019). Higher polymer concentration contributed to greater formulation viscosity (Section 3.4. *Zero shear viscosity*), which lead to formation of larger spray droplets [20,61,66–68].

The models obtained by regression analysis showed a complex influence of P80 concentration on DSD. Nonlinear dependence on P80 concentration suggested that lower values are expected in the middle of design space, while higher values of droplet size are expected at the edges of design space. Dayal et al. [20] investigated, among other parameters, the influence of surfactant on the DSD of nasal sprays. They reported lower droplet size after addition of P80 but also noticed an increase in D_v50 values with the addition of higher surfactant concentrations, probably caused by the changes in viscosity and surface tension due to the interactions between P80 and polymers [20]. The obtained regression model included also the influence of interaction between SH and FP concentration on DSD. The aforementioned interaction can be linked to the SH adsorption on FP nanocrystals (Rouse 2007) building structured network with hydrophobic drug particles.

3.1.6. Surface tension

Surface tension of prepared *in situ* gelling FP nanosuspensions (35.66 ± 0.14 to 37.89 ± 0.18 mN m^{-1}; Table 3) falls well within the acceptable surface tension range for nasal formulations (30 – 44 mN m^{-1}; [21]. Drop in surface tension in relation to purified water (70.62 ± 0.67 mN m^{-1}) can be ascribed to the presence of surfactant P80 and dissolved polymers in the prepared formulations. Regression modelling revealed no statistically significant correlation between constituent concentrations (or their interactions) and surface tension within the design space. Such an observation can be explained by the fact that the levels of surface-active compound P80 in nanosuspensions are well above its critical micellar concentration [69], rendering the surface tension of the nanosuspension relatively unchanged.

Surface tension of nasal nanosuspensions is an important parameter from both, formulation and administration point of view. For nanosuspensions prepared by wet media milling it can modulate the wetting process. Lower surface tension of a liquid system enables better wetting of the particles and therefore allows for their easier disaggregation during the wet media milling process, resulting in less aggregation in the milled nanosuspension [70].

In order to spray the formulation, it is necessary to overcome its surface tension. Generally, the lower the surface tension of the liquid, the higher is its tendency to atomise [21], and spray plume with a narrower geometry is generated [71]. Moreover, lower surface tension of the nasal formulation facilitates its distribution on the surface of the nasal mucosa, allowing it to cover a larger area and enhance drug availability at the site of action [67,72]. The tested formulations had surface tension below that of the normal mucosal lining fluid (reported to be 56 mN m^{-1}), proving the potential for adequate spreading on the mucosal surface [72].

3.1.7. Spray cone angle

Spray cone angle of prepared formulations ranged between 17.0 ± 0.7° and 36.2 ± 0.5° (Table 3). The model obtained from the regression

modelling showed a good fit (R-squared 0.88, RMSE 2.50, PRESS R-squared 0.78, and PRESS RMSE 2.94) and is given by the Eq. (9):

$$CA = 27.20 - 6.01 \times SH - 0.69 \times FP - 2.55 \times SH \times FP \quad (9)$$

Spray cone angle was negatively influenced by increase in concentrations of SH and FP, as well as their interaction. The decrease of the spray cone angle due to formulation viscosity increase derived from the higher polymer concentration is well-described in literature [3,21,23,61,73]. The negative influence of interaction between SH and FP concentration on the spray cone angle could be ascribed to the SH adsorption on FP nanocrystals [47] building structured network with hydrophobic drug particles. The observed effect is in line with influence of the same parameters in interaction on spray droplets size described in section *3.5. Droplet size distribution*.

Spray cone angle is one of the most important features of nasal sprays as it has a direct influence on nasal deposition pattern. Cone angles obtained within this work fit within appropriate range for nasal spray delivery. Even though nasal deposition of the formulation depends on multiple factors, it has generally been shown that narrower spray cone angles result in higher formulation deposition beyond the nasal valve [3,23,61,73–75].

3.1.8. Nasal deposition

Nasal deposition of *in situ* gelling FP nanosuspensions prepared according to DoE was determined using a 3D printed multi-sectional nasal cast. FP is a locally acting corticosteroid drug widely used for treatment of nasal mucosa diseases, including allergic rhinitis and chronic rhinosinusitis with or without nasal polyps [1]. Nasal cast used in this study was developed according to a CT scan of a patient with chronic rhinosinusitis (without nasal polyps), as the anatomical changes due to the swelling of the mucosa caused by inflammation may significantly influence nasal deposition [76]. The length of the nasal cavity (measured from the nostril to the end of the turbinate region) was 86.37 mm (Fig. 2 A), while the smallest vertical cross-sectional areas (valve region) were 109.92/111.02 mm^2 (left/right, respectively; Fig. 2 B) [75], fitting into the reported range of 20–160 mm^2 [77]. In addition to formulation parameters, influences of three administration parameters (inspiratory flow, angles from the horizontal and vertical plane) were studied as well. In order to eliminate the variability in deposition profiles originating from anatomical inequalities in two nasal halves, right nasal half was used in all deposition studies. The spray was administered in the right nostril while the other nostril was closed. To enable inspiration simulation, nasal cavity model was connected to a respiratory pump which generated airflow up to 60 L min^{-1} [73,75]. The model was placed on a stand which facilitated the determination of angles from both horizontal (45–75°) and vertical plane (0–20°). Fraction of the applied dose deposited in the turbinate region, i.e. beyond the nasal valve, was determined by weighing all the nasal cast regions prior to and after spray actuation in the nasal cavity. Additionally, since oedema/mucosal obstruction and nasal polyps primarily occur in the middle turbinate region, fraction of the formulation deposited on that particular region was also included in DoE as a separate response.

The fraction of the applied dose deposited in turbinate region ranged from 21.5 ± 4.9 to 84.4 ± 2.0% (Table 3). The model obtained by regression analysis exhibited an excellent fit (R-squared 0.93, RMSE 8.28, PRESS R-squared 0.75, and PRESS RMSE 11.69) and is given by the following equation (Eq. (10)):

$$TD = 64.73 + 8.84 \times SH - 7.37 \times IF - 18.59 \times AAH + 2.10 \times AAV + 12.10 \times SH \times IF + 4.95 \times AAH \times AAV - 16.47 \times AAV^2 \quad (10)$$

where TD is total turbinate deposition, IF is inspiratory flow, AAH is the angle of administration from the horizontal plane and AAV is the angle of administration from the vertical plane.

Regression model revealed SH concentration as the leading formulation parameter in optimisation of nasal deposition pattern. The increase in SH concentration led to increased total turbinate deposition. This result is not surprising, as SH has shown to have impact on all the observed responses so far. Increase in SH concentration increased droplet size and decreased spray cone angle, both of which may contribute to improved nasal deposition profile [3,61,73,75].

All tested administration parameters showed influence on total turbinate deposition (Fig. 3), with the angle of administration from the horizontal plane having the greatest impact. The increase of total turbinate deposition with the decrease of angle of administration from the horizontal plane has already been observed [3,73,75,76] and is connected to the complex nasal geometry due to which lower administration angles enable more efficient delivery beyond the nasal valve with lower extent of impaction in the anterior nasal cavity area [75]. Interaction of the angles from the horizontal and vertical plane has also shown an influence on total turbinate deposition, presumably due to the differences in droplet shape, deformation, breakup and collision after administration at different angles [78] which may have an impact on nasal deposition. Increased angle of administration from the vertical plane resulted in an increased total turbinate deposition, but has also shown a quadratic effect, indicating that the highest value of total turbinate deposition may be expected in the middle of design space (Fig. 3). This is in accordance with patient instructions for nasal spray administration which often advise directing the spray pump tip away from the nasal septum [1].

Although inspiratory flow as an individual parameter showed negative influence on total turbinate deposition, a positive influence is observed for its interaction with SH. This could be explained by the fact that the inspiratory flow may cause distortion of the emitted spray plume, reducing its cone angle [23]. Since both cone angle and droplet size strongly depended on sodium hyaluronate concentration, their influence on total turbinate deposition may be manifested in the form of

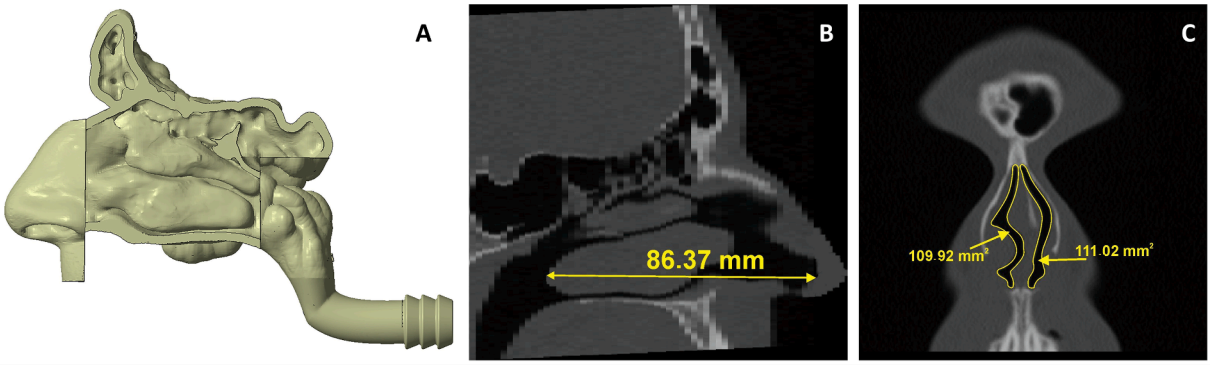

Fig. 2. Scheme of a 3D-printed nasal cavity model (A) and nasal geometry measurements: length of a nasal cavity (86.37 mm; B) and smallest vertical cross-sectional areas (left: 109.92 mm^2/right 111.02 mm^2; C).

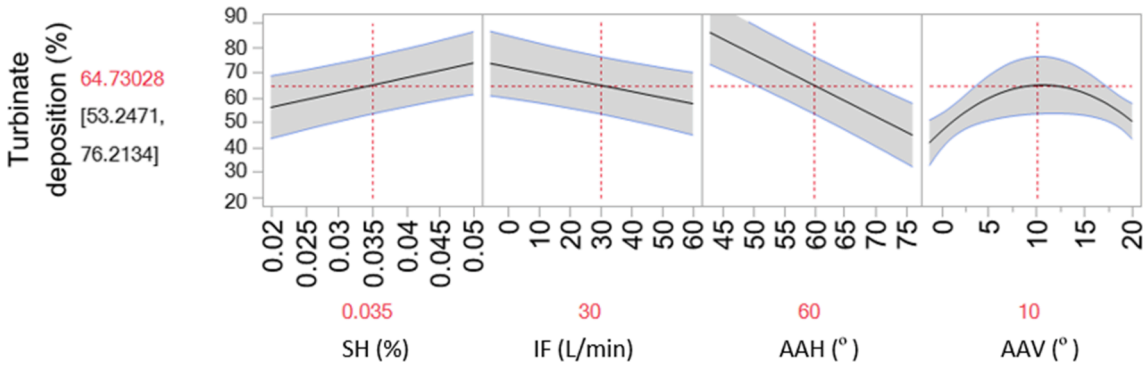

Fig. 3. Prediction of total turbinate deposition of the *in situ* gelling fluticasone propionate nanosuspension in relation to sodium hyaluronate (SH) concentration, inspiratory flow (IF), angles from the horizontal (AAH) and vertical (AAV) plane. Values in brackets refer to 95% confidence interval.

SH and inspiratory flow interaction.

In order to elucidate formulation and administration parameters that influence deposition in the middle turbinate region, that response has been analysed separately. Middle turbinate deposition (MTD) ranged from 0.1 ± 0.1 to 40.3 ± 2.6% (Table 3). The model obtained by regression analysis exhibited a good fit (R-squared 0.79, RMSE 8.08, PRESS R-squared −0.02, and PRESS RMSE 12.31) and is given by the following equation (Eq. (11)):

$$MTD = 5.77 - 2.59 \times P80 + 3.65 \times SH - 4.27 \times AAV - 3.42 \times FP + 12.24 \times P80^2 + 10.55 \times AAV^2 + 5.99 \times AAV \times FP - 17.70 \times FP^2 \quad (11)$$

The regression model for middle turbinate deposition differs significantly from the model for the total turbinate region. Namely, P80 had a pronounced influence on middle turbinate deposition, both as an individual parameter and with quadratic effect (Fig. 4), while that impact was not observed for total turbinate deposition. Similarly, FP concentration showed an influence on middle turbinate deposition, while that influence lacked for total turbinate deposition. Quadratic effects of P80 concentration and angle of administration from the vertical plane indicate that the lowest value of middle turbinate deposition may be expected in the middle of design space, while the opposite effect is noticeable for FP concentration. Contrary to the model for total turbinate deposition, angle of administration from the horizontal plane exhibited no influence on middle turbinate deposition. Even though lower angles of administration from the horizontal plane increase deposition in the turbinate region, i.e. beyond the nasal valve, most of the formulation gets deposited in lower parts of nasal cavity [73], in some cases not even reaching the middle turbinate region. Differences in regression models for total and middle turbinate deposition highlight the complexity of the nasal cavity anatomy and targeted nasal drug delivery.

Chronic rhinosinusitis (with or without nasal polyps) is a pathophysiological condition that requires treatment of inflammatory processes in the middle meatus [79], hence it is crucial to establish the formulation potential to reach the aforementioned region.

3.2. Selection of the leading *in situ* gelling FP nanosuspension and statistical model verification

Comprehensive characterisation of *in situ* gelling FP nanosuspensions disclosed their appropriateness for nasal administration in the form of spray. Studying wide variety of responses including formulation intrinsic properties and behaviour upon aerosolization revealed the headmost parameters for their fine-tuning. The selection of the leading *in situ* gelling FP nanosuspension and corresponding mode of administration was performed based on the fraction deposited within middle turbinate region, recognized for its importance in rhinosinusitis development. Namely, the formulation and administration parameters for further studies were derived from statistical model developed for middle turbinate deposition (Eq. (9)) and are given in Table 4. After the preparation, the leading *in situ* gelling FP nanosuspension was firstly

Table 4
Statistical model derived formulation with predicted high middle turbinate deposition.

Sample name	FP% (*w/w*)	P80% (*w/w*)	SH% (*w/w*)	AAH (°)	AAV (°)	IF (L min^{-1})
ISG-NS	0.041	0.030	0.050	60	0	60

ISG-NS = leading *in situ* gelling fluticasone propionate nanosuspension; FP = fluticasone propionate concentration; P80 = polysorbate 80 concentration; SH = sodium hyaluronate concentration; AAH = administration angle in relation to horizontal plane; AAV = administration angle in relation to vertical plane; IF = inspiratory flow.

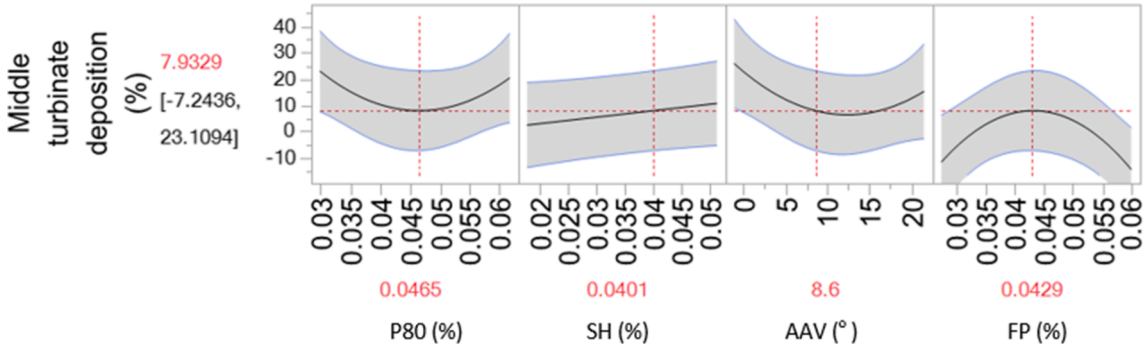

Fig. 4. Prediction of the middle turbinate deposition of the *in situ* gelling fluticasone propionate nanosuspension in relation to polysorbate 80 (P80), sodium hyaluronate (SH) and fluticasone propionate (FP) concentrations, as well as angle from the vertical (AAV) plane. Values in brackets refer to 95% confidence interval.

characterised in the same manner as the formulations included in DoE. To evaluate the impact of FP nanonisation on inspected properties, a corresponding *in situ* gelling FP microsuspension was prepared by the same procedure omitting wet media milling and was used as control (Table 5). Commercially available conventional FP microsuspension was used for comparison of spray properties, including droplet size distribution, spray cone angle and nasal deposition profile.

Leading *in situ* gelling FP nanosuspension showed similar properties to the formulations included in DoE (Table 5), confirming its suitability for nasal drug delivery. TEM analysis confirmed particle size results obtained by photon correlation spectroscopy (Fig. 5). Moreover, obtained values for inspected formulation-related responses confirmed the predictive value of the regression models developed based on DoE results. Particle size reduction to nanometre-scale induced no significant change in intrinsic formulation properties such as surface tension and osmolality.

Middle turbinate deposition of leading formulation was 51.8 ± 9.4%, while the spray cone angle was 21.3 ± 0.3°, revealing appropriate fit between experimental and predicted value (Table 5) and verifying the suitability of the developed statistical model in nasal formulation development. Furthermore, middle turbinate deposition of corresponding *in situ* gelling microsuspension was 31.5 ± 1.8%, which was substantially lower than deposition of nanoformulation (Table 5). Spray cone angle of *in situ* gelling microsuspension was 24.3 ± 1.2°, confirming the previous findings which show reciprocal correlation between cone angle and nasal deposition [3,23,61,73–75]. The regression model for middle turbinate deposition of *in situ* gelling FP nanosuspensions showed influence of FP concentration, both as an individual parameter and a parameter with quadratic effect. Hence, it can be expected that the particle size of suspended drug may impact the formulation deposition pattern, demonstrating once again that drug delivery targeted beyond the nasal valve is a multifactorial process [80]. For comparison, commercially available conventional FP microsuspension was characterised in terms of sprayability and nasal deposition profile. Results on droplet size distribution (D_v10 = 20.4 ± 0.7 μm, D_v50 = 57.9 ± 2.2 μm, D_v90 = 123.3 ± 3.6 μm), spray cone angle (30.7 ± 1.4°) and middle turbinate deposition (18.0 ± 7.3%) in comparison with those obtained for *in situ* FP gelling micro and nanosuspension clearly show that smaller droplet size corresponds to higher spray cone angle and, consequently, less effective middle turbinate deposition.

Upon verification of regression models obtained, the leading *in situ* gelling FP nanosuspension was subjected to deeper *in vitro* characterisation, predictive of its performance at nasal mucosa. In order to clarify the role of FP nanonisation and formulation gelling behavior in inspected properties, corresponding *in situ* gelling FP microsuspension as well as conventional FP nano and microsuspension (prepared with no addition of polymers) were used as controls.

3.3. In vitro release

The release of FP from leading *in situ* gelling nanosuspension was determined using an automated Franz diffusion cell system, presenting a well-established approach to *in vitro* release studies of semi-solid dosage forms [3,9]. SNF/ethanol (1:1, *v/v*) was used as the receptor medium [3,81], ensuring instant gelation of the formulation and sink conditions during the experiment. Corresponding *in situ* gelling FP microsuspension as well as conventional FP nano and microsuspension were used as controls. Fig. 6 shows the obtained FP release profiles. Using f2 as criteria for estimation of similarity between *in vitro* release profiles revealed similarity only between release profiles of leading *in situ* gelling FP nanosuspension and conventional FP microsuspension (f2 = 64.8). Other comparisons resulted in f2 values between 31.9 and 49.4, indicating release profiles dissimilarity.

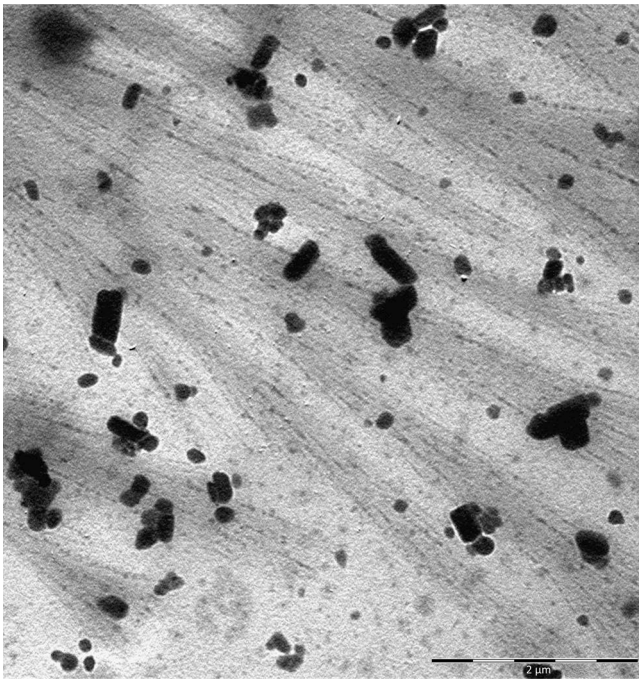

Fig. 5. TEM image of leading *in situ* gelling nanosuspension containing fluticasone propionate, polysorbate 80, pectin, sodium hyaluronate and mannitol in concentrations of 0.041, 0.03, 0.9, 0.05 and 4% (*w/w*), respectively. Size bar refers to 2 μm.

For both, conventional and *in situ* gelling suspensions, higher FP release rate was observed for nanosuspensions than microsuspensions. Furthermore, the addition of *in situ* gelling polymers ensured slower FP release when compared to conventional suspensions. Thus, the slowest release profile was observed for *in situ* gelling microsuspension, with only about 50% of the drug released after 8 h. Similar results were obtained previously by our research group, where the release profiles of FP from microsuspensions containing pectin, SH and gellan gum were studied [3]. *In situ* gelling nanosuspension ensured almost complete (about 85%) release of FP after 8 h indicating that, as expected, reduction in particle size increased the dissolution rate due to the higher

Table 5
The main characteristics of leading *in situ* gelling fluticasone propionate nanosuspension (ISG-NS) and *in situ* gelling fluticasone propionate microsuspension used as a control (ISG-MS).

Sample	d_{mean} (nm)	PDI	ζ (mV)	η_0 (mPa s)	D_v10 (μm)	D_v50 (μm)	D_v90 (μm)	σ (mN m^{-1})	CA (°)	MTD (%)
ISG-NS	156.0 ± 2.7 [138.4, 149.4]	0.295 ± 0.013	−86.1 ± 2.3 [−88.94, −84.68]	11.48 ± 0.38 [11.35, 12.52]	27.2 ± 0.7 [25.6, 28.0]	85.6 ± 1.6 [81.3, 92.3]	179.4 ± 2.1 [176.2, 201.0]	38.70 ± 0.35	21.1 ± 0.6 [20.0, 24.1]	51.8 ± 9.4 [25.8, 54.8]
ISG-MS	4245.0 ± 403.6	0.477 ± 0.106	−83.4 ± 2.3	11.10 ± 0.02	29.6 ± 0.4	92.9 ± 3.0	192.0 ± 4.2	37.94 ± 0.38	24.3 ± 1.2	31.5 ± 1.8

d_{mean} = nanoparticle diameter; PDI = polydispersity index; ζ = zeta potential;l η_0 = zero shear viscosity; D_v10, D_v50, D_v90 = volume diameters; σ = surface tension; CA = cone angle; MTD = middle turbinate deposition.
Presented values are mean ± SD, n = 3. Values in brackets refer to 95% confidence interval.

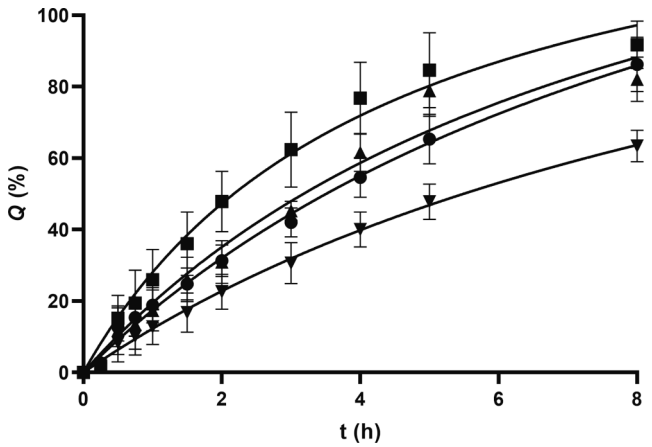

Fig. 6. *In vitro* release profiles of fluticasone propionate (FP) from leading *in situ* gelling FP nanosuspension (circle), *in situ* gelling FP microsuspension (reverse triangle), conventional FP nanosuspension (square) and conventional FP microsuspension (triangle). All formulations contained FP (0.041%, *w/w*), polysorbate 80 (0.03%, *w/w*) and mannitol (4%, *w/w*). *In situ* gelling systems also contained pectin (0.9%, *w/w*) and sodium hyaluronate (0.05%, *w/w*). The profiles were determined using Franz diffusion cell with SNF/ethanol (1:1, *v/v*) as the receptor medium. *Q* represents the cumulative amount of drug released at time *t*. Data are expressed as the mean ± SD, n = 3.

surface area of nanoparticles in contact with the solvent [7]. Dissolution of the drug is necessary for its pharmacological activity to take place. Development of nanosystems with the aim to improve dissolution rate and solubility of poorly water-soluble drugs has already been described in literature [7,9]. FP is a highly lipophilic drug with rather low aqueous solubility of about 0.1 mg L^{-1} [82,83], which makes it practically insoluble in aqueous medium [27]. Within this work, saturation solubility of nanonised and micronised FP in water/SNF mixture (1:1, *v/v*) in presence of P80 (0.03%, *w/w*) at 34 °C was determined as 44.3 ± 3.3 and 3.8 ± 0.8 mg L^{-1}, respectively. Results obtained simulating solvent electrolyte content and temperature *in vivo* indicated 11.8-fold increase in saturation solubility due to nanonisation. Observed increase was in line with literature reports on nanonisation-related solubility increase [84–88]. Yang et al. (2008) prepared conventional FP nanosuspension for pulmonary delivery and reported increased solubility in simulated lung fluid of 0.5 mg L^{-1} [89]. Furthermore, Hao et al. [9] investigated ionic-sensitive *in situ* gel loaded with resveratrol nanosuspension. Reducing resveratrol particle size to nano-scale resulted in a higher dissolution rate compared to coarse resveratrol suspensions [9]. Formulating FP as an *in situ* gelling nanosuspension offered advantage of increased release rate in relation to *in situ* gelling microsuspension, while retaining the advantage of prolonged retention due to the gel formation in contact with mucosa. In addition, gel structure formed moderated drug release in relation to that of conventional nanosuspension, reducing the risk of higher extent of systemic drug exposure.

3.4. Volume expansion coefficient of the in situ gels

After intranasal administration, pectin-based *in situ* gelling system interacts with calcium ions at the nasal mucosa. As the system goes through sol-gel phase transition, volume increase may occur, causing the clogging of the nasal cavity and discomfort for the patient [9,10]. Volume expansion study for leading *in situ* gelling FP nanosuspension and corresponding *in situ* gelling FP microsuspension (3.7 ± 2.6% and 1.9 ± 2.6%, respectively) revealed only a slight increase in volume due to sol-gel transition, indicating no significant risk of clogging-related discomfort during nasal application [9,10,90]. Both systems demonstrated good volume expansion properties, indicating that pectin from the systems forms well-arranged three-dimensional structure with calcium ions present in SNF [9]. Furthermore, SH polymeric chains form hydrogen bonds with water molecules, thus creating an organised structure which contributes to volume consistency [91].

3.5. In vitro biocompatibility

All the components of *in situ* gelling systems prepared within this work are well-known substances already widely used in approved nasal drug formulations. Pectin is a GRAS (generally recognized as safe) substance used as an *in situ* gelling polymer in nasal fentanyl formulation PecFent [92,93]. SH is a bioactive constituent used as a humectant in nasal irrigation sprays [94,95]. It is a biocompatible polymer that exhibits healing properties on nasal mucosa [96] and is currently under investigation for the treatment of both allergic and non-allergic rhinitis [97], as well as chronic rhinosinusitis [98–100]. P80 is also used as a suspending agent in approved nasal corticosteroid sprays [101]. Biocompatibility of leading *in situ* gelling FP nanosuspension and non-milled control was determined *in vitro* using Calu-3 cells, a human airway epithelial immortalized cell line. Since Calu-3 cells have cilia, produce mucus and exhibit tight junctions, they are considered an adequate model for nasal epithelia [102]. Hank's balanced salt solution (HBSS) with the addition of calcium ions in concentration identical to the one in SNF was used as a negative control (HBSS-Ca^{2+}). Prior to cell treatment, the formulations were mixed with HBSS-Ca^{2+} to induce gel formation. With the aim to examine the suitability of the formulation for *in vitro* biocompatibility studies, osmolality after mixing with HBSS-Ca^{2+} was also determined for nanoformulation and its non-milled control and has proven to be adequate (283.0 ± 1.4 mOsm kg^{-1} and 278.0 ± 1.0 mOsm kg^{-1}, respectively). No cytotoxic effect has been observed. The viability of cells treated with leading *in situ* gelling FP nanosuspension and corresponding non-milled control formulation in relation to HBSS-Ca^{2+} treated cells was 96.7 ± 7.9% and 100.3 ± 6.9%, respectively. The obtained results revealed appropriate biocompatibility profile of tested formulations with Calu-3 cell model irrespective of the FP particle size range.

3.6. Mucoadhesive properties

Mucoadhesiveness is one of the main properties to be considered in development of nasal drug delivery systems. Mucociliary clearance presents a considerable limitation in the efficacy of nasal drug delivery as it reduces the contact time between the formulation and mucosa [103]. Current trends in overcoming this issue include development of *in situ* gelling systems containing mucoadhesive polymers [67,96,104,105]. In this work, pectin was used as both *in situ* gelling and mucoadhesive polymer [103], while SH was used as bioactive and mucoadhesive constituent [97]. Mucoadhesion test was performed using porcine nasal mucosa due to its similarity to human nasal mucosa [26,106,107]. Maximum detachment force and work of adhesion were used to describe the mucoadhesive properties of leading *in situ* gelling FP nanosuspension upon mixing with SNF in volume ratio of 1:1 (Fig. 7). Corresponding *in situ* gelling FP microsuspension as well as conventional FP nano- and microsuspension were used to elucidate the impact of nanonisation and/or gelling behaviour on mucoadhesive properties, while filter paper was used as negative control. Leading *in situ* gelling FP nanosuspension and *in situ* gelling FP microsuspension showed statistically significant difference in F_A with respect to control ($p < 0.05$). Significant difference in W_{ad} with respect to control ($p < 0.05$) was observed in case of leading *in situ* gelling FP nanosuspension, *in situ* gelling FP microsuspension and conventional FP nanosuspension.

Leading *in situ* gelling FP nanosuspension showed the highest detachment force and work of adhesion (Fig. 7) among the tested formulations. Mucoadhesive properties decreased in the following order: *in situ* gelling FP nanosuspension > *in situ* gelling FP microsuspension > conventional FP nanosuspension > conventional FP microsuspension, clearly indicating that both, the presence of mucoadhesive polymers and the reduction of particle size to nanometre scale contributed to the

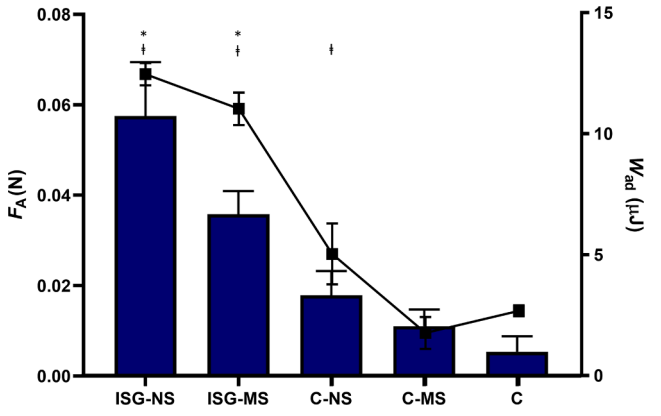

Fig. 7. Detachment force (F_A; columns) and work of adhesion (W_{ad}; squares) of the leading *in situ* gelling fluticasone propionate (FP) nanosuspension (ISG-NS), *in situ* gelling FP microsuspension (ISG-MS), conventional FP nanosuspension (C-NS) and conventional FP microsuspension (C-MS)) mixed with SNF 1:1 (*v/v*). All formulations contained FP (0.041%, *w/w*), polysorbate 80 (0.03%, *w/w*) and mannitol (4%, *w/w*). *In situ* gelling systems also contained pectin (0.9%, *w/w*) and sodium hyaluronate (0.05%, *w/w*). C = control (filter paper). Values are mean ± SD, n = 3. *-statistically significant difference in F_A with respect to control, $p < 0.05$; ǂ- statistically significant difference in W_{ad} with respect to control, $p < 0.05$.

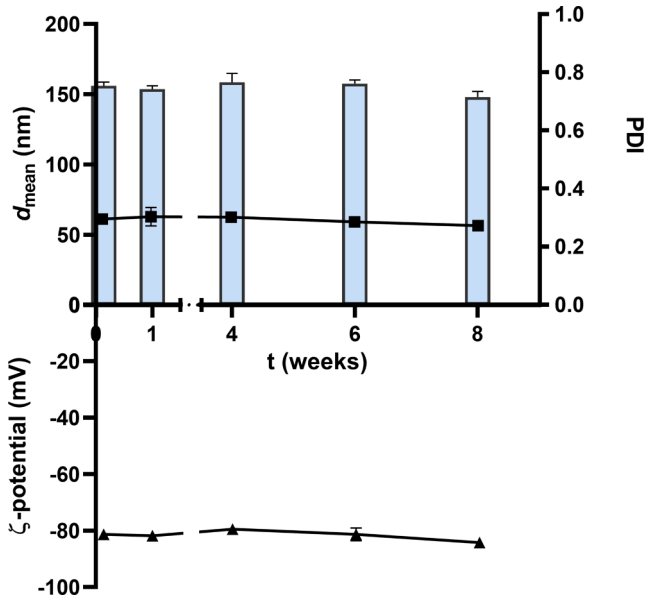

Fig. 8. Mean particle diameter (d_{mean}, columns), polydispersity index (PDI, squares) and zeta (ζ)-potential (triangles) of *in situ* gelling nanosuspension containing fluticasone propionate, polysorbate 80, sodium hyaluronate, pectin and mannitol (0.041%, 0.03%, 0.05%, 0.9% and 4%, *w/w*; respectively) after 0, 1, 4, 6 and 8 weeks. Values are mean ± SD, n = 3. Statistical analysis revealed no significant change in inspected properties at sampling time points ($p > 0.05$).

mucoadhesion of the formulation. Pectin and SH are anionic polymers that form hydrogen bonds with mucus glycoproteins, thus exhibiting mucoadhesive properties [103]. Another mechanism contributing to mucoadhesion is the entanglement of polymeric chains with the mucin molecules [108]. SH is frequently used in development of mucoadhesive nasal delivery systems [96,105]. Xu et al. (2014) developed a thermosensitive poloxamer/SH based *in situ* gelling system with similar mucoadhesive properties to the ones in this work [105].

Higher detachment force and work of adhesion observed for nanoformulations compared to non-milled formulations (Fig. 7) could be explained by more pronounced interaction of mucin chains with dispersed FP nanoparticles compared to non-milled FP microparticles, as former are characterised by larger specific surface area [7].

3.7. Rheological characterisation

To get a deeper insight in the structure properties of the formed gel, frequency sweep test of leading *in situ* gelling FP nanosuspension mixed with SNF was performed. Frequency sweep is an oscillatory test that may indicate short- and long-term gel behaviour [56]. The test was conducted under constant strain from the LVE range as to ensure no structure disruption. Storage modulus (G') was higher than loss modulus (G'') over a large angular frequency range (0.1 to 100 rad s^{-1}). Both moduli showed behaviour nearly independent of frequency, indicating appropriate stability of the formed *in situ* gel [9,109].

3.8. Formulation stability

Physico-chemical stability of the leading *in situ* gelling FP nanosuspension was monitored over a period of 8 weeks. The formulation was stored in an impermeable container at 4 °C/RH 65% and inspected for drug content, formulation appearance, physical attributes and functionality (colour, phase separation, resuspendibility, particle size, polydispersity index, zeta potential and gelation properties).

No change in formulation colour was observed. After settling due to gravity, nanoparticle precipitate was easily redispersed. Mean particle diameter, PDI and zeta-potential remained unchanged during 8-week storage (Fig. 8), revealing suitable formulation stability. Statistical analysis revealed no significant change in inspected properties at sampling time points ($p > 0.05$). Drug content upon 8-week storage was in line with that of freshly prepared *in situ* gelling FP nanosuspension (97.4 ± 0.8% vs. 98.2 ± 1.1%, respectively).

To monitor the gelling behaviour, gelation time and frequency sweep tests were employed. During the monitored storage period, the leading formulation retained instant gelation ability. Furthermore, no significant changes were observed in storage and loss moduli behaviour of the formed gel, as shown by the frequency sweep test (Fig. 9), proving the rheological stability of the formulation. The performed stability tests confirmed preservation of key advantages of developed formulation, referring to drug particle size in nanoscale and rheological behaviour tailored for advanced nasal delivery.

4. Conclusion

Within this study, *in situ* gelling nanosuspension has proven to be a

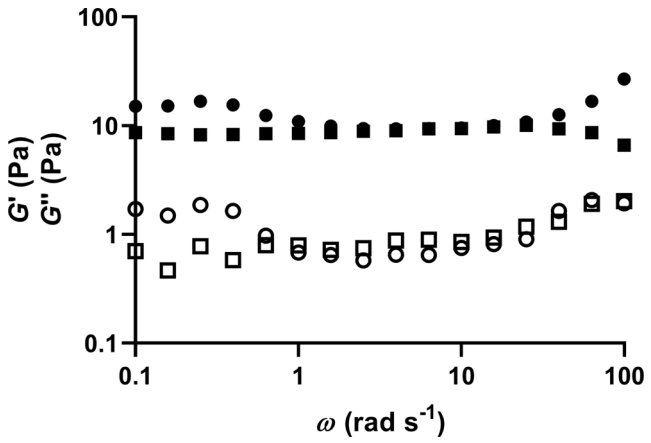

Fig. 9. Storage (G'; filled symbol) and loss (G''; open symbol) modulus as a function of angular frequency (ω) of *in situ* gelling nanosuspension containing fluticasone propionate, polysorbate 80, sodium hyaluronate, pectin and mannitol (0.041%, 0.03%, 0.05%, 0.9% and 4%, *w/w*; respectively) mixed with SNF 1:1 (*v/v*) after 0 (circle) and 8 (square) weeks.

promising platform for efficient fluticasone propionate nasal delivery. Combined strategy of incorporation of drug nanocrystals into *in situ* gelling system resulted in well-tailored formulation with sprayability, gelling ability, mucoadhesion and drug release properties optimised for nasal delivery. QbD approach coupling formulation and administration parameters in the deposition studies enabled drug targeting to the middle meatus, the critical region in the treatment of rhinosinusitis and nasal polyposis. Biocompatibility and stability profile of the leading *in situ* gelling FP nanosuspension strengthen the basis for further evaluation of its therapeutic potential.

Declaration of Competing Interest

The authors declare that they have no known competing financial interests or personal relationships that could have appeared to influence the work reported in this paper.

Acknowledgements

This work has been supported in part by Croatian Science Foundation under the project UIP-2017-05-4592, European Social Fund under the Croatian Science Foundation project DOK-2020-01-2473 and Strengthening the scientific research and innovation capacities of the Faculty of Pharmacy and Biochemistry, University of Zagreb (FarmInova; project number KK.01.1.1.02.0021), financed from the European Regional Development Fund, Operational Program Competitiveness and Cohesion for the period 2014–2020. The authors thank Miodrag Katalenić and Mladen Šercer (Cateh d.o.o., Zagreb) for help in the production of 3D nasal cavity model and assoc. prof. Petra Peharec Štefanić, PhD for TEM analysis.

References

[1] W.J. Fokkens, V.J. Lund, C. Hopkins, P.W. Hellings, R. Kern, S. Reitsma, et al., EPOS 2020, Off. J. Eur. Int. Rhinol. Soc. Confederation European ORL-HNS (Suppl. 29) (2020) 1–464.
[2] P.T. Daley-Yates, D. Larenas-Linnemann, C. Bhargave, M. Verma, Intranasal corticosteroids: Topical potency, systemic activity and therapeutic index, J. Asthma Allergy 14 (2021) 1093–1104.
[3] L. Nižić, I. Ugrina, D. Špoljarić, V. Saršon, M.S. Kučuk, I. Pepić, A. Hafner, Innovative sprayable in situ gelling fluticasone suspension: Development and optimization of nasal deposition, Int. J. Pharm. 563 (2019) 445–456.
[4] C. Karavasili, D.G. Fatouros, Smart materials: in situ gel-forming systems for nasal delivery, Drug Discovery Today 21 (1) (2016) 157–166.
[5] V.B. Patravale, A.A. Date, R.M. Kulkarni, Nanosuspensions: a promising drug delivery strategy, J. Pharm. Pharmacol. 56 (7) (2004) 827–840.
[6] N.S. Saindane, K.P. Pagar, P.R. Vavia, Nanosuspension based in situ gelling nasal spray of carvedilol: Development, in vitro and in vivo characterization, AAPS PharmSciTech. 14 (1) (2013) 189–199.
[7] A. Alshweiat, Ildikó Csóka, F. Tömösi, T. Janáky, A. Kovács, R. Gáspár, A. Sztojkov-Ivanov, E. Ducza, Á. Márki, P. Szabó-Révész, R. Ambrus, Nasal delivery of nanosuspension-based mucoadhesive formulation with improved bioavailability of loratadine: Preparation, characterization, and in vivo evaluation, Int. J. Pharm. 579 (2020) 119166, https://doi.org/10.1016/j.ijpharm.2020.119166.
[8] Bhavna, S. Md, M. Ali, R. Ali, A. Bhatnagar, S. Baboota, J. Ali, Donepezil nanosuspension intended for nose to brain targeting: In vitro and in vivo safety evaluation, Int. J. Biol. Macromol. 67 (2014) 418–425.
[9] J. Hao, J. Zhao, S. Zhang, T. Tong, Q. Zhuang, K. Jin, W. Chen, H. Tang, Fabrication of an ionic-sensitive in situ gel loaded with resveratrol nanosuspensions intended for direct nose-to-brain delivery, Colloids Surf., B 147 (2016) 376–386.
[10] Y. Chen, Y. Liu, J. Xie, Q. Zheng, P. Yue, L. Chen, et al., Nose-to-brain delivery by nanosuspensions-based in situ gel for breviscapine, Int. J. Nanomed. 15 (2020) 10435–10451.
[11] S.R. Pailla, S. Talluri, N. Rangaraj, R. Ramavath, V.S. Challa, N. Doijad, S. Sampathi, Intranasal Zotepine Nanosuspension: intended for improved brain distribution in rats, DARU, J. Pharm. Sci. 27 (2) (2019) 541–556.
[12] G.F. Racaniello, V. Laquintana, S. Summonte, A. Lopedota, A. Cutrignelli, A. Lopalco, M. Franco, A. Bernkop-Schnürch, N. Denora, Spray-dried mucoadhesive microparticles based on S-protected thiolated hydroxypropyl-β-cyclodextrin for budesonide nasal delivery, Int. J. Pharm. 603 (2021) 120728, https://doi.org/10.1016/j.ijpharm.2021.120728.
[13] Z.F. Aref, S.E.E.S. Bazeed, M.H. Hassan, A.S. Hassan, A. Rashad, R.G. Hassan, A. A. Abdelmaksoud, Clinical, biochemical and molecular evaluations of ivermectin mucoadhesive nanosuspension nasal spray in reducing upper respiratory symptoms of mild covid-19, Int. J. Nanomed. 16 (2021) 4063–4072.
[14] J. Dai, B.H. Ruan, Y. Zhu, X. Liang, F. Su, W. Su, Priprema nano-strukturiranog flutikazon-propionat nazalnog spreja sa poboljšanom stabilnošću i uniformnošću, Chem. Ind. Chem. Eng. Quart. 21 (3) (2015) 457–464.
[15] J. Liang, A.P. Lane, Topical Drug Delivery for Chronic Rhinosinusitis, Curr. Otorhinolaryngol. Rep. 1 (1) (2013) 51–60.
[16] E.L. Cummings, S.N. Fassas, K.J. Sykes, A. Sisson, A.G. Chiu, M.G. Fox, Positional Installation of Intranasal Corticosteroids in the Treatment of Chronic Rhinosinusitis: A Systematic Review of the Literature, Ear Nose Throat J. 100 (5) (2021) 302–308.
[17] A. Tsikoudas, J.J. Homer, The delivery of topical nasal sprays and drops to the middle meatus: A semiquantitative analysis, Clin. Otolaryngol. Allied Sci. 26 (4) (2001) 294–297.
[18] G.B. Romero, C.M. Keck, R.H. Müller, Simple low-cost miniaturization approach for pharmaceutical nanocrystals production, Int. J. Pharm. 501 (1-2) (2016) 236–244.
[19] H.H. Winter, F. Chambon, Analysis of Linear Viscoelasticity of a Crosslinking Polymer at the Gel Point Analysis of Linear Viscoelasticity of a Crosslinking Polymer at the, Gel Point. 367 (1986).
[20] P. Dayal, M.S. Shaik, M. Singh, Evaluation of different parameters that affect droplet-size distribution from nasal sprays using the Malvern Spraytec®, J. Pharm. Sci. 93 (7) (2004) 1725–1742.
[21] K. Shrestha, J. van Strien, N. Singh, K. Inthavong, Primary break-up and atomization characteristics of a nasal spray, PLoS ONE [Internet]. 15(8 August 2020) (2020)1–16. Available from: https://doi.org/10.1371/journal.pone.0236063.
[22] N.B. Vargaftik, B.N. Volkov, L.D. Voljak, International Tables of Water Surface Tension, J. Phys. Chem. Ref. Data 12 (3) (1983) 817–820.
[23] D. Moraga-Espinoza, Z. Warnken, A. Moore, R.O. Williams, H.D.C. Smyth, A modified USP induction port to characterize nasal spray plume geometry and predict turbinate deposition under flow, Int. J. Pharm. 548 (1) (2018) 305–313.
[24] C. Hong, Y. Dang, G. Lin, Y. Yao, G. Li, G. Ji, H. Shen, Y. Xie, Effects of stabilizing agents on the development of myricetin nanosuspension and its characterization: An in vitro and in vivo evaluation, Int. J. Pharm. 477 (1-2) (2014) 251–260.
[25] F.N.S. Fachel, B. Medeiros-Neves, M. Dal Prá, R.S. Schuh, K.S. Veras, V.L. Bassani, L.S. Koester, A.T. Henriques, E. Braganhol, H.F. Teixeira, Box-Behnken design optimization of mucoadhesive chitosan-coated nanoemulsions for rosmarinic acid nasal delivery—In vitro studies, Carbohydr. Polym. 199 (2018) 572–582.
[26] L. Nižić Nodilo, I. Ugrina, D. Špoljarić, D. Amidžić Klarić, C. Jakobušić Brala, M. Perkušić, I. Pepić, J. Lovrić, V. Saršon, M. Safundžić Kučuk, D. Zadravec, L. Kalogjera, A. Hafner, A dry powder platform for nose-to-brain delivery of dexamethasone: Formulation development and nasal deposition studies, Pharmaceutics 13 (6) (2021) 795, https://doi.org/10.3390/pharmaceutics13060795.
[27] Ph. Eur. Commission. European Pharmacopoeia (Ph. Eur.) 10th Edition [Internet]. 2021 [cited 2021 Dec 1]. Available from: https://www.edqm.eu/en/european-pharmacopoeia-ph-eur-10th-edition.
[28] European Medicines Agency London UK. European Medicines Agency. Validation of Analytical Procedures: Text and Methodology Q2(R1) [Internet]. 2005. Available from: https://database.ich.org/sites/default/files/Q2%28R1%29Guideline.pdf.
[29] ICH Q1A(R2). International Conference on Harmonization (ICH). Guidance for industry: Q1A(R2) STABILITY TESTING OF NEW DRUG SUBSTANCES AND PRODUCTS. Ich Harmonised Tripartite Guideline. 2003;4(February):24.
[30] C.P. Costa, S. Cunha, J.N. Moreira, R. Silva, E. Gil-Martins, V. Silva, L. Azevedo, A.F. Peixoto, J.M. Sousa Lobo, A.C. Silva, Quality by design (QbD) optimization of diazepam-loaded nanostructured lipid carriers (NLC) for nose-to-brain delivery: Toxicological effect of surface charge on human neuronal cells, Int. J. Pharm. 607 (2021) 120933, https://doi.org/10.1016/j.ijpharm.2021.120933.
[31] S. Gupta, M.K. Samanta, A.M. Raichur, Dual-drug delivery system based on in situ gel-forming nanosuspension of forskolin to enhance antiglaucoma efficacy, AAPS PharmSciTech. 11 (1) (2010) 322–335.
[32] S. Nippe, C. Preuße, S. General, Evaluation of the in vitro release and pharmacokinetics of parenteral injectable formulations for steroids, Eur. J. Pharm. Biopharm. 83 (2) (2013) 253–265.
[33] F. Blažević, T. Milekić, M.D. Romić, M. Juretić, I. Pepić, J. Filipović-Grčić, J. Lovrić, A. Hafner, Nanoparticle-mediated interplay of chitosan and melatonin for improved wound epithelialisation, Carbohydr. Polym. 146 (2016) 445–454.
[34] Goos P, Jones B. Optimal Design of Experiments. 1st ed. Wiley, editor. 2011.
[35] C. Bitter, K. Suter-Zimmermann, C. Surbera, Nasal Drug Delivery in Humans, Curr. Probl. Dermatol. 40 (2011) 20–35.
[36] M.C.C. Peters, I.F. de Oliveira, M.G.M. Machado, D.C. Ferreira, M.H.A. Zanin, N. Bou-Chacra, The glucocorticoid derivative with the phthalimide group cationic nanocrystal for ophthalmic application: a design space development approach, Mater. Today Chem. 19 (2021) 100396, https://doi.org/10.1016/j.mtchem.2020.100396.
[37] K.J.C. Melo, M.A.B. Henostroza, R. Löbenberg, N.A. Bou-Chacra, Rifampicin nanocrystals: Towards an innovative approach to treat tuberculosis, Mater. Sci. Eng., C 112 (2020) 110895, https://doi.org/10.1016/j.msec.2020.110895.
[38] S. Meruva, P. Thool, Y. Gong, S. Karki, W. Bowen, S. Kumar, 119026, Available from: 577 (2020) 119026, https://doi.org/10.1016/j.ijpharm.2020.119026.
[39] X. Liu, B. Shen, C. Shen, R. Zhong, X. Wang, H. Yuan, Nanoparticle-loaded gels for topical delivery of nitrofurazone: Effect of particle size on skin permeation and retention, J. Drug Delivery Sci. Technol. 45 (2018) 367–372.

[40] J. Zuo, G.L.B. de Araujo, M.A. Stephano, Z. Zuo, N.A. Bou-Chacra, R. Löbenberg, Design space approach in the development of esculetin nanocrystals by a small-scale wet-bead milling process, J. Drug Deliv. Sci. Technol. [Internet] 55 (October 2019) (2020) 101486, https://doi.org/10.1016/j.jddst.2019.101486.
[41] I. Tomić, M. Juretić, M. Jug, I. Pepić, B. Cetina Čižmek, J. Filipović-Grčić, Preparation of in situ hydrogels loaded with azelaic acid nanocrystals and their dermal application performance study, Int. J. Pharm. 563 (April) (2019) 249–258.
[42] E. Merisko-Liversidge, G.G. Liversidge, Nanosizing for oral and parenteral drug delivery: A perspective on formulating poorly-water soluble compounds using wet media milling technology, Adv. Drug Deliv. Rev. 63 (6) (2011) 427–440.
[43] H. Akel, R. Ismail, G. Katona, F. Sabir, R. Ambrus, I. Csóka, A comparison study of lipid and polymeric nanoparticles in the nasal delivery of meloxicam: Formulation, characterization, and in vitro evaluation, Int. J. Pharm. 604 (2021) 120724, https://doi.org/10.1016/j.ijpharm.2021.120724.
[44] H. Shen, S. Shi, Z. Zhang, T. Gong, X. Sun, Coating solid lipid nanoparticles with hyaluronic acid enhances antitumor activity against melanoma stem-like cells, Theranostics 5 (7) (2015) 755–771.
[45] S. Sharma, J. Singh, A. Verma, B.V. Teja, R.P. Shukla, S.K. Singh, V. Sharma, R. Konwar, P.R. Mishra, Hyaluronic acid anchored paclitaxel nanocrystals improves chemotherapeutic efficacy and inhibits lung metastasis in tumor-bearing rat model, RSC Adv. 6 (77) (2016) 73083–73095.
[46] C. Shen, B. Shen, X. Liu, H. Yuan, Nanosuspensions based gel as delivery system of nitrofurazone for enhanced dermal bioavailability, J. Drug Delivery Sci. Technol. 43 (2018) 1–11.
[47] J.J. Rouse, T.L. Whateley, M. Thomas, G.M. Eccleston, Controlled drug delivery to the lung: Influence of hyaluronic acid solution conformation on its adsorption to hydrophobic drug particles, Int. J. Pharm. 330 (1-2) (2007) 175–182.
[48] J. Zhao, Y. Wang, Y. Ma, Y. Liu, B. Yan, L. Wang, Smart nanocarrier based on PEGylated hyaluronic acid for deacetyl mycoepoxydience: High stability with enhanced bioavailability and efficiency, Carbohydr. Polym. 203 (2019) 356–368.
[49] L. Wu, J. Zhang, W. Watanabe, Physical and chemical stability of drug nanoparticles, Adv. Drug Deliv. Rev. 63 (6) (2011) 456–469.
[50] P.R. Mishra, L.A. Shaal, R.H. Müller, C.M. Keck, Production and characterization of Hesperetin nanosuspensions for dermal delivery, Int. J. Pharm. 371 (1-2) (2009) 182–189.
[51] Alshora DH, Ibrahim MA, Elzayat E, Almeanazel OT, Alanazi F. Rosuvastatin calcium nanoparticles: Improving bioavailability by formulation and stabilization codesign. PLoS ONE [Internet]. 2018;13(7):1–17. Available from: https://doi.org/10.1371/journal.pone.0200218.
[52] J.R. Rodriguez Amado, A.L. Prada, J.L. Duarte, H. Keita, H.R. da Silva, A. M. Ferreira, E.H. Sosa, J.C.T. Carvalho, Development, stability and in vitro delivery profile of new loratadine-loaded nanoparticles, Saudi Pharm. J. 25 (8) (2017) 1158–1168.
[53] A. Soroushnia, F. Ganji, E. Vasheghani-Farahani, H. Mobedi, Preparation, optimization, and evaluation of midazolam nanosuspension: enhanced bioavailability for buccal administration, Prog. Biomater. 10 (1) (2021) 19–28.
[54] T. Chuacharoen, S. Prasongsuk, C.M. Sabliov, Effect of surfactant concentrations on physicochemical properties and functionality of curcumin nanoemulsions under conditions relevant to commercial utilization, Molecules 24 (15) (2019) 1–12.
[55] T.P. Sari, B. Mann, R. Kumar, R.R.B. Singh, R. Sharma, M. Bhardwaj, S. Athira, Preparation and characterization of nanoemulsion encapsulating curcumin, Food Hydrocolloids 43 (2015) 540–546.
[56] T.G. Mezger, The Rheology Handbook For users of rotational and oscillatory rheometers. 2nd ed. Vincentz Network, Hanover, Germany; 2006.
[57] M.H. Mahdi, B.R. Conway, A.M. Smith, Development of mucoadhesive sprayable gellan gum fluid gels, Int. J. Pharm. 488 (1-2) (2015) 12–19.
[58] C. Guo, K.J. Stine, J.F. Kauffman, W.H. Doub, Assessment of the influence factors on in vitro testing of nasal sprays using Box-Behnken experimental design, Eur. J. Pharm. Sci. 35 (5) (2008) 417–426.
[59] D.-S. Yin, W.-Y. Yang, Z.-Q. Ge, Y.-J. Yuan, A fluorescence study of sodium hyaluronate/surfactant interactions in aqueous media, Carbohydr. Res. 340 (6) (2005) 1201–1206.
[60] V. Kundoor, R.N. Dalby, Assessment of nasal spray deposition pattern in a silicone human nose model using a color-based method, Pharm. Res. 27 (1) (2010) 30–36.
[61] Y.u. Pu, A.P. Goodey, X. Fang, K. Jacob, A comparison of the deposition patterns of different nasal spray formulations using a nasal cast, Aerosol Sci. Technol. 48 (9) (2014) 930–938.
[62] C.T. Uppuluri, P.R. Ravi, A.V. Dalvi, S.S. Shaikh, S.R. Kale, Piribedil loaded thermo-responsive nasal in situ gelling system for enhanced delivery to the brain: formulation optimization, physical characterization, and in vitro and in vivo evaluation, Drug Delivery and Translational Res. 11 (3) (2021) 909–926.
[63] K. Dua, D. Mathure, J.R. Madan, K.N. Gujar, A. Tupsamundre, H.A. Ranpise, Formulation and evaluation of niosomal in-situ nasal gel of Buspirone Hydrochloride for brain delivery, Pharmaceutical Nanotechnol. 06 (2018) 69–78.
[64] European Medicines Agency. Committee for medicinal products for human use (CHMP): Guideline on the pharmaceutical quality of inhalation and nasal products. 2006. p. 27.
[65] US Food and Drug Administration. Guidance for Industry Nasal Spray and Inhalation Solution, Suspension, and Spray Drug Products — Chemistry, Manufacturing, and Controls Documentation ' U.S. Department of Health and Human Services Food and Drug Administration Center for Drug Evaluation an. Online [Internet]. 2002;(July):10–5. Available from: https://www.fda.gov/media/70857/download.
[66] J. Grmaš, K. Stare, D. Božič, R. Injac, R. Dreu, Elucidation of Formulation and Delivery Device-Related Effects on in Vitro Performance of Nasal Spray with Implication to Rational Product Specification Identification, J. Aerosol Med. Pulmonary Drug Delivery 30 (4) (2017) 230–246.
[67] T. Jullaphant, T. Nakpeng, T. Srichana, Montelukast nasal spray: formulation development and in vitro evaluation, Pharm. Dev. Technol. 24 (4) (2019) 494–503.
[68] E. Casula, M.L. Manca, M. Perra, J.L. Pedraz, T.B. Lopez-Mendez, A. Lozano, E. Calvo, M. Zaru, M. Manconi, Nasal spray formulations based on combined hyalurosomes and glycerosomes loading zingiber officinalis extract as green and natural strategy for the treatment of rhinitis and rhinosinusitis, Antioxidants. 10 (7) (2021) 1109, https://doi.org/10.3390/antiox10071109.
[69] A.C. Braun, D. Ilko, B. Merget, H. Gieseler, O. Germershaus, U. Holzgrabe, L. Meinel, Predicting critical micelle concentration and micelle molecular weight of polysorbate 80 using compendial methods, Eur. J. Pharm. Biopharm. 94 (2015) 559–568.
[70] M. Li, P. Alvarez, P. Orbe, E. Bilgili, Multi-faceted Characterization of Wet-milled Griseofulvin Nanosuspensions for Elucidation of Aggregation State and Stabilization Mechanisms, AAPS PharmSciTech. 19 (4) (2018) 1789–1801.
[71] T.R. Sosnowski, P. Rapiejko, J. Sova, K. Dobrowolska, Impact of physicochemical properties of nasal spray products on drug deposition and transport in the pediatric nasal cavity model, Int. J. Pharm. 574 (2020) 118911, https://doi.org/10.1016/j.ijpharm.2019.118911.
[72] K. Han, O.E. Woghiren, R. Priefer, Surface tension examination of various liquid oral, nasal, and ophthalmic dosage forms, Chem. Cent. J. 10 (1) (2016) 1–5.
[73] M.Y. Foo, Y.-S. Cheng, W.-C. Su, M.D. Donovan, The influence of spray properties on intranasal deposition, J. Aerosol Med.: Deposition, Clearance, and Effects in the Lung 20 (4) (2007) 495–508.
[74] Cheng YS, Holmes TD, Gao J, Guilmette RA, Li S, Surakitbanharn Y, et al. Characterization of Nasal Spray Pumps and Deposition Pattern in a Replica of the Human Nasal Airway. Journal of Aerosol Medicine [Internet]. 2001;14(2): 267–80. Available from: http://www.liebertonline.com/doi/abs/10.1089/08942680152484199.
[75] Z.N. Warnken, H.D.C. Smyth, D.A. Davis, S. Weitman, J.G. Kuhn, R.O. Williams, Personalized Medicine in Nasal Delivery: The Use of Patient-Specific Administration Parameters to Improve Nasal Drug Targeting Using 3D-Printed Nasal Replica Casts, Mol. Pharm. 15 (4) (2018) 1392–1402.
[76] J.Z. Chen, M. Kiaee, A.R. Martin, W.H. Finlay, In vitro assessment of an idealized nose for nasal spray testing: Comparison with regional deposition in realistic nasal replicas, Int. J. Pharm. 582 (2020) 119341, https://doi.org/10.1016/j.ijpharm.2020.119341.
[77] P.G. Djupesland, R.A. Mahmoud, Role of nasal casts for in vitro evaluation of nasal drug delivery and quantitative evaluation of various nasal casts. 11 (2020) 485–95.
[78] S. Ghaemi, P. Rahimi, D.S. Nobes, Assesment of parameters for distinguishing droplet shape in a spray field using image based techniques, Atom. Sprays 19 (9) (2009) 809–831.
[79] E. Chiarella, N. Lombardo, N. Lobello, A. Aloisio, T. Aragona, C. Pelaia, S. Scicchitano, H.M. Bond, M. Mesuraca, Nasal polyposis: Insights in epithelial-mesenchymal transition and differentiation of polyp mesenchymal stem cells, Int. J. Mol. Sci. 21 (18) (2020) 6878, https://doi.org/10.3390/ijms21186878.
[80] M.D. Manniello, S. Hosseini, A. Alfaifi, A.R. Esmaeili, A.V. Kolanjiyil, R. Walenga, A. Babiskin, D. Sandell, R. Mohammadi, T. Schuman, M. Hindle, L. Golshahi, In vitro evaluation of regional nasal drug delivery using multiple anatomical nasal replicas of adult human subjects and two nasal sprays, Int. J. Pharm. 593 (2021) 120103, https://doi.org/10.1016/j.ijpharm.2020.120103.
[81] A. Lopedota, A. Cutrignelli, N. Denora, V. Laquintana, A. Lopalco, S. Selva, et al., New ethanol and propylene glycol free gel formulations containing a minoxidil-methyl- b -cyclodextrin complex as promising tools for alopecia treatment, Drug Dev. Ind. Pharm. 41 (5) (2014) 1–9.
[82] D. Baumann, C. Bachert, P. Högger, Dissolution in nasal fluid, retention and anti-inflammatory activity of fluticasone furoate in human nasal tissue ex vivo, Clin. Exp. Allergy 39 (10) (2009) 1540–1550.
[83] T. Tokumura, H. Isaka, M. Kanou, E. Miyazaki, N. Kaneko, T. Kurita, An inclusion complex of fluticasone propionate with γ-cyclodextrin in aqueous solution and in a solid state, J. Drug Delivery Sci. Technol. 26 (2015) 24–27.
[84] M. Colombo, S. Staufenbiel, E. Rühl, R. Bodmeier, In situ determination of the saturation solubility of nanocrystals of poorly soluble drugs for dermal application, Int. J. Pharm. 521 (1-2) (2017) 156–166.
[85] K. Mitri, R. Shegokar, S. Gohla, C. Anselmi, R.H. Müller, Lutein nanocrystals as antioxidant formulation for oral and dermal delivery, Int. J. Pharm. 420 (1) (2011) 141–146.
[86] N.V. Gandhi, U.A. Deokate, S.S. Angadi, Development of Nanonized Nitrendipine and Its Transformation into Nanoparticulate Oral Fast Dissolving Drug Delivery System, AAPS PharmSciTech. 22 (3) (2021) 1–15.
[87] E.C. Arrua, O. Hartwig, D.-K. Ho, B. Loretz, X. Murgia, C.J. Salomon, C.-M. Lehr, Surfactant-Free Glibenclamide Nanoparticles: Formulation, Characterization and Evaluation of Interactions with Biological Barriers, Pharm. Res. 38 (6) (2021) 1081–1092.
[88] R. Xu, C. Jiang, L. Zhou, B. Li, Y.i. Hu, Y. Guo, X. Xiao, S. Lu, Fabrication of Stable Apigenin Nanosuspension with PEG 400 as Antisolvent for Enhancing the Solubility and Bioavailability, AAPS PharmSciTech. 23 (1) (2022), https://doi.org/10.1208/s12249-021-02164-x.
[89] J.Z. Yang, A.L. Young, P.-C. Chiang, A. Thurston, D.K. Pretzer, Fluticasone and Budesonide Nanosuspensions for Pulmonary Delivery: Preparation,

Characterization, and Pharmacokinetic Studies, J. Pharm. Sci. 97 (11) (2008) 4869–4878.
[90] V. Shah, M. Sharma, R. Pandya, R.K. Parikh, B. Bharatiya, A. Shukla, H.-C. Tsai, Quality by Design approach for an in situ gelling microemulsion of Lorazepam via intranasal route, Mater. Sci. Eng., C 75 (2017) 1231–1241.
[91] P. Snetkov, K. Zakharova, S. Morozkina, R. Olekhnovich, M. Uspenskaya, Hyaluronic acid: The influence of molecular weight on structural, physical, physico-chemical, and degradable properties of biopolymer, Polymers. 12 (8) (2020) 1800, https://doi.org/10.3390/polym12081800.
[92] P. Watts, A. Smith, M. Perelman, Nasal delivery of fentanyl. Drug Delivery and Translational, Research. 3 (1) (2013) 75–83.
[93] PecFent SmPC. PecFent [Internet]. European Medicines Agency. [cited 2021 Dec 1]. Available from: www.ema.europa.ea.
[94] SmPC. Hysan [Internet]. [cited 2021 Dec 1]. Available from: https://hysan.prohealth.com.mt/.
[95] Sterimar [Internet]. [cited 2021 Dec 1]. Available from: https://www.sterimarnasal.co.uk/.
[96] M. Cirri, F. Maestrelli, G. Nerli, N. Mennini, M. D'Ambrosio, C. Luceri, P.A. Mura, Development of a cyclodextrin-based mucoadhesive-thermo-sensitive in situ gel for clonazepam intranasal delivery, Pharmaceutics 13 (7) (2021) 969, https://doi.org/10.3390/pharmaceutics13070969.
[97] M. Gelardi, L. Iannuzzi, N. Quaranta, Intranasal sodium hyaluronate on the nasal cytology of patients with allergic and nonallergic rhinitis, Int. Forum Allergy Rhinol. 3 (10) (2013) 807–813.
[98] E. Cantone, M. Iengo, Effect of sodium hyaluronate added to topical corticosteroids in chronic rhinosinusitis with nasal polyposis, Am. J. Rhinol. Allergy 30 (5) (2016) 340–343.
[99] D. Monzani, G. Molinari, C. Gherpelli, L. Michellini, M. Alicandri-Ciufelli, Evaluation of Performance and Tolerability of Nebulized Hyaluronic Acid Nasal Hypertonic Solution in the Treatment of Chronic Rhinosinusitis, Am. J. Rhinol. Allergy 34 (6) (2020) 725–733.
[100] E. Savietto, G. Marioni, P. Maculan, A. Pettorelli, B. Scarpa, E. Simoni, L. Astolfi, R. Marchese-Ragona, G. Ottaviano, Effectiveness of micronized nasal irrigations with hyaluronic acid/isotonic saline solution in non-polipoid chronic rhinosinusitis: a prospective, randomized, double-blind, controlled study, Am. J. Otolaryngol. 41 (4) (2020) 102502, https://doi.org/10.1016/j.amjoto.2020.102502.
[101] Flixonase [Internet]. [cited 2021 Dec 1]. Available from: https://www.medicines.org.uk/emc/product/5503/smpc#gref.
[102] L. Salade, N. Wauthoz, J. Goole, K. Amighi, How to characterize a nasal product. The state of the art of in vitro and ex vivo specific methods, Int. J. Pharmaceutics. Elsevier B.V. 561 (2019) 47–65.
[103] F. Zahir-Jouzdani, J.D. Wolf, F. Atyabi, A. Bernkop-Schnürch, In situ gelling and mucoadhesive polymers: why do they need each other? Expert Opin. Drug Deliv. 15 (10) (2018) 1007–1019.
[104] V.S. Belgamwar, D.S. Chauk, H.S. Mahajan, S.A. Jain, S.G. Gattani, S.J. Surana, Formulation and evaluation of in situ gelling system of dimenhydrinate for nasal administration, Pharm. Dev. Technol. 14 (3) (2009) 240–248.
[105] X. Xu, Y. Shen, W. Wang, C. Sun, C. Li, Y. Xiong, et al., Preparation and in vitro characterization of thermosensitive and mucoadhesive hydrogels for nasal delivery of phenylephrine hydrochloride, Eur. J. Pharm. Biopharm. 88 (3) (2014) 998–1004.
[106] J. Yang, L. Dai, Q. Yu, Q. Yang, Histological and anatomical structure of the nasal cavity of Bama minipigs, PLoS ONE 12 (3) (2017) 1–14.
[107] S. Ladel, P. Schlossbauer, J. Flamm, H. Luksch, B. Mizaikoff, K. Schindowski, Improved in vitro model for intranasal mucosal drug delivery: Primary olfactory and respiratory epithelial cells compared with the permanent Nasal cell line RPMI 2650, Pharmaceutics 11 (8) (2019).
[108] L. Joergensen, B. Klösgen, A.C. Simonsen, J. Borch, E. Hagesaether, New insights into the mucoadhesion of pectins by AFM roughness parameters in combination with SPR, Int. J. Pharm. 411 (1–2) (2011) 162–168.
[109] J.F. Douglas, Weak and strong gels and the emergence of the amorphous solid state, Gels 4 (1) (2018) 1–14.

5. RASPRAVA

Primjena lijeka u nos put je izbora u liječenju lokalnih oboljenja nosne sluznice, ali pruža i mogućnost za sistemsku dostavu te izravnu dostavu lijeka u središnji živčani sustav (147). Nazalni kortikosteroidi u širokoj su upotrebi u liječenju upalnih bolesti nosne sluznice, kao što su alergijski i nealergijski rinitis, kronični rinosinuitis i nosna polipoza (39), a u novije vrijeme istražuju se i u liječenju neuroupale povezane s teškim oblikom bolesti Covid-19 (45). Složena anatomija nosne šupljine otežava dostavu lijeka u ciljnu regiju, a mukocilijarni mehanizam čišćenja u kratkom vremenu uklanja lijek s nosne sluznice. Jedno od rješenja leži u razvoju inovativnih tekućih i praškastih *in situ* gelirajućih sustava koji se u kontaktu sa sluznicom nosa umrežavaju ili bubre te stvaraju gel, produljujući vrijeme zadržavanja na sluznici i prilagođavajući oslobađanje lijeka (63,72). Istodobno, za ostvarenje željenog učinka, važno je u ranoj fazi razvoja formulacije lijeka razmatrati profil njegove nazalne depozicije te optimirati formulaciju i način primjene za dostavljanje lijeka u ciljno područje nosne šupljine (125).

Cilj ovog rada bio je prilagođavanjem procesnih, formulacijskih i/ili parametara primjene korištenjem statističkog dizajna eksperimenta razviti inovativne farmaceutske oblike kortikosterioda za nazalnu primjenu, uključujući *in situ* gelirajuću mikro- i nanosuspenziju flutikazonpropionata (FP-a) te polimerne mikrosfere s natrijevim deksametazonfosfatom (NDF-om), kao i optimirati smjesu mikrosfera s NDF-om i inertnog nosača. Navedeni tekući *in situ* gelirajući sustavi FP-a namijenjeni su liječenju kroničnog rinosinuitisa i nosne polipoze, a praškasti sustavi s NDF-om liječenju neuroupalnih procesa izravnom dostavom nazalno primijenjenog kortikosteroida u središnji živčani sustav. Cilj je bio razviti farmaceutske oblike povoljnih biofarmaceutskih svojstava, optimalne depozicije u nosnoj šupljini, produljenog vremena zadržavanja na mjestu primjene te prikladnog profila oslobađanja lijeka s obzirom na željeni učinak. U izradi *in situ* gelirajućih mikro- i nanosuspenzija FP-a korišten je polisorbat 80 kao površinski aktivna tvar i stabilizator, niskometoksilirani visokoamidirani pektin i gelan guma prvenstveno kao *in situ* gelirajući polimeri te natrijev hijaluronat kao mukoadhezivni i bioaktivni polimer. Manitol je korišten kao sredstvo za izotonizaciju, a natrijev hidroksid za prilagodbu pH. NDF je također kortikosteroid koji je u upotrebi za razne indikacije. Njegova dobra topljivost u vodi čini ga pogodnim za oblikovanje pomoću sušenja raspršivanjem. Za pripravu *in situ* gelirajućih praškastih sustava NDF-a namijenjenih za izravnu dostavu kortikosteroida iz nosne šupljine u u središnji živčani sustav korišteni su niskometoksilirani pektin kao *in situ* gelirajući polimer i hipromeloza, mukoadhezivni polimer s pokazanim potencijalom stvaranja mehaničke barijere na nosnoj sluznici i sprječavanja difuzije alergena ili virusa do nazalnog epitela (148,149). Kao inertni nosači korišteni su laktoza i manitol. Sve

navedene pomoćne tvari pripadaju GRAS (engl. *generally recognised as safe*) popisu tvari Američke agencije za hranu i lijekove (engl. *Food and Drug Administration,* FDA). Pripravljeni tekući i praškasti *in situ* gelirajući sustavi karakterizirani su i optimirani s obzirom na sadržaj lijeka, fizičko-kemijska svojstva, posebice reološka svojstva, zatim svojstva spreja, profil oslobađanja lijeka, mukoadhezivnost, biokompatibilnost, permeabilnost i profil nazalne depozicije. Sveobuhvatni pristup razvoju inovativnih farmaceutskih oblika kortikosteroida omogućen je primjenom statističkog dizajna eksperimenta koji je obuhvaćao dio navedenih karakterizacijskih postupaka, ključnih za pojedini razvijani oblik. Daljni probir ili potvrda potencijala vodećih formulacija osigurani su temeljem *in vitro* ispitivanja ponašanja formulacija u kontaktu s nosnom sluznicom te određivanjem profila stabilnosti.

Kako je prikazano u nastavku, plan eksperimenata u razvoju inovativnih formulacija odabranih kortikosteroida bio je prilagođen vrsti razvijanog farmaceutskog oblika (*in situ* gelirajući oblici: mikrosuspenzija, nanosuspenzija ili praškasti sustav), svojstvima oblikovane djelatne tvari (u vodi slabo topljivi FP *vs*. dobro topljivi NDF) te ciljnom učinku (učinkovita dostava lijeka u nosnu šupljinu; lokalni učinak *vs*. izravna dostava u središnji živčani sustav, odnosno ciljanje turbinatne ili olfaktorne regije nosne šupljine).

In situ gelirajuće mikrosuspenzije pripravljene su rastrljavanjem mikroniziranog FP-a s polisorbatom 80 te dodavanjem otopina polimera. U razvoju formulacije primijenjena su QbD načela te je korišten prilagođeni definitivni pretražni dizajn eksperimenta u kojem je varirano sedam parametara na dvije ili tri razine. Formulacijski parametri uključivali su koncentraciju FP-a, polisorbata 80, pektina, gelan gume i natrijevog hijaluronata, dok su kut primjene u odnosu na horizontalnu ravninu i protok zraka pri udahu bili parametri primjene. Navedene postavke rezultirale su matricom od 52 kombinacije parametara (42 različite kombinacije + 10 replikata). Kao odgovori u dizajnu eksperimenta pri razvoju *in situ* gelirajuće mikrosuspenzije FP-a ispitani su: vrijeme geliranja formulacije nakon miješanja sa simuliranim nosnim fluidom (SNF-om), viskoznost pri mirovanju, veličina raspršenih kapljica, kut raspršenja i depozicija u nosnoj šupljini. Vrijednost primjene statističkog dizajna u razvoju *in situ* gelirajuće mikrosuspenzije FP-a ogleda se u generiranim visoko prediktivnim regresijskim modelima utjecaja variranih parametara na promatrane odgovore. Temeljem modela za turbinatnu depoziciju izvedeno je šest prikladnih formulacija vrlo učinkovite turbinatne depozicije među kojima je, temeljem dublje reološke karakterizacije gela koji nastaje u kontaktu s nosnim fluidom te ispitivanja profila oslobađanja uklopljenog FP-a *in vitro,* prepoznata formulacija najvećeg terapijskog potencijala.

Radi proučavanja utjecaja veličine suspendiranih kristala FP-a na svojstva *in situ* gelirajuće formulacije, pripravljeni su nanokristali FP-a metodom vlažnog mljevenja. Njihovim uklapanjem u *in situ* gelirajuću otopinu polimera dobivena je *in situ* gelirajuća nanosuspenzija FP-a. Prilikom razvoja *in situ* gelirajuće nanosuspenzije FP-a, u dizajnu eksperimenta varirana su tri formulacijska parametra (koncentracija FP-a, polisorbata 80 i natrijevog hijaluronata) i tri parametra primjene (kut u odnosu na horizontalnu ravninu, kut u odnosu na vertikalnu ravninu i protok zraka), što je rezultiralo matricom od 17 kombinacija parametara. Kao odgovori u dizajnu eksperimenta, jednako kao i pri razvoju *in situ* gelirajuće mikrosuspenzije FP-a, ispitani su: vrijeme geliranja formulacije nakon miješanja sa simuliranim nosnim fluidom (SNF-om), viskoznost pri mirovanju, veličina raspršenih kapljica, kut raspršenja i depozicija u nosnoj šupljini, uz veličinu i zeta potencijal nanokristala u suspenziji te površinsku napetost sustava kao dodatne odgovore. Primjena statističkog dizajna eksperimenta i proučavanje velikog broja odgovora koji se odnose na intrinzična svojstva formulacije i ponašanje nakon aerosolizacije razotkrili su glavne parametre za njihovo fino ugađanje. Odabir vodeće *in situ* gelirajuće nanosuspenzije FP-a i odgovarajućih parametara primjene izvršen je temeljem regresijskog modela za depoziciju u srednjoj turbinatnoj regiji, važnoj u razvoju rinosinuitisa. Terapijski potencijal razvijene *in situ* gelirajuće nanosuspenzije FP-a potvrđen je usporedbom s odgovarajućom *in situ* gelirajućom mikrosuspenzijom s obzirom na profil *in vitro* oslobađanja lijeka, ekspanziju volumena geliranjem, reološka svojstva nastalog gela, *in vitro* biokompatibilnost te mukoadhezivnost, a pokazana je i adekvatna stabilnost razvijenog sustava.

Mikrosfere s NDF-om pripravljene su sušenjem raspršivanjem. Dizajn eksperimenta uključivao je dva formulacijska (koncentracija hipromeloze i NDF-a u otopini za sušenje) i dva procesna (ulazna temperatura i protok uzorka) parametra, koji su varirani s ciljem dobivanja mikrosfera povoljnih svojstava, dajući matricu od 32 kombinacije parametara. U pripravi mikrosfera s NDF-om kao odgovori su promatrani iskorištenje procesa sušenja raspršivanjem, uspješnost uklapanja i sadržaj lijeka u mikrosferama, veličina mikrosfera, sadržaj vlage te bubrenje u vodi i SNF-u. Primjenom statističkog dizajna eksperimenta razlučeni su optimalni procesni i formulacijski parametri za pripravu mikrosfera s NDF-om. Optimirane mikrosfere s NDF-om miješane su s inertnim nosačem (laktozom ili manitolom) te su pripravljene smjese prašaka detaljno okarakterizirane s obzirom na homogenost, svojstva tečenja, svojstva spreja, mukoadhezivnost i biokmpatibilnost. Terapijski potencijal smjese optimiranih mikrosfera s NDF-om i manitola kao odabranog nosača, potvrđen je ispitivanjima permeabilnosti *in vitro* i depozicije u nosnoj šupljini.

In situ gelirajuće mikrosuspenzije FP-a izrađene su korištenjem komercijalno dostupnog mikroniziranog FP-a veličine čestica u rasponu od 0,097 do 10 μm. U izradi *in situ* gelirajućih nanosuspenzija FP-a, metoda vlažnog mljevenja u laboratorijskom mjerilu pokazala se primjenjivom za pripravu nanokristala FP-a. Srednji promjer nanokristala u *in situ* gelirajućim nanosuspenzijama predviđenima dizajnom eksperimenta (od 133,0 ± 0,8 nm do 160,7 ± 3,6 nm) i indeks polidisperznosti (0,227 ± 0,027 do 0,273 ± 0,011) potvrdili su odgovarajući stupanj usitnjenosti i monodisperznu raspodjelu veličina (88). Veličina nanokristala potvrđena je transmisijskom elektronskom mikroskopijom (engl. *transmission electron microscopy,* TEM). Zeta potencijal u *in situ* gelirajućim nanosuspenzijama FP-a bio je u rasponu od − 93,1 ± 0,6 mV do − 77,2 ± 3,7 mV, osiguravajući dostatnu fizičku stabilnost pripravljenih sustava. Naime, nanosuspenzije se smatraju stabilnima pri vrijednostima zeta potencijala od ± 30 mV, dok apsolutne vrijednosti veće od 60 mV ukazuju na izrazitu stabilnost (150). Zabilježeni negativni zeta potencijal posljedica je adsorpcije polisorbata 80 i natrijevog hijaluronata na površinu FP nanokristala. Površinska napetost *in situ* gelirajućih nanosuspenzija FP-a pripravljenih pri omjeru FP-a i polisorbata 80 od 1:1 do 2:1 (*m*/*m*) odgovarala je vrijednostima prikladnim za nazalnu primjenu (151). Polimerni sastav *in situ* gelirajućih mikro- i nanosuspenzija FP-a, uz povećanje viskoznosti i povoljan učinak na stabilnost suspenzija, osigurao je pseudoplastično ponašanje i prikladnost za primjenu raspršivanjem, kao i svojstvo geliranja u kontaktu sa SNF-om.

Mikrosfere s uklopljenim NDF-om pripravljene su sušenjem raspršivanjem. Iskorištenje procesa sušenja raspršivanjem bilo je u rasponu od 13,9 % do 68,6 %. Vrijednost iskorištenja rasla je s porastom ulazne temperature, smanjivala se s povećanjem protoka uzorka i koncentracije hipromeloze, a uočen je i utjecaj interakcije procesnih parametara na iskorištenje. Visoka uspješnost uklapanja NDF-a (od 85,2±4,8 % do 101,9±0,3 %) postignuta je za sve pripravljene uzorke te nije ovisila o promatranim formulacijskim niti procesnim parametrima. Sadržaj NDF-a u pripravljenim mikrosferama bio je u rasponu od 1,4 % do 33,5 % te je korelirao s masenim omjerom polimera i lijeka u sušenim otopinama. Pektin i hipromeloza su biokompatibilni, mukoadhezivni polimeri koji su već u upotrebi u tekućim farmaceutskim oblicima za nazalnu primjenu (63,152). Kombiniranje pektina i hipromeloze kao polimera izbora za pripravu mikrosfera s NDF-om omogućilo je prilagođavanje svojstava polimernog matriksa s obzirom na željena svojstva mikrosfera. Bitno svojstvo mikrosfera pripravljenih sušenjem raspršivanjem je sadržaj ostatne vlage, koja može utjecati na kemijsku i mikrobiološku stabilnost lijeka. Sadržaj ostatne vlage u mikrosferama s NDF-om iznosio je od

3,2 ± 0,8 % do 9,1 ± 0,2 %, što je unutar prihvatljivog raspona za praškaste sustave s hidrofilnim polimerima (153). Porast koncentracije hipromeloze i smanjenje koncentracije NDF-a rezultirali su smanjenjem sadržaja vlage. NDF je zbog svoje higroskopnosti povećavao sadržaj vlage u mikrosferama, dok je porast koncentracije hipromeloze u otopini za sušenje značio smanjenje udjela higroskopnijeg pektina u mikrosferama (147), što je konačno rezultiralo i manjim sadržajem ostatne vlage.

Usprkos razlikama u temeljnim značajkama razvijanih farmaceutskih oblika FP-a i NDF-a (tekući vs. praškasti oblik), geliranje u kontaktu s nosnim fluidom predstavlja njihovo zajedničko svojstvo koje ima za cilj osigurati adheziju farmaceutskog oblika za nosnu sluznicu te produljeno zadržavanje i prilagođeno oslobađanje uklopljenog lijeka na mjestu primjene (153). Vrijeme geliranja *in situ* gelirajućih mikro- i nanosuspenzija FP-a određeno je nakon miješanja s SNF-om u volumnom omjeru 1:1, čime su simulirani uvjeti *in vivo* pri kontaktu kapljice nazalnog spreja s nosnom sluznicom (154). SNF sadrži kalcijeve ione koji umrežavaju pektin te nastaje trodimenzionalna struktura gela. Koncentracija pektina u *in situ* gelirajućim mikrosuspenzijama FP-a bila je od 0,5 % do 0,7 % (*m*/*m*), a gelan gume od 0 do 0,2 % (*m*/*m*). Kod svih ispitanih *in situ* gelirajućih mikrosuspenzija FP-a, modul pohrane bio je veći od modula gubitka već na početku mjerenja, ukazujući na trenutno geliranje sustava. S ciljem smanjenja broja sastavnica formulacije, a zadržavanja trenutnog geliranja, u izradi *in situ* gelirajućih nanosuspenzija FP-a korišten je pektin kao jedini *in situ* gelirajući polimer pri koncentraciji od 0,9 % (*m*/*m*) te su i ti sustavi gelirali odmah nakon miješanja s SNF-om. Faktor gubitka za sve *in situ* gelirajuće mikro- i nanosuspenzije FP iznosio je oko 0,1, što odgovara slabim gelovima prikladnima za nazalnu primjenu (66). Za razliku od opisanih tekućih sustava FP-a, mikrosfere s uklopljenim NDF-om stvaraju gel bubrenjem u kontaktu s vodenim medijem. Bubrenje mikrosfera ispitano je u kontaktu s SNF-om te pročišćenom vodom kao kontrolom, kako bi se mogao vrednovati utjecaj umreženosti polimernog matriksa temeljenog na pektinu kalcijevim ionima na stupanj bubrenja. Mikrosfere s NDF-om apsorbirale su manje volumene SNF-a (6,1 ± 1,6 μl mg^{-1} – 23,5 ± 1,9 μl mg^{-1}) nego vode (6,7 ± 2,7 μl mg^{-1} – 41,6 ± 3,4 μl mg^{-1}) uslijed umrežavanja pektinskih lanaca ionima kalcija iz SNF-a koji je prepoznat kao glavni čimbenik s utjecajem na bubrenje. Umjereno bubrenje mikrosfera prilikom kontakta s nosnim fluidom sprječava pretjeranu hidrataciju polimernih lanaca te posljedično smanjenje adhezivnosti, dok istovremeno omogućava produljeno zadržavanje mikrosfera na nosnoj sluznici te prikladno oslobađanje uklopljenog lijeka.

Farmaceutski oblici FP-a i NDF-a razvijani u ovom radu namijenjeni su nazalnoj primjeni u obliku spreja, pri čemu je veličina aerosloziranih kapljica/čestica od ključne važnosti za ciljanu depoziciju unutar nosne šupljine. Prema smjernicama EMA-e i FDA-e, većina raspršenih kapljica/čestica proizvoda za nazalnu primjenu mora biti promjera većeg od 10 μm, dok gornja granica veličine nije navedena (94,155). U slučaju *in situ* gelirajućih suspenzija FP-a raspodjela veličina kapljica određena je nakon raspršivanja nazalnom sprej pumpicom prilagođenom raspršivanju viskoznih sustava. Raspodjela veličina mikrosfera NDF-a određena je nakon temeljitog dispergiranja suhog praška u etanolu, kako bi se dobili podaci o raspodjeli veličina pojedinačnih čestica, kao krajnjem slučaju aerosoliziranog praškastog oblika. Raspodjele veličina raspršenih kapljica *in situ* gelirajućih suspenzija FP-a te mikrosfera NDF-a određene su metodom laserske difrakcije, a izražene su volumnim promjerima D_v10, D_v50 i D_v90.

Sve dizajnom predviđene *in situ* gelirajuće mikro- i nanosuspenzije FP-a udovoljavaju kriteriju vezanom uz veličinu raspršenih kapljica pri nazalnoj primjeni u obliku spreja (Tablica 2.).

Tablica 2. Rasponi D_v10, D_v50 i D_v90 raspršenih kapljica *in situ* gelirajućih mikro- i nanosuspenzija FP-a te mikrosfera s NDF-om dispergiranih u etanolu

Uzorak	D_v10 (μm)	D_v50 (μm)	D_v90 (μm)
ISG-M-FP	16,4 ± 0,6 – 40,6 ± 1,9	35,9 ± 1,2 – 132,1 ± 6,3	86,9 ± 5,5 – 280,6 ± 30,9
ISG-N-FP	16,9 ± 0,4 – 30,4 ± 8,4	38,7 ± 1,1 – 100,7 ± 30,3	98,2 ± 3,0 – 219,3 ± 45,3
MS-NDF	1,4 ± 0,0 – 2,6 ± 0,3	2,2 ± 0,0 – 14,9 ± 3,4	3,7 ± 0,0 – 42,9 ± 0,6

ISG-M-FP – *in situ* gelirajuće mikrosuspenzije flutikazonpropionata; ISG-N-FP – *in situ* gelirajuće nanosuspenzije flutikazonpropionata; MS-NDF – mikrosfere s natrijevim deksametazonfosfatom. Prikazane su srednje vrijednosti ± standardna devijacija (n=3).

Rasponi vrijednosti volumnih promjera D_v10, D_v50 i D_v90 raspršenih kapljica *in situ* gelirajućih mikro- i nanosuspenzija FP-a vrlo su slični usprkos razlikama u polimernom sastavu (prisustvo gelan gume u mikrosuspenzijama te veća koncentracija pektina u nanosuspenzijama), ističući važan utjecaj koncentracije natrijevog hijaluronata na veličinu raspršenih kapljica. Navedeni parametar sadržan je u regresijskim modelima za promatrane volumne promjere obaju tipova suspenzija FP-a. Raspodjela veličina mikrosfera s NDF-om ukazuje na veliki udio čestica u praškastim uzorcima promjera manjeg od 10 μm (Tablica 2.), stoga su se mikrosfere s NDF-om pokazale prikladnima za miješanje s inertnim nosačima s ciljem osiguranja adekvatne raspodjele veličine čestica i depozicije u nosnoj šupljini (140). Nastavno na takvo zapažanje, temeljem regresijskih modela dobivenih statističkom analizom utjecaja parametara na svojstva

mikrosfera s NDF-om, razlučeni su optimalni procesni i formulacijski parametri za pripravu mikrosfera koje su u daljnjem postupku miješane s inertnim nosačem. Odabrani parametri rezultirali su velikim iskorištenjem procesa sušenja raspršivanjem te mikrosferama relativno male veličine, s visokim udjelom NDF-a (33,5 ± 0,4 %) i umjerenog bubrenja u SNF-u. Očekivano je da će se manje čestice lakše uklopiti u brazde hrapave površine nosača te tako bolje adherirati na isti (77). Visoki udio NDF-a u mikrosferama omogućio je miješanje mikrosfera s inertnim nosačem na način da se osigura primjena potrebne doze lijeka u količini praška koja se može primijeniti u nos (najviše 25 mg po nosnici) (72). Smjese prašaka pripravljene su miješanjem odabranih mikrosfera s NDF-om s laktozom ili manitolom prikladne veličine čestica za nazalnu primjenu (od 45 do 63 μm; (72)), u omjerima 1:9 i 1:19 (*m*/*m*). Adekvatnost odabranih omjera razvidna je iz mikrografija praškastih sustava mikrosfera s laktozom i manitolom u omjeru 1:9 (*m*/*m*) snimljenih pretražnom elektronskom mikroskopijom (engl. *scanning electron microscopy,* SEM). Čestice nosača nepravilnog su oblika i hrapave površine, a vidljive su i na njih adherirane mikrosfere s NDF-om koje ujednačeno prekrivaju površinu nosača. Smjesama prašaka utvrđena je homogenost s obzirom na sadržaj NDF-a, što je nužan preduvjet za osiguravanje ujednačenosti doziranja lijeka (156).

Viskoznost tekućih *in situ* gelirajućih sustava i svojstva tečenja praškastih sustava za nazalnu primjenu od ključne su važnosti u njihovom razvoju. Pseudoplastičnost polimernih otopina u kojima su suspendirani (nano)kristali FP-a te dobra svojstva tečenja smjese mikrosfera s NDF-om i inertnog nosača preduvjet su za njihovu adekvatnu primjenu u obliku spreja za nos. U slučaju *in situ* gelirajućih mikro- i nanosuspenzija FP-a, viskoznost pri mirovanju uključena je kao odgovor u dizajn eksperimenta. Kod oba tipa tekućih sustava, uočen je znatan utjecaj koncentracije polimera na viskoznost sustava pri mirovanju. Veći raspon viskoznosti u mirovanju primijećen je za *in situ* gelirajuće mikrosuspenzije FP-a (3,84 ± 0,01 mPa s do 127,16 ± 4,62 mPa s) u odnosu na nanosuspenzije (9,3 ± 0,3 mPa s do 13,4 ± 0,1 mPa s), ukazujući na gotovo eksponencijalni utjecaj koncentracije gelan gume prisutne u mikrosuspenzijama na viskoznost sustava. U slučaju mikrosuspenzije, koncentracija polisorbata 80 nije utjecala na viskoznost, dok je viskoznost nanosuspenzija, osim o koncentraciji natrijevog hijaluronata, ovisila i o koncentraciji površinski aktivne tvari. Povećanje viskoznosti *in situ* gelirajućih mikro- i nanosuspenzija FP-a usporavalo je taloženje čestica u usporedbi s odgovarajućim konvencionalnim vodenim suspenzijama FP-a. Zamijećeno je i sporije taloženje nanokristala FP-a u usporedbi s mikroniziranim, nemljevenim FP-om u odgovarajućim uzorcima. Viskoznost *in situ* gelirajućih mikro- i nanosuspenzija FP-a opadala je s porastom brzine

smicanja, što je karakteristika pseudoplastičnih sustava. Opisano smanjenje viskoznosti pridonosi učinkovitijem raspršivanju sustava pri primjeni u nosnu šupljinu, što može utjecati na depoziciju lijeka u nosnoj šupljini (110). Svojstva tečenja smjesa mikrosfera s NDF-om i laktoze ili manitola izražena su putem Hausnerovog omjera i ostatka u kapsuli iz koje se prašak pomoću uređaja za nazalnu dostavu prašaka raspršuje u nosnu šupljinu. Hausnerov omjer smjesa prašaka te samih nosača bio je u rasponu od 1,14 ± 0,0 do 1,43 ± 0,1, dok je za same mikrosfere iznosio 1,96 ± 0,18, što potvrđuje poboljšanje svojstava tečenja nakon dodatka inertnog nosača. Farmakopejska klasifikacija vrijednosti Hausnerovog omjera odnosi se na praške koji slobodno teku, primjerice pri tabletiranju ili punjenju kapsula te kao takva nije nužno primjenjiva i za praškaste sustave za primjenu u nos koji se raspršuju u nosnu šupljinu pod utjecajem vanjske sile, odnosno protoka zraka (72). Ipak, svojstva tečenja prašaka mogu utjecati na sposobnost praška da napusti uređaj za nazalnu primjenu, odnosno na ujednačenost primijenjenih doza (116). Stoga je smjesama mikrosfera s NDF-om i laktoze ili manitola određen ostatak u kapsuli, odnosno masa praška koja nije raspršena nakon aktivacije uređaja za nazalnu dostavu prašaka. Ostatak samih nosača i smjesa mikrosfera s NDF-om i laktoze ili manitola u kapsuli bio je u rasponu od 0,0 ± 0,0 % do 6,3 ± 1,7 %, a za same mikrosfere s NDF-om iznosio je 14,8 ± 2,8 % doze izvagane u kapsuli. Statističkom analizom utvrđena je pozitivna korelacija između Hausnerovog omjera i ostatka u kapsuli, što potvrđuje važnost optimiranja svojstava tečenja praškastih farmaceutskih oblika za nazalnu primjenu.

Kut raspršenja tekućih i praškastih oblika lijeka još je jedno od ključnih svojstava s utjecajem na depoziciju lijeka primijenjenog u obliku spreja u nosnu šupljinu. Kut raspršenja *in situ* gelirajućih mikro- i nanosuspenzija FP-a te smjese mikrosfera s NDP-om i nosača određen je analizom slike raspršenog oblaka dobivene nakon raspršivanja formulacija iz prikladne nazalne sprej pumpice naspram tamne pozadine (Slika 5). Za *in situ* gelirajuće mikrosuspenzije FP-a kut raspršenja iznosio je od 26,9 ± 0,2 ° do 57,4 ± 0,9 °, dok je za *in situ* gelirajuće nanosuspenzije FP-a zabilježen puno manji raspon kutova, od 17,0 ± 0,7 ° do 36,2 ± 0,5 °. Kod praškastih sustava, same mikrosfere s NDF-om, laktoza, manitol te smjese mikrosfera s NDF-om i laktoze ili manitola karakterizirani su kutom raspršenja u rasponu od 18,7 ± 0,5 ° do 26,5 ± 0,3 °. Pokazano je da manji kutovi raspršenja rezultiraju povećanom depozicijom lijeka iza nosne valvule (112). Kutovi raspršenja za sve sustave pokazuju sličan trend kao i svojstva tečenja. U slučaju prašaka, to je potvrđeno statističkom analizom kojom je utvrđena pozitivna korelacija između Hausnerovog omjera i kuta raspršenja. Kod tekućih sustava moguće je uočiti povezanost između viskoznosti i kuta raspršenja; što je viskoznost tekućeg sustava veća, kut

raspršenja je manji (110). Ipak, za *in situ* gelirajuće mikrosuspenzije FP-a karakterizirane najmanjim sadržajem pektina i odsustvom gelan gume te nižom viskoznosti pri mirovanju, a s natrijevim hijaluronatom u sastavu, uočeni su uži kut raspršenja i veća raspodjela veličina kapljica u odnosu na uzorke s većim sadržajem pektina i gelan gume, a bez natrijevog hijaluronata, što pokazuje da je, osim viskoznosti sustava, bitan parametar s utjecajem na svojstva spreja upravo i vrsta polimera u sustavu, odnosno njegovo ponašanje pod utjecajem velikih brzina smicanja prilikom raspršivanja iz sprej pumpice.

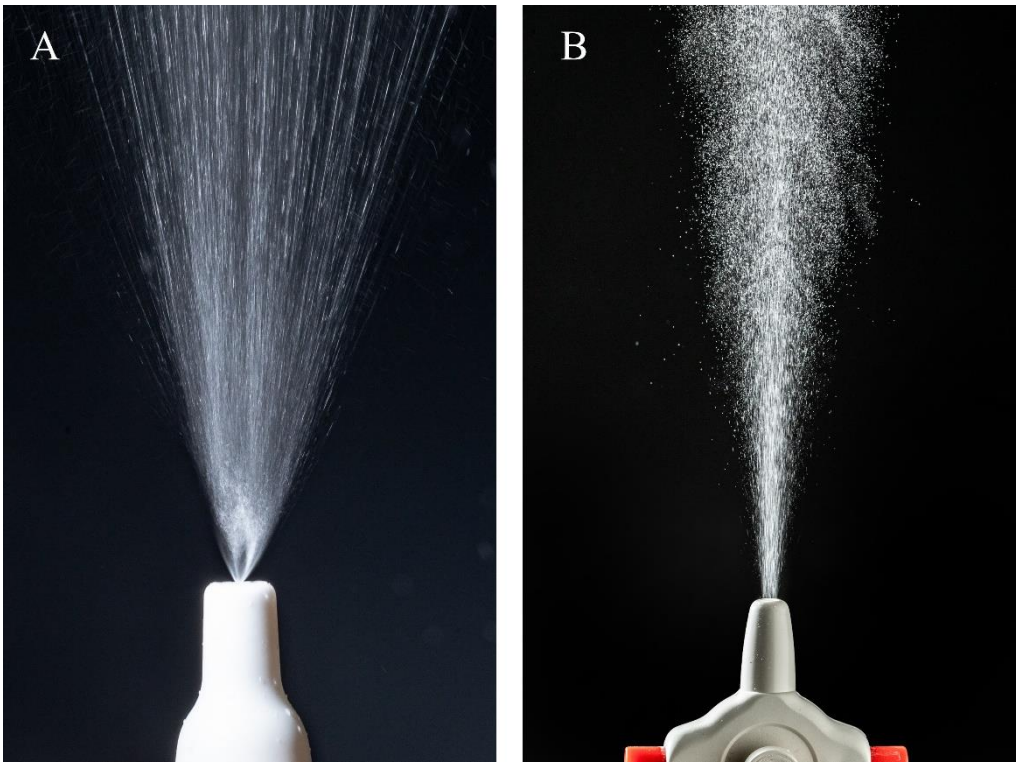

Slika 5. Prikaz raspršenih oblaka: (A) *in situ* gelirajuće mikrosuspenzije koja sadrži flutikazonpropionat (0,1 %, *m*/*m*), polisorbat 80 (0,03 %, *m*/*m*), pektin (0,5 %, *m*/*m*), gelan gumu (0,1 %, *m*/*m*) te manitol (4 %, *m*/*m*); i (B) praškastog sustava mikrosfera s natrijevim deksametazonfosfatom i manitola 1:9 (*m*/*m*).

Ispitivanje i optimiranje depozicije farmaceutskih oblika FP-a i NDF-a predstavlja jedan od ključnih segmenata njihovog razvoja. U slučaju *in situ* gelirajućih mikro- i nano suspenzija FP-a, nazalna depozicija uključena je kao odgovor u statistički dizajn eksperimenta koji je služio kao temelj za razvoj i probir formulacije. U slučaju praškastih sustava s NDF-om, ispitivanjima nazalne depozicije optimirani su parametri primjene smjese vodećih mikrosfera s NDF-om (razvijenih u okviru statističkog dizajna eksperimenta) i manitola kao odabranog nosača. Depozicija razvijanih sustava određena je u tri različita modela nosne šupljine. Tako je za

ispitivanje depozicije *in situ* gelirajućih mikrosuspenzija FP-a korišten je komercijalno dostupni, transparentni, silikonski model nosne šupljine Koken, dok su za ispitivanje depozicije *in situ* gelirajuće nanosuspenzije FP-a i praškastog sustava s NDF-om razvijeni 3D printani modeli nosne šupljine izrađeni prema CT snimkama glave pacijenta (Slika 6).

Ciljna regija za dostavu *in situ* gelirajuće mikrosuspenzije FP-a bila je cijela turbinatna regija kao mjesto razvoja upale kod kroničnog rinosinuitisa i nosnih polipa. Korišteni komercijalno dostupni silikonski model omogućavao je precizno određivanje frakcije lijeka dostavljene u navedenu regiju.

U razvoju *in situ* gelirajuće nanosuspenzije FP-a, a s ciljem vjernije simulacije uvjeta *in vivo,* korišten je 3D printani model nosne šupljine pacijenta s kroničnim rinosinuitisom. Model je sastavljen od više dijelova, uključujući donju, srednju i gornju turbinatnu regiju, što omogućuje precizno određivanje količine dostavljenog lijeka u pojedinom dijelu turbinatne regije.

Slika 6. Modeli nosne šupljine: komercijalno dostupni silikonski model Koken (lijevo), 3D printani model nosne šupljine pacijenta s kroničnim rinosinuitisom (sredina) i 3D printani model nosne šupljine zdrave osobe (desno; preuzeto i prilagođeno prema Nižić Nodilo i sur., 2021).

Uzevši u obzir najčešću zahvaćenost srednje turbinatne regije upalom te posljedični razvoj polipa uslijed neadekvatnog liječenja, *in situ* gelirajuća nanosuspenzija FP-a i parametri primjene optimirani su prema udjelu formulacije dostavljene u srednju turbinatnu regiju.

Praškasti sustav s NDF-om namijenjen je izravnoj dostavi lijeka iz nosne šupljine u mozak. Olfaktorna regija nosne šupljine predstavljala je ciljnu regiju za nazalnu dostavu razvijanog praškastog sustava, s obzirom da olfaktorni živac predstavlja glavni put izravne dostave nazalno primijenjenog lijeka u mozak (88). Izravnu dostavu nazalno primijenjenog lijeka u središnji

živčani sustav u određenoj mjeri je moguće postići i dostavljanjem lijeka u turbinatnu regiju, gdje se nalaze ogranci trigeminalnog živca (4). Međutim, zbog iznimno dobre prokrvljenosti nosne sluznice, udio lijeka koji dospije u turbinatnu regiju podložan je i sistemskoj apsorpciji (1). Ispitivanja depozicije praškastog farmaceutskog oblika također su provedena korištenjem 3D printanog modela nosne šupljine, u ovom slučaju zdrave osobe. Kako je ranije naglašeno, za *in situ* gelirajuće mikro- i nanosuspenzije FP-a, depozicija u ciljnoj regiji bila je uvrštena kao odgovor u dizajnu eksperimenta te je bila temelj za odabir vodeće formulacije. U ispitivanju depozicije *in situ* gelirajuće mikrosuspenzije FP statističkom analizom je potvrđen značajan utjecaj parametara primjene na depoziciju lijeka u turbinatnoj regiji. Smanjenje kuta primjene u odnosu na horizontalnu ravninu poboljšalo je depoziciju, kao i primjena spreja uz protok zraka, odnosno simulirani udah. Najveći utjecaj među formulacijskim parametrima imala je koncentracija natrijevog hijaluronata, što se može povezati s vrijednostima raspodjele veličina kapljica i kuta raspršenja. Depozicija lijeka u ciljnoj regiji bila je u vrlo širokom rasponu od 0,1 ± 0,05 % do 98,8 ± 0,8 %. Pri optimalnim postavkama gotovo cijela doza primijenjene formulacije dostavljena je u turbinatnu regiju. Temeljem statističke analize, a s ciljem potvrde regresijskih modela, izračunati su formulacijski parametri za šest vodećih formulacija te su predviđeni parametri primjene pod kojima se očekuje visoka turbinatna depozicija za navedene sustave. Detaljnom karakterizacijom tih šest sustava potvrđena je prediktivna vrijednost razvijenih regresijskih modela te je omogućen odabir formulacije s najvećim potencijalom.

Nakon uspješne dostave *in situ* gelirajuće mikrosuspenzije FP-a u turbinatnu regiju, cilj je bio dostaviti *in situ* gelirajuću nanosuspenziju FP-a još preciznije, odnosno u srednju turbinatnu regiju. Depozicija nanosuspenzije FP-a u cijeloj turbinatnoj regiji iznosila je od 21,5 ± 4,9 % do 84,4 ± 2,0 % te je najviše ovisila o koncentraciji natrijevog hijaluronata, slično kao kod mikrosuspenzije FP-a. Najveći utjecaj na depoziciju među parametrima primjene imao je kut u odnosu na horizontalnu ravninu, na isti način kao i kod mikrosuspenzije FP-a. Uočen je i utjecaj interakcije kutova raspršenja u odnosu na vertikalnu i horizontalnu ravninu, što se može objasniti razlikama u obliku, deformaciji i sudaranju kapljica prilikom primjene pri različitim kutovima (157). Depozicija u srednjoj turbinatnoj regiji bila je u rasponu od 0,1 ± 0,1 % do 40,3 ± 2,6 %. Parametri s utjecajem na depoziciju u srednjoj turbinatnoj regiji određeni regresijskim modelom značajno se razlikuju od onih za depoziciju u cijeloj turbinatnoj regiji. Naime, koncentracije FP-a i polisorbata 80 nisu utjecale na depoziciju u cijeloj turbinatnoj regiji, dok su imale utjecaj na depoziciju u srednjoj turbinatnoj regiji. Nadalje, kut primjene u odnosu na horizontalnu ravninu nije imao utjecaja na depoziciju u srednjoj turbinatnoj regiji.

Taj rezultat može se objasniti činjenicom da iako niži kutovi primjene u odnosu na horizontalnu ravninu rezultiraju boljom depozicijom u turbinatnoj regiji, odnosno iza nosne valvule, većina doze dostavi se u donje dijelove nosne šupljine (126), u nekim slučajevima ni ne dospijevajući do srednje turbinatne regije. Navedene razlike u parametrima koji utječu na depoziciju lijeka u cijeloj te samo srednjoj turbinatnoj regiji pojačavaju naglasak na složenost anatomije nosne šupljine te ciljane dostave lijeka u nos.

Kao što je ranije istaknuto, u slučaju praškastih sustava s NDF-om, ispitivanjima nazalne depozicije optimirani su parametri primjene smjese vodećih mikrosfera s NDF-om (razvijenih u okviru statističkog dizajna eksperimenta) i manitola kao odabranog nosača u omjeru 1:9 (*m*/*m*). Prilikom ispitivanja depozicije varirani su kut primjene u odnosu na horizontalnu ravninu te protok zraka, a s ciljem dostave što veće količine lijeka u olfaktornu regiju, najteže dostupno područje nosne šupljine. Uspoređen je profil depozicije lijeka nakon primjene u obje nosnice. Kao optimalni parametri primjene praškastog sustava s NDF-om pokazali su se kut primjene od 75 ° i primjena bez protoka zraka. Prilikom primjene praškastog lijeka u nos uz simulaciju udaha, velik dio primijenjene doze može biti udahnut i otići u nazofarinks te probavni sustav (77). Depozicija u olfaktornoj regiji bila je u rasponu od 5,1 ± 0,9 % do 17,0 ± 1,6 %, što je visoki udio u usporedbi s većinom prijavljenih rezultata depozicije u olfaktornoj regiji (127,142). Dobiveni rezultati ukazuju na potencijal razvijenog praškastog sustava za izravnu dostavu lijeka u središnji živčani sustav. Primjena lijeka u desnu polovicu nosne šupljine rezultirala je boljim profilom depozicije u usporedbi s lijevom polovicom, stavljajući još jednom naglasak na važnost razmatranja depozicije u nosnoj šupljini u ranim fazama razvoja formulacije te na potrebu za individualiziranim pristupom liječenju.

Za konačan probir ili potvrdu terapijskog potencijala vodećih formulacija FP-a i NDF-a provedena je detaljna biofarmaceutska karakterizacija *in vitro* koja je uključivala ispitivanje profila oslobađanja lijeka, mukoadhezivnosti, biokompatibilnosti razvijenih sustava i/ili permeacije uklopljenog lijeka kroz biološku barijeru *in vitro* te procjenu stabilnosti, ovisno o vrsti farmaceutskog oblika i namjeni uklopljenog kortikosteroida.

Oslobađanje lijeka *in vitro* iz *in situ* gelirajućih farmaceutskih oblika FP-a i NDF-a ispitano je pomoću Franzove difuzijske ćelije. Pri ispitivanju oslobađanja lijeka iz svih formulacija bili su uspostavljeni uvjeti osigurane topljivosti. Razvijeni farmaceutski oblici osigurali su produljeno oslobađanje djelatne tvari u usporedbi s konvencionalnim oblicima. Profili oslobađanja FP-a iz *in situ* gelirajuće mikro- i nanosuspenzije te NDF-a iz smjese mikrosfera i manitola prikazani su na Slici 7. Oslobađanje FP-a iz *in situ* gelirajuće mikro- i nanosuspenzije

bilo je značajno sporije od oslobađanja NDF-a iz polimernih mikrosfera, što se može prvenstveno pripisati razlici u topljivosti uspoređenih lijekova, a onda i razlikama u odgovarajućim farmaceutskim oblicima. Usitnjavanjem FP-a na nanometarsku veličinu postignuto je brže oslobađanje FP-a iz *in situ* gela u odnosu na mikronizirani FP zbog veće specifične površine čestica izložene otapalu (90). Nadalje, topljivost nanokristala FP-a u smjesi vode i SNF-a u omjeru 1:1 (*V*/*V*) pri 34 °C bila je 11,8 puta veća u usporedbi s mikroniziranim FP (redom 44,3 ± 3,3 mg l^{-1} i 3,8 ± 0,8 mg l^{-1}). S obzirom na vrlo malu topljivost FP-a u vodenom mediju, pretjerano usporavanje njegovog oslobađanja moglo bi narušiti terapijski učinak (75), stoga je usitnjavanje čestica prikladna metoda optimiranja formulacije. Relativno brzo oslobađanje NDF-a iz mikrosfera u prisutnosti manitola posljedica je brzog otapanja čestica manitola zbog kojega ravnomjerno raspodijeljene mikrosfere velikom površinom dolaze u kontakt s SNF-om i bubre, stvarajući strukturu slabog gela. Takav profil oslobađanja prikladan je za nazalnu dostavu NDF-a jer može osigurati visoku početnu koncentraciju lijeka na nosnoj sluznici, što potiče apsorpciju, te potpuno oslobađanje lijeka tijekom očekivanog vremena kontakta formulacije s nosnom sluznicom.

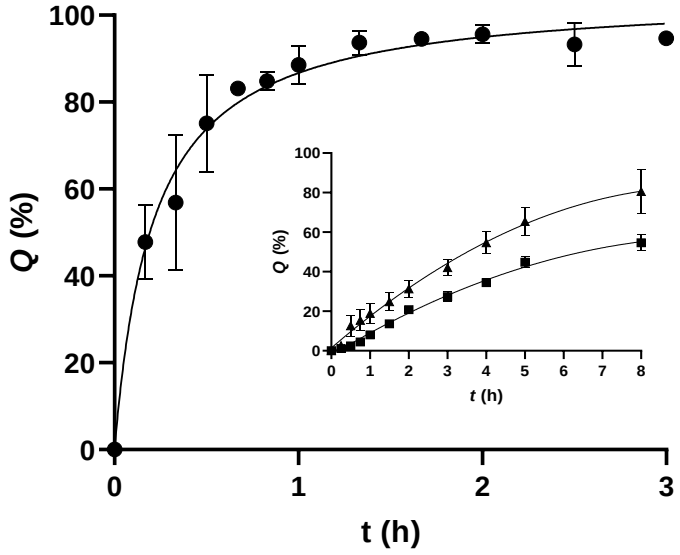

Slika 7. Profil *in vitro* oslobađanja natrijevog deksametazonfosfata iz praškastog sustava mikrosfera i manitola (1:9, *m*/*m*; krugovi). Umetak: profili *in vitro* oslobađanja flutikazonpropionata iz *in* situ gelirajuće mikrosuspenzije (kvadrati) i *in* situ gelirajuće nanosuspenzije (trokuti). *Q* predstavlja kumulativni udio oslobođenog lijeka u vremenu *t*. Prikazane su srednje vrijednosti ± standardna devijacija (n=3).

Odabranim tekućim *in situ* gelirajućim sustavima FP-a nakon miješanja s SNF-om ispitana je ovisnost modula pohrane i gubitka o kutnoj frekvenciji. Prilikom promjene frekvencije u rasponu od 0,1 do 100 rad s^{-1}, moduli pohrane i gubitka *in situ* gelova s mikro- i nanokristalima FP-a bili su gotovo paralelni (Slika 8), ukazujući na povoljna svojstva i stabilnost dobivenih *in situ* gelova te da promjena veličine čestica nije značajno utjecala na svojstva gela. *In situ* gelirajućoj nanosuspenziji FP-a i njezinoj nemljevenoj kontroli ispitana je i ekspanzija volumena gela. Volumen gela vrlo se malo razlikovao u odnosu na teorijski (3,7 ± 2,6 % i 1,9 ± 2,6 % redom za *in situ* gelirajuću nanosuspenziju i nemljevenu kontrolu), ukazujući na gotovo nepostojeći rizik od nelagode prilikom nazalne primjene zbog začepljenja nosne šupljine gelom.

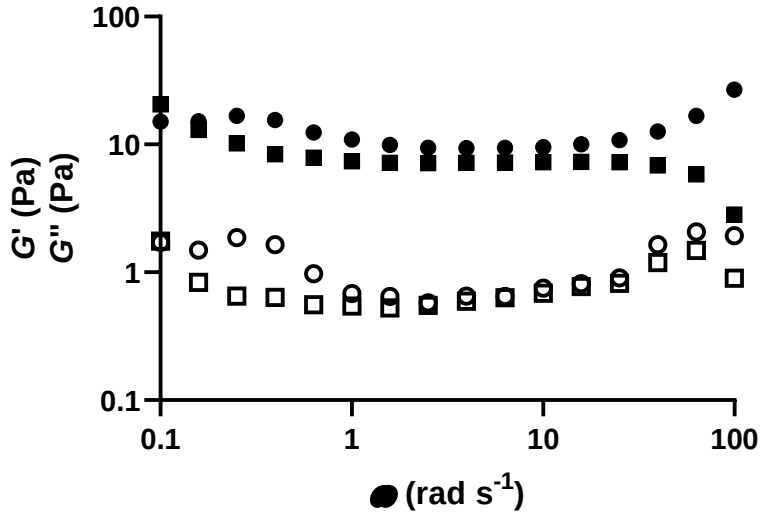

Slika 8. Ovisnost modula pohrane (puni znakovi) i gubitka (prazni znakovi) o kutnoj frekvenciji za *in situ* gelirajuću mikrosuspenziju (kvadrati) i nanosuspenziju (krugovi) flutikazonpropionata.

Mukoadhezivnost *in situ* gelirajućih sustava FP-a i NDF-a određena je *ex vivo* pomoću analizatora teksture korištenjem nazalne sluznice izolirane iz glave svinje. Izražena je preko sile odvajanja (F_A) i rada adhezije (W_{ad}). Najveća mukoadhezivnost uočena je za praškasti sustav mikrosfera s NDF-om i manitola. Mikrosfere s NDF-om ravnomjerno su adherirane na veće čestice manitola. Prilikom kontakta s SNF-om, čestice manitola brzo se otapaju te su mikrosfere velikom površinom izložene sluznici, omogućujući interakciju izbubrenih polimernih lanaca i mucina, što rezultira izraženim mukoadhezivnim svojstvima. Za *in situ* gelirajuću nanosuspenziju FP-a te njenu kontrolnu *in situ* gelirajuću mikrosuspenziju izmjereni

su značajno manji rad adhezije i sila odvajanja od sluznice u usporedbi s praškastim sustavom, no i dalje su mukoadhezivnije od konvencionalnih vodenih mikro- i nanosuspenzija FP-a. Opisani rezultati pokazuju potencijal duljeg zadržavanja farmaceutskih oblika pripravljenih iz *in situ* gelirajućih i mukoadhezivnih polimera na nosnoj sluznici. Mehanizmi mukoadhezije obuhvaćaju stvaranje vodikovih veza između polimera i glikoproteina iz sluzi (68) te zaplitanje polimernih lanaca s mucinom (158). Bolja mukoadhezivna svojstva *in situ* gelirajuće nanosuspenzije FP-a naspram *in situ* gelirajuće mikrosuspenzije FP-a mogu se objasniti boljom interakcijom lanaca mucina sa suspendiranim nanokristalima FP-a u usporedbi u usporedbi sa suspendiranim mikrokristalima FP zbog veće specifične površine (90).

Biokompatibilnost *in situ* gelirajućih sustava FP-a i NDF-a potvrđena je *in vitro* ispitivanjima na Calu-3 staničnom monosloju. Prije nanošenja na stanice, tekući *in situ* gelirajući sustavi FP-a pomiješani su s Hankovom uravnoteženom otopinom soli (engl. *Hank's balanced salt solution,* HBSS) s dodatkom iona kalcija pri biorelevantnoj koncentraciji istoj kao i u nosnom fluidu (HBSS-Ca^{2+}) u volumnom omjeru 1:1, a za postizanje trenutnog geliranja. Praškasti sustav NDF-a dispergiran je prvo u pročišćenoj vodi, nakon čega je ta disperzija također pomiješana s HBSS-Ca^{2+} (1:1, *V*/*V*) prije nanošenja na stanični monosloj. Provedeno je ispitivanje s 3-(4,5-dimetiltiazol-2-il)-2,5-difeniltetrazolin bromidom (MTT reagensom) koji se u metabolički aktivnim stanicama reducira u netopljive ljubičaste kristale formazana. Kao negativna kontrola služile su stanice inkubirane u samom HBSS-Ca^{2+}. Vijabilnost stanica izražena je kao postotni omjer apsorbancija otopina formazana iz tretiranih stanica i stanica inkubiranih u HBSS-Ca^{2+}. Ni za jedan od ispitanih *in situ* gelirajućih sustava nije uočen citotoksični učinak, odnosno vijabilnost stanica za sve ispitane formulacije bila je veća od 80 % u odnosu na kontrolu (159). U slučaju *in situ* gelirajućih suspenzija FP-a, sustavi su bili biokompatibilni neovisno o veličini kristala FP-a u suspenziji. Time je potvrđen potencijal razvijenih tekućih i praškastih sustava za primjenu na nosnu sluznicu.

Za razliku od *in situ* gelirajućih sustava s FP-om koji su namijenjeni lokalnom djelovanju, cilj razvoja praškastog sustava s NDF-om je izravna dostava lijeka u središnji živčani sustav. Iz tog razloga provedeno je *in vitro* ispitivanje permeabilnosti NDF-a kroz Calu-3 stanični monosloj iz praškastog sustava mikrosfera i manitola u masenom omjeru 1:19. Navedeni omjer mikrosfera s NDF-om i manitola odabran je za ispitivanje permeabilnosti radi osiguravanja hipertoničnih uvjeta (koji se očekuju pri nazalnoj primjeni praškastog sustava NDF-a *in vivo*) te uvjeta osigurane topljivosti uzevši u obzir volumen medija u receptorskom odjeljku. Permeabilnost lijeka izražena je pomoću prividnog koeficijenta permeabilnosti, P_{app}. Uočena je

ovisnost permeabilnosti NDF-a o osmotskim uvjetima: vrijednosti P_{app} bile su slične pri izoosmotskim i blago hiperosmotskim uvjetima, dok su hipoosmotski uvjeti uzrokovali porast prijenosa NDF-a preko modela epitelne barijere, odnosno porast vrijednosti P_{app}. Razlog tome je preferirani paracelularni transport polarnog NDF-a koji se povećava zbog pada transepitelnog električnog otpora uslijed hipoosmotskih uvjeta (75,160). Uklapanje NDF-a u mikrosfere rezultiralo je povećanjem vrijednosti P_{app}, što je vidljivo iz usporedbe vrijednost P_{app} za fizičku smjesu manitola i NDF-a te za praškasti sustav mikrosfera s NDF-om i manitola koje su iznosile redom $(0{,}39 \pm 0{,}01) \times 10^{-6}$ cm s^{-1} i $(0{,}65 \pm 0{,}12) \times 10^{-6}$ cm s^{-1}. Zamijećeni učinak poboljšanja permeacije statistički je značajan ($p < 0{,}05$) te uz produljeno oslobađanje lijeka iz izbubrenih mikrosfera i svojstvo mukoadhezivnosti ukazuje na potencijal praškastog sustava mikrosfera s NDF-om i manitola za povećanje permeacije NDF-a putem olfaktornog epitela *in vivo.*

Stabilnost *in situ* gelirajućih sustava FP-a i NDF-a ispitana je praćenjem ključnih svojstava za pojedini oblik lijeka tijekom prikladnog vremenskog perioda. Rezultati su sumirani u Tablici 3. U naznačenom vremenskom periodu, sve formulacije zadržale su svojstva ista kao i neposredno nakon priprave, čime je potvrđen njihov potencijal u nazalnoj primjeni kortikosteroida. Ostvareni rezultati predstavljaju čvrst temelj za daljnja ispitivanja *in vivo.*

Tablica 3. Stabilnost praškastog i tekućih *in situ* gelirajućih sustava

	Promatrano svojstvo	Vremenski period	Uvjeti skladištenja	Vrijednosti redom nakon pripreme i na kraju ispitivanja stabilnosti
ISG-M-FP	Mogućnost resuspendiranja	6 mjeseci	4 °C, nepropusni spremnik	nepromijenjena
	Veličina čestica (μm)			2,03 ± 0,05 – 2,28 ± 0,1 μm (nepromijenjena)
ISG-N-FP	Mogućnost resuspendiranja	8 tjedana	4 °C, nepropusni spremnik	nepromijenjena
	Sadržaj lijeka (%)			97,4 ± 0,8 98,2 ± 1,1
	Veličina čestica (nm)			156,0 ± 2,7 148,0 ± 4,1
	PDI			0,295 ± 0,013 0,275 ± 0,003
	Zeta potencijal (mV)			−81,3 ± 1,4 −84,2 ± 1,3
	Stabilnost *in situ* gela nakon miješanja s SNF-om			*G*' i *G*" ostali su nepromijenjeni
MS-NDF	Sadržaj lijeka (%)	12 mjeseci	4 °C, nepropusni spremnik	33,5 ± 0,4 31,9 ± 0,8
	D_v10; D_v50; D_v90 (μm)			1,1; 3,2; 7,6 1,5; 2,9; 8,2
	Zeta potencijal (mV)			−23,1 ± 1,4 −22,0 ± 2,2
MS-NDF/ manitol 1:9	Sadržaj lijeka (%)			100,2 95,8
	RSD (%)			4,6 3,4

ISG-M-FP – *in situ* gelirajuće mikrosuspenzije flutikazonpropionata; ISG-N-FP – *in situ* gelirajuće nanosuspenzije flutikazonpropionata; *G*' – modul pohrane; *G*" – modul gubitka; MS-NDF – mikrosfere s natrijevim deksametazonfosfatom; RSD – relativna standardna devijacija.
Gornja vrijednost u posljednjem stupcu predstavlja vrijednost izmjerenu neposredno nakon priprave sustava, dok donja predstavlja vrijednost izmjerenu na kraju ispitivanja stabilnosti.

6. ZAKLJUČAK

U sklopu ovog doktorskog rada, primjenom QbD načela uspješno su razvijeni: (i) *in situ* gelirajuća mikrosuspenzija FP-a, (ii) *in situ* gelirajuća nanosuspenzija FP-a te (iii) praškasti sustav mikrosfera s NDF-om sušenih raspršivanjem i inertnog nosača. *In situ* gelirajuće mikrosuspenzije FP-a pripravljene su korištenjem komercijalno dostupnog mikroniziranog FP-a, a *in situ* gelirajuće nanosuspenzije korištenjem nanokristala FP-a pripravljenih vlažnim mljevenjem. Veličina i polidisperznost pripravljenih nanokristala potvrđuju prikladnost vlažnog mljevenja za nanonizaciju FP-a. Zeta potencijal *in situ* gelirajućih nanosuspenzija FP-a (< −60 mV), osigurao je fizičku stabilnost pripravljenih sustava. Površinska napetost *in situ* gelirajućih nanosuspenzija bila je unutar raspona vrijednosti prikladnih za nazalni sprej. Odabir i koncentracija polimera u *in situ* gelirajućim mikro- i nanosuspenzijama FP-a osigurali su odgovarajuću viskoznost, stabilizaciju suspenzije, pseudoplastično ponašanje, prikladnost za primjenu raspršivanjem i geliranje nakon miješanja sa SNF-om u biorelevantnom volumnom omjeru. Optimiranje procesa sušenja raspršivanjem rezultiralo je velikim prinosom te pripravom mikrosfera visoke uspješnosti uklapanja lijeka, relativno niskog sadržaja ostatne vlage, male veličine čestica te prikladnih svojstava bubrenja (geliranja) u SNF-u. *In situ* gelirajuće mikro- i nanosuspenzije FP-a, kao i mikrosfere s NDF-om stvarale su gel odmah nakon kontakta s SNF-om. Sve dizajnom predviđene formulacije FP-a udovoljavaju kriteriju vezanom uz veličinu raspršenih kapljica pri nazalnoj primjeni u obliku spreja. Raspodjela veličina mikrosfera s NDF-om ukazuje na veliki udio čestica promjera manjeg od 10 μm, što ih čini prikladnima za miješanje s inertnim nosačem odgovarajuće veličine čestica za nazalnu primjenu. Pripravljene su homogene smjese mikrosfera s NDF-om i nosača laktoze ili manitola (veličina čestica 45 – 63 μm) u masenim omjerima 1:9 i 1:19. Adhezija mikrosfera na čestice nosača rezultirala je odgovarajućom veličinom čestica, boljim svojstvima tečenja i užim kutom raspršenja u usporedbi sa samim mikrosferama.

Viskoznost *in situ* gelirajućih mikro- i nanosuspenzija FP-a bila je prikladna za nazalnu primjenu, a rasla je s porastom koncentracije polimera. Kut raspršenja tekućih *in situ* gelirajućih sustava također je ovisio o polimernom sastavu; na njega je najviše utjecala koncentracija natrijevog hijaluronata s čijim porastom se kut raspršenja smanjivao. U slučaju praškastih sustava, kut raspršenja ovisio je o prisustvu nosača u smjesi. Pokazana je pozitivna korelacija između Hausnerovog omjera i kuta raspršenja.

Sveobuhvatni pristup ispitivanju nazalne depozicije uzimajući u obzir formulacijske, procesne i parametre primjene rezultirao je uspješnom dostavom *in situ* gelirajuće mikrosuspenzije FP-a, *in situ* gelirajuće nanosuspenzije FP-a te praškastog sustava mikrosfera

s NDF-om i manitola (1:9, *m*/*m*) redom u cijelo turbinatno područje (> 90 % primijenjene doze), srednje turbinatno područje (51,8 % primijenjene doze) i olfaktorno područje (17,0 % primijenjene doze) modela nosne šupljine. Primjena praškastog sustava mikrosfera s NDF-om i manitola u lijevu i desnu nosnicu, rezultirala je različitim profilima depozicije zbog različite površine lijeve i desne nosne valvule, naglašavajući važnost razmatranja depozicije u nosnoj šupljini u ranim fazama razvoja formulacije te potrebu i potencijal za individualizirani pristup liječenju.

Produljeno oslobađanje FP-a i NDF-a *in vitro* iz razvijenih *in situ* gelirajućih sustava odgovaralo je nazalnoj primjeni. Nanonizacija u vodi netopljivog FP-a rezultirala je povećanjem topljivosti FP-a te bržim oslobađanjem lijeka iz *in situ* gelirajuće nanosuspenzije u usporedbi s *in situ* gelirajućom mikrosuspenzijom FP-a. *In situ* gelovi bili su reološki stabilni pri širokom rasponu kutnih frekvencija te su iskazivali vrlo malu ekspanziju volumena, pokazujući da usitnjavanje FP-a nije narušilo svojstva gela.

Sve razvijene formulacije iskazivale su mukoadhezivna svojstva koja su rasla u sljedećem nizu: *in situ* gelirajuća mikrosuspenzija FP-a < *in situ* gelirajuća nanosuspenzija FP-a < smjesa mikrosfera s NDF-om i manitola. *In situ* gelirajuća nanosuspenzija FP-a pokazala je poboljšana mukoadhezivna svojstva u usporedbi sa odgovarajućom nemljevenom kontrolom, potvrđujući prednost nanonizacije FP-a.

Biokompatibilnost razvijenih *in situ* gelirajućih formulacija FP-a i NDF-a potvrđena je *in vitro* ispitivanjima na Calu-3 stanicama. Permeacija NDF-a ovisila je o osmotskim uvjetima; vrijednosti P_{app} bile su slične pri izoosmotskim i blago hiperosmotskim uvjetima, dok je u hipoosmotskim uvjetima vrijednost P_{app} rasla, pokazujući povećani potencijal za izravnu dostavu lijeka u središnji živčani sustav.

Tekući i praškasti *in situ* gelirajući sustavi karakterizirani su odgovarajućim profilom stabilnosti, čime je potvrđen njihov potencijal za nazalnu primjenu kortikosteroida.

Sveobuhvatni pristup s implementiranim QbD načelima primijenjen u okviru ovog rada rezultirao je razvojem funkcionalnih *in situ* gelirajućih farmaceutskih oblika kortikosteroida za nazalnu primjenu s potencijalom produljenog zadržavanja na mjestu primjene, optimirane depozicije u nosnoj šupljini i povoljnih biofarmaceutskih svojstava.

7. LITERATURA

1. Lobaina Mato Y. Nasal route for vaccine and drug delivery: Features and current opportunities. Int J Pharm 2019; 118813.

2. Khan AR, Liu M, Khan MW, Zhai G. Progress in brain targeting drug delivery system by nasal route. J Con Rel 2017. 364–389.

3. Paulsen J, Wachke F, editors. Sobotta Atlas of Human Anatomy: Head, Neck and Neuroanatomy. 15th Ed. Munich: Urban & Fischer, Elsevier GmbH 2010.

4. Djupesland PG, Messina JC, Mahmoud RA. The nasal approach to delivering treatment for brain diseases: An anatomic, physiologic, and delivery technology overview. Ther Deliv 2014;5(6): 709–733.

5. Jalšovec D. Sustavna i topografska anatomija čovjeka. Prvo izdan. Zagreb: Školska knjiga d. d., 2005.

6. Guyton AC, Hall JE. Textbook of Medical Physiology. 12th Ed. Philadelphia: Saunders Elsevier Ltd.; 2011.

7. Djupesland PG, Messina JC, Palmer JN. Deposition of drugs in the nose and sinuses with an exhalation delivery system vs conventional nasal spray or high-volume irrigation in draf II/III post-surgical anatomy. Rhinology 2020;58(2): 175–183.

8. Gray H, Carter HV. Gray's Anatomy: The Anatomical Basis of Clinical Practice. 42nd Ed. Amsterdam: Elsevier 2020.

9. Cappello ZJ, Dublin AB. Anatomy, Head and Neck, Nose Paranasal Sinuses. StatPearls 2019; 1–9.

10. Scherzad A, Hagen R, Hackenberg S. Current understanding of nasal epithelial cell mis-differentiation. J Inflamm Res 2019;12: 309–317.

11. Hamlett KEL, Yaneza MMC, Grimmond N. Epistaxis. Surg (United Kingdom) 2021;39(9): 577–590.

12. Li C, Jiang J, Dong H, Zhao K. Computational modelling and validation of human nasal airflow under various breathing conditions. J Biomech 2017;64: 59–68.

13. Berillo D, Zharkinbekov Z, Kim Y, Raziyeva K, Temirkhanova K, Saparov A. Stimuli-responsive polymers for transdermal, transmucosal and ocular drug delivery. Pharmaceutics 2021;13(12): 1–30.

14. Leal J, Smyth HDC, Ghosh D. Physicochemical properties of mucus and their impact on transmucosal drug delivery. Int J Pharm 2017;532(1): 555–572.

15. Scherließ R. Nasal formulations for drug administration and characterization of nasal preparations in drug delivery. Ther Deliv 2020;11(3): 183–191.

16. Male D, Peebles S, Male V. Immunology. 9th Ed. Philadelphia: Elsevier Ltd.; 2020.

17. Maigler F, Ladel S, Flamm J, Gänger S, Kurpiers B, Kiderlen S, et al. Selective CNS targeting and distribution with a refined region-specific intranasal delivery technique via the olfactory mucosa. Pharmaceutics 2021;13(11):1–22.

18. Gänger S, Schindowski K. Tailoring formulations for intranasal nose-to-brain delivery: A review on architecture, physico-chemical characteristics and mucociliary clearance of the nasal olfactory mucosa. Pharmaceutics 2018;10(3).

19. Djupesland PG. Nasal drug delivery devices: characteristics and performance in a clinical perspective — a review. Drug Deliv and Transl Res 2013;42–62.

20. Wu EL, Harris WC, Babcock CM, Alexander BH, Riley CA, McCoul ED. Epistaxis Risk Associated with Intranasal Corticosteroid Sprays: A Systematic Review and Meta-analysis. Otolaryngol - Head Neck Surg (United States). 2019;161(1): 18–27.

21. Ganesh V, Banigo A, McMurran AEL, Shakeel M, Ram B. Does intranasal steroid spray technique affect side effects and compliance? Results of a patient survey. J Laryngol Otol 2017;131(11): 991–996.

22. Viehweg TL, Roberson JB, Hudson JW. Epistaxis: Diagnosis and treatment. J Oral Maxillofac Surg. 2006;64(3): 511–518.

23. Butina BG, Poje G, Baudoin T, Kalogjera L, Matić IP, Damjanović D. Guidelines for epistaxis. Medica Jadertina 2020;50(3): 185–187.

24. Meng Y, Wang C, Zhang L. Recent developments and highlights in allergic rhinitis. Allergy: Eur J Allergy Clin Immunol 2019;74(12): 2320–2328.

25. Hellings PW, Klimek L, Cingi C, Agache I, Akdis C, Bachert C, et al. Non-allergic rhinitis: Position paper of the European Academy of Allergy and Clinical Immunology. Allergy: Eur J Allergy Clin Immunol 2017;72(11): 1657–1665.

26. Meng Y, Wang C, Zhang L. Diagnosis and treatment of non-allergic rhinitis: focus on immunologic mechanisms. Expert Rev Clin Immunol Taylor & Francis; 2021.

27. Daley-Yates PT, Larenas-Linnemann D, Bhargave C, Verma M. Intranasal corticosteroids: Topical potency, systemic activity and therapeutic index. J Asthma Allergy 2021;14: 1093–1104.

28. Meltzer EO. The Role of Nasal Corticosteroids in the Treatment of Rhinitis. Immunol Allergy Clin North Am 2011;31(3): 545–560.

29. Fokkens WJ, Lund VJ, Hopkins C, Hellings PW, Kern R, Reitsma S, et al. EPOS 2020. Official Journal of the European and International Rhinologic Societies and of the Confederation of European ORL-HNS 2020;Suppl 29: 1–464.

30. Koennecke M, Klimek L, Mullol J, Gevaert P, Wollenberg B. Subtyping of polyposis nasi: phenotypes, endotypes and comorbidities. Allergo J Int 2018;27(2): 56–65.

31. Chiarella E, Lombardo N, Lobello N, Aloisio A, Aragona T, Pelaia C, et al. Nasal polyposis: Insights in epithelial-mesenchymal transition and differentiation of polyp mesenchymal stem cells. Int J Mol Sci 2020;21(18): 1–16.

32. Papadakis CE, Chimona TS, Chaidas K, Ladias A, Zisoglou M, Proimos EK. Effect of oral steroids on olfactory function in chronic rhinosinusitis with nasal polyps. Eur Ann Otorhinolaryngol Head Neck Dis 2021;138(5): 343–348.

33. Mathis S, le Masson G, Soulages A, Duval F, Carla L, Vallat JM, et al. Olfaction and anosmia: From ancient times to COVID-19. J Neurol Sci 2021;425.

34. Rashid RA, Zgair A, Al-Ani RM. Effect of nasal corticosteroid in the treatment of anosmia due to COVID-19: A randomised double-blind placebo-controlled study. Am J Otolaryngol - Head Neck Med Surg 2021;42(5): 103033.

35. Cho SH, Kim DW, Gevaert P. Chronic Rhinosinusitis without Nasal Polyps. J Allergy Clin Immunol Pract 2016;4(4): 575–582.

36. Leopold DA, Elkayam D, Messina JC, Kosik-Gonzalez C, Djupesland PG, Mahmoud RA. NAVIGATE II: Randomized, double-blind trial of the exhalation delivery system with fluticasone for nasal polyposis. J Allergy Clin Immunol 2019;143(1): 126-134.e5.

37. Messina JC, Offman E, Carothers JL, Mahmoud RA. A Randomized Comparison of the Pharmacokinetics and Bioavailability of Fluticasone Propionate Delivered via Xhance® Exhalation Delivery System Versus Flonase® Nasal Spray and Flovent® HFA Inhalational Aerosol. Clin Ther 2019;41(11): 2343–2356.

38. Stevens WW, Schleimer RP, Kern RC. Chronic Rhinosinusitis with Nasal Polyps. . J Allergy Clin Immunol Pract 2016;4(4): 565–572.

39. Fokkens W, Reitsma S. New delivery forms of nasal corticosteroids. J Allergy Clin Immunol 2019;144(1):351

40. Pilicheva B, Boyuklieva R. Can the nasal cavity help tackle COVID-19? Pharmaceutics 2021;13(10): 1–25.

41. Higgins TS, Wu AW, Illing EA, Sokoloski KJ, Weaver BA, Anthony BP, et al. Intranasal Antiviral Drug Delivery and Coronavirus Disease 2019 (COVID-19): A State of the Art Review. Otolaryngol - Head Neck Surg (United States) 2020;163(4): 682–694.

42. Basu S, Holbrook LT, Kudlaty K, Fasanmade O, Wu J, Burke A, et al. Numerical evaluation of spray position for improved nasal drug delivery Sci Rep. 2020;10(1): 1–18.

43. Cooper GM, Hausman RE. Stanica: molekularni pristup. Peto izd. Zagreb:Medicinska naklada; 2010.

44. Katzung BG, Trevor AJ. Basic and Clinical Pharmacology. 13th ed. New York:McGraw-Hill Education; 2015.

45. Cárdenas G, Torres-García D, Cervantes-Torres J, Rosales-Mendoza S, Fleury A, Fragoso G, et al. Role of Systemic and Nasal Glucocorticoid Treatment in the Regulation of the Inflammatory Response in Patients with SARS-Cov-2 Infection. Arch Med Res 2020;52(2):143-150

46. www.ema.europa.eu. *European Medicines Agency*. https://www.edqm.eu/sites/default/files/medias/fichiers/Consumer_Health_Protection/pharmaceutical_care_evidence-based_reviews_atc_group_r01.pdf (pristupljeno 17. 2. 2022.)

47. www.ema.europa.eu. *List of nationally authorised medicinal products: dexamethasone*. https://www.ema.europa.eu/en/documents/psusa/dexamethasone-apart-centrally-authorised-products-list-nationally-authorised-medicinal-products/00000973/201601_en.pdf (pristupljeno 16. 2. 2022.)

48. www.ema.europa.eu. *Budesonide: List of nationally authorised medicinal products*. https://www.ema.europa.eu/en/documents/psusa/budesonide-list-nationally-authorised-medicinal-products-psusa/00000449/201604_en.pdf (pristupljeno 16. 2. 2022.)

49. www.halmed.hr. *Sažetak opisa svojstava lijeka "Dymista."* https://www.halmed.hr/Lijekovi/Baza-lijekova/Dymista-137-mikrograma-50-mikrograma-po-potisku-sprej-za-nos-suspenzija/15327/ (pristupljeno 16. 2. 2022.)

50. www.halmed.hr. *Sažetak opisa svojstava lijeka "Synaze."* https://www.halmed.hr/Lijekovi/Baza-lijekova/Synaze-137-mikrograma-50-mikrograma-po-potisku-sprej-za-nos-suspenzija/15360/ (pristupljeno 16. 2. 2022.)

51. www.halmed.hr. *Sažetak opisa svojstava lijeka "Rinoco."* https://www.halmed.hr/Lijekovi/Baza-lijekova/Rinoco-50-mikrograma-po-potisku-sprej-za-nos-suspenzija/10540/ (pristupljeno 16. 2. 2022.)

52. www.halmed.hr. *Sažetak opisa svojstava lijeka "Flixonase sprej za nos, suspenzija."* https://www.halmed.hr/Lijekovi/Baza-lijekova/Flixonase-sprej-za-nos-suspenzija/10899/ (pristupljeno 16. 2. 2022.)

53. www.halmed.hr. *Sažetak opisa svojstava lijeka "Flixonase kapi za nos, suspenzija."* https://www.halmed.hr/Lijekovi/Baza-lijekova/Flixonase-400-mikrograma-kapi-za-nos-suspenzija/13642/ (pristupljeno 16. 2. 2022.)

54. www.halmed.hr. *Sažetak opisa svojstava lijeka "Deksametazon Krka 4 mg/ml otopina za injekciju/infuziju."* https://www.halmed.hr/Lijekovi/Baza-lijekova/Deksametazon-Krka-4-mg-ml-otopina-za-injekciju-infuziju/10298/ (pristupljeno 16. 2. 2022.)

55. www.halmed.hr. *Sažetak opisa svojstava lijeka "Dexagel 0,985 mg/g gel za oko."* https://www.halmed.hr/Lijekovi/Baza-lijekova/Dexagel-0985-mg-g-gel-za-oko/12498/ - (pristupljeno 16. 2. 2022.)

56. *Agencija za lijekove i medicinske proizvode*. www.halmed.hr (pristupljeno 16. 2. 2022.)

57. www.pmda.go.jp. *Products Approved in FY 2009: New Drugs - Erizas*. https://www.pmda.go.jp/files/000153452.pdf (pristupljeno 16. 2. 2022.)

58. Martino BJ, Church CA, Seiberling KA. Effect of intranasal dexamethasone on endogenous cortisol level and intraocular pressure. Int Forum Allergy Rhinol 2015;5(7): 605–609.

59. Manniello MD, Hosseini S, Alfaifi A, Esmaeili AR, Kolanjiyil A v., Walenga R, et al. In vitro evaluation of regional nasal drug delivery using multiple anatomical nasal replicas of adult human subjects and two nasal sprays. Int J Pharm 2021;593:120103.

60. Warnken ZN, Smyth HDC, Davis DA, Weitman S, Kuhn JG, Williams RO. Personalized Medicine in Nasal Delivery: The Use of Patient-Specific Administration

Parameters to Improve Nasal Drug Targeting Using 3D-Printed Nasal Replica Casts. Mol Pharm 2018;15(4): 1392–1402.

61. Maaz A, Blagbrough IS, de Bank PA. In vitro evaluation of nasal aerosol depositions: An insight for direct nose to brain drug delivery. Pharmaceutics 2021;13(7).

62. Sahin-Yilmaz A, Naclerio RM. Anatomy and physiology of the upper airway. Proc Am Thorac Soc 2011;8: 31–39.

63. Karavasili C, Fatouros DG. Smart materials: In situ gel-forming systems for nasal delivery. Drug Discov Today 2016;21(1): 157–166.

64. Altuntaş E, Yener G. Formulation and Evaluation of Thermoreversible In Situ Nasal Gels Containing Mometasone Furoate for Allergic Rhinitis. AAPS PharmSciTech 2017;18(7): 2673–2682.

65. Cantone E, Iengo M. Effect of sodium hyaluronate added to topical corticosteroids in chronic rhinosinusitis with nasal polyposis. Am J Rhinol Allergy 2016;30(5): 340–343.

66. Mahdi MH, Conway BR, Smith AM. Development of mucoadhesive sprayable gellan gum fluid gels. Int J Pharm 2015;488(1–2): 12–19.

67. Vigani B, Rossi S, Sandri G, Bonferoni MC, Caramella CM, Ferrari F. Recent advances in the development of in situ gelling drug delivery systems for non-parenteral administration routes. Pharmaceutics 2020;12(9): 1–29.

68. Zahir-Jouzdani F, Wolf JD, Atyabi F, Bernkop-Schnürch A. In situ gelling and mucoadhesive polymers: why do they need each other? Expert Opin Drug Deliv 2018;15(10): 1007–1019.

69. Tomić I, Juretić M, Jug M, Pepić I, Cetina Čižmek B, Filipović-Grčić J. Preparation of in situ hydrogels loaded with azelaic acid nanocrystals and their dermal application performance study. Int J Pharm 2019;563:249–258.

70. Gupta S, Vyas SP. Carbopol/chitosan based pH triggered in situ gelling system for ocular delivery of timolol maleate. Sci Pharm 2010;78(4): 959–976.

71. www.ema.europa.eu. *Sažetak opisa svojstava lijeka "PecFent."* https://www.ema.europa.eu/en/documents/product-information/pecfent-epar-product-information_hr (pristupljeno 16. 2. 2022.)

72. Tiozzo Fasiolo L, Manniello MD, Tratta E, Buttini F, Rossi A, Sonvico F, et al. Opportunity and challenges of nasal powders: Drug formulation and delivery. Eur J Pharm Sci 2018;113(May 2017): 2–17.

73. Pozzoli M, Rogueda P, Zhu B, Smith T, Young PM, Traini D, et al. Dry powder nasal drug delivery: challenges, opportunities and a study of the commercial Teijin Puvlizer Rhinocort device and formulation. Drug Dev Ind Pharm 2016;42(10): 1660–1668.

74. Salade L, Wauthoz N, Vermeersch M, Amighi K, Goole J. Chitosan-coated liposome dry-powder formulations loaded with ghrelin for nose-to-brain delivery. Eur J Pharm Biopharm 2018;129: 257–266.

75. Jurišić Dukovski B, Mrak L, Winnicka K, Szekalska M, Juretić M, Filipović-Grčić J, et al. Spray-dried nanoparticle-loaded pectin microspheres for dexamethasone nasal delivery. Dry Technol 2019;0(0): 1–11.

76. Nižić L, Potaś J, Winnicka K, Szekalska M, Erak I, Gretić M, et al. Development, characterisation and nasal deposition of melatonin-loaded pectin/hypromellose microspheres. Eur J Pharm Sci 2020;141:105-115.

77. Trows S, Scherließ R. Carrier-based dry powder formulation for nasal delivery of vaccines utilizing BSA as model drug. Powder Technol 2016;292: 223–231.

78. Ziaee A, Albadarin AB, Padrela L, Femmer T, O'Reilly E, Walker G. Spray drying of pharmaceuticals and biopharmaceuticals: Critical parameters and experimental process optimization approaches. Eur J Pharm Sci 2019;127: 300–318.

79. De Souza Lima R, Ré MI, Arlabosse P. Drying droplet as a template for solid formation: A review. Powder Technol 2020;359: 161–171.

80. Li X, Anton N, Arpagaus C, Belleteix F, Vandamme TF. Nanoparticles by spray drying using innovative new technology: The Büchi Nano Spray Dryer B-90. J Control Rel 2010;147(2): 304–310.

81. Sosnik A, Seremeta KP. Advantages and challenges of the spray-drying technology for the production of pure drug particles and drug-loaded polymeric carriers. Adv Colloid Interface Sci 2015;223: 40–54.

82. Fissore D. Drying technologies for biotechnology and pharmaceutical applications. Dry Technol 2020.

83. Focaroli S, Mah PT, Hastedt JE, Gitlin I, Oscarson S, Fahy J v., et al. A Design of Experiment (DoE) approach to optimise spray drying process conditions for the production of trehalose/leucine formulations with application in pulmonary delivery. Int J Pharm 2019;562: 228–240.

84. Gallo L, Verónica Ramírez-Rigo M, Bucalá V. Development of porous spray-dried inhalable particles using an organic solvent-free technique. Powder Technol 2019;342: 642–652.

85. Duvnjak Romić M, Šegvić Klarić M, Lovrić J, Pepić I, Cetina-Čižmek B, Filipović-Grčić J, et al. Melatonin-loaded chitosan/Pluronic® F127 microspheres as in situ forming hydrogel: An innovative antimicrobial wound dressing. Eur J Pharm Biopharm 2016;107: 67–79.

86. Merisko-Liversidge E, Liversidge GG. Nanosizing for oral and parenteral drug delivery: A perspective on formulating poorly-water soluble compounds using wet media milling technology. Adv Drug Deliv Rev 2011;63(6): 427–440.

87. Noyes AA, Whitney WR. The rate of solution of solid substances in their own solutions. J Am Chem Soc 1897;19: 930–934.

88. Akel H, Ismail R, Katona G, Sabir F, Ambrus R, Csóka I. A comparison study of lipid and polymeric nanoparticles in the nasal delivery of meloxicam: Formulation, characterization, and in vitro evaluation. Int J Pharm 2021;604.

89. Aref ZF, Bazeed SEES, Hassan MH, Hassan AS, Rashad A, Hassan RG, et al. Clinical, biochemical and molecular evaluations of ivermectin mucoadhesive nanosuspension nasal spray in reducing upper respiratory symptoms of mild covid-19. Int J Nanomedicine 2021;16:4063–4072.

90. Alshweiat A, Csóka IiI, Tömösi F, Janáky T, Kovács A, Gáspár R, et al. Nasal delivery of nanosuspension-based mucoadhesive formulation with improved bioavailability of loratadine: Preparation, characterization, and in vivo evaluation. Int J Pharm 2020;579:119166.

91. Peltonen L. Design space and QbD approach for production of drug nanocrystals by wet media milling techniques. Pharmaceutics 2018;10(3).

92. Lovrić J, Hafner A, Radiković M, Juretić M, Dürrigl M, Perina Lakoš G, et al. Nanokristali djelatne tvari : fizičko-kemijska , farmaceutsko-tehnološka, biofarmaceutska i terapijska svojstva. Farm glas 2015;71: 355–384.

93. Li M, Azad M, Davé R, Bilgili E. Nanomilling of drugs for bioavailability enhancement: A holistic formulation-process perspective. Pharmaceutics 2016;8(2).

94. European Medicines Agency. Committee for medicinal products for human use (CHMP): Guideline on the pharmaceutical quality of inhalation and nasal products. 2006.

95. Mezger TG. The Rheology Handbook For users of rotational and oscillatory rheometers. 2nd ed. Hanover:Vincentz Network; 2006.

96. Hao J, Zhao J, Zhang S, Tong T, Zhuang Q, Jin K, et al. Fabrication of an ionic-sensitive in situ gel loaded with resveratrol nanosuspensions intended for direct nose-to-brain delivery. Colloids Surf B Biointerfaces 2016;147: 376–386.

97. Watts P, Smith A, Perelman M. Nasal delivery of fentanyl. Drug Deliv 2013; 75–83.

98. Zaki NM, Awad GA, Mortada ND, Abd SS. Enhanced bioavailability of metoclopramide HCl by intranasal administration of a mucoadhesive in situ gel with modulated rheological and mucociliary transport properties. Eur J Pharm Sci 2007;2: 296–307.

99. Pennington J, Pandey P, Tat H, Willson J, Donovan B. Spray pattern and droplet size analyses for high-shear viscosity determination of aqueous suspension corticosteroid nasal sprays. Drug Dev Ind Pharm 2008;34(9): 923–929.

100. Gao M, Shen X, Mao S. Factors influencing drug deposition in the nasal cavity upon delivery via nasal sprays. J Pharm Investig 2020;50(3): 251–259.

101. Winter HH, Chambon F. Analysis of Linear Viscoelasticity of a Crosslinking Polymer at the Gel Point Analysis of Linear Viscoelasticity of a Crosslinking Polymer at the Gel Point. J Rheol 1986;30:367.

102. Moura MJ, Figueiredo MM, Gil MH. Rheological Study of Genipin Cross-Linked Chitosan Hydrogels. Biomacromolecules 2007;8(12):3823-9.

103. Ye X, Li X, Shen Y, Chang G, Yang J, Gu Z. Self-healing pH-sensitive cytosine- and guanosine-modified hyaluronic acid hydrogels via hydrogen bonding. Polymer 2017;108: 348-60.

104. Ta HT, Han H, Larson I, Dass CR, Dunstan DE. Chitosan-dibasic orthophosphate hydrogel: A potential drug delivery system. Int J Pharm 2009;371: 134–141.

105. Dabbaghi M, Namjoshi S, Panchal B, Grice JE, Prakash S, Roberts MS, et al. Viscoelastic and deformation characteristics of structurally different commercial topical systems. Pharmaceutics 2021;13(9): 1–11.

106. Aulton ME, Taylor KMG. Aulton's Pharmaceutics - The Design and Manufacture of Medicines. 5th Ed. London:Harcourt Publishers Limited. 2013.

107. Jüptner A, Scherließ R. Spray dried formulations for inhalation—meaningful characterisation of powder properties. Pharmaceutics 2020;12(1).

108. Hertel N, Birk G, Scherließ R. Particle engineered mannitol for carrier-based inhalation – A serious alternative? Int J Pharm 2020;577: 118901.

109. Dayal P, Shaik MS, Singh M. Evaluation of different parameters that affect droplet-size distribution from nasal sprays using the Malvern Spraytec®. J Pharm Sci 2004;93(7): 1725–42.

110. Moraga-Espinoza D, Warnken Z, Moore A, Williams RO, Smyth HDC. A modified USP induction port to characterize nasal spray plume geometry and predict turbinate deposition under flow. Int J Pharm 2018;548(1): 305-313.

111. Guo C, Doub WH. The influence of actuation parameters on in vitro testing of nasal spray products. J Pharm Sci 2006;95(9): 2029-40.

112. Pu Y, Goodey AP, Fang X, Jacob K. A comparison of the deposition patterns of different nasal spray formulations using a nasal cast. Aerosol Sci Technol 2014;48(9): 930–8.

113. Salunke SR, Patil SB. Ion activated in situ gel of gellan gum containing salbutamol sulphate for nasal administration. Int J Biol Macromol 2016;87:41–47.

114. Balzus B, Colombo M, Sahle FF, Zoubari G, Staufenbiel S, Bodmeier R. Comparison of different in vitro release methods used to investigate nanocarriers intended for dermal application. Int J Pharm 2016;513(1–2):247–54.

115. Chu K, Chen L, Xu W, Li H, Zhang Y, Xie W, et al. Preparation of a paeonol-containing temperature-sensitive in situ gel and its preliminary efficacy on allergic rhinitis. Int J Mol Sci 2013;14(3): 6499–6515.

116. Salade L, Wauthoz N, Goole J, Amighi K. *How to characterize a nasal product. The state of the art of in vitro and ex vivo specific methods*. Int J Pharm 2019; 47–65.

117. Sibinovska N, Žakelj S, Roškar R, Kristan K. Suitability and functional characterization of two Calu-3 cell models for prediction of drug permeability across the airway epithelial barrier. Int J Pharm 2020;585:119484.

118. Sibinovska N, Božič D, Bošković Ribarski M, Kristan K. Prediction of pharmacokinetic studies outcome for locally acting nasal sprays by using different in vitro methods. Int J Pharm 2021;120569.

119. Yang J, Dai L, Yu Q, Yang Q. Histological and anatomical structure of the nasal cavity of Bama minipigs. PLoS ONE 2017;12(3):1–14.

120. Fachel FNS, Medeiros-Neves B, Dal Prá M, Schuh RS, Veras KS, Bassani VL, et al. Box-Behnken design optimization of mucoadhesive chitosan-coated nanoemulsions for rosmarinic acid nasal delivery—In vitro studies. Carbohydr Polym 2018;199: 572–582.

121. Lungare S, Bowen J, Badhan R. Development and Evaluation of a Novel Intranasal Spray for the Delivery of Amantadine. J Pharm Sci 2016;105(3): 1209–1220.

122. Yarragudi SB, Richter R, Lee H, Walker GF, Clarkson AN, Kumar H, et al. Formulation of olfactory-targeted microparticles with tamarind seed polysaccharide to improve nose-to-brain transport of drugs. Carbohydr Polym 2017;163: 216–226.

123. Castile J, Cheng YH, Simmons B, Perelman M, Smith A, Watts P. Development of in vitro models to demonstrate the ability of PecSys®, an *in situ* nasal gelling technology, to reduce nasal run-off and drip. Drug Dev Ind Pharm 2013;39(5): 816–824.

124. Chen JZ, Kiaee M, Martin AR, Finlay WH. In vitro assessment of an idealized nose for nasal spray testing: Comparison with regional deposition in realistic nasal replicas. Int J Pharm 2020;582:119341.

125. Le Guellec S, Ehrmann S, Vecellio L. In vitro – in vivo correlation of intranasal drug deposition. Adv Drug Deliv Rev 2021;170:340–352.

126. Foo MY, Cheng YS, Su WC, Donovan MD. The influence of spray properties on intranasal deposition. J Aerosol Med Depos Clear Eff Lung 2007;20(4):495–508.

127. Xi J, Wang Z, Nevorski D, White T, Zhou Y. Nasal and Olfactory Deposition with Normal and Bidirectional Intranasal Delivery Techniques: In Vitro Tests and Numerical Simulations. J Aerosol Med Pulm Drug Deliv 2017;30(2):118-31.

128. www.halmed.hr. *Sažetak opisa svojstava lijeka "Avamys."* https://www.halmed.hr/Lijekovi/Baza-lijekova/Avamys/9450/ (pristupljeno 16. 2. 2022.)

129. www.halmed.hr. *Sažetak opisa svojstava lijeka "Tafen."* https://www.halmed.hr/Lijekovi/Baza-lijekova/Tafen-nasal-50-mikrograma-po-potisku-sprej-za-nos-suspenzija/14364/ (pristupljeno 16. 2. 2022.)

130. Guo Y, Laube B, Dalby R. The Effect of Formulation Variables and Breathing Patterns on the Site of Nasal Deposition in an Anatomically Correct Model. Pharm Res 2005;22(11):1871–78.

131. www.halmed.hr. *Sažetak opisa svojstava lijeka "Bloctimo."* https://www.halmed.hr/Lijekovi/Baza-lijekova/Bloctimo-50-mikrograma-po-potisku-sprej-za-nos-suspenzija/14968/ (pristupljeno 16. 2. 2022.)

132. www.halmed.hr. *Sažetak opisa svojstava lijeka "Momanose."* https://www.halmed.hr/Lijekovi/Baza-lijekova/Momanose-50-mikrograma-po-potisku-sprej-za-nos-suspenzija/14861/ (pristupljeno 16. 2. 2022.)

133. www.halmed.hr. *Sažetak opisa svojstava lijeka "Mometazonfuroat Cipla."* https://www.halmed.hr/Lijekovi/Baza-lijekova/Mometazonfuroat-Cipla-50-mikrograma-po-potisku-sprej-za-nos-suspenzija/10649/ (pristupljeno 16. 2. 2022.)

134. www.halmed.hr. *Sažetak opisa svojstava lijeka "Nasonex."* https://www.halmed.hr/Lijekovi/Baza-lijekova/Nasonex-50-mikrograma-po-potisku-sprej-za-nos-suspenzija/ (pristupljeno 16. 2. 2022.)

135. www.halmed.hr. *Sažetak opisa svojstava lijeka "Nasacort."* https://www.halmed.hr/Lijekovi/Baza-lijekova/Nasacort-55-mikrograma-po-potisku-sprej-za-nos-suspenzija/14451/ (pristupljeno 16. 2. 2022.)

136. Kundoor V, Dalby RN. Assessment of nasal spray deposition pattern in a silicone human nose model using a color-based method. Pharm Res 2010;27(1): 30–6.

137. Colombo G, Bortolotti F, Chiapponi V, Buttini F, Sonvico F, Invernizzi R. Nasal powders of thalidomide for local treatment of nose bleeding in persons affected by hereditary hemorrhagic telangiectasia. Int J Pharm 2016;514(1): 229–37.

138. Kundoor V, Dalby RN. Effect of formulation- and administration-related variables on deposition pattern of nasal spray pumps evaluated using a nasal cast. Pharm Res 2011;28(8): 1895–1904.

139. Shah SA, Dickens CJ, Ward DJ, Banaszek AA, George C, Horodnik W. Design of experiments to optimize an in vitro cast to predict human nasal drug deposition. J Aerosol Med Pulm Drug Deliv 2014;27(1):21–9.

140. Kaye RS, Purewal TS, Alpar OH. Development and testing of particulate formulations for the nasal delivery of antibodies. J Control Rel 2009;135(2):127-35.

141. Shah SA, Berger RL, McDermott J, Gupta P, Monteith D, Connor A, et al. Regional deposition of mometasone furoate nasal spray suspension in humans. Allergy Asthma Proc 2015;36(1).

142. Xi J, Wang Z, Si XA, Zhou Y. Nasal dilation effects on olfactory deposition in unilateral and bi-directional deliveries: In vitro tests and numerical modeling. Eur J Pharm Sci 2018;118:113–23.

143. Politis SN, Colombo P, Colombo G, Rekkas DM. Design of experiments (DoE) in pharmaceutical development. Drug Dev Ind Pharm 2017;43(6): 889–901.

144. Grangeia HB, Silva C, Simões SP, Reis MS. Quality by design in pharmaceutical manufacturing: A systematic review of current status, challenges and future perspectives. Eur J Pharm Biopharm 2020;147:19–37.

145. von Mentzer B, Russo AF, Zhang Z, Kuburas A, Killoran PM, D'Aloisio V, et al. A CGRP receptor antagonist peptide formulated for nasal administration to treat migraine. J Pharm Pharmacol 2020;72(10):1352–60.

146. Silva DM, Vyas HKN, Sanderson-Smith ML, Sencadas V. Development and optimization of ciprofloxacin-loaded gelatin microparticles by single-step spray-drying technique. Powder Technol 2018;330:201–209.

147. Trenkel M, Scherließ R. Nasal Powder Formulations: In-Vitro Characterisation of the Impact of Powders on Nasal Residence Time and Sensory Effects. Pharmaceutics 2021;13(3):385.

148. Popov TA, Åberg N, Emberlin J, Josling P, Ilyina NI, Nikitin NP, et al. Methyl-cellulose powder for prevention and management of nasal symptoms. Expert Rev Respir Med 2017;11:885–892.

149. Chen X, Guan WJ, Sun SX, Zheng PY, Sun LH, Chen DH, et al. Effects of Intranasal Cellulose Powder on Asthma Control in Children With Mild-to-Moderate Perennial Allergic Rhinitis: A Randomized, Placebo-Controlled Trial. Am J Rhinol Allergy 2019;33(2):184–193.

150. Wu L, Zhang J, Watanabe W. Physical and chemical stability of drug nanoparticles. Adv Drug Deliv Rev 2011;63(6):456–469.

151. Shrestha K, Strien J van, Singh N, Inthavong K. Primary break-up and atomization characteristics of a nasal spray. PLoS ONE 2020;15:1–16.

152. Jiang L, Gao L, Wang X, Tang L. The application of mucoadhesive polymers in nasal drug delivery. Drug Dev Ind Pharm 2010;36(3):323–336.

153. Shahin HI, Vinjamuri BP, Mahmoud AA, Shamma RN, Mansour SM, Ammar HO, et al. Design and evaluation of novel inhalable sildenafil citrate spray-dried microparticles for pulmonary arterial hypertension. J Control Rel 2019;302:126–139.

154. Jurišić Dukovski B, Plantić I, Čunčić I, Krtalić I, Juretić M, Pepić I, et al. Lipid/alginate nanoparticle-loaded in situ gelling system tailored for dexamethasone nasal delivery. Int J Pharm 2017;533(2) 480–487.

155. US Food and Drug Administration. Guidance for Industry Nasal Spray and Inhalation Solution, Suspension, and Spray Drug Products — Chemistry, Manufacturing, and Controls Documentation ` U.S. Department of Health and Human Services Food and Drug Administration Center for Drug Evaluation an. 2002;10–15. https://www.fda.gov/media/70857/download (pristupljeno 16. 2. 2022.)

156. Lee HJ, Lee HG, Kwon YB, Kim JY, Rhee YS, Chon J, et al. The role of lactose carrier on the powder behavior and aerodynamic performance of bosentan microparticles for dry powder inhalation. Eur J Pharm Sci 2018;117:279-89.

157. Ghaemi S, Rahimi P, Nobes DS. Assesment of parameters for distinguishing droplet shape in a spray field using image based techniques. At Sprays 2009;19(9):809-831.

158. Joergensen L, Klösgen B, Simonsen AC, Borch J, Hagesaether E. New insights into the mucoadhesion of pectins by AFM roughness parameters in combination with SPR. Int J Pharm 2011;411(1–2):162–168.

159. Scherließ R. The MTT assay as tool to evaluate and compare excipient toxicity in vitro on respiratory epithelial cells. Int J Pharm 2011;411(1–2):98–105.

160. Noach AB, Sakai M, Blom-Roosemalen MC, de Jonge HR, de Boer AG, Breimer DD. Effect of anisotonic conditions on the transport of hydrophilic model compounds across monolayers of human colonic cell lines. J Pharmacol Exp Ther 1994;270(3):1373–80.

8. ŽIVOTOPIS

Laura Nižić Nodilo (r. Nižić) rođena je u Splitu 10. srpnja 1993. godine. Osnovnu školu i opću gimnaziju te osnovnu i srednju glazbenu školu završila je u Zadru, a 2012. godine upisala je integrirani preddiplomski i diplomski studij farmacije na Farmaceutsko-biokemijskom fakultetu Sveučilišta u Zagrebu. Diplomski rad pod naslovom "Utjecaj brzine dotoka uzorka i protoka medija za sušenje na svojstva alginatnih mikročestica pripravljenih sušenjem raspršivanjem" izradila je u Zavodu za farmaceutsku tehnologiju Farmaceutsko-biokemijskog fakulteta Sveučilišta u Zagrebu pod stručnim vodstvom prof. dr. sc. Anite Hafner. Diplomirala je 2017. godine i stekla naslov magistre farmacije te dobila odobrenje za samostalan rad u ljekarničkoj djelatnosti. Nakon diplome odlazi na Erasmus + stručnu praksu u Liverpool, Velika Britanija, gdje radi na razvoju mikrosfera s peptidnim antimigrenikom pripravljenih sušenjem raspršivanjem. 2018. godine zapošljava se kao doktorand – asistent na Zavodu za farmaceutsku tehnologiju Farmaceutsko-biokemijskog fakulteta Sveučilišta u Zagrebu, u sklopu uspostavnog istraživačkog projekta sufinanciranog od strane Hrvatske zaklade za znanost, voditeljice prof. dr. sc. Anite Hafner. Poslijediplomski doktorski studij Farmaceutsko-biokemijske znanosti (grana Farmacija) na Farmaceutsko-biokemijskom fakultetu Sveučilišta u Zagrebu upisala je 2018. godine. Sudjeluje u izvođenju nastave predmeta Biofarmacija s farmakokinetikom, Magistralna receptura i Kozmetologija na integriranom preddiplomskom i diplomskom studiju farmacije te Nosači i aktivne supstancije u dermatološkim i kozmetičkim pripravcima na poslijediplomskom specijalističkom studiju Dermatofarmacija i kozmetologija. Do sada je u koautorstvu objavila pet znanstvenih radova zastupljenih u bazi Web of Science Core Collection te jedan rad u drugom časopisu. Aktivno je sudjelovala na stranim i domaćim znanstvenim skupovima s četrnaest posterskih priopćenja. Osvojila je nagradu publike za najbolju postersku prezentaciju na 12. CESPT-u 2018. godine te nagradu stručnog povjerenstva za najbolju postersku prezentaciju na godišnjem skupu FIGON/EUFEPS 2022. Održala je nekoliko radionica na Danima otvorenih vrata Farmaceutsko-biokemijskog fakulteta i Festivalu znanosti. Držala je prezentacije na Danu znanosti, Infodanu doktorskog studija te na Danu brucoša. Od 2017. godine članica je Hrvatske ljekarničke komore.

Znanstveni radovi (CC):

1. Nižić L, Ugrina I, Špoljarić D, Saršon V, Safundžić Kučuk M, Pepić I, et al. Innovative sprayable *in situ* gelling fluticasone suspension: Development and optimization of nasal deposition. Int J Pharm. 2019;563:445–456.

2. Nižić L, Potaś J, Winnicka K, Szekalska M, Erak I, Gretić M, et al. Development, characterisation and nasal deposition of melatonin-loaded pectin/hypromellose microspheres. Eur J Pharm Sci. 2020;141:105115.

3. von Mentzer B, Russo AF, Zhang Z, Kuburas A, Killoran PM, D'Aloisio V, et al. A CGRP receptor antagonist peptide formulated for nasal administration to treat migraine. J Pharm Pharmacol. 2020;72:1352–1360.

4. Nižić Nodilo L, Ugrina I, Špoljarić D, Amidžić Klarić D, Jakobušić Brala C, Perkušić M, et al. A dry powder platform for nose-to-brain delivery of dexamethasone: Formulation development and nasal deposition studies. Pharmaceutics. 2021;13:1–30.

5. Nižić Nodilo L, Perkušić M, Ugrina I, Špoljarić D, Jakobušić Brala C, Amidžić Klarić D, et al. *In situ* gelling nanosuspension as an advanced platform for fluticasone propionate nasal delivery. Eur J Pharm Biopharm. 2022;175:27–42.

Ostali znanstveni radovi:

1. Nižić L, Keser S, Duvnjak Romić M, Hafner A. Utjecaj parametara sušenja raspršivanjem na svojstva alginatnih mikročestica. Farm Glas. 2018;74:619–632.

TEMELJNA DOKUMENTACIJSKA KARTICA

Sveučilište u Zagrebu
Farmaceutsko-biokemijski fakultet
Zavod za farmaceutsku tehnologiju
A. Kovačića 1, 10000 Zagreb, Hrvatska

Doktorski rad

RAZVOJ I OPTIMIRANJE NAZALNE DEPOZICIJE INOVATIVNIH FARMACEUTSKIH OBLIKA KORTIKOSTEROIDA

Laura Nižić Nodilo

SAŽETAK

Nazalna primjena lijeka uobičajena je u liječenju lokalnih oboljenja nosne sluznice. Istražuje se i kao alternativni put sistemske primjene lijekova, a pruža mogućnost i izravne dostave lijeka u središnji živčani sustav. Ograničenja nazalne primjene lijeka uključuju otežanu dostavu lijeka u ciljno područje te mukocilijarni klirens koji skraćuje vrijeme kontakta lijeka i nosne sluznice. Nazalna primjena kortikosteroida česta je u liječenju bolesti nosne sluznice i paranazalnih sinusa, a u novije vrijeme predlaže se i u liječenju neuroupalnih procesa. U okviru ovog doktorskog rada, primjenjujući načela kakvoće utemeljene kroz dizajn, razvijena su tri inovativna *in situ* gelirajuća sustava s uklopljenim kortikosteroidom za nazalnu primjenu u obliku spreja: (i) *in situ* gelirajuća mikrosuspenzija flutikazonpropionata (FP-a), (ii) *in situ* gelirajuća nanosuspenzija FP-a pripravljena uz vlažno mljevenje te (iii) praškasti sustav mikrosfera s natrijevim deksametazonfosfatom (NDF-om) i inertnog nosača. Provedena je njihova temeljita fizičko-kemijska i biofarmaceutska karakterizacija. Polimerni sastav *in situ* gelirajućih mikro- i nanosuspenzija FP-a osigurao je pseudoplastično ponašanje, prikladnost za primjenu raspršivanjem (tj. prikladnu veličinu raspršenih kapljica i kut raspršenja) te svojstvo geliranja u kontaktu sa simuliranim nosnim fluidom (SNF). Mikrosfere s NDF-om, pripravljene sušenjem raspršivanjem, karakterizirane su velikom uspješnošću uklapanja lijeka, odgovarajućim sadržajem ostatne vlage te sposobnošću bubrenja u SNF-u pri čemu nastaje gel. Smjese mikrosfera s NDF-om i inertnog nosača bile su homogene te boljih svojstava tečenja i užeg kuta raspršenja od samih mikrosfera. Postignuta je uspješna depozicija sva tri farmaceutska oblika u ciljnoj regiji nosne šupljine, ovisno o željenom učinku. Razvijeni farmaceutski oblici karakterizirani su boljom mukoadhezivnošću u usporedbi s konvencionalnim oblicima. Oslobađanje lijeka iz svih razvijenih oblika bilo je prikladno za nazalnu primjenu. Nanonizacija FP-a rezultirala je većom mukoadhezivnošću formulacije te većom topljivošću i brzinom oslobađanja FP-a iz *in situ* gela, pružajući mogućnost smanjenja primijenjene doze. Svim sustavima potvrđena je biokompatibilnost *in vitro* na modelu Calu-3 stanica te fizičko-kemijska stabilnost. Praškasti sustav s NDF-om pokazao je potencijal poboljšanja permeacije lijeka kroz nazalni epitel. Prilagođavanjem procesnih, formulacijskih i/ili parametara primjene korištenjem dizajna eksperimenta razvijeni su inovativni farmaceutski oblici kortikosteroida s potencijalom produljenog zadržavanja na mjestu primjene, povoljnih biofarmaceutskih svojstava i optimirane depozicije u nosnoj šupljini.

Rad je pohranjen u Središnjoj knjižnici Sveučilišta u Zagrebu Farmaceutsko-biokemijskog fakulteta.

Rad sadrži: 121 stranicu, 8 grafičkih prikaza, 3 tablice i 160 literaturnih navoda. Izvornik je na hrvatskom jeziku.

Ključne riječi: *in situ* gelirajući sustav, nanosuspenzija, mikrosfere, sušenje raspršivanjem, flutikazonpropionat, natrijev deksametazonfosfat, nazalna depozicija

Mentor: **Dr. sc. Anita Hafner**, *redovita profesorica Sveučilišta u Zagrebu Farmaceutsko-biokemijskog fakulteta*.

Ocjenjivači: **Dr. sc. Jasmina Lovrić**, *redovita profesorica Sveučilišta u Zagrebu Farmaceutsko-biokemijskog fakulteta*.

Dr. sc. Ana Mornar Turk, *redovita profesorica Sveučilišta u Zagrebu Farmaceutsko-biokemijskog fakulteta*.

Dr. sc. Marjana Dürrigl, *znanstvena suradnica, PLIVA Hrvatska d.o.o., Farmaceutsko-biokemijski fakultet Sveučilišta u Zagrebu*

Rad prihvaćen: lipanj 2022.

BASIC DOCUMENTATION CARD

University of Zagreb
Faculty of Pharmacy and Biochemistry
Department of Pharmaceutical Technology
A. Kovačića 1, 10000 Zagreb, Croatia

Doctoral thesis

DEVELOPMENT AND NASAL DEPOSITION OPTIMISATION OF INNOVATIVE PHARMACEUTICAL FORMS OF CORTICOSTEROIDS

Laura Nižić Nodilo

SUMMARY

Nasal drug delivery is well estabilshed in the treatment of local nasal mucosa diseases. It is also being investigated as an alternative route of systemic drug delivery, as well as the possibility of direct drug delivery to the central nervous system. Limitations of nasal drug administration include difficult drug delivery to the target area and mucociliary clearance, which shortens the contact time between the drug and the nasal mucosa. Nasal use of corticosteroids is common in the treatment of diseases of the nasal mucosa and paranasal sinuse. Recently it has been suggested in the treatment of neuroinflammatory processes. Within this doctoral thesis, employing quality by design principles, three innovative *in situ* gelling pharmaceutical forms of corticosteroid for nasal spray application have been developed: (i) *in situ* gelling microsuspension of fluticasone propionate (FP), (ii) *in situ* gelling nanosuspension of FP prepared by wet media milling; and (iii) powder platform consisting of dexamethasone sodium phosphate (DSP)-loaded microspheres blended with an inert carrier. Thorough physicochemical and biopharmaceutical characterization of developed systems was performed. The polymer composition of the *in situ* gelling micro- and nanosuspensions of FP ensured shear thinning behavior, suitability for administration as a spray (i.e., suitable droplet size and spray angle), and immediate gelling in contact with simulated nasal fluid (SNF). Microspheres with DSP, prepared by spray drying, are characterized by high drug entrapment efficiency, adequate residual moisture content, and good swelling ability in SNF, forming a gel. Blends of microspheres with DSP and inert carrier were homogeneous and had better flow properties and a narrower spray cone angle than the microspheres alone. Successful deposition of all three pharmaceutical forms in the target region of the nasal cavity model was achieved, depending on the desired effect. Developed pharmaceutical forms are characterized by better mucoadhesiveness compared to conventional forms. Drug release from all developed forms was suitable for nasal administration. Nanonization of FP resulted in greater mucoadhesiveness of the formulation and increased solubility and release rate of FP from the *in situ* gel, providing the possibility of reducing the applied dose. Biocompatibility on the *in vitro* Calu-3 cell model and the physicochemical stability was confirmed for all developed formulations. The powder system with DSP showed the potential to improve drug permeation through the nasal epithelium. By varying process, formulation and/or administration parameters, employing design of experiments, innovative pharmaceutical forms of corticosteroids with the potential for prolonged retention at the site of administration, favourable biopharmaceutical properties and optimized deposition in the nasal cavity have been successfully developed.

The thesis is deposited in the Central Library of the University of Zagreb Faculty of Pharmacy and Biochemistry.

Thesis includes: 121 pages, 8 figures, 3 tables and 160 references. Original is in Croatian language.

Keywords: *in situ* gelling system, nanosuspension, microspheres, spray drying, fluticasone propionate, dexamethasone sodium phosphate, nasal deposition

Mentor: **Anita Hafner, PhD,** *Full Professor, University of Zagreb Faculty of Pharmacy and Biochemistry*

Reviewers: **Jasmina Lovrić, PhD,** *Full Professor, University of Zagreb Faculty of Pharmacy and Biochemistry*

Ana Mornar Turk, PhD, *Full Professor, University of Zagreb Faculty of Pharmacy and Biochemistry*

Marjana Dürrigl, PhD, *Research Associate, PLIVA Croatia Ltd., University of Zagreb Faculty of Pharmacy and Biochemistry*

The thesis was accepted: June 2022